

UNCLASSIFIED

| |
|---|
| |
| |
| |
| |
| AD NUMBER |
| ADB270660 |
| NEW LIMITATION CHANGE |
| TO Approved for public release, distribution unlimited |
| FROM Distribution authorized to U.S. Gov't. agencies only; Proprietary Info.; Sep 2000. Other requests shall be referred to U.S. Army Medical Research and Materiel Command, 504 Scott St., Fort Detrick, MD 21702-5012. |
| AUTHORITY |
| USAMRMC ltr, 26 Aug 2002 |

THIS PAGE IS UNCLASSIFIED

AD _____

Award Number: DAMD17-97-1-7076

TITLE: Combinatorial Synthesis for the Expedited Discovery of
Novel Selective Antiestrogens for Breast Cancer Prevention
and Therapy

PRINCIPAL INVESTIGATOR: John A. Katzenellenbogen, Ph.D.

CONTRACTING ORGANIZATION: University of Illinois
Champaign, Illinois 61820

REPORT DATE: September 2000

TYPE OF REPORT: Annual

PREPARED FOR: U.S. Army Medical Research and Materiel Command
Fort Detrick, Maryland 21702-5012

DISTRIBUTION STATEMENT: Distribution authorized to U.S.
Government agencies only (proprietary information, Sep 00).
Other requests for this document shall be referred to U.S.
Army Medical Research and Materiel Command, 504 Scott Street,
Fort Detrick, Maryland 21702-5012.

The views, opinions and/or findings contained in this report are
those of the author(s) and should not be construed as an official
Department of the Army position, policy or decision unless so
designated by other documentation.

20010924 031

NOTICE

USING GOVERNMENT DRAWINGS, SPECIFICATIONS, OR OTHER DATA INCLUDED IN THIS DOCUMENT FOR ANY PURPOSE OTHER THAN GOVERNMENT PROCUREMENT DOES NOT IN ANY WAY OBLIGATE THE U.S. GOVERNMENT. THE FACT THAT THE GOVERNMENT FORMULATED OR SUPPLIED THE DRAWINGS, SPECIFICATIONS, OR OTHER DATA DOES NOT LICENSE THE HOLDER OR ANY OTHER PERSON OR CORPORATION; OR CONVEY ANY RIGHTS OR PERMISSION TO MANUFACTURE, USE, OR SELL ANY PATENTED INVENTION THAT MAY RELATE TO THEM.

LIMITED RIGHTS LEGEND

Award Number: DAMD17-97-1-7076

Organization: University of Illinois

Location of Limited Rights Data (Pages):

Those portions of the technical data contained in this report marked as limited rights data shall not, without the written permission of the above contractor, be (a) released or disclosed outside the government, (b) used by the Government for manufacture or, in the case of computer software documentation, for preparing the same or similar computer software, or (c) used by a party other than the Government, except that the Government may release or disclose technical data to persons outside the Government, or permit the use of technical data by such persons, if (i) such release, disclosure, or use is necessary for emergency repair or overhaul or (ii) is a release or disclosure of technical data (other than detailed manufacturing or process data) to, or use of such data by, a foreign government that is in the interest of the Government and is required for evaluational or informational purposes, provided in either case that such release, disclosure or use is made subject to a prohibition that the person to whom the data is released or disclosed may not further use, release or disclose such data, and the contractor or subcontractor or subcontractor asserting the restriction is notified of such release, disclosure or use. This legend, together with the indications of the portions of this data which are subject to such limitations, shall be included on any reproduction hereof which includes any part of the portions subject to such limitations.

THIS TECHNICAL REPORT HAS BEEN REVIEWED AND IS APPROVED FOR PUBLICATION.

Earl Hunt Jr. LTC, MS
17 Aug 01

REPORT DOCUMENTATION PAGEForm Approved
OMB No. 074-0188

*Public reporting burden for this collection of information is estimated to average 1 hour per response, including the time for reviewing instructions, searching existing data sources, gathering and maintaining the data needed, and completing and reviewing this collection of information. Send comments regarding this burden estimate or any other aspect of this collection of information, including suggestions for reducing this burden to Washington Headquarters Services, Directorate for Information Operations and Reports, 1215 Jefferson Davis Highway, Suite 1204, Arlington, VA 22202-4302, and to the Office of Management and Budget, Paperwork Reduction Project (0704-0188), Washington, DC 20503

| | | | | |
|---|---|--|--|--|
| 1. AGENCY USE ONLY (Leave blank) | | 2. REPORT DATE September 2000 | 3. REPORT TYPE AND DATES COVERED Annual (1 Sep 99 - 31 Aug 00) | |
| 4. TITLE AND SUBTITLE Combinatorial Synthesis for the Expedited Discovery of Novel Selective Antiestrogens for Breast Cancer Prevention and Therapy | | | 5. FUNDING NUMBERS DAMD17-97-1-7076 | |
| 6. AUTHOR(S) John A. Katzenellenbogen, Ph.D. | | | | |
| 7. PERFORMING ORGANIZATION NAME(S) AND ADDRESS(ES) University of Illinois Champaign, Illinois 61820 E-MAIL: jkatzene@uiuc.edu | | | 8. PERFORMING ORGANIZATION REPORT NUMBER | |
| 9. SPONSORING / MONITORING AGENCY NAME(S) AND ADDRESS(ES) U.S. Army Medical Research and Materiel Command Fort Detrick, Maryland 21702-5012 | | | 10. SPONSORING / MONITORING AGENCY REPORT NUMBER | |
| 11. SUPPLEMENTARY NOTES This report contains colored photos | | | | |
| 12a. DISTRIBUTION / AVAILABILITY STATEMENT DISTRIBUTION STATEMENT: Distribution authorized to U.S. Government agencies only (proprietary information, Sep 00). Other requests for this document shall be referred to U.S. Army Medical Research and Materiel Command, 504 Scott Street, Fort Detrick, Maryland 21702-5012. | | | 12b. DISTRIBUTION CODE | |
| 13. ABSTRACT (Maximum 200 Words) We have conceived of an approach to prepare by combinatorial methods, libraries of novel ligands for the estrogen receptor, by the creation of simple amide or five-membered ring heterocyclic core structures that display peripheral substituents (phenols, aliphatic groups, etc.) commonly found in non-steroidal estrogens. These novel estrogens might be useful in the treatment or prevention of breast cancer. We have made excellent progress on the preparation of novel estrogens of the diphenyl carboxamide class, the diphenylsulfonamide class, the phenyl benzylcarboxamide and sulfonamide classes, and the pyrazole, oxazole, thiazole, and imidazole classes. Members of some classes have high affinity for the estrogen receptor, and some of them show high binding and potency selectivity for the estrogen receptor subtype alpha and can be adapted as selective estrogen receptor alpha antagonists. We have also developed a convenient solid phase synthesis of the pyrazole class, so that we can prepare conveniently and rapidly larger libraries of the members of what appear presently to be the most promising of these classes of novel estrogens. | | | | |
| 14. SUBJECT TERMS Breast Cancer | | | 15. NUMBER OF PAGES 175 | |
| | | | 16. PRICE CODE | |
| 17. SECURITY CLASSIFICATION OF REPORT Unclassified | 18. SECURITY CLASSIFICATION OF THIS PAGE Unclassified | 19. SECURITY CLASSIFICATION OF ABSTRACT Unclassified | 20. LIMITATION OF ABSTRACT Unlimited | |

NSN 7540-01-280-5500

Standard Form 298 (Rev. 2-89)
Prescribed by ANSI Std. Z39-18
298-102

TABLE OF CONTENTS

| <u>Section</u> | <u>Page</u> |
|---|-------------|
| Front Cover | |
| Report Documentation Page (SF 298) | 2 |
| Table of Contents | 3 |
| Introduction | 4 |
| Body | 5 |
| Key Research Accomplishments | 11 |
| Reportable Outcomes | 13 |
| Conclusions | 14 |
| References | 15 |
| Publications, Patents, Meeting Abstracts, and Personnel Supported | 18 |
| Appendices | 20 |

PRINCIPAL INVESTIGATOR: John A. Katzenellenbogen

TITLE: Combinatorial Synthesis For The Expedited Discovery Of Novel Selective Antiestrogens For Breast Cancer Prevention And Therapy

ORGANIZATION: University Of Illinois

+++++

INTRODUCTION, GOALS OF THE PROJECT AND APPROACH

[NOTE: For the purpose of continuity, the three Schemes in the attached Appendix have been taken directly from the original proposal. The details of this final report are contained in three reprints and four manuscripts that are appended. Specific reference is made to these as "Publications No. 1-7".]

Antiestrogens such as tamoxifen are widely used in the treatment of hormone responsive breast cancer and recently shown to be effective in breast cancer prevention¹⁻⁵. Tamoxifen, however, as well as the pure ICI antiestrogens, are not ideal agents, because they cause vaginal atrophy and menopausal hot flashes, induce osteoporosis (pure antiestrogens), and may cause endometrial and liver cancer (tamoxifen)⁶⁻¹⁴. Thus, there is a need for the development of selective antiestrogens with an improved endocrine profile for use in the treatment and prevention of breast cancer¹⁵⁻¹⁶.

Recent advances in our understanding of the molecular pharmacology of estrogens and the development of new selective antiestrogens for menopausal bone maintenance, suggest that new selective antiestrogens of this type can be discovered¹⁶⁻²⁵. Up to now, however, this search has not been approached in a systematic fashion²⁶. Furthermore, the structures of antiestrogens that have been studied to date are quite complex and their synthesis sufficiently challenging, so as not to be amenable to synthesis by solid-phase combinatorial means. Combinatorial synthesis is the fastest growing new technology in pharmaceutical chemistry, and is proving to be a highly expeditious and promising approach to new drug discovery²⁷⁻³⁵.

In preparing for this project, we analyzed the structures of many selective antiestrogens and found that they possess three common peripheral groups (a phenol, a second aromatic group, and a basic side chain) attached to various core structures. Because the core structure appears to function as a scaffold simply to hold these other appendages together, we then designed six novel core structures that will perform the same scaffold function for the peripheral groups, yet are sufficiently simple that they can be readily prepared by solid-phase combinatorial synthesis.

In this project, we proposed to prepare six novel classes of ligands for the estrogen receptor, based on four functional group so far unexplored in the antiestrogen literature: a carboxamide, a sulfonamide, a pyrazole, and an oxazole (and related thiazole and imidazole). Solution-phase syntheses were first to be developed, and then adapted to solid-phase synthesis using an acid-labile linker attached to the common phenol function. Libraries containing larger numbers of the best of these classes were then to be prepared, and all of these compounds then to be assayed for their binding affinity for the estrogen receptor. The estrogen agonist and antagonist activity of those members with high affinity was then later to be determined in cell transfection and proliferation assays, and those with the most appropriate endocrine activity tested in a uterotrophic assay.

The combination of this novel structural insight leading to the design of new core structures for estrogen receptor ligands that can be readily prepared by combinatorial synthesis, together with a set of simple, but effective assays to establish their hormonal activity, should assist in the discovery of novel selective antiestrogens for the treatment and prevention of breast cancer.

+++++

BODY

Experimental Approach

A General Structural Description of Selective Estrogen Receptor Ligands Suggests Alternate Core Structures that Can be Prepared by Solid Phase Combinatorial Chemistry Methods

As a class, selective antiestrogens can be envisioned as having four structural components (Schemes 1 and 2 in attached Appendix [taken from the original proposal]): *a core structure (A)* onto which are appended three other structural elements, *a phenol (B)*, *a second aromatic group (C)* and *a basic side chain (D)*. The achievement of an appropriate balance of estrogenic vs antiestrogenic activities in each of these series of selective antiestrogens appears to involve a delicate interaction between these component parts of their structure. Curiously, whereas

components **B**, **C**, and **D** are rather similar in almost all of the selective antiestrogens (cf. Scheme 1, selective antiestrogens), the central core structure **A**, which links together the other three components like a scaffold, is quite variable. This suggests that other core structures could replace this central component in selective antiestrogens.

In the original proposal we proposed to explore new antiestrogens specifically designed to have novel core structures that are readily amenable to solid phase combinatorial synthesis and which may prove to be more tissue selective and efficacious for breast cancer. As explained in Scheme 3 in attached Appendix [taken from the original proposal], we identified three simple structure motifs that are found in ER ligands, around which we designed six new classes of potential ligands for the ER that are based on four new core structures (Scheme 3, right column). We anticipated that these four core structures—a carboxamide, a sulfonamide, a pyrazole, and an oxazole (and a related thiazole and imidazole)—would provide a suitable molecular scaffold for the other three components typically found in selective antiestrogens—the phenol, the second aromatic unit, and the basic side chain—so that these new structural classes would also have selective antiestrogenic activity. The unique feature of these new core structures is that, unlike most antiestrogens developed to date, they can be prepared by combinatorial chemistry means.

The first of the motifs, *motif A is an anti-bibenzyl system*, a structural subunit that is found in the potent estrogen hexestrol, as well as in the antiestrogen hydroxytamoxifen (Scheme 3). The structural analogs of this motif that we planned to explore, the diphenylcarboxamide and diphenylsulfonamide (Classes I and II), are well suited to three-component combinatorial solid phase synthesis methods (see below and Scheme 6). *Motif B is the homolog of the bibenzyl motif*, a substructure that is exemplified in the potent estrogen benzestrol and the selective estrogen raloxifene, but is otherwise largely undeveloped. We planned to explore several structural analogs of the homobibenzyl motif that are better suited for solid phase three-component combinatorial synthesis, benzylic homologs of the carboxamides and sulfonamides (Classes III and IV) and pyrazoles (Class V) (see below and Schemes 6 and 7). Finally, *Motif C, a syn-bibenzyl system* found in tamoxifen and centchroman, is the motivation for the three-component combinatorial synthesis of a series of heterocyclic analogs, oxazoles, thiazoles, and imidazoles (Class VI; see below and Scheme 8).

As we discuss below, we have made good progress evaluating the synthetic feasibility and ER binding affinity of members of all of these classes, as well as some others.

Results and Discussion for total project, years 1-3.

The statement of work for years 1-3 of this project are listed below.

ORIGINAL STATEMENT OF WORK

Project Period: July 1, 1997– June 30, 2000 (3 years)

Year 1

- Synthesis of representative members of Class I-VI ligands by solution phase methods.
- Isolate, purify, and fully characterize these members.
- Measure estrogen receptor binding affinity of representative members of Class I-VI ligands
- Begin to adapt solution phase syntheses to solid phase.

Year 2

- Complete adaptation of solution phase synthesis to solid phase.
- Isolate and fully characterize representative members produced by solid phase synthesis.
Determine yield and characterize impurities.
- Compare estrogen receptor binding of representative members of Class I-VI ligands prepared by solution vs solid phase.
- Begin synthesis of full Class I-VI libraries.
- Begin cell proliferation and cell-based transfection assays.

Year 3

- Complete synthesis of full Class I-VI libraries.
 - Complete estrogen receptor assay of full libraries at two concentrations.
 - Reassay the members with detectable estrogen receptor binding affinity by quantitative titration assay.
 - Assay the members with high estrogen receptor binding affinity in the cell proliferation and cell-based transfection assays.
 - Assay uterotrophic activity of the most promising members in rats.
-
-

Summary — Through the work we have engaged in on this project over the past three years, we have completed all of the goals of the original proposal, as summarized in the original Statement of Work. This has involved an exploration of the promise of all of the proposed acyclic amide and 5-membered ring heterocyclic systems, and the development of solid phase synthesis methods and large library synthesis and analysis. In addition, we have discovered in

the process that some of the most promising heterocyclic ligands, the pyrazoles, have high affinity and potency selectivity for one of the estrogen receptor subtypes, ER α . Because the development of estrogen receptor subtype selective ligands is a very important issue and one of great current interest, we have devoted considerable efforts in years 2 and 3 to pursue this further. We have completed a careful structure-activity relationship study on the pyrazoles, obtaining ultimately a compound that is almost a completely specific activator of ER α , having essentially no activity on ER β at doses where it maximally stimulated ER α , and, based on these findings, we have developed a series of pyrazole basic side chain derivatives that hold considerable promise as potency selective antagonists of ER α . Such compounds could be used to block the action of estradiol through this receptor subtype without interfering with its effect on ER β .

The work that we have done on this project has also spawned several related lines of inquiry that are currently being pursued in my laboratory with independent support. These include investigations of other 5-membered ring heterocyclic systems as estrogen receptor ligands, namely furans, thiophenes, and pyrroles, as well as carbocyclic analogs, cyclopentadienes and related cyclopentadienones. In addition, based on the favorable results of the work under this project, we have begun to synthesize 6-membered ring heterocycles such as pyrazines, pyrimidines, and pyridazines as estrogen receptor ligands. This work is still in an early state of development, but already we know that we have compounds that show high affinity for the receptor and are therefore potentially quite interesting, because their structures are unique in the estrogen receptor field.

We certainly appreciate the support that has been provided to our research efforts in this area through this US Army grant. It has served as a stimulus to us to thrust our laboratory research into new directions that have proved to be very fruitful and potentially useful for the prevention and treatment of breast cancer.

The details of this final report are contained in three reprints and four manuscripts that are appended. Specific reference is made to these as "Publications No. 1-7".

Publication No. 1: B. E. Fink, D. S. Mortensen, S. R. Stauffer, Z. D. Aron, J. A. Katzenellenbogen. Novel Structural Templates for Estrogen-Receptor Ligands and Prospects for Combinatorial Synthesis of Estrogens. *Chem. & Biol.*, 1999, 6, 205-219.

Publication No. 2: S. R. Stauffer, J. Sun, B. S. Katzenellenbogen, J. A. Katzenellenbogen. Acyclic Amides as Estrogen Receptor Ligands: Synthesis, Binding, Activity, and Receptor Interaction. *Bio. Med. Chem.*, 2000, 8, 1293-1316.

- Publication No. 3:** S. R. Stauffer, J. A. Katzenellenbogen. Solid-Phase Synthesis of Tetra-Substituted Pyrazoles, Novel Ligands for the Estrogen Receptor. *J. Comb. Chem.*, 2000, 2, 318-329.
- Publication No. 4:** S. R. Stauffer, C. J. Coletta, J. Sun, B. S. Katzenellenbogen, J. A. Katzenellenbogen. Pyrazole Ligands: Structure-Affinity/Activity Relationships of Estrogen Receptor- α Selective Agonists. *J. Med. Chem.*, 1999, submitted.
- Publication No. 5:** S. R. Stauffer, Y. Huang, C. J. Coletta, R. Tedesco, J. A. Katzenellenbogen. Estrogen Pyrazoles: Defining the Pyrazole Core Structure and the Orientation of Substituents in the Ligand Binding Pocket of the Estrogen Receptor. *Bio. Med. Chem.*, 2000, in press.
- Publication No. 6:** S. R. Stauffer, Y. R. Huang, Z. D. Aron, C. J. Coletta, J. Sun, B. S. Katzenellenbogen, J. A. Katzenellenbogen. Triarylpyrazoles with Basic Side Chains: Development of Pyrazole-Based Estrogen Receptor Antagonists. *Bio. Med. Chem.*, 2000, in press.
- Publication No. 7:** Y. R. Huang, J. A. Katzenellenbogen. Regioselective Synthesis of 1,3,5-Triaryl-4-alkylpyrazoles: Novel Ligands for the Estrogen Receptor. *Org. Lett.*, 2000, in press.

Investigation of Novel Core Structures of Estrogen Receptor Ligands [Publications No. 1 and 2]

In the first of these publications [Publication No. 1], we surveyed a series of heterocyclic systems to identify which core structure from among those originally proposed (pyrazole, imidazole, oxazole, thiazole, isoxazole and isothiazole classes) were capable of giving ligands with high affinity for the estrogen receptor. This work definitively identified the pyrazole class as the most promising one, and one tetrasubstituted pyrazole, in particular, had a binding affinity that reached 19% that of estradiol, a truly remarkable finding. This compound is numbered **38d** in this publication.

The second of these publications [Publication No. 2] we surveyed a series of amides (carboxamides, thiocarboxamides, and sulfonamides) as potential ligands for the estrogen receptor. Again, we found that high affinity for the receptor was restricted to the diphenylcarboxamide class and then only to those analogs having appropriate substituents. The most promising agent, compound **16g** in this publication, has an affinity 15% that of estradiol. This work included extensive analysis of the conformation of these flexible ligands with the aim of understanding how they fit into the ligand binding pocket.

Development of Solid Phase Synthesis Methods to Prepare the Most Promising Ligands [Publication No. 3]

In this publication, we describe the systematic approach that we took to develop an efficient method to synthesize the pyrazole system on a solid phase. In this included a careful determination of the conditions required to attach the precursor to the support and to effect all of the ensuing reactions, including cleavage of the final product. We used NMR and IR analysis directly on the derivatized beads to assess the progress of the reactions. Finally, we used the optimized methods to prepare a small library (12 members) and then a large library (96 members) of the tetrasubstituted pyrazole class. We also measured the receptor binding affinities of these 96 compounds and thereby developed an interesting structure affinity relationship [See Figure 6, **Publication No. 3**]. The highest affinity ligands are those in which at least two of the aromatic rings bear a 4-hydroxy group.

Structure-Activity Relationships of Tetrasubstituted Pyrazoles and Development of an Estrogen Receptor Alpha Specific Ligand [Publication No. 4]

In this publication, we have taken the most favorable results from Publication Nos. 1 and 3 and extended further the structure-activity analysis of the tetrasubstituted pyrazole ligands. In addition, we have assayed their affinity for the estrogen receptor subtypes ER α and ER β . Remarkably, we find that some of the pyrazoles have especially high affinity for ER α , reaching as high as 75% that of estradiol, yet very low affinity for ER β . The best of these compounds [numbered **4g (PPT)** in **Publication No. 4**] has a 410-fold affinity preference for ER α . This compound also shows extremely high potency selectivity for ER α in cell-based transcription assays [Figure 2 in **Publication No. 4**]. This compound has proved to be of great interest to the molecular endocrinology community as a probe for assessing the biological roles of ER α and ER β . We have supplied samples of this ER α selective ligand to more than 20 laboratories who are engaged with use in collaborative studies. In this study we also endeavored to use molecular modeling to supplement the results of our structure-activity study so as to be able to predict the orientational mode with which these rather symmetrical pyrazole core ligands are bound by the estrogen receptor.

Synthesis of Pyrazole Core Isomers in a Further Structure Activity Relationship Study of Tetrasubstituted Pyrazole Estrogen Receptor Ligands [Publication No. 5]

Originally, we explored only one isomeric series of tetrasubstituted pyrazoles as ligands for the estrogen receptor, ones in which the three aryl groups were at N-1, C-3 and C-5, and the alkyl group at C-4. In this publication [**Publication No. 5**] we explore pyrazoles of the isomeric series (i.e., 1,3,4-triaryl-5-alkyl). This required the development of a completely new synthetic

method, because the original method, when applied to the corresponding monoaryl 1,3-diones underwent a Fischer indole reaction rather than a pyrazole cyclization. We were able to overcome this side reaction by performing the synthesis on a 1,3-dione of lesser substitution and then to introduce the final aryl group by a Suzuki coupling method. The overall process proved to be both regioselective for this series and efficient. The most interesting products from this study were those listed as compounds **10a** and **10b** in **Publication No. 5**.

Investigation of Pyrazoles with Basic Side Chains as Potential Potency-Selective Estrogen Receptor Alpha Antagonists [Publication No. 6]

Because of the high affinity and potency selectivity of certain of the pyrazoles as agonists for ER α , we were interested in seeing whether we could convert them to ER α potency selective antagonists by adding a basic side chain to the pyrazole core structure. In this publication [Publication No. 6], we attached a basic side chain to the four substituent positions on the tetrasubstituted pyrazoles, and we found that only one of these showed high affinity for the estrogen receptor. This compound showed about a 10-fold potency preference as an antagonist for ER α vs ER β [see compound **5** and Figure 3 in **Publication No. 6**]. It is the basis for continued studies on pyrazole ligands with basic side chains, which stimulated in part the development of the regioselective method for pyrazole synthesis discussed below.

Development of a Regioselective Synthesis of Pyrazoles [Publication No. 7]

The method we originally devised for the synthesis of the pyrazoles involved the reaction of a hydrazine with a 1,3-diketone and was, therefore, not regioselective. This increasingly became a problem as we wanted to prepare more and more non-symmetrical pyrazoles. In this publication, we have developed an efficient regioselective synthesis of these pyrazoles by the addition of the hydrazine to an enone to give a pyrazoline intermediate. The corresponding anion of this pyrazoline can be alkylated and then oxidized to produce unsymmetrical pyrazoles in high yield and with complete regioselectivity. We have used this method to prepare more than 20 different unsymmetrical pyrazoles, including a variety of ones having different basic side chain substituents on the position where it is most favorable (see discussion above).

+++++

KEY RESEARCH OUTCOMES

Progress in Relation to the Statement of Work

The complete three year Statement of Work, presented in the original proposal of July 1996, is shown below. Our accomplishments are noted in *italics*:

=====

ORIGINAL STATEMENT OF WORK

Project Period: July 1, 1997– June 30, 2000 (3 years)

Year 1

- Synthesis of representative members of Class I-VI ligands by solution phase methods. *completed*
- Isolate, purify, and fully characterize these members. *completed*
- Measure estrogen receptor binding affinity of representative members of Class I-VI ligands. *completed*
- Begin to adapt solution phase syntheses to solid phase. *completed for the most promising series (pyrazoles)*

Year 2

- Complete adaptation of solution phase synthesis to solid phase. *completed for the most promising series (pyrazoles)*
- Isolate and fully characterize representative members produced by solid phase synthesis. *completed for the most promising series (pyrazoles)* Determine yield and characterize impurities. *completed for the most promising series (pyrazoles)*
- Compare estrogen receptor binding of representative members of Class I-VI ligands prepared by solution vs solid phase. *completed for the most promising series (pyrazoles)*
- Begin synthesis of full Class I-VI libraries. *completed for the most promising series (pyrazoles)*
- Begin cell proliferation and cell-based transfection assays. *completed for the most promising series (pyrazoles)*

Year 3

- Complete synthesis of full Class I-VI libraries. *completed for the most promising series (pyrazoles)*
- Complete estrogen receptor assay of full libraries at two concentrations. *completed for the most promising series (pyrazoles)*

- Reassay the members with detectable estrogen receptor binding affinity by quantitative titration assay. *completed for the most promising series (pyrazoles)*
- Assay the members with high estrogen receptor binding affinity in the cell proliferation and cell-based transfection assays. *completed for the most promising series (pyrazoles)*
- Assay uterotrophic activity of the most promising members in rats. *In vivo assays are currently underway and will probably require pharmaceutical development*

Please see **Summary** at the conclusion of the preceeding section that outlines additional accomplishments beyond those outlined in the original Statement of Work.

=====

+++++

REPORTABLE OUTCOMES

- Two full papers have been published, four full manuscripts have been accepted and a fifth has been submitted and is in the final stages of revision, likely to be accepted. These publications are attached as the appendix and are listed as **Publications Nos. 1-7**.
- Presentations have been made at three American Chemical Society meeting by the PI and the principal co-worker, Shaun Stauffer, and by Stauffer at a meeting on solid phase synthesis. Numerous seminars given by the PI have included work developed under this project.
- A PCT patent has been submitted to the US Patent Office covering the 5-membered ring heterocyclic estrogens.
- Shaun Stauffer, my principal co-worker on this project, has completed his Ph.D. degree in the fall of 1999.
- He is currently a postdoctoral fellow with Professor John Hartwig at Yale University, supported by a postdoctoral fellowship from the National Institutes of Health. The topic of Shaun's NIH postdoctoral fellowship derived from the experience he developed working on this project. He will soon be looking for positions in the pharmaceutical industry and, in advance of his formal expression of interest, has already been contacted by interested employers.
- Ying Huang, a postdoctoral fellow in my laboratory who worked on this project, has completed her studies and has moved to a job in new drug discovery at Schering-Plough in New Jersey.

- Rosanna Tedesco, a graduate student who has worked on this project, will complete her Ph.D. studies in October, 2000, and she has accepted a position in new drug discovery at SmithKline Beecham.
- Christopher Coletta and Zachary Aron, two undergraduate students who worked on this project for their senior research, have graduated with high honors, based in part on their excellent undergraduate theses. Chris is working as a B. S. Chemist in new drug discovery at Pfizer, in Connecticut, and Zachary is in a Ph.D. graduate program at the University of California, Irvine, working with Professor Larry Overman.

+++++

CONCLUSIONS [The Summary, presented earlier, is repeated for convenience]

Summary — Through the work we have engaged in on this project over the past three years, we have completed all of the goals of the original proposal, as summarized in the original Statement of Work. This has involved an exploration of the promise of all of the proposed acyclic amide and 5-membered ring heterocyclic systems, and the development of solid phase synthesis methods and large library synthesis and analysis. In addition, we have discovered in the process that some of the most promising heterocyclic ligands, the pyrazoles, have high affinity and potency selectivity for one of the estrogen receptor subtypes, ER α . Because the development of estrogen receptor subtype selective ligands is a very important issue and one of great current interest, we have devoted considerable efforts in years 2 and 3 to pursue this further. We have completed a careful structure-activity relationship study on the pyrazoles, obtaining ultimately a compound that is almost a completely specific activator of ER α , having essentially no activity on ER β at doses where it maximally stimulated ER α , and, based on these findings, we have developed a series of pyrazole basic side chain derivatives that hold considerable promise as potency selective antagonists of ER α . Such compounds could be used to block the action of estradiol through this receptor subtype without interfering with its effect on ER β .

The work that we have done on this project has also spawned several related lines of inquiry that are currently being pursued in my laboratory with independent support. These include investigations of other 5-membered ring heterocyclic systems as estrogen receptor ligands, namely furans, thiophenes, and pyrroles, as well as carbocyclic analogs, cyclopentadienes and related cyclopentadienones. In addition, based on the favorable results of the work under this project, we have begun to synthesize 6-membered ring heterocycles such as pyrazines, pyrimidines, and pyridazines as estrogen receptor ligands. This work is still in an

early state of development, but already we know that we have compounds that show high affinity for the receptor and are therefore potentially quite interesting, because their structures are unique in the estrogen receptor field.

We certainly appreciate the support that has been provided to our research efforts in this area through this US Army grant. It has served as a stimulus to us to thrust our laboratory research into new directions that have proved to be very fruitful and potentially useful for the prevention and treatment of breast cancer.

+++++

REFERENCES

1. Katzenellenbogen BS, Montano M, Le Goff P, Schodin DJ, Kraus WL, Bhardwaj B, Fujimoto N. Antiestrogens: Mechanisms and actions in target cells. *J. Steroid Biochem. Molec. Biol.* 1995; 53:387-393.
2. Katzenellenbogen BS, Fang H, Ince BA, Pakdel F, Reese JC, Wooge CH, Wrenn CK. Estrogen receptors: Ligand discrimination and antiestrogen action. *Breast Cancer Res. Treat.* 1993; 27:17-26.
3. Pasqualini JR, Katzenellenbogen BS. Hormone-Dependent Cancer. New York: Marcel Dekker, 1996.
4. Read LD, Katzenellenbogen BS. Characterization and regulation of estrogen and progesterone receptors in breast cancer. In: Dickson RB, Lippman ME, eds. Genes, Oncogenes, and Hormones: Advances in Cellular and Molecular Biology of Breast Cancer. Boston: Kluwer Academic Publishers, 1991; 277-299.
5. Chang JCN, A Review of Breast Cancer Chemoprevention. *Biomedicine & Pharmacotherapy* 1998; 52:133-136.
6. Jordan VC, Morrow M. Should clinicians be concerned about the carcinogenic potential of tamoxifen? *Eur. J. Cancer* 1994; 30A:1714-1721.
7. Katzenellenbogen BS. Antiestrogen resistance: Mechanisms by which breast cancer cells undermine the effectiveness of endocrine therapy. *J. Natl. Cancer Inst.* 1991; 83:1434-1435.
8. Davidson NE. Hormone-replacement therapy—breast versus heart versus bone. *N. Engl. J. Med.* 1995; 332:1638-1639.
9. Nique F, Van de Velde P, Bremaud J, Hardy M, Philibert D, Teutsch G. 11 β -Amidoalkoxyphenyl estradiols, a new series of pure antiestrogens. *J. Steroid Biochem. Molec. Biol.* 1994; 50:21-29.
10. Nicholson RI, Gee JMW, Francis AB, Manning DL, Wakeling AE, Katzenellenbogen BS. Observations arising from the use of pure antioestrogens on oestrogen-responsive (MCF-7) and oestrogen growth-independent (K3) human breast cancer cells. *Endocrine Related Cancer* 1995; 2:1-7.
11. Wakeling AE, Bowler J. Biology and mode of action of pure antiestrogens. *J Steroid Biochem* 1988; 30:141-147.
12. Wakeling AE, Dukes M, Bowler J. A potent specific pure antiestrogen with clinical potential. *Cancer Res* 1991; 51:3867-3873.
13. Osborne CK, Coronado-Heinsohn EB, Hilsenbeck SG, McCue BL, Wakeling AE, McClelland RA, Manning DL, Nicholson RI. Comparison of the effects of a pure steroidal antiestrogen with those of tamoxifen in a model of human breast cancer. *J. Natl. Cancer Inst.* 1995; 87:746-750.
14. Howell A, DeFriend D, Robertson J, Blamey R, Walton P. Response to a specific antiestrogen (ICI 182780) in tamoxifen-resistant breast cancer. *Lancet* 1995; 345:29-30.

15. Katzenellenbogen BS. Estrogen receptors: Bioactivities and interactions with cell signaling pathways. *Biol. Reprod.* 1996; 54:287-293.
16. Katzenellenbogen JA, O'Malley BW, Katzenellenbogen BS. Tripartite steroid hormone receptor pharmacology: Interaction with multiple effector sites as a basis for the cell- and promoter-specific action of these hormones. *Mol. Endocrinol.* 1996; 10:119-131.
17. Montano MM, Ekena KE, Krueger KD, Keller AL, Katzenellenbogen BS. Human estrogen receptor ligand activity inversion mutants: Receptors that interpret antiestrogens as estrogens and estrogens as antiestrogens and discriminate among different antiestrogens. *Mol. Endocrinol.* 1996; 10:230-242.
18. Montano MM, Müller V, Trobaugh A, Katzenellenbogen BS. The carboxy-terminal F domain of the human estrogen receptor: Role in the transcriptional activity of the receptor and the effectiveness of antiestrogens as estrogen antagonists. *Mol Endocrinol* 1995; 9:814-825.
19. Tzukerman MT, Esty A, Santiso-Mere D, Danielian P, Parker MG, Stein RB, Pike JW, McDonnell DP. Human estrogen receptor transactivational capacity is determined by both cellular and promoter context and mediated by two functionally distinct intramolecular regions. *Mol Endocrinol* 1994; 8:21-30.
20. Berry M, Metzger D, Chambon P. Role of the two activating domains of the oestrogen receptor in the cell-type and promoter-context dependent agonistic activity of the anti-oestrogen 4-hydroxytamoxifen. *EMBO J.* 1990; 9:2811-2818.
21. McDonnell DP, Clemm DL, Hermann T, Goldman ME, Pike JW. Analysis of estrogen receptor function in vitro reveals three distinct classes of antiestrogens. *Mol Endocrinol* 1995; 9:659-669.
22. Yang NN, Hardikar S, Kim J. Raloxifene, an anti-estrogen, simulates the effects of estrogen on inhibiting bone resorption through regulating TGF β -3 expression in bone. *J. Bone Miner. Res.* 1993; 8 (Suppl 1):S118.
23. Yang NN, Bryant HU, Hardikar S, Sato M, Galvin RJS, Glasebrook AL, Termine JD. Estrogen and raloxifene stimulate transforming growth factor- β 3 gene expression in rat bone: A potential mechanism for estrogen- or raloxifene-mediated bone maintenance. *Endocrinology* 1996; 137:2075-2084.
24. Sato M, Glasebrook AL, Bryant HU. Raloxifene: A selective estrogen receptor modulator. *J Bone Miner Met* 1994; 12 (Suppl 2):S9-S20.
25. Sato M, Rippey MK, Bryant HU. Raloxifene, tamoxifen, nafoxidine, or estrogen effects on reproductive and nonreproductive tissues in ovariectomized rats. *FASEB J.* 1996; 10:905-912.
26. von Angerer E. The Estrogen Receptor as a Target for Rational Drug Design. Austin: R.G. Landes Company, 1995.
27. Gordon EM, Barrett RW, Dower WJ, Fodor SPA, Gallop MA. Applications of combinatorial technologies to drug discovery. 2. Combinatorial organic synthesis, library screening strategies, and future directions. *J. Med. Chem.* 1994; 37:1385-1401.
28. Gallop MA, Barrett RW, Dower WJ, Fodor SPA, Gordon EM. Applications of combinatorial technologies to drug discovery. 1. Background and peptide combinatorial libraries. *J. Med. Chem.* 1994; 37:1233-1251.
29. Geysen HM, Houghten RA, Kauffman S, Lebl M, Moos WH, Pavia MR, Szostak JW. Molecular diversity comes of age! *Molecular Diversity* 1995; 1:2-3.
30. Murphy MM, Schullek JR, Gordon EM, Gallop MA. Combinatorial organic synthesis of highly functionalized pyrrolidines: Identification of a potent angiotensin converting enzyme inhibitor from a mercaptoacyl proline library. *J. Am. Chem. Soc.* 1995; 117:7029-7030.
31. Terrett NK, Bojanic D, Brown D, Bungay PJ, Gardner M, Gordon DW, Mayers CJ, Steele J. The combinatorial synthesis of a 30,752-compound library: Discovery of SAR around the endothelin antagonist, FR-139,317. *Bioorg. Med. Chem. Lett.* 1995; 5:917-922.
32. Booramra CG, Burow KM, Ellman JA. An expedient and high-yielding method for the solid-phase synthesis of diverse 1,4-benzodiazepine-2,5-diones. *J. Org. Chem.* 1995; 60:5742-5743.

33. Goff DA, Zuckermann RN. Solid-phase synthesis of defined 1,4-benzodiazepine-2,5-dione mixtures. *J. Org. Chem.* 1995; 60:5744-5745.
34. Plunkett MJ, Ellman JA. Solid-phase synthesis of structurally diverse 1,4-benzodiazepine derivatives using the Stille coupling reaction. *J. Am. Chem. Soc.* 1995; 117:3306-3307.
35. DeWitt SH, Kiely JS, Stankovic CJ, Schroeder MC, Cody DMR, Pavia MR. "Diversomers": An approach to nonpeptide, nonoligomeric chemical diversity. *Proc. Natl. Acad. Sci. U.S.A.* 1993; 90:6909-6913.

Publications, Patents, Meeting Abstracts, and Personnel Supported

Publications:

- Publication No. 1:** B. E. Fink, D. S. Mortensen, S. R. Stauffer, Z. D. Aron, J. A. Katzenellenbogen. Novel Structural Templates for Estrogen-Receptor Ligands and Prospects for Combinatorial Synthesis of Estrogens. *Chem. & Biol.*, 1999, 6, 205-219.
- Publication No. 2:** S. R. Stauffer, J. Sun, B. S. Katzenellenbogen, J. A. Katzenellenbogen. Acyclic Amides as Estrogen Receptor Ligands: Synthesis, Binding, Activity, and Receptor Interaction. *Bio. Med. Chem.*, 2000, 8, 1293-1316.
- Publication No. 3:** S. R. Stauffer, J. A. Katzenellenbogen. Solid-Phase Synthesis of Tetra-Substituted Pyrazoles, Novel Ligands for the Estrogen Receptor. *J. Comb. Chem.*, 2000, 2, 318-329.
- Publication No. 4:** S. R. Stauffer, C. J. Coletta, J. Sun, B. S. Katzenellenbogen, J. A. Katzenellenbogen. Pyrazole Ligands: Structure-Affinity/Activity Relationships of Estrogen Receptor- α Selective Agonists. *J. Med. Chem.*, 1999, submitted.
- Publication No. 5:** S. R. Stauffer, Y. Huang, C. J. Coletta, R. Tedesco, J. A. Katzenellenbogen. Estrogen Pyrazoles: Defining the Pyrazole Core Structure and the Orientation of Substituents in the Ligand Binding Pocket of the Estrogen Receptor. *Bio. Med. Chem.*, 2000, in press.
- Publication No. 6:** S. R. Stauffer, Y. R. Huang, Z. D. Aron, C. J. Coletta, J. Sun, B. S. Katzenellenbogen, J. A. Katzenellenbogen. Triarylpyrazoles with Basic Side Chains: Development of Pyrazole-Based Estrogen Receptor Antagonists. *Bio. Med. Chem.*, 2000, in press.
- Publication No. 7:** Y. R. Huang, J. A. Katzenellenbogen. Regioselective Synthesis of 1,3,5-Triaryl-4-alkylpyrazoles: Novel Ligands for the Estrogen Receptor. *Org. Lett.*, 2000, in press.

Patents:

PCT Patent Application No. PCT/US99/22747 "Estrogen Receptor Ligands", October 1, 1999.

U. S. Patent Application No. US/09/483,233 "Selective Estrogens and Antiestrogens", January 14, 2000.

Meeting Abstracts:

S. R. Stauffer and J. A. Katzenellenbogen. Conformationally Biased s-cis Anilidoamides as Novel Ligands for the Estrogen Receptor. 216th National Meeting of the American Chemical Society, Boston, August 23-27, **1998**.

D. Mortensen and J. A. Katzenellenbogen, Novel Heterocyclic Ligands for the Estrogen Receptor. 219th ACS National Meeting, San Francisco, CA, March, **2000**.

J. A. Katzenellenbogen, Estrogen Receptor Ligands: Design and Dynamics. Frontiers in Estrogen Action, April, Manalapan, FL, April **2000**.

S. R. Stauffer, K. E. Carlson, J. A. Katzenellenbogen. Solid Phase Synthesis and Relative Binding Affinity Assessment of a Tetrasubstituted Pyrazole Library, Novel Ligands for the Estrogen Receptor. 6th Annual Conference and Exhibition "Screening in the New Millennium". Vancouver, British Columbia, Canada, September 6-9, **2000**.

D. S. Mortensen, B. F. Fink, S. R. Stauffer, Y. Huang, J. Sun, B. S. Katzenellenbogen, J. A. Katzenellenbogen, Heterocyclic Non-Steroidal Ligands for the Estrogen Receptor with Very High Receptor Subtype Specificity. ICE 2000, Sydney, Australia, October 29-November 3, **2000**.

J. A. Katzenellenbogen and S R., Stauffer, Design and Combinatorial Synthesis of Novel Heterocyclic Antiestrogens. Era of Hope, Department of Defense Breast Cancer Research Program Meeting. Atlanta, GA, June 8-11, **2000**.

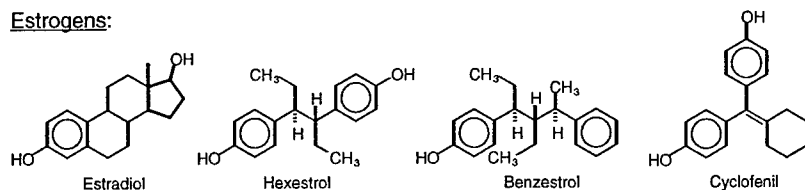
Personnel Supported:

Shaun R. Stauffer

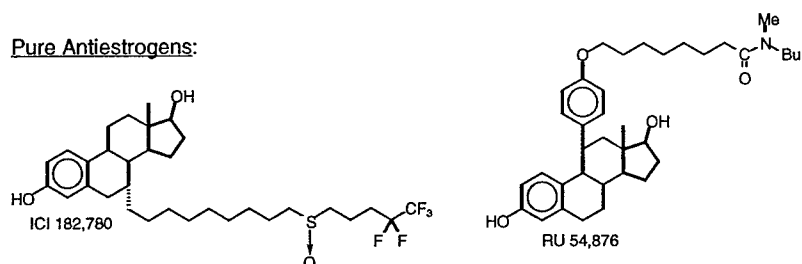
Ying R. Huang

Scheme 1. Estrogens, Pure Antiestrogens, and Selective Antiestrogens – From the Original Proposal

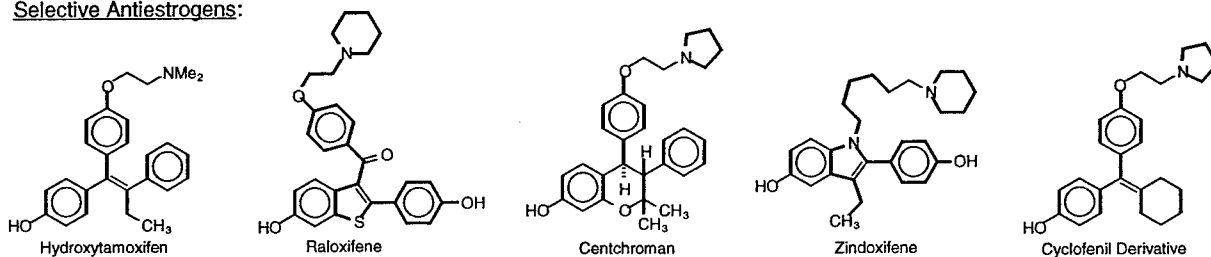
Estrogens:



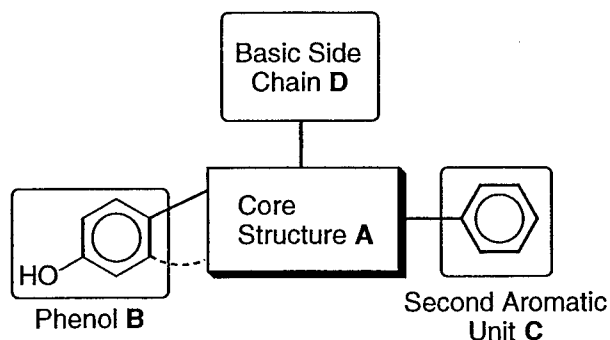
Pure Antiestrogens:



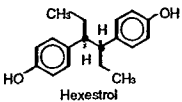
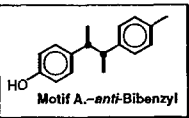
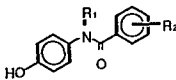
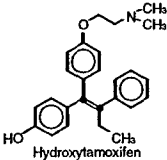
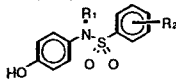
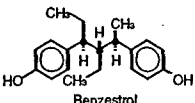
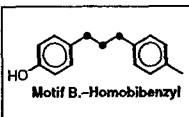

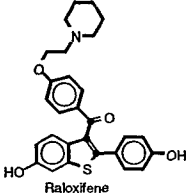
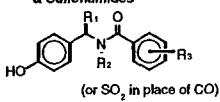
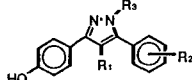
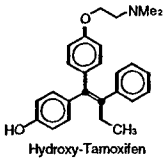
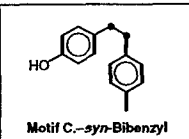
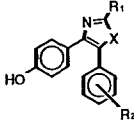
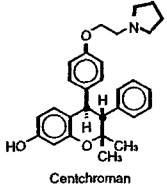
Selective Antiestrogens:



Scheme 2. Structural Components of Selective Antiestrogens – From the Original Proposal



Scheme 3. Structural Motifs for Estrogen Receptor Ligands
and Their Combinatorial Analogs – From the Original Proposal

| Estrogen Receptor Ligand | Structural Motif | Combinatorial Analog (Class) |
|--|--|---|
|  Hexestrol |  Motif A, <i>anti</i> -Bibenzyl | I. Diphenyl Carboxamides  |
|  Hydroxytamoxifen | | II. Diphenyl Sulfonamides  |
|  Benzestrol |  Motif B, <i>Homobibenzyl</i> | III. Phenyl Benzylcarboxamides & Sulfonamides  (or SO ₂ in place of CO) |
|  Raloxifene | | IV. Benzyl Phenylcarboxamides & Sulfonamides  (or SO ₂ in place of CO) |
| | | V. Pyrazoles  |
|  Hydroxy-Tamoxifen |  Motif C, <i>syn</i> -Bibenzyl | VI. Oxazoles, Thiazoles, and Imidazoles  (X = O, S, NR) |
|  Centchroman | | |

Novel structural templates for estrogen-receptor ligands and prospects for combinatorial synthesis of estrogens

Brian E Fink, Deborah S Mortensen, Shaun R Stauffer, Zachary D Aron and John A Katzenellenbogen

Introduction: The development of estrogen pharmaceutical agents with appropriate tissue-selectivity profiles has not yet benefited substantially from the application of combinatorial synthetic approaches to the preparation of structural classes that are known to be ligands for the estrogen receptor (ER). We have developed an estrogen pharmacophore that consists of a simple heterocyclic core scaffold, amenable to construction by combinatorial methods, onto which are appended 3–4 peripheral substituents that embody substructural motifs commonly found in nonsteroidal estrogens. The issue addressed here is whether these heterocyclic core structures can be used to prepare ligands with good affinity for the ER.

Results: We prepared representative members of various azole core structures. Although members of the imidazole, thiazole or isoxazole classes generally have weak binding for the ER, several members of the pyrazole class show good binding affinity. The high-affinity pyrazoles bear close conformational relationship to the nonsteroidal ligand raloxifene, and they can be fitted into the ligand-binding pocket of the ER–raloxifene X-ray structure.

Conclusions: Compounds such as these pyrazoles, which are novel ER ligands, are well suited for combinatorial synthesis using solid-phase methods.

Address: Department of Chemistry, University of Illinois, 600 S. Mathews Avenue, Urbana, IL 61801, USA.

Correspondence: John A Katzenellenbogen
E-mail: jkatzene@uiuc.edu

Key words: arylpyrazoles, combinatorial chemistry, estrogen receptor, estrogen ligands, nonsteroidal estrogens

Received: 16 November 1998
Revisions requested: 15 December 1998
Revisions received: 20 January 1999
Accepted: 28 January 1999

Published: 18 March 1999

Chemistry & Biology April 1999, 6:205–219
<http://biomednet.com/elecref/1074552100600205>

© Elsevier Science Ltd ISSN 1074-5521

Introduction

Estrogens are endocrine regulators of the vertebrate reproductive system that have important effects in many non-reproductive tissues as well (bone, liver, cardiovascular system, CNS and so on). Many estrogen pharmaceuticals, based on both natural and synthetic substances, have been developed as agents for regulating fertility, preventing and controlling hormone-responsive breast cancer, and menopausal hormone replacement. These substances display a spectrum of agonist to antagonist activity that can show remarkable tissue and cell selectivity [1].

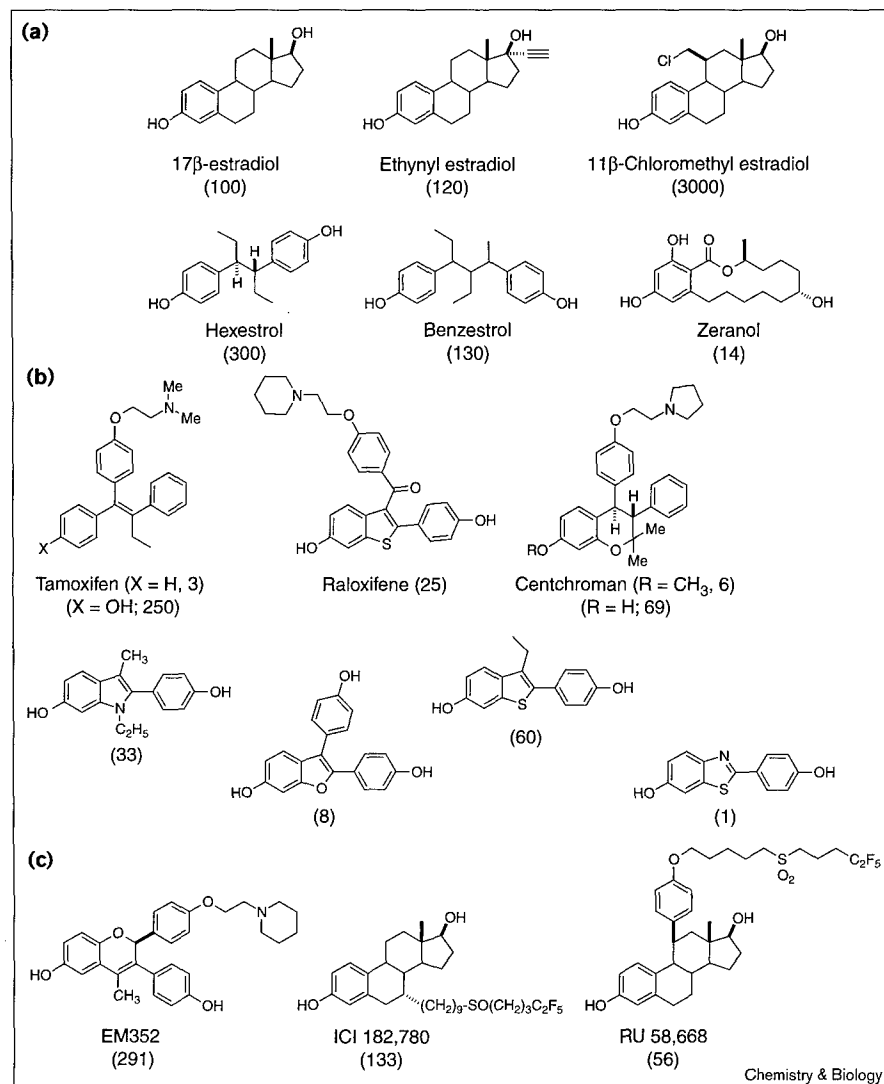
The molecular target of estrogens is the estrogen receptor (ER), of which there are now known to be two subtypes, ER- α and ER- β , that have different patterns of tissue expression and somewhat different ligand-binding specificities [2,3]. ER is a transcription factor that binds to specific estrogen-response elements in the promoter region of estrogen-regulated genes and whose activity is modulated by the estrogen ligands [4]. The capacity of ER–ligand complexes to activate gene transcription is mediated by a series of co-regulator proteins [5]. These co-regulators have interaction functions that tether ER to the RNA polymerase II preinitiation complex and enzymatic activities to modify chromatin structure [6]. It is the fact that each cell and each gene presents to an ER(subtype)–ligand complex a unique combination of these effector components—various estrogen-response elements and

co-regulators—that appears to underlie, in part, the cell and gene selectivity of various estrogens [7].

Among known ligands for ER, the natural estrogens are the simplest of the steroidal hormones, distinguished by their phenolic A-ring (Figure 1). Synthetic estrogens, especially those of nonsteroidal nature, generally retain a phenolic function (at least for those of high potency), but otherwise span a remarkable range of structural motifs that encompass simple acyclic core structures of various lengths and sizes, as well as a variety of ring-size fused and nonfused carbocyclic and heterocyclic systems [8–10]. It is clear from many decades of medicinal-chemistry investigations that minor changes in the structure and stereochemistry of these ligands can have profound effects on both their affinity and their biocharacter (i.e. the agonist versus antagonist balance in various tissues). Major efforts have been directed at optimizing ER ligand structure to obtain desired profiles of tissue selectivity, but, even so, the ideal profile for various uses has not yet been achieved [1,11,12].

As currently explored, ER ligands are, by and large, not well suited for synthesis using combinatorial approaches, because their preparation generally involves a series of carbon–carbon bond forming reactions that do not give uniformly high yields, nor are they well adapted to solid-phase-synthesis methods. There are two examples of the preparation of estrogen combinatorial libraries on solid

Figure 1



Examples of ligands with high affinity for the estrogen receptor. In each case, the binding affinity relative to that of estradiol (100%) is given in parentheses. The compounds are grouped according to their activity in a standard rat uterine weight gain assay as (a) agonists, (b) mixed or selective agonist/antagonists or (c) pure antagonists.

phase, both involving stilbene-like structures [13,14], but the application of combinatorial approaches for the preparation of ER ligands has, so far, been limited.

To expand possible combinatorial approaches to the synthesis of ER ligands, we have begun investigating simple structural motifs that might be used for the construction of molecules with high affinity for ER. The goal was to identify core structures that could be readily prepared by the types of simple condensation reactions that typify those used in solid-phase combinatorial approaches for the preparation of drug-like molecules, and from these to select ones that would support the development of high-affinity ligands for ER.

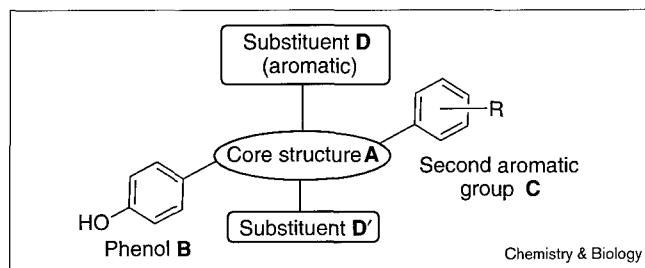
Here, we describe the investigation of prototype 1,2- and 1,3-azole systems as potential ligands for the ER. We examine the issue of whether ER ligands can be considered

simply as an assembly of a phenol unit together with 2–3 auxiliary peripheral groups linked together by a functionally inert core scaffold, or whether the core scaffold itself plays an integral role in ligand binding. In the process, we have discovered a new class of high-affinity ligands for ER, 4-alkyl-1,3,5-triarylpyrazoles, that bear an unexpected topological resemblance to the nonsteroidal estrogen raloxifene and show an interesting structure-binding affinity pattern.

Results and discussion

Structural motifs found in estrogen-receptor ligands and proposed heterocyclic surrogates

Selected examples of nonsteroidal ligands for the estrogen receptor are shown in Figure 1, together with an indication of their ER-binding affinity and their agonist (Ag) versus antagonist (Antag) character in a standard rat uterine weight gain assay. Collectively, these molecules exemplify a recognizable structural gestalt (Figure 2): a core structure (A) onto

Figure 2

Estrogen ligand pharmacophore model.

which are attached other, peripheral structural elements, a phenolic unit (B) that is always preserved, a second aromatic group (C) that is usually present, and another substituent (D) or two (D'), one of which might be aromatic. In the case of ER antagonists or mixed agonist/antagonists, one of the substituents generally contains a basic or polar function.

Comparisons of the various specific manifestations of this basic structure (Figure 1) suggest that, to achieve high

ER-binding affinity, the peripheral substituents (B–D') need to be displayed in a certain geometric arrangement, so that they will be 'in register' with their corresponding subsites in the ligand-binding pocket in ER. It seems that this peripheral group 'display function' can be accomplished by using core elements that encompass a considerable structural variety. This raises the interesting question of whether the core element itself plays any direct role in ER binding or whether it serves merely as an inert molecular scaffold whose function is simply to display these peripheral elements with appropriate topology. If the latter is true, it should be possible to replace the core scaffold with a variety of other units, providing they also are able to display the peripheral elements with the appropriate geometry. Some of these core scaffolds, namely small-ring heterocycles, could be assembled by facile condensation reactions from simpler components, a situation that is favorable for the development of large chemical libraries of related compounds by combinatorial synthesis approaches.

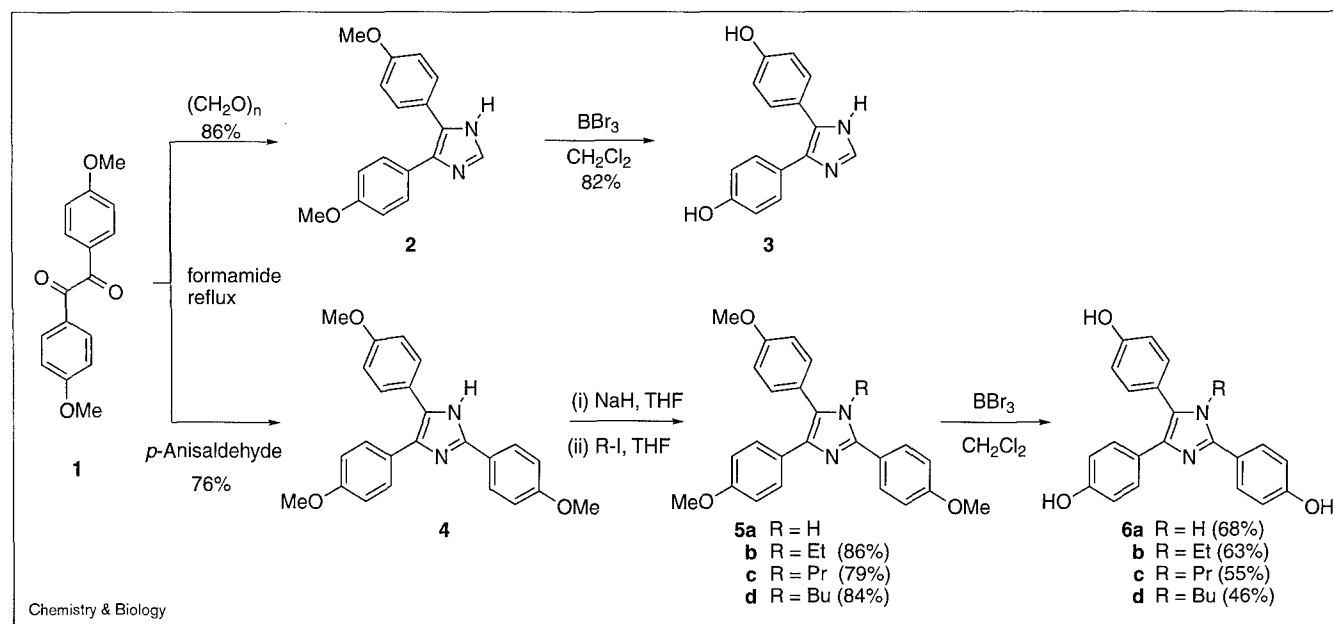
In Table 1 we have outlined two (out of many possible) manifestations of this conceptual approach, based on the incorporation of certain substructural motifs into 1,2- and

Table 1**Structural motifs found in ER ligands and proposed surrogates.**

| Estrogen-receptor ligand | Structural motif | Combinatorial analog (class) |
|--------------------------|----------------------------|--|
| Benzestrol | Motif A. Homobibenzyl* | 3,5-Diaryl pyrazoles |
| Raloxifene | Motif B. Bibenzyl* | 3,5-Diaryl isoxazoles |
| Hydroxytamoxifen | | 2,4-Diaryl imidazoles, thiazoles, oxazoles |
| | | 4,5-Diaryl imidazoles, oxazoles, thiazoles |

*These structural motifs are meant to highlight alternative atom connections between the phenol and a second aromatic substituent, without specific consideration of conformational factors. Structural motifs found in ER ligands and proposed surrogates.

Figure 3

Synthesis of imidazoles **3** and **6a-d**.

1,3-azole systems. Here, the homobibenzyl motif A, exemplified in the nonsteroidal ligands benzestrol and raloxifene, is represented in various 3,5-diaryl-1,2-azoles (pyrazoles and isoxazoles) and 2,4-diaryl-1,3-azoles (imidazoles, thiazoles and oxazoles). Similarly, the bibenzyl motif B is represented in various 4,5-diaryl-1,3-azoles. In each case, the diazole N,N-systems (namely pyrazoles and imidazoles) can accommodate up to four peripheral substituents, whereas the N,O- and N,S-heterocycles (oxazoles, isoxazoles and thiazoles) are limited to three substituents.

Synthesis of representative diaryl and triaryl 1,2- and 1,3-azoles as potential ligands for the estrogen receptor

Imidazoles

The synthesis of representative symmetrical members of the imidazole class and their N-alkyl analogs was accomplished by a well-precedented approach [15] shown in Figure 3. Refluxing 4,4'-dimethoxybenzil (**1**) in formamide in the presence of *para*-formaldehyde afforded the 4,5-disubstituted imidazole **2** [16], which upon deprotection with BBr_3 in CH_2Cl_2 afforded imidazole **3** in good yield. A similar reaction using 4-methoxybenzaldehyde afforded the 2,4,5-tri-substituted imidazole **4** [17–19] in good yield. To prepare tetra-substituted systems, the sodium salt of imidazole **4** was alkylated with ethyl, propyl and butyl iodide, and then deprotected to afford free phenols **6a-d**.

Two additional, unsymmetrical, imidazoles were synthesized as outlined in Figure 4. The top reaction sequence illustrates the synthetic approach to N-ethyl imidazole **12**. Reaction of 4-methoxy-deoxybenzoin (**7**) [20] with bromine

Figure 4

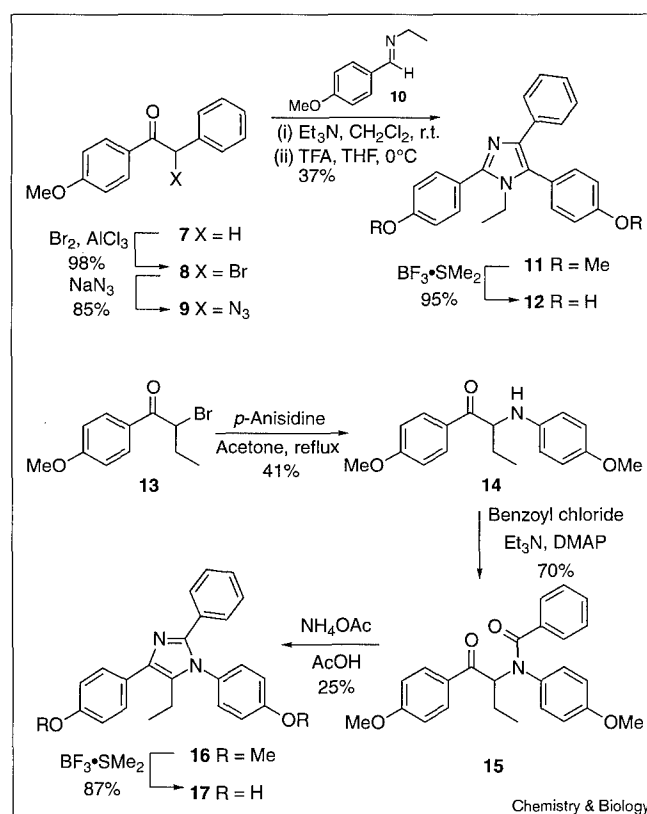
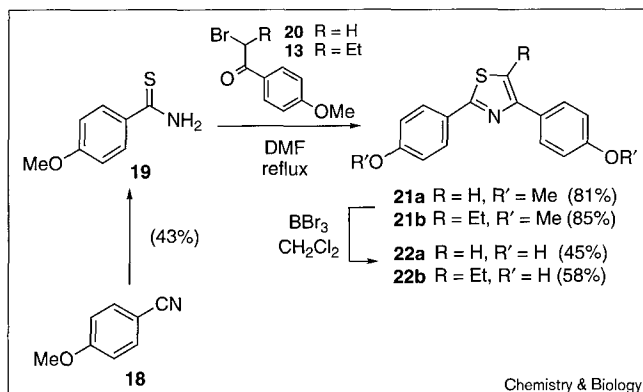
Synthesis of imidazoles **12** and **17**.

Figure 5

Synthesis of thiazoles **22a** and **22b**.

and a trace of AlCl_3 in Et_2O gave α -bromoketone **8** [21], which, upon reaction with sodium azide in acetone, afforded the corresponding azide **9**. The azido-ketone **9** was treated with one equivalent of Et_3N and imine **10** in tetrahydrofuran (THF). Removal of solvent and excess Et_3N followed by treatment of the crude intermediate 2,5-dihydro-2-hydroxyimidazole with TFA in CH_2Cl_2 , according to the procedure of Patonay and Hoffman [22], resulted in the formation of *N*-ethyl imidazole **11**. Deprotection with $\text{BF}_3 \cdot \text{SMe}_2$ in CH_2Cl_2 produced imidazole **12** in good yield.

The synthesis of *N*-aryl substituted imidazole **17** is also shown in Figure 4. Refluxing 4'-methoxy- α -bromobutyrophenone (**13**) with *p*-anisidine in acetone gave the α -amino-ketone **14**, which was converted into the benzamide **15** upon reaction with benzoyl chloride and base. Cyclization with ammonium acetate in refluxing acetic acid afforded the 1,2,4,5 tetra-substituted imidazole **16**, which upon deprotection with $\text{BF}_3 \cdot \text{SMe}_2$ in CH_2Cl_2 produced the free phenol **17**.

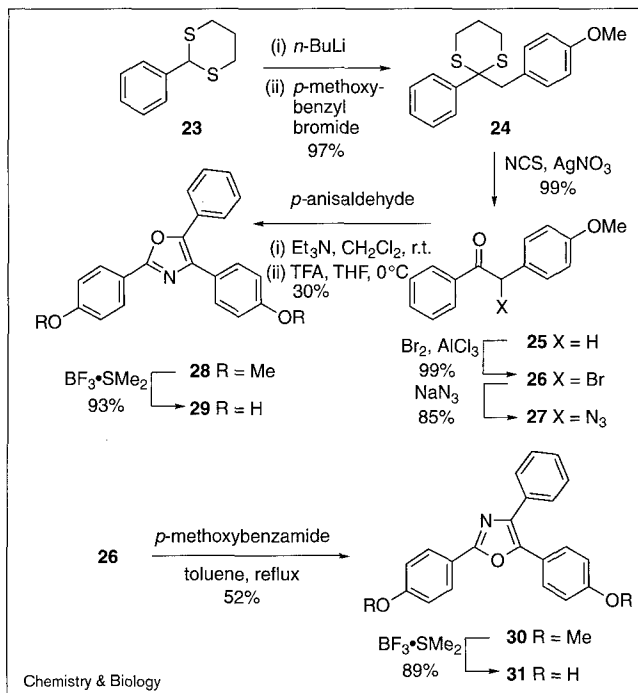
Thiazoles

The synthesis of representative thiazoles is shown in Figure 5. Thioamide **19**, derived from 4-methoxybenzothioamide (**18**) [23], was condensed with 4'-methoxy- α -bromoacetophenone (**20**) or 4'-methoxy- α -bromobutyrophenone (**13**) in refluxing DMF to give high yields of the 2,4-disubstituted thiazole **21a** [24] or 2,4,5-trisubstituted thiazole **21b**, respectively. Deprotection with BBr_3 afforded moderate yields of the free phenols **22a** and **22b**.

Oxazoles

Two representative oxazoles were synthesized as shown in Figure 6. Reaction of the lithium anion of dithiane **23** with *p*-methoxybenzyl bromide gave the alkylated product **24**, which upon hydrolysis afforded 4'-methoxy-deoxybenzoin (**25**) [25] in excellent yield. Conversion to the

Figure 6

Synthesis of oxazoles **29** and **31**.

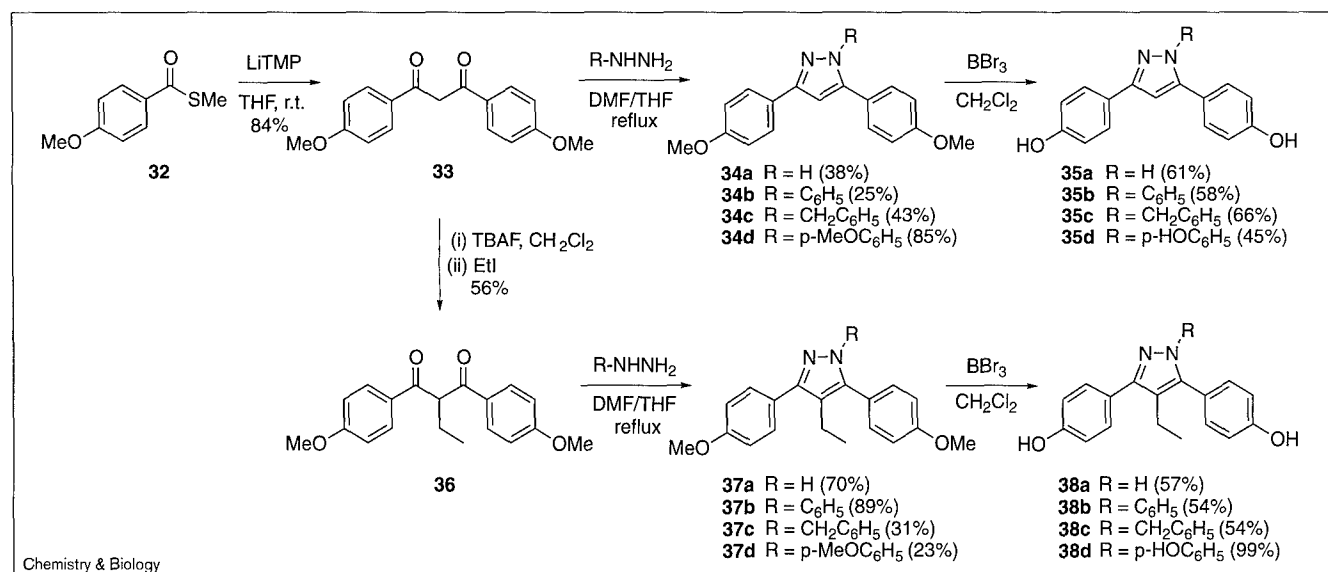
bromide **26** [26] and azide **27** was accomplished as described for analogous compounds **8** and **9** above. The azido-ketone **27** was then treated with one equivalent of Et_3N and *p*-anisaldehyde, and then with TFA to afford oxazole **28** [27]. Oxazole **30** resulted from the condensation of bromo-ketone **26** with *p*-methoxybenzamide in refluxing toluene, analogous to the thiazole synthesis discussed above. Deprotection of **28** and **30** with $\text{BF}_3 \cdot \text{SMe}_2$ gave oxazoles **29** and **31**, respectively.

Pyrazoles

The synthesis of the pyrazoles involves the condensation of a hydrazine with a 1,3-diketone [28]. Using the method of Beak and coworkers [29], we obtained 1,3-diketone **33** from the reaction of the methyl thioester **32** and lithium tetramethylpiperidide in good yield (Figure 7). Condensation of the diketone with hydrazine hydrochloride or *N*-substituted hydrazine hydrochlorides in refluxing DMF/THF (3:1) afforded the 3,5-disubstituted pyrazole **34a** or 1,3,5-trisubstituted pyrazoles **34b-d**; yields were higher with aryl-substituted hydrazines than with hydrazine itself. Deprotection of **34a-d** with BBr_3 afforded the free phenols **35a-d** in moderate yield.

The introduction of a 4-alkyl substituent was accomplished through the alkylation of diketone **33** with TBAF and ethyl iodide to afford **36** in moderate yield [30,31]. Attempts to increase the yield of this alkylation were

Figure 7

Synthesis of pyrazoles **35a-d** and **38a-d**.

unsuccessful. Conversion of diketone **36** to the corresponding pyrazoles was accomplished as with the unsubstituted case, to afford pyrazoles **38a-d**.

Isoxazoles

The preparation of a single isoxazole is shown in Figure 8 [32]. Double deprotonation of the ketoxime **39** derived from 4-methoxyacetophenone with *n*BuLi, followed by addition of methyl 4-methoxybenzoate afforded the 3,5-disubstituted isoxazole **40** in low yield [33]. Deprotection with BBr₃ afforded the free phenol **41** in moderate yield [34].

Estrogen-receptor binding

The binding affinities of the heterocycles prepared above for the estrogen receptor are shown in Tables 2-4, organized according to heterocyclic core structure. The binding values were obtained from a competitive radiometric binding assay, using [³H]estradiol as the tracer, dextran-coated charcoal

to adsorb free tracer and lamb uterine cytosol as a source of ER. The values are expressed as relative binding affinities (RBA), with estradiol having an affinity of 100% [35]. In replicate assays, these values are reproducible with a coefficient of variation of 30% (K.E. Carlson and J.A.K., unpublished observations).

Imidazoles, oxazoles and thiazoles

The receptor-binding data for the imidazole series are shown in Table 2. Although the members of this series have rather low affinity, there is an increase in RBA with the addition of alkyl substituents at the 1-position (**3**, **6a-d**); this trend reaches a maximum for propyl **6c**, reversing for the butyl substituent **6d**. Such trends, where affinity

Figure 8

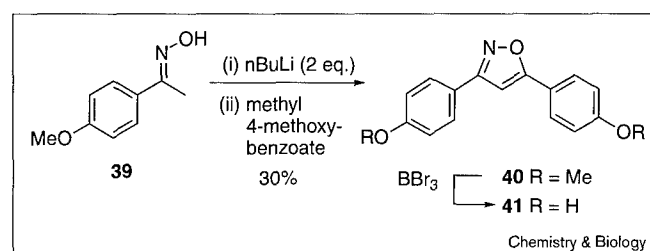
Synthesis of isoxazole **41**.

Table 2

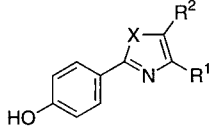
Estrogen receptor binding data for imidazoles **3**, **6a-d**, **12** and **17**.

| Compound | | | | | RBA* |
|-----------|-------------------------------------|-------------------------------------|-------------------------------------|-------------------------------------|--------|
| | R ¹ | R ² | R ³ | R ⁴ | |
| 3 | 4'-HO-C ₆ H ₄ | 4'-HO-C ₆ H ₄ | H | H | <0.001 |
| 6a | 4'-HO-C ₆ H ₄ | 4'-HO-C ₆ H ₄ | H | 4'-HO-C ₆ H ₄ | 0.007 |
| 6b | 4'-HO-C ₆ H ₄ | 4'-HO-C ₆ H ₄ | C ₂ H ₅ | 4'-HO-C ₆ H ₄ | 0.38 |
| 6c | 4'-HO-C ₆ H ₄ | 4'-HO-C ₆ H ₄ | C ₃ H ₇ | 4'-HO-C ₆ H ₄ | 0.62 |
| 6d | 4'-HO-C ₆ H ₄ | 4'-HO-C ₆ H ₄ | C ₄ H ₉ | 4'-HO-C ₆ H ₄ | 0.17 |
| 12 | C ₆ H ₅ | 4'-HO-C ₆ H ₄ | C ₂ H ₅ | 4'-HO-C ₆ H ₄ | 0.25 |
| 17 | 4'-HO-C ₆ H ₄ | C ₂ H ₅ | 4'-HO-C ₆ H ₄ | C ₆ H ₅ | 0.37 |

*RBA, relative binding affinity (estradiol = 100%).

Table 3

Estrogen receptor binding data for thiazoles **22a**, **22b** and oxazoles **29** and **31**.

|  | | | | |
|---|---|-------------------------------------|-------------------------------------|--------|
| Compound | X | R ¹ | R ² | RBA |
| 22a | S | 4'-HO-C ₆ H ₄ | H | 0.018 |
| 22b | S | 4'-HO-C ₆ H ₄ | C ₂ H ₅ | 0.041 |
| 29 | O | 4'-HO-C ₆ H ₄ | C ₆ H ₅ | <0.001 |
| 31 | O | C ₆ H ₅ | 4'-HO-C ₆ H ₄ | 0.027 |

increases with substituent size up to a point, are well known both in steroidal systems (11 β - and 16 α -substituents) [36] and in other non-steroidal ligand series (such as 2-phenylindoles [37], tetrahydrochrysenes [38] and so on), and probably represent the filling of preformed pockets of limited volume in the receptor by these substituents [37]. The principal difference in binding, however, is between the tetra-substituted imidazoles (**6b-d**, **12** and **17**) and the di- or tri-substituted imidazole (**3** and **6a**), the tetra-substituted ones having much higher affinity. There is little difference in binding between imidazoles **12** and **17**, which have a different arrangement of nitrogen atoms in the heterocyclic core but display their four substituents in an identical fashion (Figure 9). The overall low binding affinity of the imidazoles as a class might be the result of the high inherent polarity of this heterocyclic system as compared with the pyrazoles, reflected by their higher chromatographic polarity in both normal and reversed phases systems. It is also of note that the dipole moment for imidazole is very

Table 4

Estrogen receptor binding affinity data for pyrazoles and an isoxazole.

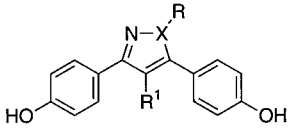
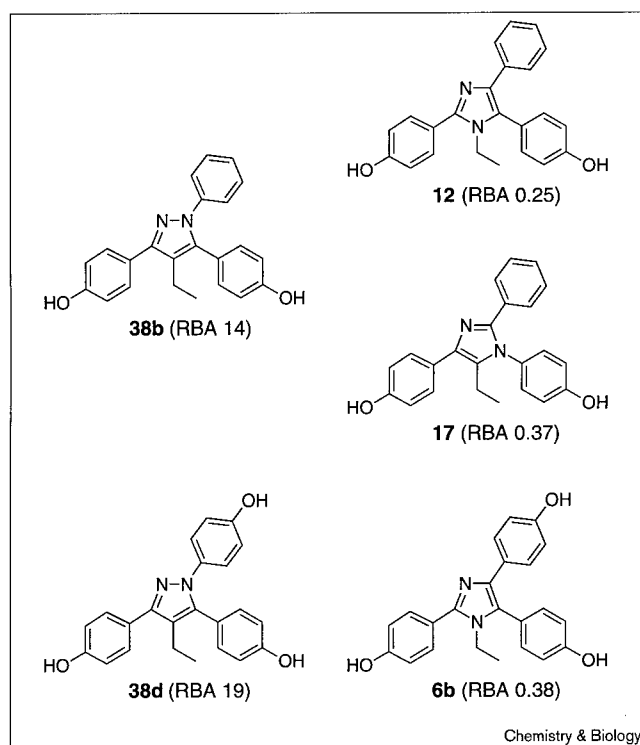
|  | | | | |
|---|---|---|-------------------------------|--------|
| Compound | X | R | R ¹ | RBA |
| 35a | N | H | H | 0.009 |
| 35b | N | C ₆ H ₅ - | H | 0.028 |
| 35c | N | C ₆ H ₅ CH ₂ - | H | <0.007 |
| 35d | N | 4'-HO-C ₆ H ₄ - | H | 0.059 |
| 38a | N | H | C ₂ H ₅ | 0.015 |
| 38b | N | C ₆ H ₅ - | C ₂ H ₅ | 14.0 |
| 38c | N | C ₆ H ₅ CH ₂ - | C ₂ H ₅ | 0.150 |
| 38d | N | 4'-HO-C ₆ H ₄ - | C ₂ H ₅ | 19.0 |
| 41 | O | - | C ₂ H ₅ | 0.006 |

Figure 9



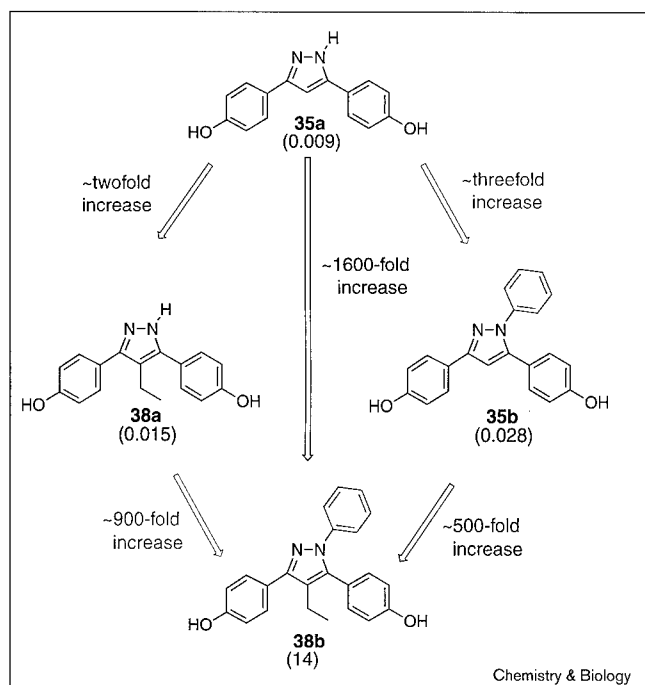
Comparisons between ring pyrazoles (**38b**, **38d**) and imidazoles (**6b**, **12** and **17**).

large, 5.56 D [39], and this might be unfavorable for binding to the estrogen receptor.

Table 3 shows the binding data for the two thiazoles and oxazoles. Although affinities are again very low, the more highly substituted thiazole again has the higher affinity (**22a** compared with **22b**). The oxazole **29** has undetectable affinity for ER. The isomer **31**, however, does have measurable, albeit low, binding. In contrast to imidazoles, thiazoles and oxazoles do not have very high dipole moments [39]; so overall polarity is not likely to be the cause of their low ER binding affinity, although heteroatom orientation appears to play a role (**29** compared with **31**). In the imidazole series, the compounds with the highest affinities were all tetra-substituted, however. As it is only possible to tri-substitute a thiazole or oxazole, this core structure might be unable to present sufficient peripheral substituents to afford ligands with good ER binding affinities, at least as far as we have investigated.

The low binding affinities of the imidazoles, thiazoles and oxazoles are disappointing, although not surprising, considering the relatively poor affinity of the most closely related benzothiazole reported by von Angerer [40] (Figure 1). The sparsely substituted monocyclic or polycyclic aromatic systems are also expected to be rather

Figure 10



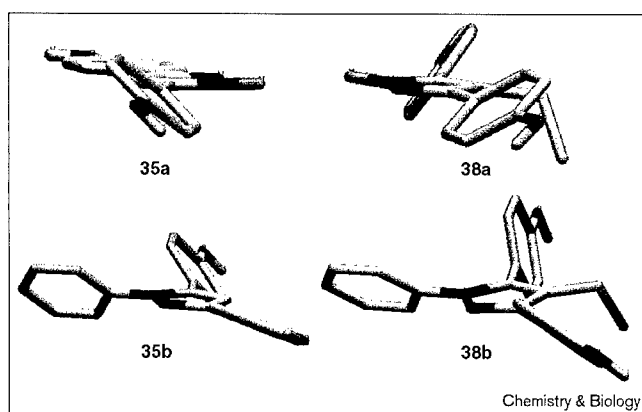
Comparison of the estrogen receptor binding affinity of four related pyrazoles with increasing substitution.

planar. It is generally agreed that good ligands for the estrogen receptor need to have some degree of 'thickness' in the central portion of the ligand [38]. When alkyl substituents are added to either the imidazoles or thiazoles, their RBA increases (Tables 2,3). This increased binding could be due to an increase in steric bulk around the central portion of the molecule, the result, in part, of a twisting of some of the aromatic substituents (see below) or to an increase in lipophilicity. Regardless, the effects are not great, and in general the 1,3-azoles seem to present some special challenges that might best be investigated further by combinatorial approaches.

Pyrazoles and isoxazoles

The RBA data for the 1,2-azoles are presented in Table 4. Immediately apparent is the relatively high binding affinity of pyrazoles **38b** and **38d**. An interesting comparison can be made among compounds **35a**, **35b**, **38a** and **38b** (Figure 10). The disubstituted progenitor **35a** has very low affinity; addition of a third substituent, 1-phenyl in **35b** or 4-ethyl in **38a**, causes only a twofold or threefold increase in binding affinity, respectively. By contrast, addition of the fourth substituent (to give **38b**) causes either an 900- or 500-fold increase in binding affinity, respectively. Clearly, this is not additive behavior—two groups that each alone raise binding affinity twofold and threefold, together raise binding not sixfold but 1600-fold. This suggests that to achieve high binding affinity there needs to be a detailed

Figure 11



Ab initio calculated conformations for **35a**, **35b**, **38a** and **38b**.

and proper match between the peripheral substituents and several subsites on the receptor, and in the azole systems we have explored, it appears that this requires a tetra-substituted ring (see below). Consistent with this is the low affinity of the isoxazole **41**, whose affinity is similar to the most closely related tri-substituted pyrazole **38a**.

There are other interesting trends in the pyrazole series: replacement of the N-phenyl substituent (**38b**) with an N-benzyl group (**38c**) causes a dramatic 100-fold reduction in binding. Both of these compounds are tetra-substituted pyrazoles, and they contain the homobibenzyl motif A that was considered to be an important factor for receptor binding (as do all of the other compounds in Table 1). The decrease in binding affinity in **38b** compared with **38c** again suggests the need for a detailed match between ligand substituents and receptor subsites: the extra 'kink' in the benzyl substituent in **38c** might be repositioning the peripheral substituents in a less favorable geometry. The addition of a hydroxyl group at the *para* position of the N-phenyl substituent (compound **38d** compared with **38b**) causes a minor increase in binding, indicating that polarity is well tolerated in this region of the receptor.

Structural comparisons between high-affinity pyrazole ligands and other nonsteroidal ligands

The conformation of pyrazoles **35a,b** and **38a,b** was determined by *ab initio* calculations at the 3-G21* level (Figure 11). The action of A-strain is evident in these structures: even in the disubstituted system **35a**, the 5-phenyl group is twisted ~60° out of the plane; this twisting increases as the third (**35b**, **38a**) and fourth (**38b**) substituents are added to the pyrazole ring, so that in **38b** the 5-phenyl substituent is nearly perpendicular to the pyrazole core. In this conformation **38b** resembles the general propeller-type conformation of the triarylethylene nonsteroidal estrogens such as tamoxifen [41].

Although the comparison of the conformations of tamoxifen with pyrazole **38b** might give some idea of the reason **38b** binds to ER with high affinity, it does not adequately explain why **35a**, **35b** and **38a** have so much lower binding affinities. When the latter three pyrazoles are compared with **38b**, it is apparent that there is little difference in conformation that could account for the large discrepancy in binding within the series. The reasons for the marked changes in RBA in response to very small changes in structure, noted especially for the pyrazole series, are therefore not intuitively obvious from an examination of the structure of the ligands alone, although they are not entirely unexpected on the basis of the behavior of other nonsteroidal ligands and the detailed fit of these congeners in the ligand-binding pocket of the estrogen receptor (see below).

Analysis of the X-ray structure of the estrogen-receptor ligand-binding domain complexed with estradiol and the nonsteroidal ligand raloxifene

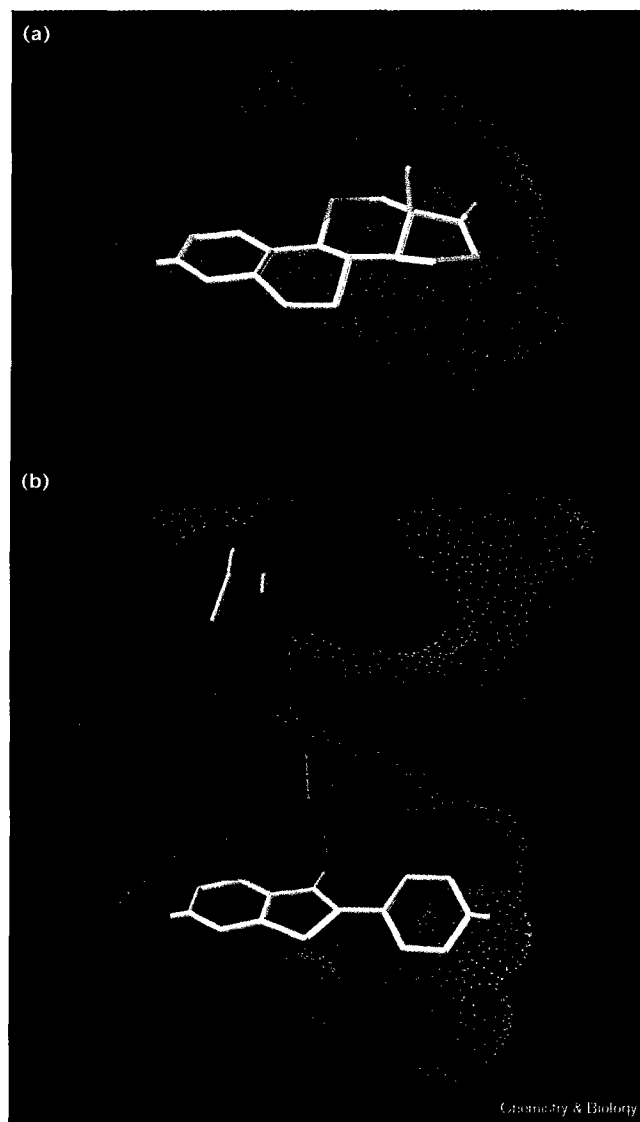
The explanation that was previously proposed — that high-affinity binding to ER derives from a proper match between the peripheral substituents on the ligand and their complementary binding regions on the receptor — can now be considered in some detail, because, recently, the X-ray structures of the estrogen receptor- α bound to estradiol and the nonsteroidal ligand raloxifene have been reported [42].

The ligand-binding pocket in the ER-estradiol structure has a volume of approximately 450 \AA^3 , which is $\sim 200 \text{ \AA}^3$ larger than the volume of estradiol [43] (Figure 12a). As a result, there is a large hydrophobic space around the central portion of the binding pocket, especially in the regions corresponding to the 11β position and, to a lesser degree, 7α position (Figure 12a), which is consistent with the tolerance that ER shows for binding steroids with large substituents at these positions [36]. A view of the ER-raloxifene structure is shown in Figure 12b. The core of this ligand is oriented in the same manner as estradiol and occupies much of the same space in the binding pocket, but the benzoyl substituent projects outward, askew of the ligand core, with the piperidinyl sidechain extending into an upper hydrophobic region, which is much more open due to the displacement of helix 12 [42].

Comparison between raloxifene and the tetra-substituted pyrazole (**38b**)

The structure of the high-affinity pyrazole (**38b**) can be overlayed onto the structure of raloxifene (Figure 13a). In such a superposition, it is evident that the centroids of all three aromatic rings lie quite close to one another. This structural alignment can be used to place the pyrazole **38b** into the ligand-binding pocket of the ER-raloxifene structure (Figure 13b). With a minimal, energetically reasonable rearrangement of nearby residues (see Figure 13 legend), this ligand can fit quite comfortably in the raloxifene pocket (compare Figure 13b with Figure 12b).

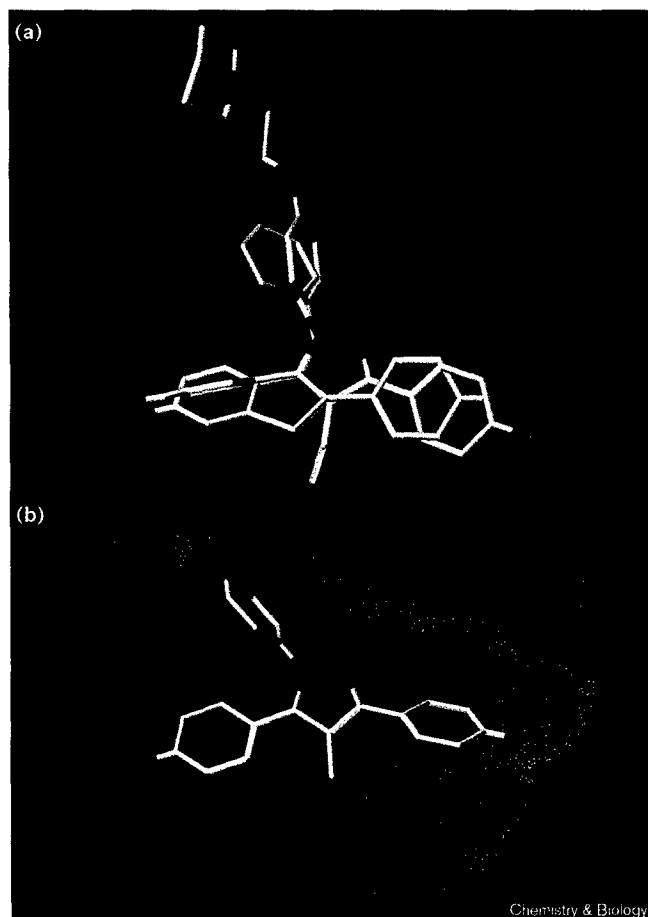
Figure 12



Ligand binding pockets for (a) estradiol and (b) raloxifene. Structures were prepared from the crystallographic coordinates [43] by generating a solvent-accessible surface for the protein (green-blue dot surface) and for the ligand (purple).

In the arrangement shown in Figure 13b, the two hydroxyl groups are positioned in such a manner that they could engage the same protein hydrogen-bonding partners as do the corresponding hydroxyl groups in raloxifene; the 3-(*p*-hydroxyphenyl) substituent of **38b** is mimicking the estradiol A-ring surrogate of raloxifene (i.e. the fused phenol of the benzothiophene unit) and the 5-(*p*-hydroxyphenyl) group of **38b** is mimicking the pendant *p*-hydroxyphenyl group at position 2 of the benzothiophene (compare with Figure 12b). The 1-phenyl group of **38b** overlies the benzoyl arene of raloxifene and projects into channel that exists in roughly the 11β direction in the ER-raloxifene

Figure 13



(a) Overlay of pyrazole **38b** with raloxifene and (b) pyrazole **38b** in the binding pocket of the ER-raloxifene structure. (a) The overlay of the two ligands was obtained by a least-squares multifitting seven atoms in each molecule ($\text{rms}=0.924 \text{ \AA}$): in each of the three benzene rings, the two atoms selected were the ones at the site of attachment and the ones *para* to this site; in addition, the *p*-hydroxy group on the 5-phenyl substituent in pyrazole **38b** was overlaid with the benzothiophene hydroxyl group. (b) Pyrazole **38b** was pre-positioned into the ER-raloxifene crystal structure [42] from the overlay shown in (a). From this structure additional docking studies using FlexiDock (Tripos, St Louis, MO) followed by a three-step minimization using the TRIPOS Forcefield were conducted to afford the final model (see the Materials and methods section). This minimization caused only small changes in the protein and ligand, but reduced the ligand-protein interaction energy to a reasonable level.

structure. The 4-ethyl substituent on pyrazole **38b** projects outwards from the heterocycle from a position that corresponds roughly to the sulfur atom of the benzothiophene ring system, and extends into an open pocket in the ER.

When analyzed in this manner, one can appreciate that the pyrazole core can display these four substituents in a manner congruent with the same regions in the binding pocket of the estrogen receptor that accommodate corresponding portions of raloxifene. In addition, the high cost in binding affinity that results from the absence of

either the 1-phenyl or the 4-ethyl substituent (compare with Figure 10) suggests that proper registration of each of the four peripheral substituents into its appropriate binding subsite is supported by the interaction of the other three. By this analysis, it is therefore not surprising that all of the other heterocyclic systems that were only di-substituted or tri-substituted were low affinity ligands, at least with the substituents we have thus far investigated. The low-affinity of the tetra-substituted imidazoles, however, most likely derives from their high polarity, as noted (see below).

The importance of core structural element in ligand binding: passive or active?

The question raised initially—does the core scaffold in these novel ER ligands play only a passive role in their binding, merely displaying the peripheral substituents in an appropriate topology, or is its role more active or functional?—can be answered reasonably definitively from the results we have obtained so far. Clearly, with the substituents we have examined, high-affinity binding was obtained only with those azoles that afforded the possibility of tetra-substitution. But of these, the 1,2-diazoles (pyrazoles) and the 1,3-diazoles (imidazoles), only the pyrazoles gave good binding. Although there are not many direct comparisons that can be made between these two diazole systems, pyrazole **38b** and imidazoles **12** and **17** are, in fact, just ring nitrogen isomers of one another, having otherwise identical peripheral groups and functionality (Figure 9). The same is true for pyrazole **38d** and imidazole **6b**. In both cases, however, the pyrazole partner binds to ER with ~30–36-fold higher affinity than the isomeric imidazole(s). This would suggest that the core structure does play more than a passive role in ER binding, although, as noted before, the high polarity and significant dipole moment of the imidazole might be the principal reason for the difference in this case. The issue of the functional role of the core scaffold in ER binding needs to be investigated further in these and other heterocyclic systems.

Significance

Compounds with a remarkable variety of structures bind with high affinity to the estrogen receptor (ER), and many nonsteroidal ligands have been prepared in the search for agents that have improved tissue-selectivity profiles. The application of combinatorial approaches to the development of selective ER ligands, however, is still in a state of infancy.

Based on a simple pharmacophore model consisting of a core scaffold and various peripheral groups we have designed systems that display the peripheral groups on simple heterocyclic core systems, which are readily prepared by simple condensation reactions. Here, we describe the synthesis and ER-binding affinity of various substituted 1,2- and 1,3-azoles.

No significant binding was found for members of the imidazole, thiazole or isoxazole classes, and this is rationalized either by the inherent polarity of these compounds (imidazoles) or by their inability to carry a sufficient number of the types of peripheral substituents we have explored so far (thiazoles, oxazoles and isoxazoles). Several members of the pyrazole class did show good binding affinity, however, the best being a tetra-substituted pyrazole **38d**. Both **38b** and **38d** bear an unexpectedly close conformational relationship to the nonsteroidal ligand raloxifene.

Compounds such as **38b** and **38d** are well suited to combinatorial synthesis using solid-phase methods. The large differences in binding affinity that result from small structural changes suggest that a thorough investigation of many possible combinations of core structures and peripheral substituents will be needed to identify novel high-affinity ligands for the ER that can be evaluated for their selective biological activity. The solid-phase combinatorial synthesis of pyrazole libraries is currently underway and has yielded other high-affinity ligands for the estrogen receptor (S.R.S. and J.A.K., unpublished observations). Some of these heterocycles have also shown intriguing biological activity [43].

Materials and methods

General methods

All reactions using water- or air-sensitive reagents were conducted under an Ar atmosphere with dry solvents. Solvents were distilled under N₂ as follows: CH₂Cl₂ from CaH₂, tetrahydrofuran (THF) from sodium benzophenone ketyl, dimethylformamide (DMF) from MgSO₄, and hexanes from CaSO₄. Triethylamine was distilled over CaH₂. All other reagents were purchased from commercial suppliers and used without further purification. Reactions were all monitored using thin-layer chromatography (TLC), performed on 0.25 mm silica gel glass plates containing F-254 indicator. Visualization on TLC was achieved by UV light (254 nm), iodine vapors, or phosphomolybdic acid indicator. Flash chromatography was performed using Woelm 32–63 µm silica gel packing unless otherwise noted.

¹H NMR and ¹³C NMR spectra were recorded on a Varian U400, Varian U500 or Varian INOVA 750. NMR spectra chemical shifts (δ) are reported in parts per million downfield from TMS and referenced with either TMS internal standard for CDCl₃, acetone-*d*₆, MeOD-*d*₄, or DMSO-*d*₆ solvent peak. NMR coupling constants are reported in Hertz. Electron ionization (EI) spectra were obtained using a Finnigan--MATCH5 spectrometer at 70 eV. Fast atom bombardment (FAB) were recorded on a VG ZAB-SE spectrometer. High-pressure liquid chromatography (HPLC) was performed on a SpectraPhysics P100 solvent delivery system with ultraviolet detection at 254 nm. Elemental analysis was performed by the Microanalytical Service Laboratory at the University of Illinois. All characterized compounds are chromatographically homogeneous.

Relative binding affinities

Assays were performed as reported previously [44] using lamb uterine cytosol diluted to approximately 1.5 nM of receptor, which was incubated with buffer of several concentrations of unlabeled competitor together with 10 nM [³H]estradiol for 18–24 h. Free ligand was removed by adsorption onto dextran-coated charcoal. Unlabeled competitors were prepared in 1:1 DMF:TEA to ensure solubility.

Molecular modeling and docking studies

Solvent-accessible surfaces were generated (Figures 12 and 13) using the QCPE Connolly Program module (Indiana University) in Sybyl 6.5 (Tripos, St. Louis, MO). Figure 13b: the pre-positioned pyrazole **38b** was used for additional docking studies using the Tripos FlexiDock module. Both hydrogen-bond donors and acceptors within the pocket surrounding the ligand and the ligand itself in addition to select rotatable torsional bonds were defined in order to afford an optimal docked-structure prior to molecular mechanics minimization. With the protein backbone held rigid, the ligand and the protein residues within 8 Å of the ligand were then minimized using a step-wise approach: first torsional bonds about the ligand were minimized holding the receptor fixed, followed by minimization of the receptor holding the ligand fixed, and then minimization of both the ligand and receptor. Minimizations were done using the TRIPOS Forcefield (as implemented in the program Sybyl) with the Powell gradient method and default settings (final RMS < 0.05 kcal/mol-Å).

Representative chemical synthesis

4,5-Di(4-methoxyphenyl)-1H-imidazole (2). To 4,4'-dimethoxybenzil (**1**) (2.0 g, 7.4 mmol) and *p*-formaldehyde (1.0 g, 11.1 mmol) was added formamide (50 ml). The bright yellow suspension was heated to reflux (220°C) for 2 h. The reaction mixture was then cooled to room temperature then to 0°C. The crystals that formed were filtered and recrystallized from EtOAc to afford **2** (2.4 g, 86%). mp 183–184°C (lit [16] mp 183–184°C); ¹H NMR (400 MHz, MeOH-*d*₄) δ 7.64 (s, 1H), 7.44 (d, 4H, *J* = 7.50), 6.89 (d, 4H, *J* = 7.50), 3.79 (s, 6H); ¹³C NMR (100 MHz, MeOH-*d*₄) δ 158.4, 135.2, 129.1, 128.9, 122.6, 114.2, 55.3.

General demethylation procedure using BBr₃. To a stirring solution of the methyl-protected heterocycle (**1** equiv) in CH₂Cl₂ at –78°C was added a solution of BBr₃ (4–5 equiv) as a 1N solution in CH₂Cl₂. The reaction were allowed to warm to room temperature and stirred for 18 h. After quenching with H₂O, the layers were separated and the aqueous layer extracted with EtOAc (3 × 5 ml). The combined organic layers were dried over Na₂SO₄, filtered and concentrated to afford the crude phenols. Flash chromatography afforded the demethylated products.

4,5-Di(4-hydroxyphenyl)-1H-imidazole (3). Imidazole **2** (100 mg, 0.35 mmol) afforded **3** (52 mg, 59%) by the general BBr₃ demethylation procedure. ¹H NMR (400 MHz, CDCl₃) δ 14.56 (br s, 1H), 9.93 (br s, 1H), 9.24 (s, 1H), 7.24 (d, 4H, *J* = 8.47), 6.82 (d, 4H, *J* = 8.40); MS (FAB) *m/z* (relative intensity, %) 253.1 (MH⁺ 24), 169.2 (100).

2,4,5-Tri(4-methoxyphenyl)-1H-imidazole (4). A suspension of 4,4'-dimethoxybenzil (**1**) (4.0 g, 15 mmol) and *p*-anisaldehyde (20 ml, 164 mmol) and formamide (100 ml) was heated to reflux (220°C) for 2 h, during which time the reaction mixture became homogeneous. The reaction was then cooled to 0°C and the precipitated product **4** was filtered. The light yellow powder was recrystallized from MeOH/H₂O to afford 3.80 g of **4** [19] (66%). mp 89–91°C (lit [19] mp 88–94°C). ¹H NMR (400 MHz, Acetone-*d*₆) δ 7.98 (d, 2H, *J* = 8.88), 7.42 (d, 4H, *J* = 8.52), 7.01 (d, 2H, *J* = 8.83), 6.92 (br s, 4H), 3.79 (s, 3H), 3.75 (s, 6H); ¹³C NMR (100 MHz, Acetone-*d*₆) δ 162.4, 159.9, 158.9, 145.4, 131.0, 129.0, 128.9, 126.6, 132.8, 114.0, 113.7, 113.6; MS (EI, 70 eV) *m/z* (relative intensity, %) 386.2 (M⁺, 100), 371 (30), 280 (100), 265 (30); HRMS calc'd for C₂₁H₁₆N₂O₃: 345.123800, found: 345.123918.

General N-alkylation procedure for imidazoles. A solution of imidazole **4** (200 mg, 0.52 mmol) in THF (10 ml) and DMF (1.5 ml) was cooled to 5°C. NaH (31 mg, 0.78 mmol) was added as 60% dispersion in mineral oil. The reaction mixture was warmed to room temperature for 1 h and respective alkyl halide (0.04 ml, 0.62 mmol) was added. The resulting suspension was heated to reflux for 12 h, then cooled to room temperature. The light precipitate was filtered, and the filtrate was concentrated under vacuum to a yellow solid which was flashed on silica (30% EtOAc/Hexanes) to afford alkylated products **5b–d** in 80–90% yields.

1-Ethyl-2,4,5-tri(4-methoxyphenyl)-imidazole (5b). ¹H NMR (400 MHz, CDCl₃) δ 7.60 (AA'XX', 2H, *J*_{AX} = 8.88, *J*_{AA} = 2.51), 7.46 (AA'XX', 2H,

$J_{AX}=8.97$, $J_{AA}=2.56$), 7.32 (AA'XX', 2H, $J_{AX}=8.88$, $J_{AA}=2.56$), 7.00 (AA'XX', 2H, $J_{AX}=8.88$, $J_{AA}=2.51$), 6.99 (AA'XX', 2H, $J_{AX}=8.88$, $J_{AA}=2.56$), 6.74 (AA'XX', 2H, $J_{AX}=8.97$, $J_{AA}=2.56$), 3.87 (q, 2H, $J=7.32$), 3.87 (s, 3H), 3.85 (s, 3H), 1.00 (t, 3H, $J=7.14$); ^{13}C NMR (100 MHz, CDCl_3) δ 160.0, 159.7, 158.1, 146.8, 137.2, 132.4, 130.5, 127.9, 127.5, 123.8, 123.7, 114.5, 114.0, 113.5, 55.3, 55.2, 55.1, 39.5, 16.2.

2,4,5-Tri(4-hydroxyphenyl)-1H-imidazole (6a). According to the general BBr_3 demethylation procedure above, imidazole 4 (3.0 g, 7.8 mmol) afforded **6a** as a green-orange solid that darkened upon exposure to air (1.8 g, 68%). mp 203–205°C; ^1H NMR (400 MHz, Acetone- d_6) δ 7.93 (AA'XX', 2H, $J_{AX}=8.97$, $J_{AA}=2.47$), 7.40 (AA'XX', 4H, $J_{AX}=8.60$, $J_{AA}=2.47$), 6.89 (AA'XX', 2H, $J_{AX}=8.97$, $J_{AA}=2.47$), 6.80 (AA'XX', 2H, $J_{AX}=8.60$, $J_{AA}=2.47$); ^{13}C NMR (100 MHz, Acetone- d_6) δ 157.9, 156.4, 145.9, 129.0, 126.8, 124.0, 123.4, 121.3, 115.0, 114.7; MS (FAB) m/z (relative intensity, %) 345.1 ($\text{M}+\text{H}^+$, 10), 353 (10), 169 (100); HRMS calc'd for $\text{C}_{21}\text{H}_{16}\text{N}_2\text{O}_3$: 345.123800, found: 345.123918.

1-Ethyl-2,4,5-tri(4-hydroxyphenyl)-imidazole (6b). According to the general BBr_3 demethylation procedure above, imidazole 5b (185 mg, 0.46 mmol) afforded **6b** (107 mg, 62%). mp 150–153°C; ^1H NMR (400 MHz, Acetone- d_6) δ 7.51 (AA'XX', 2H, $J_{AX}=8.52$, $J_{AA}=2.42$), 7.34 (AA'XX', 2H, $J_{AX}=8.71$, $J_{AA}=2.39$), 7.24 (AA'XX', 2H, $J_{AX}=8.63$, $J_{AA}=2.41$), 6.97 (AA'XX', 2H, $J_{AX}=8.58$, $J_{AA}=2.31$), 6.90 (AA'XX', 2H, $J_{AX}=8.75$, $J_{AA}=2.31$), 6.64 (AA'XX', 2H, $J_{AX}=8.96$, $J_{AA}=2.43$), 3.93 (q, 2H, $J=7.19$), 0.98 (t, 3H, $J=7.12$); ^{13}C NMR (100 MHz, Acetone- d_6) δ 158.2, 157.9, 155.9, 146.5, 136.8, 132.5, 130.3, 127.9, 127.8, 126.6, 122.5, 122.4, 116.0, 115.4, 114.8, 17.9, 15.4; MS (FAB) m/z (relative intensity, %) 372.1 (M^+ , 100), 343 (15), 275 (10), 214 (25), 162 (30), 148 (30); HRMS calc'd for $\text{C}_{23}\text{H}_{20}\text{N}_2\text{O}_3$: 372.147251, found: 372.147393.

1-Ethyl-2,5-(4-methoxyphenyl)-4-phenyl imidazole (11). Azido-ketone **9** (50.0 mg, 0.187 mmol) and imine **10** (92.0 mg, 0.564 mmol) were dissolved in THF (15 ml). Et_3N (29.0 μL , 0.208 mmol) was added via syringe and reaction stirred at room temperature for 48 h. The reaction mixture was then poured into H_2O and extracted with CH_2Cl_2 , organic fractions were pooled, dried over Na_2SO_4 , filtered and solvent removed under reduced pressure. The intermediate, 2,5-dihydro-2-hydroxyimidazole, used in next step without further purification or characterization, was taken up CH_2Cl_2 (10 ml). Solution was cooled to 0°C and TFA (14.4 μL , 0.187 mmol) was added via syringe. Reaction stirred at 0°C for 36 h. The mixture was diluted with CH_2Cl_2 (10 ml) and washed with H_2O , sat. NaHCO_3 , and sat. NaCl successively. The organic fraction was dried over Na_2SO_4 , filtered and solvent removed under reduced pressure. Purification by flash column chromatography (1:2 EtOAc:Hexanes) and recrystallization from CH_2Cl_2 /Hexanes afforded imidazole **11** as a white solid (24.6 mg, 34% yield from azide **9**). ^1H NMR (500 MHz, CDCl_3) δ 7.63 (AA'XX', 2H, $J_{AX}=8.81$, $J_{XX'}=2.53$), 7.54 (m, 2H), 7.34 (AA'XX', 2H, $J_{AX}=8.80$, $J_{XX'}=2.45$), 7.20 (m, 2H), 7.12 (m, 1H), 7.02 (AA'XX', 2H, $J_{AX}=8.78$, $J_{AA'}=2.54$), 7.01 (AA'XX', 2H, $J_{AX}=8.43$, $J_{AA'}=2.57$), 3.90 (q, 2H, $J=7.08$), 3.89 (s, 3H), 3.87 (s, 3H), 1.02 (t, 3H, $J=7.17$); ^{13}C NMR (125 MHz, CDCl_3) δ 200.8, 160.0, 159.8, 147.0, 134.8, 132.3 (2), 130.5 (2), 129.3, 128.9, 128.0 (2), 126.6 (2), 126.0, 123.6, 114.5 (2), 114.0 (2), 55.33, 55.28, 36.4, 16.2; MS (EI, 70 eV) m/z 384.2 (M^+); Anal. calc'd for $\text{C}_{25}\text{H}_{24}\text{N}_2\text{O}_2$, C: 78.10%, H: 6.29%, N: 7.29%, found, C: 77.91%, H: 6.28%, N: 7.28%.

General demethylation procedure using $\text{BF}_3\cdot\text{SMe}_2$. To a stirring solution of the methyl protected heterocycle (1 equiv) in CH_2Cl_2 (8 ml) at room temperature was added $\text{BF}_3\cdot\text{SMe}_2$ complex (75 equiv). After stirring for 24 h, solvent and excess reagent were evaporated under nitrogen stream in hood. Residue was taken up in EtOAc and washed with H_2O and sat. NaCl . Organic extract was dried over Na_2SO_4 , filtered and solvent removed under reduced pressure. The resulting residue was purified through a silica plug, eluting with EtOAc. Solvent evaporation afforded the deprotected products.

1-Ethyl-2,5-(4-hydroxyphenyl)-4-phenyl imidazole (12). Imidazole **11** (12.0 mg, 0.031 mmol) was demethylated according to the general $\text{BF}_3\cdot\text{SMe}_2$ procedure to afford imidazole **12** as an off-white powder (10.6 mg, 95%). ^1H NMR (500 MHz, Acetone- d_6) δ 7.80 (AA'XX', 2H, $J_{AX}=8.81$, $J_{XX'}=2.44$), 7.47–7.49 (m, 2H), 7.44 (AA'XX', 2H, $J_{AX}=8.65$, $J_{XX'}=2.44$), 7.37–7.40 (m, 3H), 7.14 (AA'XX', 2H, $J_{AX}=8.80$, $J_{AA'}=2.43$), 7.06 (AA'XX', 2H, $J_{AX}=8.68$, $J_{AA'}=2.46$), 4.25 (q, 2H, $J=7.28$), 1.17 (t, 3H, $J=7.29$); MS (FAB) m/z 357.2 ($\text{M}+\text{H}^+$); HRMS calc'd for $\text{C}_{23}\text{H}_{21}\text{N}_2\text{O}_2$: 357.160303, found: 357.160000.

5-Ethyl-1,4-(4-methoxyphenyl)-2-phenyl imidazole (16). Keto-amide **15** (110.0 mg, 0.273 mmol) and ammonium acetate (105.0 mg, 1.362 mmol) were heated to reflux in acetic acid (10 ml) for 48 h. Acetic acid was removed under reduced pressure, resulting residue was taken up in EtOAc, washed with sat. NaHCO_3 , H_2O , and sat. NaCl . Organic extracts were dried over Na_2SO_4 , filtered and solvent removed. Product was purified by flash column chromatography (1:4 EtOAc:Hexanes) and recrystallization from CH_2Cl_2 /Hexanes to give imidazole **16** as a white solid (25.7 mg, 25%). ^1H NMR (500 MHz, CDCl_3) δ 7.72 (AA'XX', 2H, $J_{AX}=8.29$, $J_{XX'}=2.55$), 7.14 (m, 2H), 7.21 (m, 3H), 7.19 (AA'XX', 2H, $J_{AX}=9.33$, $J_{XX'}=2.71$), 6.98 (AA'XX', 2H, $J_{AX}=8.48$, $J_{AA'}=2.52$), 6.96 (AA'XX', 2H, $J_{AX}=8.62$, $J_{AA'}=2.74$), 3.87 (s, 3H), 3.85 (s, 3H), 2.67 (q, 2H, $J=7.48$), 1.01 (t, 3H, $J=7.45$); MS (EI, 70 eV) m/z 384.2 (M^+).

5-Ethyl-1,4-(4-hydroxyphenyl)-2-phenyl imidazole (17). Imidazole **16** (25.0 mg, 0.065 mmol) was demethylated as outlined in general $\text{BF}_3\cdot\text{SMe}_2$ procedure above to give deprotected imidazole **17** as an off-white powder (20.2 mg, 87%). ^1H NMR (400 MHz, Acetone- d_6) δ 9.04 (br s, 1H), 8.51 (br s, 1H), 7.64 (AA'XX', 2H, $J_{AX}=8.73$, $J_{XX'}=2.51$), 7.50–7.47 (m, 2H), 7.31–7.27 (m, 5H), 7.01 (AA'XX', 2H, $J_{AX}=8.94$, $J_{AA'}=2.76$), 6.94 (AA'XX', 2H, $J_{AX}=8.73$, $J_{AA'}=2.52$), 2.69 (q, 2H, $J=7.48$), 1.02 (t, 3H, $J=7.49$); MS (FAB) m/z 357.1 ($\text{M}+\text{H}^+$); HRMS calc'd for $\text{C}_{23}\text{H}_{21}\text{N}_2\text{O}_2$: 357.1603, found 357.1602.

2,4-Di(4-methoxyphenyl)-thiazole (21a). A suspension of thioamide **19** (1.3 g, 7.9 mmol) and α -bromo-4'-methoxy-acetophenone (**20**) (1.8 g, 7.9 mmol) in DMF (10 ml) was heated to reflux for 1 h, until it became homogeneous. The heat was removed and the reaction was stirred for 15 h at room temperature. The reaction mixture was poured into H_2O (50 ml) and the solid precipitate was filtered to afford crude **21a**. Recrystallization from CH_2NO_2 afforded pure **21a** as light yellow crystals (1.8 g, 81%). ^1H NMR (400 MHz, CDCl_3) δ 7.98 (AA'XX', 2H, $J_{AX}=8.87$, $J_{AA}=2.53$), 7.63 (AA'XX', 2H, $J_{AX}=8.94$, $J_{AA}=2.48$), 6.86 (AA'XX', 2H, $J_{AX}=8.87$, $J_{AA}=2.53$), 6.85 (AA'XX', 2H, $J_{AX}=8.94$, $J_{AA}=2.48$), 7.26 (s, 1H), 3.86 (s, 3H), 3.85 (s, 3H); ^{13}C NMR (400 MHz, CDCl_3) δ 167.5, 160.9, 159.4, 155.6, 127.9, 127.6, 127.4, 126.6, 114.1, 113.9, 109.9, 55.3, 55.2; MS (EI, 70 eV) m/z (relative intensity, %) 297.1 (M^+ , 100), 282.1 (10), 164.1 (30), 149.1 (55), 133.1 (10), 121.1 (25), 77.1 (15); HRMS calc'd for $\text{C}_{17}\text{H}_{15}\text{NSO}_2$: 297.082469, found: 297.082351.

2,4-Di(4-hydroxyphenyl)-thiazole (22a). Thiazole **21a** (1.0 g, 3.6 mmol) was demethylated using BBr_3 as outlined in the general procedure above to afford **22a** (430 mg, 45%). mp 218–221°C; ^1H NMR (400 MHz, Acetone- d_6) δ 8.84 (br s, 2H), 7.92 (AA'XX', 4H, $J_{AX}=8.57$, $J_{AA}=2.17$), 7.58 (s, 1H), 6.96 (AA'XX', 2H, $J_{AX}=8.79$, $J_{AA}=2.51$), 6.92 (AA'XX', 2H, $J_{AX}=8.78$, $J_{AA}=2.44$); ^{13}C NMR (100 MHz, Acetone- d_6) δ 168.2, 159.3, 157.2, 155.8, 127.7, 127.3, 126.2, 125.1, 115.2, 114.9, 109.3; MS (EI, 70 eV) m/z (relative intensity, %) 296.1 (M^+ , 100), 150.1 (27), 121.1 (11), 78.1 (8); HRMS calc'd for $\text{C}_{15}\text{H}_{11}\text{NSO}_2$: 269.051163, found: 269.051051.

2,4-(4-Methoxyphenyl)-5-phenyl oxazole (28). Azido-ketone **27** (0.18 g, 0.673 mmol) and *p*-anisaldehyde (0.25 ml, 2.05 mmol) were dissolved in THF (15 ml). Et_3N (94.0 μL , 0.674 mmol) was added via syringe and reaction stirred at room temperature for 48 h. The reaction mixture was then poured into H_2O and extracted with CH_2Cl_2 , organic fraction was dried over Na_2SO_4 , filtered and solvent removed under reduced pressure. Resulting intermediate 2,5-dihydro-5-hydroxyoxazole, used in next

step without further purification or characterization, was taken up CH_2Cl_2 (10 ml). Solution was cooled to 0°C and TFA (54.0 μl , 0.701 mmol) was added via syringe. Reaction stirred at 0°C for 36 h. The mixture was diluted with CH_2Cl_2 (10 ml) and washed with H_2O , sat. NaHCO_3 , and sat. NaCl successively. Organic extracts were combined, dried over Na_2SO_4 , filtered and solvent removed under reduced pressure. Purification by flash column chromatography (1:2 EtOAc:hexanes) and recrystallization from CH_2Cl_2 /Hexanes afforded oxazole **28** as a white solid (72.4 mg, 30% yield from azide **27**). mp $125\text{--}128^\circ\text{C}$ (lit. [27] mp $126\text{--}127^\circ\text{C}$); ^1H NMR (500 MHz, CDCl_3) δ 7.84 (AA'XX', 2H, $J_{\text{AX}}=8.89$, $J_{\text{XX'}}=2.47$), 7.43 (AA'XX', 2H, $J_{\text{AX}}=8.83$, $J_{\text{XX'}}=2.48$), 7.53 (m, 2H), 7.32 (m, 2H), 7.26 (tt, 1H, $J=7.03$, 1.42), 6.97 (AA'XX', 2H, $J_{\text{AX}}=8.85$, $J_{\text{AA'}}=2.53$), 6.88 (AA'XX', 2H, $J_{\text{AX}}=8.70$, $J_{\text{AA'}}=2.53$), 3.84 (s, 3H), 3.81 (s, 3H).

2,4-(4-Hydroxyphenyl)-5-phenyl oxazole (29). Oxazole **28** (22.0 mg, 0.062 mmol) was demethylated according to the general $\text{BF}_3\cdot\text{SMe}_2$ procedure above to give deprotected oxazole **29** as an off-white powder (18.8 mg, 93%). ^1H NMR (500 MHz, Acetone- d_6) δ 9.43 (br s, 1H), 8.90 (br s, 1H), 8.08 (AA'XX', 2H, $J_{\text{AX}}=9.06$, $J_{\text{XX'}}=2.62$), 7.61 (m, 2H), 7.49 (m, 3H), 7.44 (AA'XX', 2H, $J_{\text{AX}}=8.97$, $J_{\text{XX'}}=2.44$), 7.12 (AA'XX', 2H, $J_{\text{AX}}=8.87$, $J_{\text{AA'}}=2.50$), 6.95 (AA'XX', 2H, $J_{\text{AX}}=8.86$, $J_{\text{AA'}}=2.42$); MS m/z 329.1 (M^+); HRMS calc'd. for $\text{C}_{21}\text{H}_{15}\text{NO}_3$: 329.1052, found 329.1285.

2,5-(4-Methoxyphenyl)-4-phenyl oxazole (30). A solution of bromo-ketone **26** (87.0 mg, 0.285 mmol) and *p*-methoxybenzamide (43.0 mg, 0.285 mmol) in toluene was heated to reflux for 36 h. Toluene was removed under reduced pressure and resulting residue purified by flash column chromatography (1:4 EtOAc:Hexanes). Recrystallization of desired product from CH_2Cl_2 /hexanes afforded oxazole **30** as a colorless solid (52.9 mg, 52%). mp $147\text{--}149^\circ\text{C}$; ^1H NMR (500 MHz, CDCl_3) δ 8.08 (AA'XX', 2H, $J_{\text{AX}}=8.58$, $J_{\text{XX'}}=2.24$), 7.72 (m, 2H), 7.59 (AA'XX', 2H, $J_{\text{AX}}=8.72$, $J_{\text{XX'}}=2.31$), 7.39 (m, 2H), 7.33 (m, 1H), 6.99 (AA'XX', 2H, $J_{\text{AX}}=8.63$, $J_{\text{AA'}}=2.26$), 6.92 (AA'XX', 2H, $J_{\text{AX}}=8.68$, $J_{\text{AA'}}=2.67$), 3.88 (s, 3H), 3.85 (s, 3H); ^{13}C NMR (100 MHz, CDCl_3) δ 161.2, 159.9, 159.7, 145.1, 135.3, 132.9, 128.6 (2), 128.1 (2), 128.0 (2), 127.96 (2), 127.9, 121.7, 120.3, 114.2 (2), 114.1 (2), 55.4, 55.3; MS m/z 357.2 (M^+).

2,5-(4-Hydroxyphenyl)-4-phenyl oxazole (31). Oxazole **30** (22.0 mg, 0.062 mmol) was demethylated according to the general $\text{BF}_3\cdot\text{SMe}_2$ procedure above to give deprotected oxazole **31** as an off-white powder (18.1 mg, 89%). ^1H NMR (500 MHz, Acetone- d_6) δ 8.93 (br s, 1H), 8.77 (br s, 1H), 7.99 (AA'XX', 2H, $J_{\text{AX}}=8.83$, $J_{\text{XX'}}=2.41$), 7.72 (m, 2H), 7.53 (AA'XX', 2H, $J_{\text{AX}}=8.77$, $J_{\text{XX'}}=2.46$), 7.40 (m, 2H), 7.34 (tt, 1H, $J=7.36$, 1.33), 6.99 (AA'XX', 2H, $J_{\text{AX}}=8.70$, $J_{\text{AA'}}=2.40$), 6.92 (AA'XX', 2H, $J_{\text{AX}}=8.83$, $J_{\text{AA'}}=2.46$); MS m/z 329.1 (M^+); HRMS calc'd for $\text{C}_{21}\text{H}_{15}\text{NO}_3$: 329.1052, found 329.1055.

General procedure for pyrazole synthesis. A suspension of diketone (1 equiv) and appropriate hydrazine hydrochloride (3–5 equiv) in a 3:1 mixture DMF:THF was heated to reflux for 16–24 h with reaction progress being monitored by TLC for disappearance of starting material. The reaction mixtures were cooled to room temperature and poured into iced sat. LiCl solution (10 ml) and EtOAc (10 ml). The layers were separated and the organic layer was washed with brine (10 ml), dried over MgSO_4 , filtered and concentrated. Purification using flash column chromatography (EtOAc/hexanes systems) afforded the pyrazoles.

3,5-di(4-methoxyphenyl)-1H-pyrazole (34a). Diketone **33** (91 mg, 0.32 mmol) and hydrazine (0.1 ml, 3.2 mmol) were reacted as outlined in general pyrazole procedure to afford **34a** [45] as an off-white solid (32.6 mg, 38%). mp $172\text{--}175^\circ\text{C}$ (lit [45] mp 174°C); ^1H NMR (400 MHz, CDCl_3) δ 7.73 (AA'XX', 4H, $J_{\text{AX}}=8.73$, $J_{\text{AA'}}=2.42$), 6.97 (AA'XX', 4H, $J_{\text{AX}}=8.73$, $J_{\text{AA'}}=2.42$), 6.80 (s, 1H), 3.72 (s, 6H); ^{13}C NMR (100 MHz, CDCl_3) δ 159.9, 148.3, 126.8, 123.0, 112.9, 98.6, 54.5; MS (FAB) m/z (relative intensity, %) 281 (MH^+ , 100).

1-Phenyl-3,5-di(4-methoxyphenyl)-pyrazole (34b). Diketone **33** (100 mg, 0.35 mmol) and phenyl hydrazine hydrochloride (500 mg, 3.5 mmol) were reacted as outlined in general pyrazole procedure above to afford **34b** [46] (30 mg, 25%). mp $159\text{--}161^\circ\text{C}$ (lit [46] mp 163°C); ^1H NMR (400 MHz, CDCl_3) δ 7.82 (AA'XX', 2H, $J_{\text{AX}}=8.96$, $J_{\text{AA'}}=2.44$), 7.24–7.20 (m, 5H), 7.20 (AA'XX', 2H, $J_{\text{AX}}=8.79$, $J_{\text{AA'}}=2.46$), 6.99 (AA'XX', 2H, $J_{\text{AX}}=8.79$, $J_{\text{AA'}}=2.46$), 6.84 (AA'XX', 2H, $J_{\text{AX}}=8.96$, $J_{\text{AA'}}=2.44$), 6.70 (s, 1H), 3.84 (s, 3H), 3.80 (s, 3H); ^{13}C NMR (100 MHz, CDCl_3) δ 159.4, 151.5, 144.1, 140.0, 129.9, 128.8, 127.2, 126.9, 125.5, 125.2, 122.9, 113.9, 113.8, 104.1, 55.2, 55.1; MS (EI, 70 eV) m/z (relative intensity, %) 356 (M^+ , 100), 341 (19), 135 (89); HRMS calc'd for $\text{C}_{23}\text{H}_{20}\text{N}_2\text{O}_2$: 356.15241, found: 356.152478.

3,5-Di(4-hydroxyphenyl)-1H-pyrazole (35a). Pyrazole **34a** (20 mg, 0.07 mmol) was demethylated with BBr_3 according to the general procedure to afford **35a** [47] as an off-white solid (11 mg, 63%). ^1H NMR (400 MHz, Acetone- d_6) δ 8.58 (br s, 2H), 7.75 (AA'XX', 4H, $J_{\text{AX}}=8.95$, $J_{\text{AA'}}=2.46$), 6.93 (AA'XX', 4H, $J_{\text{AX}}=8.95$, $J_{\text{AA'}}=2.46$), 6.83 (s, 1H); ^{13}C NMR (100 MHz, Acetone- d_6) δ 157.1, 148.3, 126.5, 123.0, 115.3, 97.5; MS (CI, CH_4) m/z (relative intensity, %) 253.1 (MH^+ , 100), 237 (10), 161 (5), 123 (15).

1-Phenyl-3,5-di(4-hydroxyphenyl)-pyrazole (35b). Pyrazole **34b** (20 mg, 0.06 mmol) was demethylated with BBr_3 according to the general procedure to afford **35b** [47] as an off-white solid (11.5 mg, 58%). ^1H NMR (400 MHz, CDCl_3) δ 8.64 (s, 1H), 8.45 (s, 1H), 7.79 (AA'XX', 4H, $J_{\text{AX}}=8.78$, $J_{\text{AA'}}=2.38$), 7.36 (m, 5H), 7.14 (AA'XX', 4H, $J_{\text{AX}}=8.60$, $J_{\text{AA'}}=2.47$), 6.90 (AA'XX', 2H, $J_{\text{AX}}=8.78$, $J_{\text{AA'}}=2.38$), 6.81 (AA'XX', 2H, $J_{\text{AX}}=8.78$, $J_{\text{AA'}}=2.47$), 6.80 (s, 1H); ^{13}C NMR (100 MHz, CDCl_3) δ 157.5, 157.3, 151.3, 144.1, 140.6, 129.9, 128.6, 126.8, 126.7, 124.9, 122.2, 122.1, 115.2, 115.1, 103.7; MS (EI, 70 eV) m/z (relative intensity, %) 362.1 (M^+ , 85), 328.1 (100).

4-Ethyl-3,5-di(4-methoxyphenyl)-1H-pyrazole (37a). Diketone **36** (100 mg, 0.32 mmol) and hydrazine (0.12 ml, 3.2 mmol) were reacted as outlined in the general pyrazole procedure above to afford **37a** as a white solid (69 mg, 70%). ^1H NMR (400 MHz, CDCl_3) δ 7.50 (AA'XX', 4H, $J_{\text{AX}}=8.84$, $J_{\text{AA'}}=2.48$), 6.94 (AA'XX', 4H, $J_{\text{AX}}=8.90$, $J_{\text{AA'}}=2.50$), 3.85 (s, 3H), 2.71 (q, 2H, $J=7.38$), 1.07 (t, 3H, $J=7.44$); ^{13}C NMR (100 MHz, CDCl_3) δ 159.4, 129.0, 127.4, 124.1, 116.8, 113.9, 55.1, 16.6, 15.3; MS (EI, 70 eV) m/z (relative intensity, %) 308.1 (M^+ , 100), 293.1 (73), 160.1 (7), 134 (8).

1-Phenyl-4-ethyl-3,5-di(4-methoxyphenyl)-pyrazole (37b). Diketone **36** (100 mg, 0.35 mmol) and phenyl hydrazine hydrochloride (140 mg, 0.96 mmol) were reacted as outlined in the general pyrazole procedure above to afford **37b** as an orange solid (109 mg, 87%). ^1H NMR (400 MHz, CDCl_3) δ 7.72 (AA'XX', 2H, $J_{\text{AX}}=9.03$, $J_{\text{AA'}}=2.44$), 7.24 (m, 3H), 7.20 (m, 2H), 7.17 (AA'XX', 2H, $J_{\text{AX}}=8.79$, $J_{\text{AA'}}=2.44$), 6.99 (AA'XX', 2H, $J_{\text{AX}}=8.79$, $J_{\text{AA'}}=2.56$), 6.90 (AA'XX', 2H, $J_{\text{AX}}=8.79$, $J_{\text{AA'}}=2.44$), 3.86 (s, 3H), 3.83 (s, 3H), 2.63 (q, 2H, $J=7.57$), 1.04 (t, 3H, $J=7.57$); ^{13}C NMR (100 MHz, CDCl_3) δ 159.6, 159.4, 150.8, 141.2, 140.5, 131.5, 129.3, 128.8, 127.0, 126.7, 124.8, 123.5, 120.7, 114.2, 114.1, 55.5, 55.4, 17.3, 15.8; MS (EI, 70 eV) m/z (relative intensity, %) 356 (M^+ , 100), 341 (100), 328 (15), 196 (25), 77 (40); HRMS calc'd for $\text{C}_{25}\text{H}_{24}\text{N}_2\text{O}_2$: 384.183582, found: 384.183778.

4-Ethyl-3,5-di(4-hydroxyphenyl)-1H-pyrazole (38a). Pyrazole **37a** (69 mg, 0.22 mmol) was demethylated according to the general BBr_3 procedure to afford **38a** as a white solid (35 mg, 57%). ^1H NMR (400 MHz, Acetone- d_6) δ 7.49 (AA'XX', 4H, $J_{\text{AX}}=8.85$, $J_{\text{AA'}}=2.46$), 6.93 (AA'XX', 4H, $J_{\text{AX}}=8.64$, $J_{\text{AA'}}=2.40$), 2.73 (q, 2H, $J=7.39$), 1.07 (t, 3H, $J=7.47$); ^{13}C NMR (100 MHz, Acetone- d_6) δ 156.9, 128.8, 124.3, 122.2, 115.4, 115.2, 16.5, 14.9; MS (CI, CH_4) m/z (relative intensity, %) 282.1 ($\text{M}+\text{H}^+$, 100), 263.1 (10), 187.1 (20).

1-Phenyl-4-ethyl-3,5-di(4-hydroxyphenyl)-pyrazole (38b). Pyrazole **37b** (100 mg, 0.26 mmol) was demethylated according to the general BBr_3 procedure to afford **38b** as a white solid (50 mg, 54%). ^1H NMR

(400 MHz, MeOH- d_4) δ 7.51 (AA'XX', 4H, $J_{AX} = 8.67$, $J_{AA} = 2.47$), 7.24–7.42 (m, 5H), 7.05 (AA'XX', 4H, $J_{AX} = 8.81$, $J_{AA} = 2.40$), 6.88 (AA'XX', 2H, $J_{AX} = 8.67$, $J_{AA} = 2.46$), 6.78 (AA'XX', 2H, $J_{AX} = 8.81$, $J_{AA} = 2.40$), 2.60 (q, 2H, $J = 7.53$), 0.98 (t, 3H, $J = 7.39$); MS (EI, 70 eV) m/z (relative intensity, %) 356.1 (M^+ , 100), 341.1 (100), 328.1 (15), 196.1 (25), 77 (40); HRMS calc'd for $C_{23}H_{21}N_2O_2$: 357.161155, found: 357.160303.

3,5-Di(4-methoxyphenyl)isoxazole (40). To a solution of oxime **39** (1.0 g, 6 mmol) in THF (20 mL) at 0°C was added nBuLi (9.11 mL, 13.3 mmol) as a solution in hexanes. The clear solution was stirred for 30 min at 0°C then methyl 4-methoxybenzoate (498 mg, 3 mmol) was added as a solution in THF (5 mL) over 5 min. The reaction mixture was stirred at 0°C for 30 min, then warmed to room temperature. 5 N HCl (10 mL) was added and the biphasic reaction mixture was brought to reflux overnight (12 h). Upon cooling to 0°C, isoxazole **40** precipitated [33] and was collected via filtration (450 mg, 27%). mp 174–177°C (lit [33] mp 176–177°C); 1H NMR (400 MHz, Acetone- d_6) δ 7.66 (AA'XX', 2H, $J_{AX} = 8.88$, $J_{AA} = 2.44$), 7.63 (AA'XX', 2H, $J_{AX} = 9.1$, $J_{AA} = 2.15$), 6.86 (AA'XX', 2H, $J_{AX} = 8.88$, $J_{AA} = 2.44$), 6.85 (AA'XX', 2H, $J_{AX} = 9.1$, $J_{AA} = 2.44$), 6.57 (s, 1H), 3.73 (s, 3H), 3.72 (s, 3H); ^{13}C NMR (100 MHz, Acetone- d_6) δ 169.8, 162.3, 160.8, 160.7, 127.9, 127.1, 121.5, 120.0, 114.1, 114.0, 95.7, 55.1, 55.0; MS (EI, 70 eV) m/z (relative intensity, %) 281.1 (M^+ , 5), 150.1 (20), 135.1 (100).

3,5-Di(4-hydroxyphenyl)isoxazole (41). Isoxazole **40** (300 g, 1.1 mmol) was demethylated according to the general BBr_3 procedure to afford **41** [34] as a white solid (152 mg, 56%). mp 267–269°C (lit [34] mp 255°C); 1H NMR (400 MHz, Acetone- d_6) δ 10.07 (s, 1H), 9.91 (s, 1H), 7.90 (d, 4H, $J = 8.79$), 7.21 (s, 1H), 6.88 (4H, t, $J = 9.38$); ^{13}C NMR (100 MHz, MeOH- d_4) δ 170.3, 162.8, 159.1, 127.7, 126.9, 119.9, 118.7, 116.3, 115.1, 95.3, 95.0; MS (EI, 70 eV) m/z (relative intensity, %) 253.1 (M^+ , 60), 133.1 (25), 121.1 (100), 93.0 (20), 77.0 (10), 65.0 (30).

Supplementary material available

Experimental detail regarding the preparation of all intermediates discussed in the synthesis of the above heterocycles is available with the online version of this paper.

Acknowledgements

We are grateful for support of this research through grants from the National Institutes of Health (PHS 5R37 DK15556) and the U.S. Army Breast Cancer Research Program (DAMD17-97-1-7076). We thank Kathryn Carlson for determining estrogen receptor binding affinities. NMR spectra were obtained in the Varian Oxford Instrument Center for Excellence in NMR Laboratory. Funding for this instrumentation was provided in part from the W.M. Keck Foundation, the National Institutes of Health (PHS 1 S10 RR104444-01) and the National Science Foundation (NSF CHE 96-10502). Mass spectra were obtained on instruments supported by grants from the National Institute of General Medical Sciences (GM 27029), the National Institutes of Health (RR 01575), and the National Science Foundation (PCM 8121494).

References

- Grese, T.A., et al., & Dodge, J.A. (1997). Molecular determinants of tissue selectivity in estrogen receptor modulators. *Proc. Natl Acad. Sci. USA* **94**, 14105–14110.
- Kuiper, G.G.J.M., Enmark, E., Pelto-Huikko, M., Nilsson, S. & Gustafsson, J.A. (1996). Cloning of a novel receptor expressed in rat prostate and ovary. *Proc. Natl Acad. Sci. USA* **93**, 5925–5930.
- Mosselman, S., Polman, J. & Dijkema, R. (1996). ERb: Identification and characterization of a novel human estrogen receptor. *FEBS Lett.* **392**, 49–53.
- Katzenellenbogen, J.A. & Katzenellenbogen, B.S. (1996). Nuclear hormone receptors: ligand-activated regulators of transcription and diverse cell responses. *Chem. Biol.* **3**, 529–536.
- Horwitz, K.B., et al., & Tung, L. (1996). Nuclear receptor coactivators and corepressors. *Mol. Endocrinol.* **10**, 1167–1177.
- Glass, C.K., Rose, D.W. & Rosenfeld, M.G. (1997). Nuclear receptor coactivators. *Curr. Opin. Cell Biol.* **9**, 222–232.
- Katzenellenbogen, J.A., O'Malley, B.W. & Katzenellenbogen, B.S. (1996). Tripartite steroid hormone receptor pharmacology: interaction with multiple effector sites as a basis for the cell- and promoter-specific action of these hormones. *Mol. Endocrinol.* **10**, 119–131.
- Magarian, R.A., Overacre, L.B. & Singh, S. (1994). The medicinal chemistry of nonsteroidal antiestrogens: a review. *Curr. Med. Chem.* **1**, 61–104.
- Grundy, J. (1957). Artificial estrogens. *Chem. Rev.* **57**, 281–416.
- Solmsen, U.V. (1945). Synthetic estrogens and the relation between their structure and their activity. *Chem. Rev.* **37**, 481–598.
- Grese, T.A., et al., & Bryant, H.U. (1998). Synthesis and pharmacology of conformationally restricted raloxifene analogues: highly potent selective estrogen receptor modulators. *J. Med. Chem.* **41**, 1272–1283.
- Plakowitz, A.D., et al., & Bryant, H.U. (1997). Discovery and synthesis of [6-Hydroxy-3-[4-[2-(1-piperidinyl)ethoxy]phenoxy]-2-(hydroxyphenyl)]benzo[b]thiophene: a novel, highly potent, selective estrogen receptor modulator. *J. Med. Chem.* **40**, 1407–1416.
- Brown, D.S. & Armstrong, R.W. (1996). Synthesis of tetra-substituted ethylenes on solid support via resin capture. *J. Am. Chem. Soc.* **118**, 6331–6332.
- Williard, R., et al., & Scanlan, T.S. (1995). Screening and characterization of estrogenic activity from hydroxystilbene library. *Curr. Biol.* **2**, 45–51.
- Sarshar, S., Siev, D. & Mjalli, A.M.M. (1996). Imidazole libraries on solid support. *Tetrahedron Lett.* **37**, 835–838.
- Bredereck, H., Gompper, R. & Hayer, D. (1959). Imidazole aus α -diketonen. *Chem. Ber.* **92**, 338–343.
- Lombardino, J.G. & Weisman, E.H. (1974). Preparation and antiinflammatory activity of some nonacid trisubstituted imidazoles. *J. Med. Chem.* **17**, 1182–1188.
- Schubert, V.H., Giesemann, G., Steffen, P. & Bleichert, J. (1962). p-Aryl- and p-Alkoxyphenyl-imidazole. *J. Prakt. Chem.* **18**, 192–202.
- Hayes, J.F., Mitchell, M.B. & Wicks, C. (1994). A novel synthesis of 2,4,5-triarylimidazoles. *Heterocycles* **38**, 575–585.
- Gardner, P.D. (1956). Organic peracid oxidation of some enol esters involving R' rearrangement. *J. Am. Chem. Soc.* **78**, 3421–3424.
- Jenkins, S.S. (1934). The grignard reaction in the synthesis of ketones. IV. A new method of preparing isomeric unsymmetrical benzoin. *J. Am. Chem. Soc.* **56**, 682–684.
- Patonay, T. & Hoffman, R.V. (1995). Base-promoted reactions of α -azido ketones with aldehydes and ketones: a novel entry to α -azido-hydroxy ketones and 2,5-dihydro-5-hydroxyoxazoles. *J. Org. Chem.* **60**, 2368–2377.
- Taylor, E.C. & Zoltewicz, J.A. (1960). A new synthesis of aliphatic and aromatic thioamides from nitriles. *J. Am. Chem. Soc.* **82**, 2656–2657.
- Dolling, K., Zschacke, H. & Schubert, H. (1979). Kristallin-flüssige Thiazole. [Liquid-crystalline thiazoles.] *J. Prakt. Chem.* **321**, 643–654.
- Katrzyk, A.R., Boulton, A.J. & Short, D.J. (1960). Interaction at a distance in conjugated systems. Part III. Effect of aryl and heteroaryl groups on the infrared intensities of C=C and C-C stretching bands. *J. Chem. Soc.* 1519–1523.
- Cowper, R.M. & Stevens, T.S. (1940). Mechanism of the reaction between arylamines and benzoin. *J. Chem. Soc.* 347–349.
- Strzybny, P.P.E., van ES, T. & Backeberg, O.G. (1969). Reaction of α -acyloxyketones with ammonium acetate. *J. South African Chem. Inst.* **22**, 158–164.
- Marzinzik, A.L. & Felder, E.R. (1996). Solid support synthesis of highly functionalized pyrazoles and isoxazoles; scaffolds for molecular diversity. *Tetrahedron Lett.* **37**, 1003–1006.
- Reitz, D.B., Beak, P., Farney, R.F. & Helmick, L.S. (1978). Dipole-stabilized carbanions from thioesters. Evidence for stabilization by the carbonyl group. *J. Am. Chem. Soc.* **100**, 5428–5436.
- Tewari, S.C. & Rastogi, S.N. (1979). Studies in antifertility agents: Part XXII: 1,2-diethyl-1,3-bis-(p-hydroxyphenyl)-1-propene. *Ind. J. Chem.* **18B**, 62–64.
- Clark, J.H. & Miller, J.M. (1977). Hydrogen bonding in organic synthesis. Part 6. C-Alkylation of β -dicarbonyl compounds using tetralkylammonium fluorides. *J. Chem. Soc., Perkin I*, 1743–1745.
- Perkins, M., Beam, C.F., Dyer, M.C.D. & Hauser, C.R. (1988). 3-(4-Chlorophenyl)-5-(4-methoxyphenyl)isoxazole. *Org. Syn. Coll. Vol. VI*, 278–281.
- Ichinose, N., Mizuno, K., Tami, T. & Otsuji, Y. (1988). A novel NO insertion into cyclopropane ring by use of $NOBF_4$. Formation of 2-isoxazolines. *Chem. Lett.*, 233–236.
- Murthy, A.K., Rao, K.S.R.K.M. & Rao, N.V.S. (1968). Isoxazolyphenols and their absorption spectra. *Aus. J. Chem.* **21**, 2315–2317.
- Katzenellenbogen, J.A., Myers, H.N., Johnson, H.J., Jr, Kempton, R.J. & Carlson, K.E. (1977). Estrogen photoaffinity labels. 1. Chemical and radiochemical synthesis of hexestrol diazoketone and azide derivatives; photochemical studies in solution. *Biochemistry* **16**, 1964–1970.

36. Anstead, G.M., Carlson, K.E. & Katzenellenbogen, J.A. (1997). The estradiol pharmacophore: ligand structure-estrogen receptor binding affinity relationships and a model for the receptor binding site. *Steroids* **62**, 268-303.
37. von Angerer, E., Prekajac, J. & Strohmeier, J. (1984). 2-Phenylindoles. Relationship between structure, estrogen receptor affinity, and mammary tumor inhibiting activity in the rat. *J. Med. Chem.* **27**, 1439-1447.
38. Hwang, K.J., O'Neil, J.P. & Katzenellenbogen, J.A. (1992). 5,6,11,12-Tetrahydrochrysenes: Synthesis of rigid stilbene systems designed to be fluorescent ligands for the estrogen receptor. *J. Org. Chem.* **57**, 1262-1271.
39. Joule, J.A., Mills, K. & Smith, G.F.J. (1995). *Heterocyclic Chemistry*. Third ed. p 516, Chapman and Hall, New York.
40. von Angerer, E. & Erber, S. (1992). 3-Alkyl-2-phenylbenzo[b]thiophenes: nonsteroidal estrogen antagonists with mammary tumor inhibiting activity. *J. Steroid Biochem. Mol. Biol.* **41**, 557-562.
41. Grese, T.A., *et al.*, & Sata, M. (1996). Benzopyran selective estrogen receptor modulators (SERMS): Pharmacological effects and structural correlation with raloxifene. *Bioorg. Med. Chem. Lett.* **6**, 903-908.
42. Brzozowski, A.M., *et al.* & Carlquist, M. (1997). Molecular basis of agonism and antagonism in the oestrogen receptor. *Nature* **389**, 753-758.
43. Sun, J., *et al.*, & Katzenellenbogen, B.S. (1999). Novel ligands that function as selective estrogens or antiestrogens for estrogen receptor- α or estrogen receptor- β . *Endocrinology*, **140**, 800-804.
44. Katzenellenbogen, J.A., Johnson, H.J. & Myers, H.N. (1973). Photoaffinity labels for estrogen binding proteins of rat uterus. *Biochemistry* **12**, 4085-4092.
45. van Steenis, J. (1946). The nitration of dianisoylmethane and p-methoxydesoxybenzoin. *Recl. Trav. Chim. Pays-Bas* **66**, 29-46.
46. Ando, W., Sato, R., Yamashita, M., Akasaka, T. & Miyazaki, H. (1983). Quenching of singlet oxygen by 1,3,5-triaryl-2-pyrazolines. *J. Org. Chem.* **48**, 542-546.
47. Hergenrother, P.M. (1991). New developments in thermally stable polymers. *Rec. Trav. Chim. Pays-Bas*. **110**, 481-491.



Pergamon

Bioorganic & Medicinal Chemistry 8 (2000) 1293–1316

BIOORGANIC &
MEDICINAL
CHEMISTRY

Acyclic Amides as Estrogen Receptor Ligands: Synthesis, Binding, Activity and Receptor Interaction

Shaun R. Stauffer,^a Jun Sun,^b Benita S. Katzenellenbogen^{b,c}
and John A. Katzenellenbogen^{a,*}

^aDepartment of Chemistry, University of Illinois, 461 Roger Adams Laboratory, Box 37-5, 600 S. Mathews Avenue, Urbana, IL 61801, USA

^bDepartment of Physiology, University of Illinois, 407 S. Goodwin Avenue, Urbana, IL 61801, USA

^cDepartment of Cell and Structural Biology, University of Illinois, 407 S. Goodwin Avenue, Urbana, IL 61801, USA

Received 7 November 1999; accepted 26 January 2000

Abstract—We have prepared a series of bisphenolic amides that mimic bibenzyl and homobibenzyl motifs commonly found as substructures in ligands for the estrogen receptor (ER). Representative members were prepared from three classes: *N*-phenyl benzamides, *N*-phenyl acetamides, and *N*-benzyl benzamides; in some cases the corresponding thiocarboxamides and sulfonamides were also prepared. Of these three classes, the *N*-phenyl benzamides had the highest affinity for ER, the *N*-phenyl acetamides had lower, and the *N*-benzyl benzamides were prone to fragmentation via a quinone methide intermediate. In the *N*-phenyl benzamide series, the highest affinity analogues had bulky *N*-substituents; a CF₃ group, in particular, conferred high affinity. The thiocarboxamides bound better than the corresponding carboxamides and these bound better than the corresponding sulfonamides. Binding affinity comparisons suggest that the *p*-hydroxy group on the benzoate ring, which contributes most to the binding, is playing the role of the phenolic hydroxyl of estradiol. Computational studies and NMR and X-ray crystallographic analysis indicate that the two anilide systems studied have a strong preference for the *s-cis* or *exo* amide conformation, which places the two aromatic rings in a *syn* orientation. We used this structural template, together with the X-ray structure of the ER ligand binding domain, to elaborate an additional hydrogen bonding site on a benzamide system that elevated receptor binding further. When assayed on the individual ER subtypes, ER α and ER β , these compounds show modest binding affinity preference for ER α . In a reporter gene transfection assay of transcriptional activity, the amides generally have full to nearly full agonist character on ER α , but have moderate to full antagonist character on ER β . One high affinity carboxamide is 500-fold more potent as an agonist on ER α than on ER β . This work illustrates that ER ligands having simple amide core structures can be readily prepared, but that high affinity binding requires an appropriate distribution of bulk, polarity, and functionality. The strong conformational preference of the core anilide function in all of these ligands defines a rather rigid geometry for further structural and functional expansion of these series. © 2000 Elsevier Science Ltd. All rights reserved.

Introduction

Recent advances in nuclear hormone receptor pharmacology and mechanism of action have redefined the classification of estrogen receptor (ER) ligands.¹ The selective estrogen receptor modulator class, or SERMs, are considered to be very important because of the potential of SERMs for maintaining bone mineral density and cardiovascular health, and for treating and preventing breast cancer and other hormone-dependent

disorders, without adverse stimulation of the uterus and breast.² SERMs comprise several structurally diverse classes, including the triarylethylenes, triarylnaphthalenes, benzo[b]furans, benzopyrans, and various other tetracyclic manifestations of these core structures.³ Collectively, SERMs display a wide range of tissue-selective agonist and antagonist activities, but major efforts continue to be directed toward optimizing ER ligand structure in order to obtain desired tissue-specific properties with minimal side-effects, which is an important concern in maintaining efficacy and patient compliance.⁴

*Corresponding author. Tel.: +1-217-333-6310; fax: +1-217-333-7325; e-mail: jkatzene@uiuc.edu

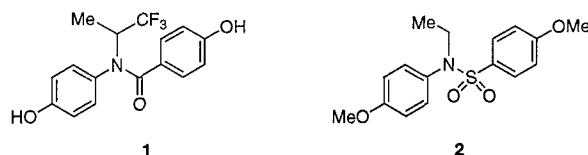
In connection with our interests in novel templates for ER ligands, especially ones that might be suitable for

combinatorial development,⁵ we wondered whether acyclic tertiary amides might be developed as mimics of common structural motifs found at the core of many ER ligands and thus support a combinatorial approach to SERM discovery and optimization. In this report, we describe the design and synthesis of three types of amide-core ER ligands, and we investigate their molecular structure, their structure binding–affinity relationships, and their activity in ER α and ER β transactivation assays. A number of interesting trends and high affinity amides were discovered during this investigation. One high affinity amide in particular (**16g**) was found to be an ER α -potency selective agonist.

Results and Discussion

Rationale and design

To the best of our knowledge, only two examples of ER ligands containing, either partially or exclusively, an amide core structure are known in the public literature. Hartmann and co-workers studied a small series of bis-phenolic carboxamides^{6,7} containing an invariant *N*-(1,1,1-trifluoro-2-propyl) substituent (e.g., **1**) and found them to be anti-estrogens with weak to moderate potency. An early example of an *N*-ethyl benzene sulfonamide (**2**)⁸ was also reported and shown to be weakly estrogenic in vivo. Neglecting amide bond stereoisomers for the moment, these ligands represent potential mimics (**I**) for either the *anti*- or *syn*-bibenzyl motifs **A** and **B**, respectively (Fig. 1, right), that are found in many common ER ligands (Fig. 1, left). In addition to the bibenzyl structural template of these leads, we envisioned two homologues (**II** and **III**, Fig. 2, right) which mimic the *homo*-bibenzyl motif **C** (Fig. 2, **II–III**), a structural element that is also well represented in high affinity ligands for the ER (Fig. 2, left).



From this analysis, model *para*-substituted bis-phenolic carboxamides, sulfonamides and thioamides containing *N*-alkyl and trifluoroalkyl substituents (**R** and **R'**) were considered as potential templates for combinatorial development (Fig. 3). Preparation for many of these compounds is straightforward and thus not unreasonable for adaptation to combinatorial library synthesis.

Chemical syntheses

***N*-Phenyl benzamides and benzene sulfonamides.** To synthesize simple *N*-alkyl amide analogues in an expeditious manner, we used catalytic phase transfer conditions (Scheme 1). Thus, *N*-alkylation of the known secondary benzene sulfonamide **3**⁸ proceeded under mild conditions using *n*-Bu₄NSO₄H, NaOH, and excess alkyl halide in CH₂Cl₂/H₂O.⁹ The target *N*-alkylated sulfonamides **5a–c** were then obtained after deprotection. The less acidic carboxamide **6** was alkylated using a solid–liquid two-phase system, consisting of powdered NaOH and cat. *n*-Bu₄NBr in refluxing benzene, to afford the tertiary amides **9a–e** in good yield.^{9,10} Carboxamides **9f** and **9g** were conveniently prepared from the secondary anilines **7** and **8**. Aniline **7** was prepared via reductive alkylation of the corresponding aldimine using a modified literature procedure.¹¹ Aniline **8** was obtained by reductive amination, using NaBH(OAc)₃, *p*-anisidine, and 3-methyl-2-butanone. Thioamides were prepared in relatively good yield by treating the carboxamide (**9a–g**) with Lawesson's reagent.¹² Deprotection with BBr₃ or

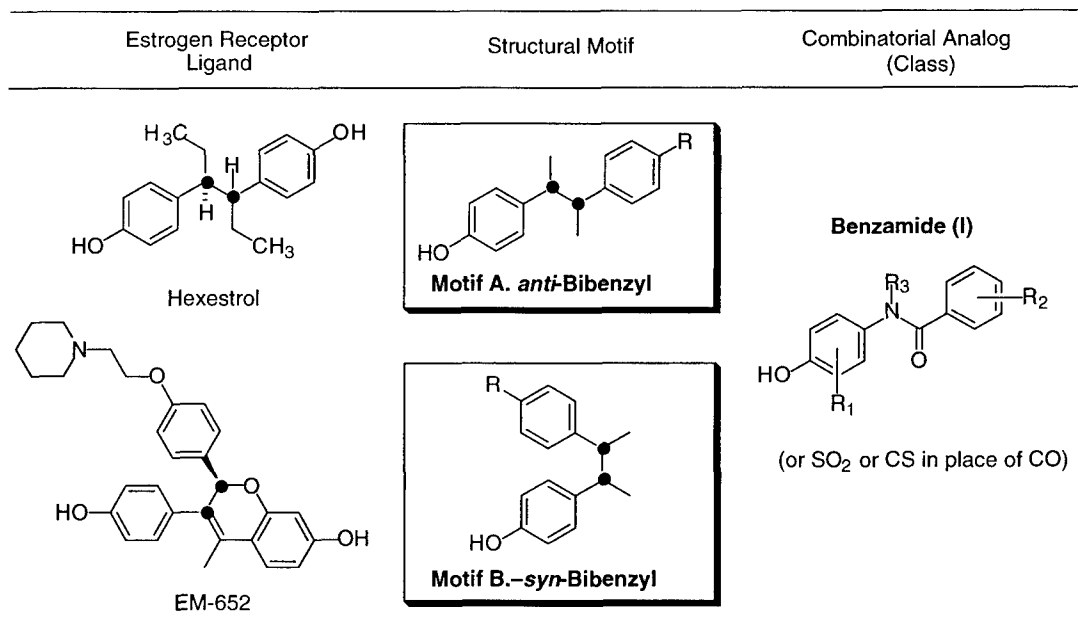


Figure 1. *Syn* and *anti*-bibenzyl motifs and proposed acyclic amide analogues.

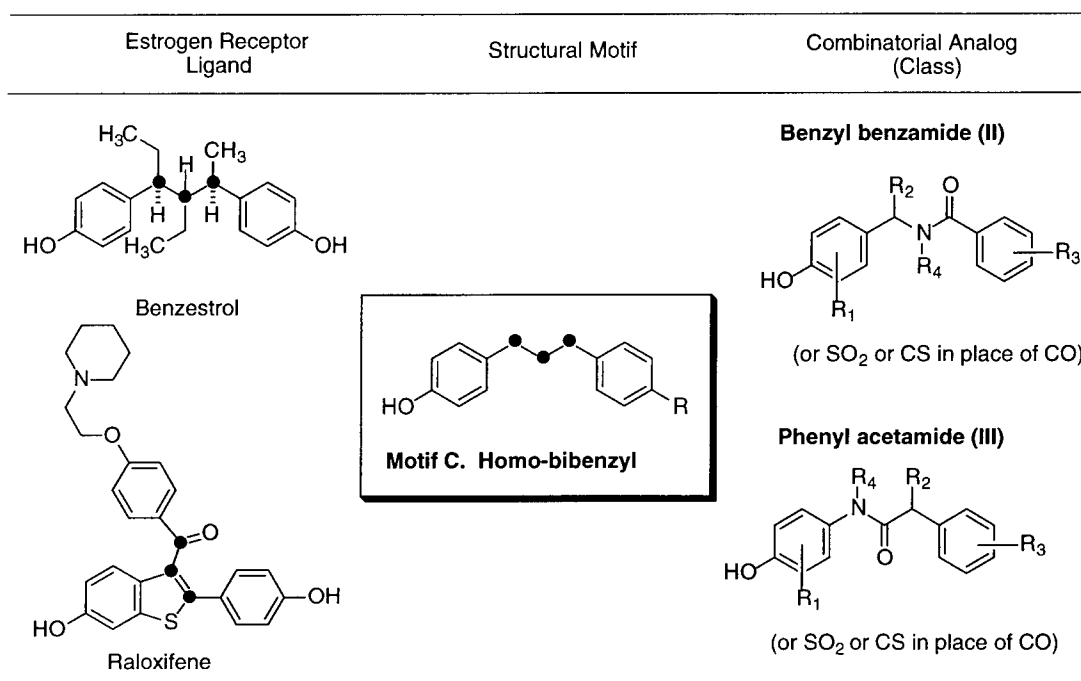


Figure 2. Homo-bibenzyl motif and proposed acyclic amide analogues.

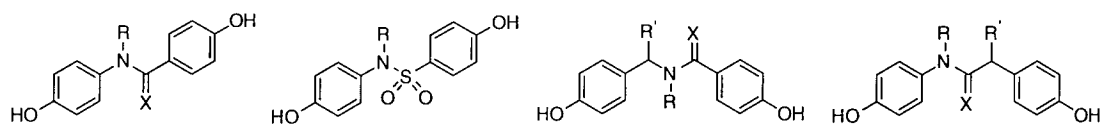
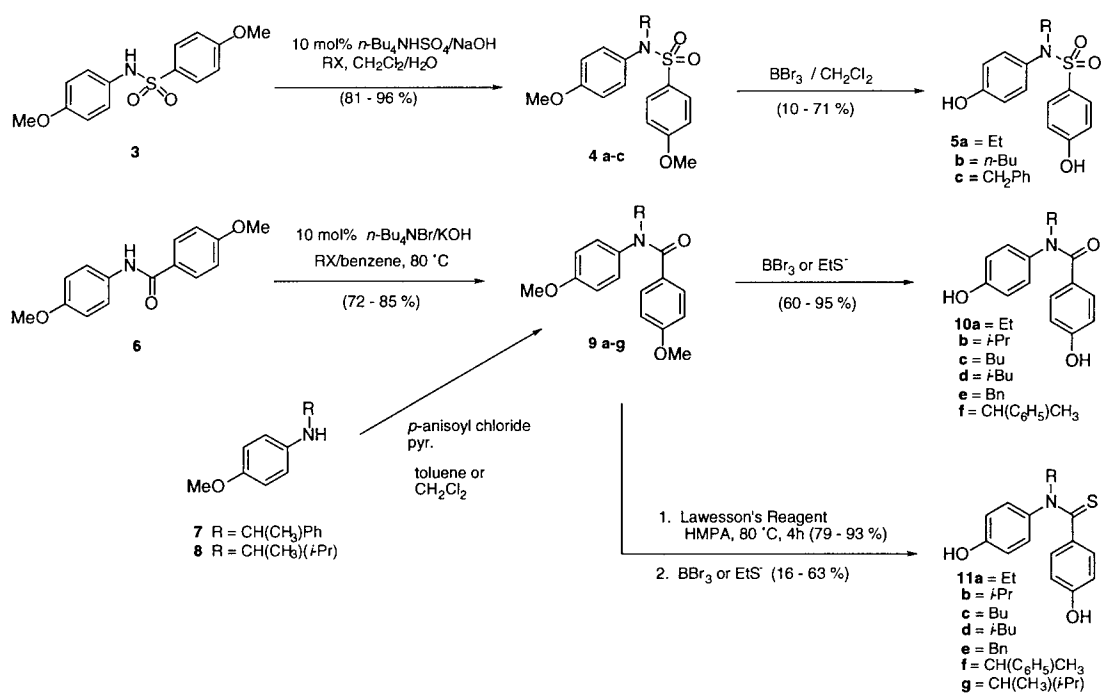


Figure 3. Potential amide ER ligand scaffolds for combinatorial chemistry (X = O, S).

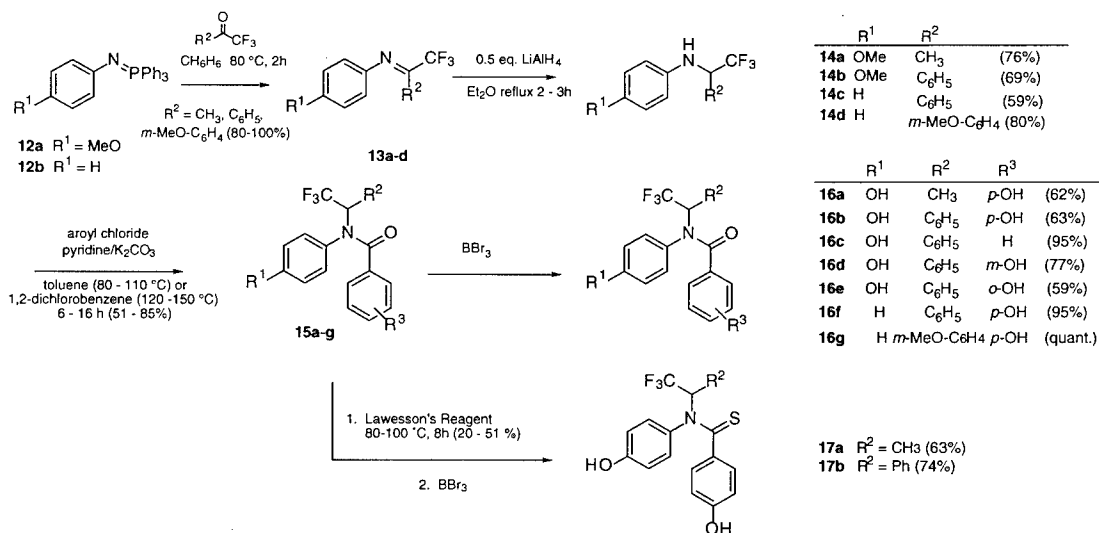
Scheme 1. Synthesis of *N*-phenyl benzamides.

ethanethiolate afforded the target benzamides **10a–f** and thiobenzamides **11a–g**.

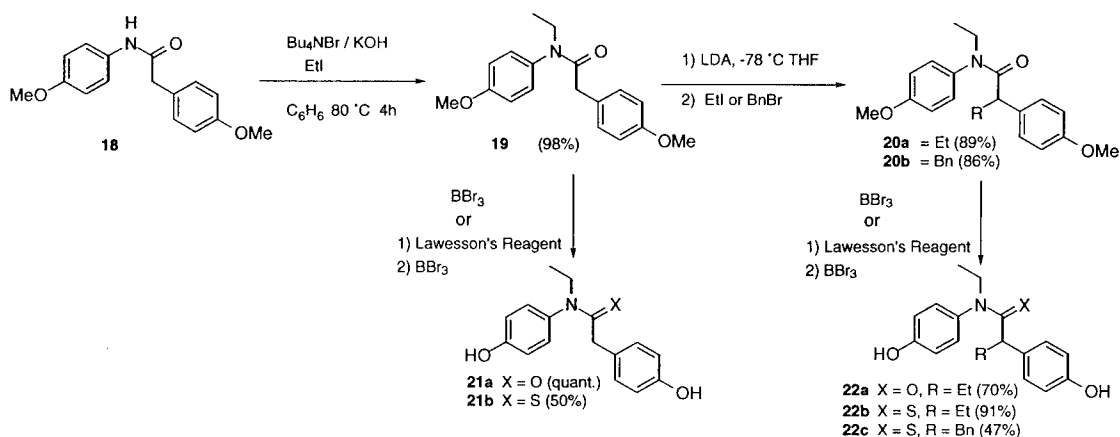
CF₃-containing *N*-phenyl benzamides. To further explore the effect that a trifluoromethyl group would have on receptor binding affinity, we prepared several carboxamide and thioamide analogues related to the weak anti-estrogen (**1**) reported by Hartmann and co-workers.⁶ The synthetic route to CF₃-amide analogues, depicted in Scheme 2, was adapted from that reported by Hartmann and required introduction of the CF₃-alkyl substituent at the aniline stage in two steps starting from the corresponding iminophosphoranes. The starting trifluoromethylketones were commercially available, with the exception of 2,2,2-trifluoro-1-(3-methoxyphenyl)ethanone, which was prepared from 3-bromoanisole according to the procedures described by Hatanaka et al. and references therein.¹³ Ylides **12a** and **12b** were readily obtained by treatment of the corresponding azides with Ph₃P.^{14,15} Subsequent Staudinger reaction to afford the CF₃-substituted imines **13a–d**, followed by LAH reduction, furnished the desired secondary anilines **14a–d** in good overall yield.

Amidation in warm toluene proceeded satisfactorily to provide carboxamides **15a–e**; however, unactivated anilines **14c** and **14d** required 1,2-dichlorobenzene as solvent and higher temperatures to afford benzamides **15f** and **15g** in satisfactory yields. Subsequent deprotection using BBr₃ afforded the desired phenols **16a–g** as before. Thionation of the protected, CF₃-substituted carboxamides proceeded in significantly lower yield (20–51%) than did those with simple *N*-alkyl substitution (>79%). Alternative thionation conditions, such as P₂S₅ and POCl₃/(TMS)₂S, did not give improved yields. Nevertheless, the two thioamides **17a** and **17b** could be obtained after deprotection with BBr₃.

***N*-Phenyl acetamides and *N*-benzyl benzamides.** Acetamides were attractive because they offer an additional site for structural diversity that is not available in benzamides (Scheme 3). *N*-Ethylation of amide **18** using PTC conditions as before afforded **19** in excellent yield. Subsequent α -alkylation using LDA at –78 °C then afforded the disubstituted carboxamides **20a–b** in high yield. Thionation and/or deprotection as before furnished



Scheme 2. Synthesis of CF₃-containing *N*-phenyl benzamides.



Scheme 3. Synthesis of *N*-phenyl-acetamides.

the desired bis-phenolic amides **21a–b** and **22a–c** without complication.

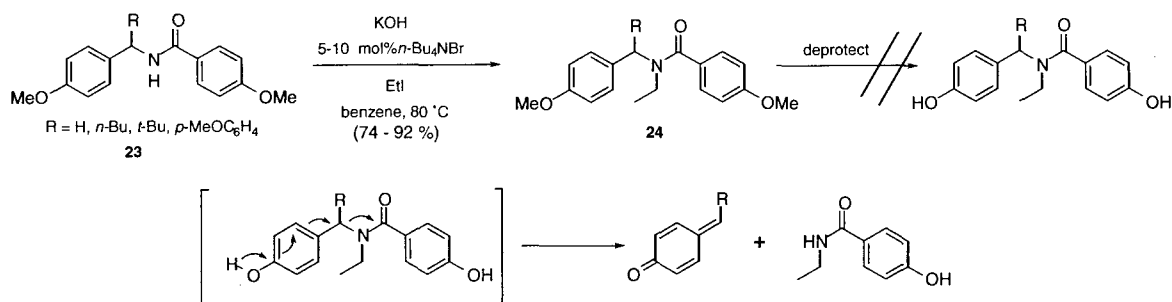
The *N*-benzyl-*N*-alkylbenzamides **24** (Scheme 4), which are essentially amide isomers of the acetamide class, and related benzenesulfonamides (not shown), were also investigated. These *N*-benzyl amides, protected as methyl ethers, could be prepared by routes that are analogous to those used in Schemes 1–3. However, these systems proved to be unstable to various deprotection conditions: BBr_3 , ethanethiolate, HBr/AcOH and TMSI all led to decomposition. The only isolatable products were the corresponding secondary amides, presumed to result from an elimination of the 4-hydroxy-*N*-benzyl substituent via a quinone-methide intermediate (Scheme 4). Due to their propensity for elimination, additional efforts were not made to prepare members of the *N*-benzyl benzamide class.

CF_3 -containing *N*-phenyl acetamides. Incorporation of the CF_3 -group was also explored in the acetamide series, and the synthesis of α -substituted acetamides containing an *N*-(1,1,1-trifluoro-2-propyl) substituent is shown in Scheme 5. Thus, the *N*-(1,1,1-trifluoro-2-propyl) substituted aniline **12a** was treated with 4-methoxyphenylacetyl chloride to afford carboxamide **25**. α -Alkylation as before using LDA at -78°C and MeI proceeded in excellent yield to give **26** as a $\sim 1:1$ mixture of diastereomers as indicated by ^1H NMR and HPLC analysis. Demethylation then afforded the di-substituted phenylacetamide **27** in good yield. Unfortunately,

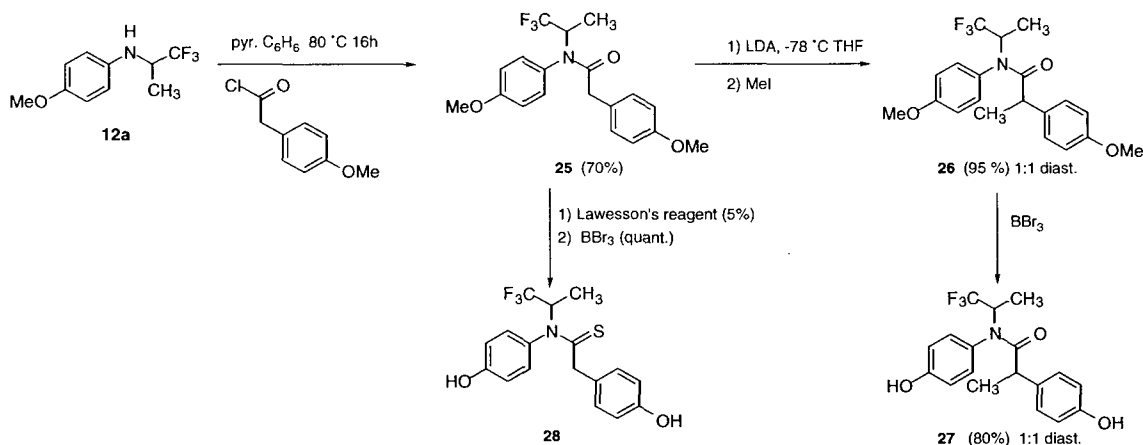
attempts to thionate **26** with Lawesson's reagent failed; however, treatment of the unsubstituted phenylacetamide **25** with Lawesson's reagent did give thioamide **28**, in albeit low yield. Repeated attempts using other reagents (P_2S_5 and $\text{POC}_{13}/(\text{TMS})_2\text{S}$) or higher temperatures failed to provide thioamide **26** or to improve the yield of **28**. Increased steric hindrance about the $\text{C}=\text{O}$ bond is thought to be responsible for the lack of reactivity of the CF_3 -substituted *N*-phenyl acetamides towards $\text{O}\text{--}\text{S}$ replacement, as lower yields for thionation were also observed for the CF_3 -containing benzamides (Scheme 2).

Molecular conformation

As was noted in Figure 1, bibenzyl motifs in ER ligands are well represented as both *syn* and *anti* conformations. Since *N*-aryl-benzamides share a similar bibenzyl-like two-atom connection between two aromatic rings, we were interested in their conformational preference to establish which structural motif they might be mimicking. From early ^1H NMR studies of *N*-substituted anilides, there is known to be a surprisingly strong preference for the *exo*-isomer (*N*-phenyl group *trans* to carbonyl oxygen).¹⁶ Even simple *N*-methyl and *N*-ethylformanilides, where steric considerations would place the bulkier alkyl group next to the formyl hydrogen in an *endo* preference, have a 95% *exo* preference in solution.¹⁷ This so-called '*exo*-rule' is quite general, and it has been stated that for *N*-substituted anilides other than formyl, the *exo*-isomer dominates to the exclusion

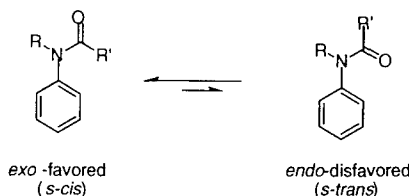


Scheme 4. Attempted synthesis of *N*-benzyl-benzamides.



Scheme 5. Synthesis of CF_3 -containing *N*-alkyl-phenylacetamides.

of the *endo*-isomer.¹⁶ The *endo*-isomer is detectable only when large *ortho* substituents are present on the *N*-phenyl ring or when $R'=H$.



Molecular modeling studies on both carboxamide **16a** and thiocarboxamide **17a** that we have performed using molecular mechanics (MM2) were in agreement with the reported NMR observations, and indicated the *exo* or *s-cis* conformer as being energetically more favorable (Fig. 4). In the case of carboxamide **16a**, a substantial ΔH of 5.3 kcal/mol between the global minimum energy *cis* and *trans* isomers was found, the major energetic difference being due to additional electrostatic contributions in the *s-trans* conformation. Thiocarboxamide **17a** has a smaller ΔH of 0.9 kcal/mol between the global minimum energy *cis* and *trans* isomers (not shown). This result is in accord with destabilization of the *s-cis* (*exo*) thioamide conformer relative to the *s-trans* (*endo*) conformer because of additional steric repulsions between sulfur and the *N*-alkyl substituent that arise from the larger covalent radii of sulfur versus oxygen (1.4 Å for sulfur, 0.74 Å for oxygen) and its longer bond length (C=S 1.64 Å; C=O 1.24 Å).

Direct structural studies of *N*-substituted thioanilides, let alone hindered systems containing a CF_3 -substituent, have not been reported, as far as we have found. For this reason and because of the relatively small energy difference found from molecular modeling for **17a**, we obtained an X-ray crystallographic structure of the methyl ether derivative of **17a** to firmly establish its preferred stereochemistry about the amide bond. In

addition, for comparison, a crystallographic structure was determined on the less hindered *N*-(*i*-propyl)-carboxamide **10b**. ORTEP representations of these molecules are shown in Figure 5.

As can be seen in Figure 5, both the *i*-propyl carboxamide and CF_3 -substituted thioamide were found to crystallize in the lower energy *s-cis* conformation. Prominent torsion angles are indicated in Table 1. Comparison of the amide torsional bonds (torsion A) reveals greater deviation of the *N*-aryl ring from the amide plane in thiocarboxamide **17a** compared to **10b** (18° versus 9.7°), consistent with the greater steric hindrance anticipated in the amide plane of the thioamide system. The greater distortion in the thioamide bond planarity is also evident from its improper torsion (torsion E) and its *N*-alkyl torsion B. Both structures also show a twisting of the phenyl rings out of the amide plane (C and D), with the thioamide being more planar. This difference appears in part to be due to additional nearby non-bonding interactions with the CF_3 -group in thioamide **17a**.

Solution VT ^1H NMR experiments (Fig. 6) were also conducted, and the results were found to be consistent with a single amide conformer. Shown in Figure 6 is the ^1H NMR spectrum of the aromatic region for thioamide **17a** at -60 , $+23$, and $+55^\circ\text{C}$ in MeOD. The spectra at -60°C and room temperature are very similar. Interestingly, there is a slow rotation about the N–C bond of the *N*-phenyl group, which results in distinct signals for the *ortho* and *meta* ring protons of the *N*-phenyl ring. Assignments are based on COSY cross couplings. Upon heating to $+55^\circ\text{C}$, no new signals are observed for either the CH_3 group (not shown), which remains a doublet at all three temperatures, or the aryl protons. However, the *ortho* and *meta* signals of the *N*-phenyl ring coalesce. This type of slow N–C rotation is well known in *N*-phenyl carboxamides and is analogous to hindered bi-phenyl rotations.¹⁶ The lack of

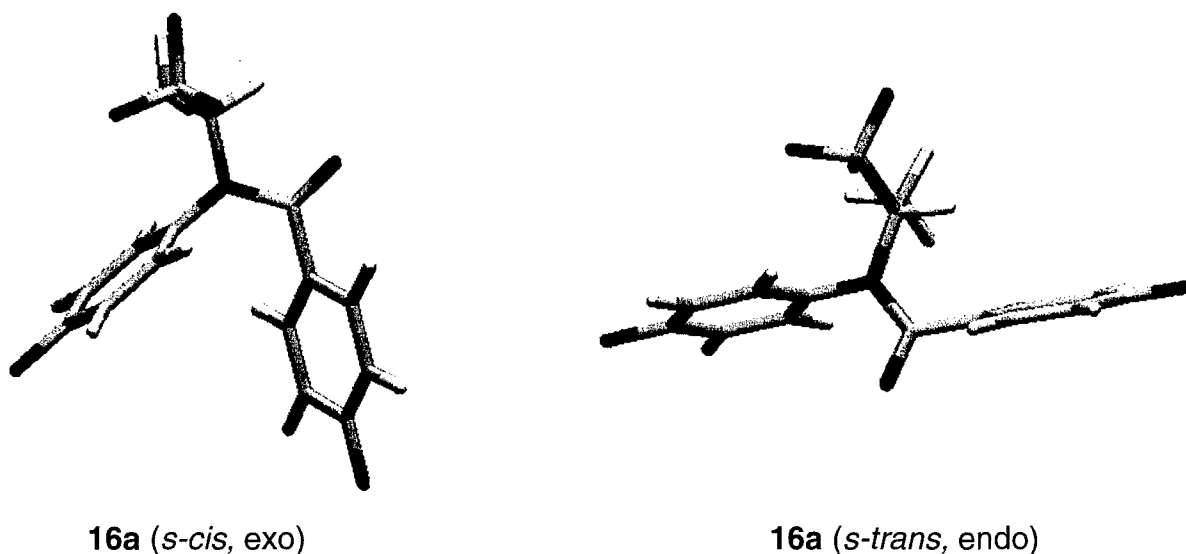


Figure 4. Capped-stick models of lowest energy *c-cis* and *s-trans* conformers of caboxamide **16a**. This *s-cis* conformer (left) has lower energy ($\Delta H=5.3$ kcal/mol).

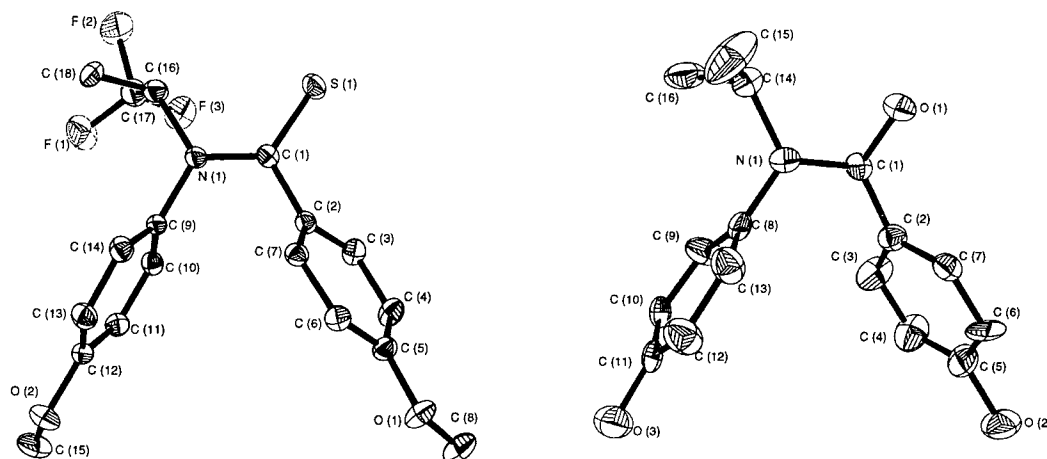


Figure 5. Molecular structures for thiocarboxamide **17a** (left) and carboxamide **10b** (right) (ORTEP; ellipsoids drawn at the 35% probability level).

Table 1. Prominent torsion angles found in carboxamide **10b** and thiocarboxamide **17a**

| Torsion | Compound 17a thioamide 1–4 atoms | Angle | Compound 10b carboxamide 1–4 atoms | Angle |
|---------|---|-------|---|-------|
| A | C(2)–C(9) | 18° | C(2)–C(8) | 9.7° |
| B | C(16)–S(1) | 7.8° | C(14)–O(1) | 3.2° |
| C | C(1)–C(10) | 76° | C(1)–C(9) | 80° |
| D | C(3)–N(1) | 50° | C(3)–N(1) | 62° |
| E | <i>N</i> -improper torsion | 5.4° | <i>N</i> -improper torsion | 4.6° |

additional signals indicates that there is a single amide conformer in solution, which we presume, on the basis of the computational and X-ray structures, to be the *s-cis*. Furthermore, for thioamides, it is worthy to note that the barrier for *cis*–*trans* inter-conversion is generally 2–5 kcal greater than it is for the analogous carboxamides. The traditional ‘resonance model’ used to rationalize the origin of the higher *cis*–*trans* barriers in thioamides has recently been challenged¹⁸ and is currently under debate.^{19–22} Nevertheless, from these studies we believe that it is reasonable to conclude that sterically hindered *N*-aryl **thiobenzamides** also have a strongly preferred *s-cis* conformation, similar to *N*-substituted **oxoanilides**. Therefore, these systems can be considered as mimics of the *syn*-biphenyl substructural motif.

Receptor binding affinities and structure–binding affinity relationships

Binding affinities for the estrogen receptor and octanol–water partition coefficients ($\text{Log } P^{o/w}$) determinations of the benzamides we have prepared are shown in Table 2 and are organized according to the substituent on the amide nitrogen (either *N*-alkyl/aryl or *N*-CF₃ containing alkyl/aryl). Binding affinities and $\text{Log } P^{o/w}$ determinations for phenylacetamides are presented in Table 3. Binding affinities were obtained from a competitive radiometric binding assay, using [³H]estradiol as tracer and lamb uterine cytosol as a source of ER, and they are expressed as relative binding affinities (RBA), with estradiol having an affinity of 100%. Additional binding

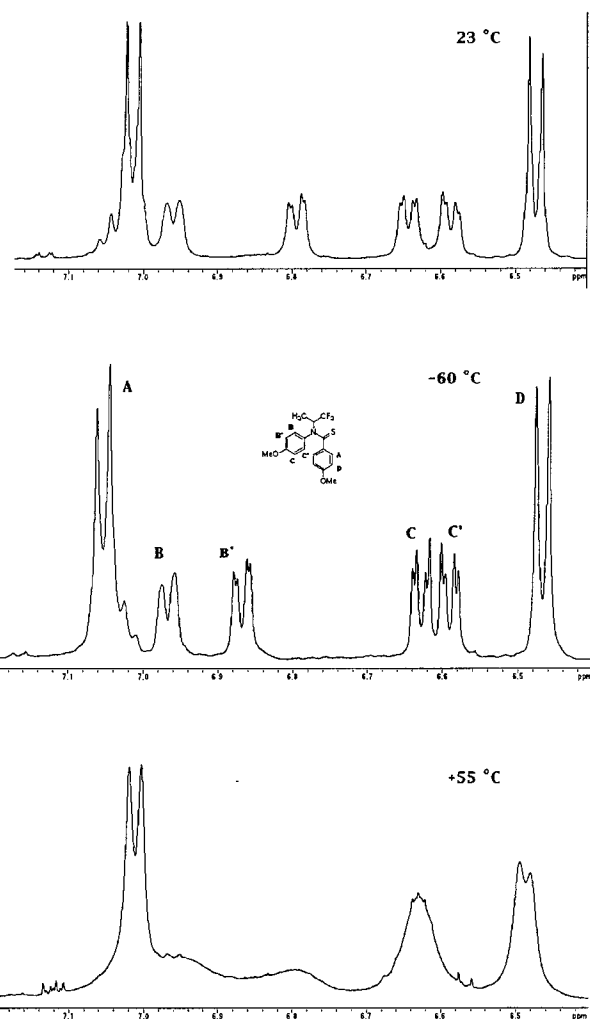
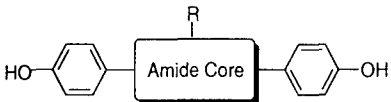


Figure 6. VT-¹H NMR for **17a**, aromatic region.

assays of select compounds for receptor subtypes ER α and ER β , as well as ER α and ER β transcriptional activation profiles in human endometrial cancer (HEC-1) cells using an estrogen-responsive reporter gene construct, are also shown in Table 4. $\text{Log } P^{o/w}$ determinations were obtained according to the method of Minick,

Table 2. Estrogen receptor relative binding affinity RBA (estradiol = 100) and log octanol–water partition coefficient (log $P^{o/w}$) data for *N*-phenyl-benzamides


| Compound | Core structure | R group | RBA ^a | Log $P^{o/w}$ |
|----------|----------------------|---|------------------|---------------|
| 5a | -CSO ₂ R- | Et | 0.23 | 2.76 |
| 5b | | <i>n</i> -Bu | 0.13 | 3.66 |
| 5c | | Bn | 0.053 | 4.62 |
| 10a | -CONR- | Et | 0.062 | 2.40 |
| 10b | | <i>i</i> -Pr | 0.009 | 2.31 |
| 10c | | <i>n</i> -Bu | 0.042 | — |
| 10d | | <i>i</i> -Bu | 0.020 | 3.15 |
| 10e | | CH ₂ Ph | 0.089 | — |
| 10f | | CH(C ₆ H ₅)CH ₃ | 0.45 | 3.96 |
| 11a | -CSNR- | Et | 0.62 | 2.80 |
| 11b | | <i>i</i> -Pr | 0.83 | 2.97 |
| 11c | | <i>n</i> -Bu | 1.3 | 3.99 |
| 11d | | <i>i</i> -Bu | 1.5 | — |
| 11e | | CH ₂ Ph | 0.15 | — |
| 11f | | CH(C ₆ H ₅)CH ₃ | 2.5 | 3.98 |
| 11g | | CH(CH ₃)(<i>i</i> -Pr) | 4.6 | 4.31 |

^aRelative binding affinities are the average of duplicate determinations (CV 0.3), measured in lamb uterine cytosol. For estradiol, RBA = 100. For details, see Experimental.

Table 3. Estrogen receptor relative binding affinity RBA (estradiol = 100) and log octanol–water partition coefficient (log $P^{o/w}$) data for *N*-CF₃-substituted benzamides

| Compound | X | R ¹ | R ² | R ³ | RBA ^a | Log $P^{o/w}$ |
|----------|---|----------------|---|----------------|------------------|---------------|
| 16a | O | HO | CH ₃ | <i>p</i> -HO | 0.49 | 3.29 |
| 16b | O | HO | C ₆ H ₅ | <i>p</i> -HO | 9.0 | 4.51 |
| 16c | O | HO | C ₆ H ₅ | H | 0.063 | 4.46 |
| 16d | O | HO | C ₆ H ₅ | <i>m</i> -HO | 0.45 | — |
| 16e | O | HO | C ₆ H ₅ | <i>o</i> -HO | 0.068 | — |
| 16f | O | H | C ₆ H ₅ | <i>p</i> -HO | 8.9 | 4.97 |
| 16g | O | H | <i>m</i> -HOC ₆ H ₄ | <i>p</i> -HO | 15 | 4.63 |
| 17a | S | HO | CH ₃ | <i>p</i> -HO | 7.5 | 3.99 |
| 17b | S | HO | C ₆ H ₅ | <i>p</i> -HO | 14 | 5.40 |

^aRelative binding affinities are the average of duplicate determinations (CV 0.3), measured in lamb uterine cytosol. For estradiol, RBA = 100. For details, see Experimental.

using a standardized Chromegabond MC8 reverse phase HPLC system.²³

Binding affinity of *N*-phenyl benzamides. The receptor binding affinities for *N*-phenyl benzamides are shown in Table 2. The sulfonamides and carboxamides all have rather low affinity, the highest being carboxamide **10f**. Within the carboxamide series (**10a–f**), it is interesting to compare the effect of branching near the amide core. For example, the ethyl (**10a**) and benzyl (**10e**) compounds have similarly low affinities, and likewise the branched *i*-propyl amide **10b** has very low affinity. However, amide **10f**, which contains both an α -phenyl and methyl substituent, shows a significant, 5- to 7-fold increase in affinity compared to either monosubstituted amide **10a** or **10e**. Overall, the analogous *N*-alkyl

Table 4. Estrogen receptor relative binding affinity RBA (estradiol = 100) and log octanol–water partition coefficient (log $P^{o/w}$) data for *N*-phenyl phenylacetamides

| Compound | X | R ¹ | R ² | RBA ^a | Log $P^{o/w}$ |
|----------|---|--|---------------------------------|------------------|---------------|
| 21a | O | CH ₂ CH ₃ | H | 0.006 | 2.68 |
| 22a | O | CH ₂ CH ₃ | CH ₂ CH ₃ | 0.004 | 3.52 |
| 27 | O | CH(CH ₃)(CF ₃) | CH ₃ | 0.010 | — |
| 28 | S | CH(CH ₃)(CF ₃) | H | 0.66 | — |
| 21b | S | CH ₂ CH ₃ | H | 0.20 | 3.40 |
| 22b | S | CH ₂ CH ₃ | CH ₂ CH ₃ | 0.089 | 4.27 |
| 22c | S | CH ₂ CH ₃ | CH ₂ Ph | 0.34 | — |

^aRelative binding affinities are the average of duplicate determinations (CV 0.3), measured in lamb uterine cytosol. For estradiol, RBA = 100. For details, see Experimental.

thioamides (**11a–g**) bind with affinity 2- to 90-fold greater than their carboxamide counterparts, which is presumably due to their greater hydrophobic character, although there are not great differences in the Log $P^{o/w}$ values, where comparisons can be made. A related trend is also observed in other non-steroidal ligands containing heteroatoms, such as benzo[*b*]furans and benzo[*b*]thiophenes, with benzo[*b*]thiophenes displaying higher affinity than benzo[*b*]furans.^{24,25}

The beneficial effect of placing more sterically encumbered groups near the amide core on receptor affinity is also evident in the thioamide series, because the same relative affinity increases which occurred for carboxamides (**10a** < **10e** < **10f**) are also reflected in the thioamides (**11e** < **11a** < **11f**). Replacement of the phenyl substituent in **11f** with an *i*-propyl group to afford thioamide **11g** results in even greater crowding near the amide plane, enhancing the relative affinity to 4.6%, the highest observed for any simple *N*-phenyl benzamide.

Binding affinity of CF₃-containing *N*-phenyl benzamides.

The RBA data for the CF₃-containing benzamides are presented in Table 3. Immediately apparent is the relatively high binding affinity for thioamide **17b** and carboxamide **16g**, and to a lesser extent amides **16b**, **16f** and **17a**. Compound **16a**, reported by Hartmann and co-workers, is included for comparison.⁶ In general, all the CF₃-substituted benzamides show affinity enhancements relative to their non-fluorinated amide counterparts (Table 2).

Shown in Figure 7 are four direct comparisons of RBA and Log $P^{o/w}$ data for benzamides from Tables 2 and 3. These four pairs of compounds clearly show the relationship between core structure (*O* and *S* substitution) and peripheral group presentation (methyl to phenyl, and methyl to trifluoromethyl) and how these components alter ER affinity.

Comparison of the relative RBAs for these four pairs of amides, starting from the *i*-propyl pair (upper left) to the CF₃-containing phenethyl pair (lower right), shows a diminishing effect of sulfur–oxygen replacement as binding affinity increases and as larger substituents are added near the amide core. The sulfur–oxygen

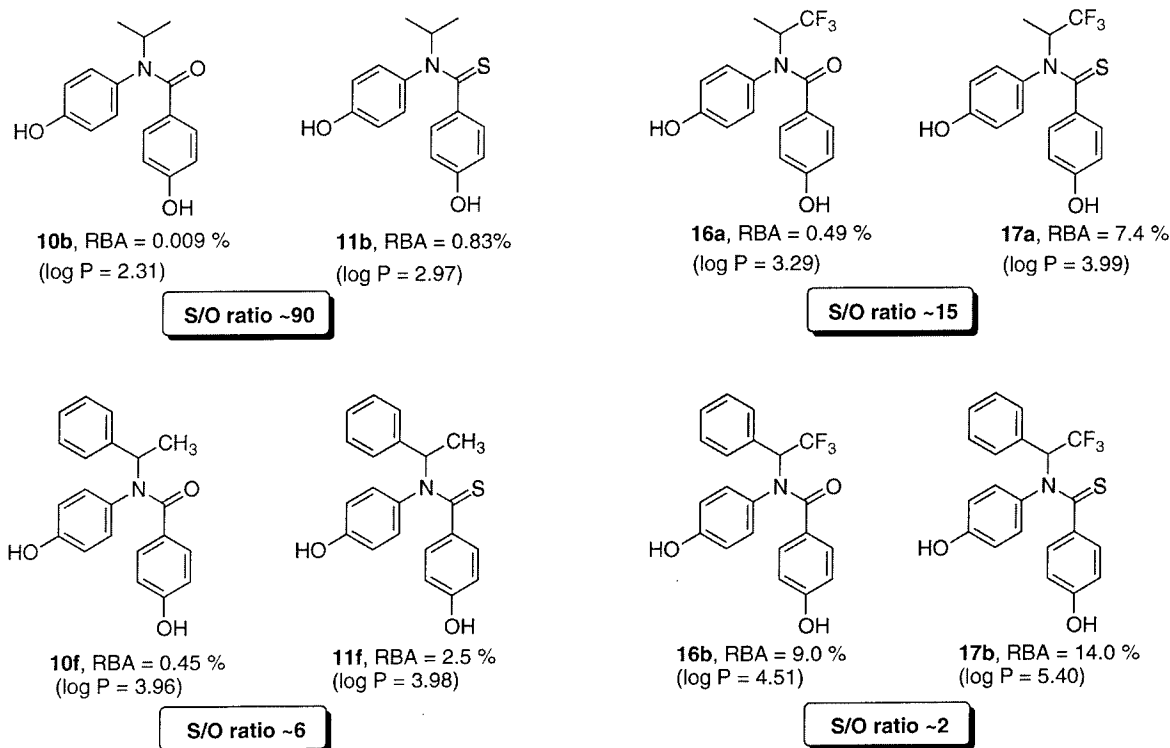


Figure 7. Comparison of the relative binding affinities of the principal carboxamides and thiocarboxamides.

enhancement is greatest in the parent *i*-propyl system (**10b** versus **11b**), where the overall affinity is lowest, and is least when the substituents are phenyl and trifluoromethyl (**16b** versus **17b**), where the overall affinity is highest. In addition, there is a general increase in binding affinity with increasing lipophilicity. The observed parallel affinity–lipophilicity increase within the series is not too surprising in light of what is known about the hydrophobic character of the ER ligand binding pocket.²⁶

CF₃ effect: lipophilic, steric or electrostatic effects? The effect of adding a CF₃ group in place of methyl on the RBA may be the result of several factors, including lipophilic, steric and/or electrostatic effects. In terms of steric effects, a recent review by O'Hagan and Rzepa²⁷ cites several studies which place an upper size limit of a CF₃-group being close to that of *i*-propyl. The greatest increases in RBA for CH₃ to CF₃ substitution are found in the carboxamide class (20- to 50-fold, versus 5- to 8-fold for thioamide), with the highest being the *i*-propyl compounds (Fig. 7, **16a** versus **10b**). In order to test whether or not RBA increases associated with CF₃-replacement are the result of its steric or its electronic property, the branched CH(CH₃)(*i*-Pr) thioamide **11g** was prepared to compare with the CF₃ analogue **17a**. Based on the above-mentioned studies, if steric effects alone operate, compound **11g** would be expected to have an RBA close to that of the CF₃-substituted thioamide **17a** (7.5%). The observed RBA, however, for compound **11g** was only 4.6%. This indicates that an additional effect may be contributing to the binding energy, either lipophilic or electrostatic. The fact that

the Log *P*_{o/w} values for **11g** and **17a** are quite similar, with **11g** being somewhat higher, suggests that the difference in binding affinity is probably not due to a lipophilic component. Thus, based on this data it would seem that the additional component has, in addition to its steric effect, an electronic effect as well.

Optimization of binding orientation and hydroxylation pattern. For unsymmetrical non-steroidal ER ligands, a common approach to determining which phenol is imitating the crucial A-ring phenol of estradiol is to prepare and test the corresponding mono-phenolic derivatives.²⁸ The highest affinity mono-phenolic analogue is then presumed to be the A-ring mimic, because the hydroxyl substituent at this position is known to be very important in binding to the ER. Many non-steroidal ER ligands benefit from a second hydroxyl hydrogen bonding partner and appear to do so in an *anti*-bibenzyl motif, which places the hydroxyl oxygen–oxygen interatomic distances approx. 10–12 Å. Thus, it was apparent to us that the rigid *s-cis* benzamide conformation (*syn*-bibenzyl motif) in our amides was likely not benefiting from a second hydrogen bonding interaction, because its hydroxyl oxygen–oxygen interatomic distance was only 7.4 Å. The importance for this second hydrogen bond is evident in the recent non-steroidal diethylstilbestrol and raloxifene ERα LBD crystal structures.^{26,29} Both of these complexes have an expected A-ring phenol mimic and a second phenol imitating the D-ring 17β-hydroxyl group of estradiol. In both cases, the second phenol uses the same hydrogen bond interaction with His₅₂₄ as does the 17β-hydroxyl group of estradiol.

To obtain an optimal hydroxylation pattern and discern which ring phenol was imitating the A-ring phenol of estradiol, we prepared benzamides **16c–g**. The results of these studies (Table 3) clearly show a pattern indicative of a preferred A-ring phenol mimic. For example, removal of the 4-hydroxyl phenol on the benzamide ring and retention of the 4-hydroxyl of the *N*-phenyl in compound **16c** lead to a nearly complete loss in binding affinity compared to the parent di-hydroxy compound **16b** (RBA = 0.063% versus 9.0%). In contrast, removal of *N*-phenyl hydroxyl and retention of the benzamide 4-hydroxyl result in an analogue **16f**, which retains a binding affinity equivalent to that of the parent compound. These findings clearly implicate the benzoyl ring phenol as the A-ring mimic of estradiol. In addition, as might be expected, positioning the hydroxyls elsewhere on the benzoyl ring is not well tolerated, as both the *ortho*- and *meta*-hydroxy analogues **16d** and **16e** have little or no affinity for the receptor.

Having discerned which phenol in the benzamide system was important for binding, we wished to explore alternative positions for a second hydroxyl group in order to benefit from the second hydrogen bonding interaction which is found in the raloxifene and DES ER binding pockets. Depicted in Figure 8 is a schematic representation of the predicted binding mode and phenol interactions for benzamide **16f** in the binding pocket of ER. This rudimentary model was derived from the interactions that were described to be present in the estradiol (E_2) X-ray crystal structure in the ER α LBD, the coordinates of which, at the time of our consideration, were not released.²⁶ Based on this view, we proposed that a hydroxyl substituent on the phenethyl ring might be positioned in the binding subpocket near His₅₂₄.

The choice of positioning the second OH at the *meta* position on the phenethyl substituent seemed somewhat obvious, since modeling showed that alternative OH substitution on the *N*-phenyl ring fails to provide O–O interatomic distances much greater than in the *para*-substituted system **16b**. Furthermore, the binding mode depicted in Figure 8 actually places the *N*-phenyl group more closely in the 11 β subpocket of the ligand binding site, rather than the D-ring subpocket. In choosing the ring-substitution for the hydroxyl on the phenethyl ring, we considered both the *para* and *meta* isomers. However, in light of the problems encountered with quinone methide elimination in the *N*-benzyl benzamide series bearing a *para*-methoxy protecting group, we opted not to prepare the *para*-hydroxy analogue of **16f**, since the electron withdrawing CF₃ group would presumably exacerbate quinone methide elimination.

With the recent release of the E_2 ER α LBD crystal structure coordinates, we performed molecular docking studies of the proposed *meta*-hydroxybenzamide (**16g**) using TRIPOS' Flexidock routine (see Experimental), to see whether or not the proposed binding mode in Figure 8 was reasonable and whether a *meta*-hydroxy derivative could participate in a hydrogen bonding interaction with His₅₂₄.

The final docked and minimized model, using the *S*-enantiomer of **16g**, is depicted in crossed-stereo in Figure 9. The *R*-enantiomer (not shown) was also modeled in the same manner but resulted in a higher energy complex. The final *S*-enantiomer model converged to an RMS of <0.05 kcal/mol-Å with a reasonably favorable binding energy. In this conformation, the benzoyl phenol is comfortably accommodated in the A-ring pocket, and the *N*-phenyl group projects into what

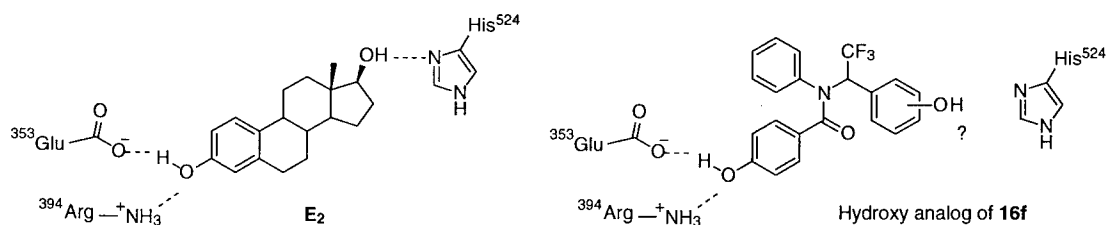


Figure 8. Putative binding mode for *N*-phenyl benzamide template with A-ring mimic interactions and a proposed site for second HO-group.

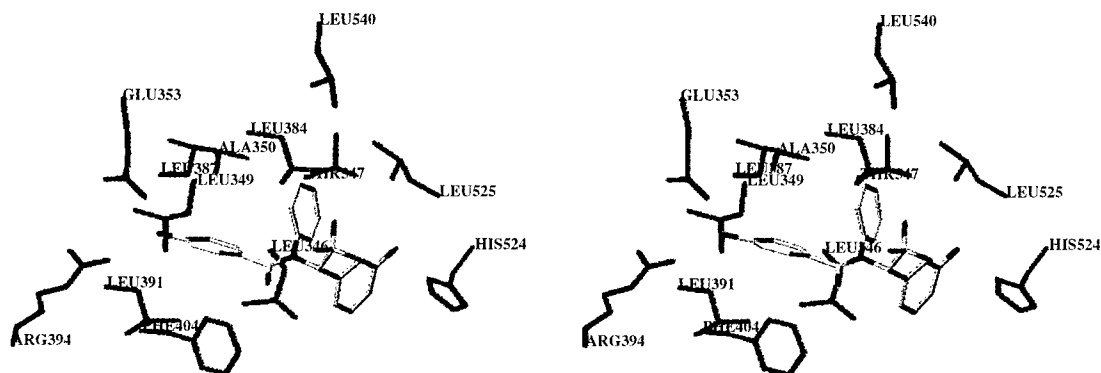


Figure 9. Crossed-stereo view of **16g** docked and minimized in ER α LBD binding pocket showing select residues within 3 Å of the benzamide.

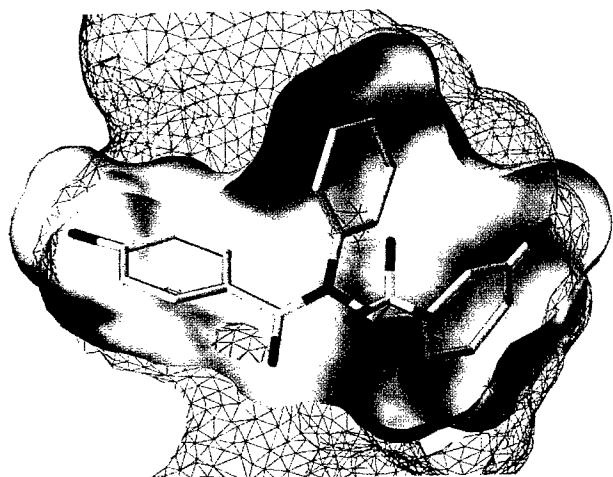


Figure 10. Depiction of solvent accessible surfaces for **16g** in ER α binding pocket.

would resemble the 11 β pocket of the ER α -E₂ structure. Interestingly, the amide bond occupies a region of the binding pocket similar to that of the isosteric ethylene unit of DES in the recently solved ER α -DES crystal structure.²⁹

Using the above model, we generated Connolly solvent accessible surfaces for the ligand and binding pocket to visualize close contacts (Fig. 10). This view reveals mostly favorable interactions within acceptable van der Waals radii. The ligand itself has a volume of 296 Å³, which is 51 Å³ greater than E₂, but is well under the total volume of 450 Å³ for the binding pocket as reported in the ER α -E₂ crystal structure.²⁶

We were grateful to find that the bis-(phenolic) benzamide **16g** had an RBA of 15%, the highest of any carboxamide ER ligand. This value represents a 1.6-fold increase over the affinity of the corresponding monophenolic benzamide **16f** and is close to what one might expect: in E₂ and other non-steroidal ER ligand systems, removal of the 17 β hydroxyl, as in E₂, or the second

D-ring hydroxyl mimic, as in raloxifene, result in a 0.6 kcal/mol reduction in binding energy, which corresponds to a 3-fold drop in affinity.³⁰ The fact that the addition of the second hydroxyl does not give a full 3-fold increase may be due to a somewhat unfavorable hydrogen bond trajectory in the binding pocket. From our model, the distance between the *m*-hydroxyl substituent and His₅₂₄ (3.69 Å) is sufficiently close for some hydrogen bonding interaction, but is not ideal either in terms of distance or geometry. A second more likely explanation may have to do with stereochemical issues: This compound (**16g**) was tested as a racemate, so only one enantiomer is likely to be able to benefit from the second hydrogen bonding interaction. The ER α and ER β RBAs and the transcriptional activation profile for *rac*-**16g** in HEC-1 cells are discussed below.

N-Phenyl acetamides as ER ligands. The RBA and Log *P_{o/w}* data for *N*-alkyl- and CF₃-containing acetamides are shown in Table 4. Disappointingly, none of these compounds were found to show appreciable affinity for the ER. Several direct comparisons can be made to other series in this investigation, which suggest that acetamides may not provide viable scaffolds for further combinatorial consideration, despite their potential to support greater structural diversity than the benzamides. Even the CF₃-containing acetamide **27** and thioacetamide **28** have affinities less than 1%, which are 50- and 11-fold lower, respectively, than their benzamide counterparts **16a** and **17a**.

One possible explanation for the low affinity in the acetamide class may lie in their conformation. Monte Carlo conformational studies of compound **27** and the unsubstituted analogue **27b**, using molecular mechanics methods, show a distinct preference for a *syn* conformation, as shown in Figure 11. The *syn*-conformer for **27** is predicted to be 5 kcal/mol lower in energy than the *anti*-conformer; even without the α -methyl substituent, which eliminates possible alkyl-*N*-phenyl steric repulsions, the *syn*-conformer is predicted to be favored by 2.5 kcal/mol (not shown). It is also noted that the barrier to rotation about the acetyl bond was estimated

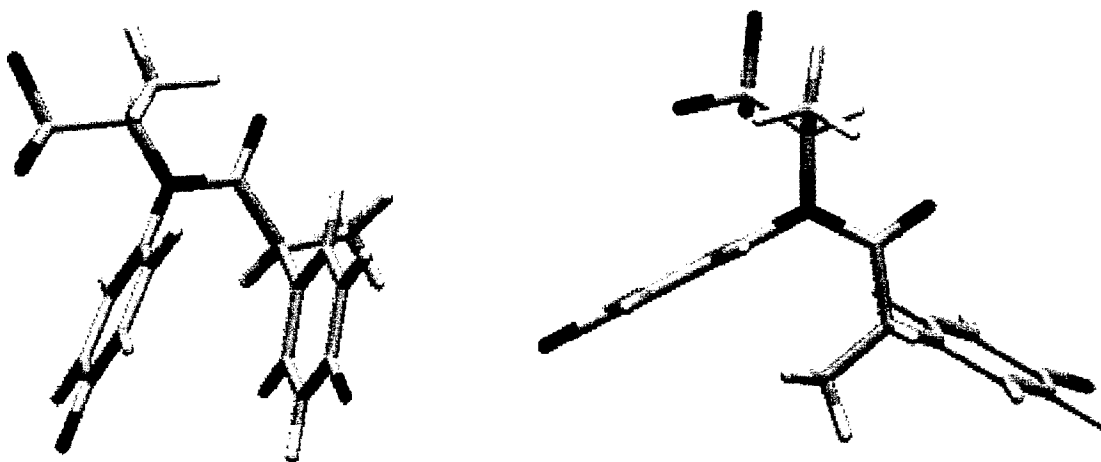


Figure 11. Conformational analysis of *N*-penyl-penylacetamide **27**.

to be between 4 and 5 kcal/mol for **27**, based on MM2 dihedral drive calculations.

As in the benzamides, in the acetyl conformations of **27** the *exo*-rule is upheld; this places the *N*-phenyl group *exo* with respect to the amide C=O, making the amide configuration *s-cis*. This *exo*-effect may also be operative for the α -phenyl substituent as well, since it also prefers to be essentially *exo* to the amide C=O rather than *endo*. Since the hydroxyl O··O interatomic distances for many estrogens requires a minimum of approximately 10.5 Å, the *syn*-conformation is excluded as a structure that is likely to fit in the ER binding pocket. Based on these studies and the RBA data available at this time, further investigations of the acetamide series did not appear to be warranted.

ER α /ER β binding affinity, transcriptional activity and enantioselectivity

Shown in Table 5 are the RBA values of select benzamides for purified ER α and ER β , along with their transcriptional activity in HEC-1 cells using an estrogen-responsive reporter gene construct ((ERE)₃-pS2-CAT) with expression vectors for either ER α or ER β and benzamide at 10⁻⁶ M. It is apparent that binding affinities show selectivity for ER α , mostly in the range of 2- to 8-fold; compound **16g** has the highest selectivity for ER α of 21-fold (27% versus 1.3%). The enantiomers of **17b**, which were separated using chiral HPLC (ChiralPak AD column), also showed interesting RBA differences between the two receptor subtypes. For example, enantiomer *ent*₂-**17b** was found to have greater selectivity for ER α than enantiomer *ent*₁-**17b** by more than 5-fold, indicating that the individual binding pockets for ER α and ER β are uniquely sensitive to subtle changes in ligand shape.

In the transcription assays,³¹ agonism is measured with 1 μ M of compound alone and is expressed as the percent of transcriptional activity with 1 nM E₂ (high values indicate agonist activity); antagonism is measured with 1 μ M compound together with 1 nM E₂ (low values indicate antagonist activity). All of the benzamides tested were full or nearly full agonists through ER α ,

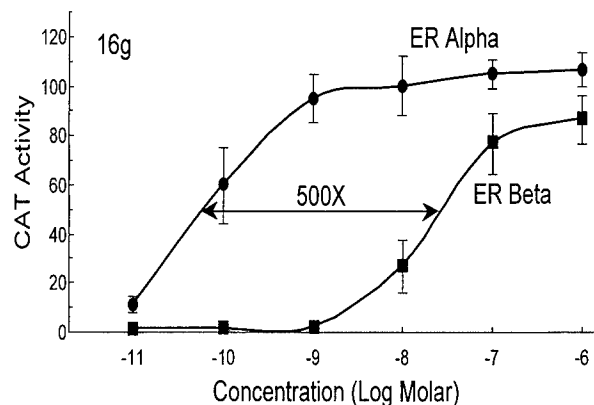


Figure 12. Transcription activation by ER α and ER β in response to benzamide **16g**. Human endometrial cancer (HEC-1) cells were transfected with expression vectors for ER α or ER β and an (ERE)₃-pS2-CAT reporter gene and were treated with the indicated concentrations of benzamide **16g** for 24 h. CAT activity was normalized for β -galactosidase activity from an internal control plasmid. Values are the mean \pm SD for three or more separate experiments, and are expressed as a percent of the ER α or ER β response with 1 nM E₂.

whereas some were effective partial antagonists through ER β . Compound **16g** was a full agonist on ER α and ER β .

Because of the high activity of amide **16g** at 10⁻⁶ M on both ER α and ER β , a full dose-response curve was determined to see whether any potency selectivity existed for either ER α or ER β . As shown in Figure 12, benzamide **16g** behaves as an ER α potency selective agonist, displaying a 500-fold higher potency for activation of ER α over ER β . It is of note that this high potency selectivity for ER α is greater than the 21-fold ER α affinity selectivity of this compound (cf. Table 5).

Conclusions

Through an analysis of potent non-steroidal estrogens, we have identified common substructural bibenzyl and homobibenzyl motifs in the structure of ER ligands. Based on this simple pharmacophore model, we have

Table 5. Benzamide ER α and ER β binding affinities and transcriptional activity

| Compound | RBA (%) (uterine) | RBA (%) ^a | | | Agonism ^b % CAT Act. | | Antagonism ^b % CAT Act. + E ₂ | |
|--------------------------------------|-------------------|----------------------|------------|----------------------|---------------------------------|------------|---|------------|
| | | ER α | ER β | α/β ratio | ER α | ER β | ER α | ER β |
| 11g | 4.6 | 14 | 2.4 | 5.8 | 65 | 20 | 90 | 40 |
| 17a | 7.5 | 23 | 15 | 1.5 | 60 | 20 | 65 | 45 |
| 16b | 9.0 | 17 | 2.7 | 6.3 | 75 | 15 | 90 | 35 |
| <i>rac</i> - 17b | 14 | 25 | 8.9 | 2.8 | 80 | 30 | 83 | 35 |
| <i>ent</i> ₁ - 17b | 10 | 18 | 11 | 1.6 | 85 | 30 | 80 | 48 |
| <i>ent</i> ₂ - 17b | 22 | 40 | 4.8 | 8.3 | 80 | 10 | 90 | 40 |
| 16g | 15 | 27 | 1.3 | 21 | 99 | 99 | 100 | 97 |

^aRelative binding affinities are the average of duplicate determinations (CV 0.3), determined with purified RD α and ER β preparations. For estradiol, RBA = 100. For details, see Experimental.

^bHEC-1 cells were transfected with either RE α or ER β expression vectors and an (ERE)₃-pS2-CAT reporter gene. CAT activity was normalized for β -galactosidase activity from an internal control plasmid and is expressed as a percent of the ER α or ER β response with 1 nM E₂. Benzamides were tested at 10⁻⁶ M concentration to test for agonism and at 10⁻⁶ M with 10⁻⁹ M E₂ to test for antagonism. These assays are generally reproducible with a CV of 30% relative.

made a substantial exploration of the amide functionality as a core replacement that might support compound libraries for developing novel SERMs. Using this approach, we prepared and tested representative examples of bis-phenolic amides which displayed both simple *N*-alkyl substituents and CF₃-containing *N*-alkyl substituents. Of the two classes examined, benzamides and acetamides, the benzamides displayed the highest affinity, in particular the CF₃-containing benzamides. The recent X-ray crystal structure of E₂ bound to ER α and structure-binding affinity relationships have allowed us to design a bis-phenolic benzamide **16g**, which has the highest affinity for any carboxamide ligand for the ER. This compound is also an ER α potency-selective agonist in cell-based assay of ER-mediated transcriptional activity. This work illustrates that ER ligands based on simple amide core structures can be readily prepared. High affinity ER binding, however, requires an appropriate distribution of bulk and functionality. The strong conformational preference of the basic anilide function in all of these ligands defines the scope of further structural and functional expansion of these series.

Experimental

General

Melting points were determined on a Thomas-Hoover UniMelt capillary apparatus and are uncorrected. All reagents and solvents were obtained from Aldrich, Fisher or Mallinckrodt. Tetrahydrofuran was distilled from sodium/benzophenone. Dimethylformamide was vacuum-distilled prior to use, and stored over 4 Å molecular sieves. *n*-Butyllithium was titrated with *N*-pivaloyl-*o*-toluidine. All reactions were performed under a dry N₂ atmosphere unless otherwise specified. Reaction progress was monitored by analytical thin-layer chromatography using GF silica plates purchased from Analtech. Visualization was achieved by short-wave UV light (254 nm) or potassium permanganate. Radial preparative-layer chromatography was performed on a Chromatotron instrument (Harrison Research, Inc., Palo Alto, CA) using EM Science silica gel Kieselgel 60 PF₂₅₄ as adsorbent. Flash column chromatography was performed using Woelm 32–63 μ m silica gel packing.

Logarithms of octanol–water partition coefficients (Log *P*_{ow}) were determined using a standardized reverse phase HPLC Chromegabond MC 8 column.²³ HPLC separation of the enantiomers for **17b** was performed on an analytical ChiralPak AD (4.6 \times 25 cm) column from Chiral Technologies using 10% *i*-propanol/hexane as solvent. ¹H and ¹³C NMR spectra were recorded on either a General Electric QE-300 (300 MHz), Varian Unity 400 or 500 MHz spectrometers using CDCl₃, MeOD or (CD₃)₂SO as solvent. Chemical shifts were reported as parts per million downfield from an internal tetramethylsilane standard (δ = 0.0 for ¹H) or from solvent references. NMR coupling constants are reported in Hertz. ¹³C NMR were determined using either the Attached Proton Test (APT) experiment or standard ¹³C pulse sequence parameters. Low resolution and high

resolution electron impact mass spectra were obtained on Finnigan MAT CH-5 or 70-VSE spectrometers. Elemental analyses were performed by the Microanalytical Service Laboratory of the University of Illinois.

Unless otherwise stated, a standard procedure for product isolation was used; this involved quenching by addition of water or an aqueous solution, exhaustive extraction with an organic solvent, washing the extracts, drying over Na₂SO₄, and solvent evaporation under reduced pressure. Quenching media, extraction solvents, and aqueous washes used are noted parenthetically after the phrase ‘product isolation’.

Biological procedures

Relative binding affinity assay. Ligand binding affinities (RBAs) using lamb uterine cytosol as a receptor source were determined by a competitive radiometric binding assay using 10 nM [³H]estradiol as tracer and dextran-coated charcoal as an adsorbant for free ligand.³² Purified ER α and ER β binding affinities were determined using a competitive radiometric binding assay using 10 nM [³H]estradiol as tracer, commercially available ER α and ER β preparations (PanVera Inc., Madison, WI), and hydroxylapatite (HAP) to adsorb bound receptor–ligand complex.³³ HAP was prepared following the recommendations of Williams and Gorski.³⁴ All incubations were done at 0 °C for 18–24 h. Binding affinities are expressed relative to estradiol on a percent scale (i.e. for estradiol, RBA = 100%). All assays were run in separate, duplicate experiments which were reproducible with a coefficient of variation of less than 30% relative.

Transcriptional activation assay. Human endometrial cancer (HEC-1) cells were maintained in culture and transfected as described previously.³¹ Transfection of HEC-1 cells in 60 mm dishes used 0.4 mL of a calcium phosphate precipitate containing 2.5 μ g of pCMV β Gal as internal control, 2 μ g of the reporter gene plasmid, 100 ng of the ER expression vector, and carrier DNA to a total of 5 μ g DNA. CAT activity, normalized for the internal control β -galactosidase activity, was assayed as previously described.³¹

Molecular modeling

Small molecule modeling. Dihedral drive and Monte Carlo conformational searches for *N*-phenyl benzamides **16a** and **17a** and *N*-phenyl acetamide **27** were conducted using the MM2 force field as implemented in MacroModel v.5.5 with CHCl₃ as a solvent model. All generated conformers from Monte Carlo searches underwent full matrix assisted minimization using the PRCG function with a convergence criteria of 0.001 kcal/mol. Dihedral drives were conducted in 5° steps with a convergence criteria of 0.05 kcal/mol using 1000 minimization steps. Analysis of the energy versus torsion angle provided the estimated rotational barrier.

Receptor docking studies. The starting conformation used for docking studies for **16g** was obtained from a

random conformational search using the TRIPOS' force field (MAXIMIN) as implemented in the program SYBYL, version 6.5.2 (Tripos Inc., St. Louis, MO). The *cis* global minima obtained for benzamide **16g** was then overlaid with E₂ in the E₂-ER α LBD crystal structure²⁶ using a least squares multifitting of five atoms: atoms C(3), C(10), C(9), C(11), and C(12) of E₂ were fitted with the 1 and 4 carbons of the benzamide phenyl ring, the C=O carbon, the nitrogen and the C(2) carbon of the phenethyl group, respectively. The pre-positioned benzamide was then optimally docked in the ER α binding pocket using TRIPOS' Flexidock. Both hydrogen-bond donors and acceptors within the pocket surrounding the ligand (Glu₃₅₃, Arg₃₉₄ and His₅₂₄) and the ligand itself, in addition to select torsional bonds were defined. The best docked receptor ligand complex from Flexidock then underwent a three-step minimization: first non-ring torsional bonds of the ligand were minimized in the context of the receptor using the torsmin command, followed by minimization of the side-chain residues within 8 Å of the ligand while holding the backbone and residues Glu₃₅₃ and Arg₃₉₄ fixed. A final third minimization of both the ligand and receptor was conducted using the anneal function (hot radius 8 Å, interesting radius 16 Å) while holding residues Glu₃₅₃ and Arg₃₉₄ fixed to afford the final model. Minimizations were done using the TRIPOS' Forcefield (MAXIMIN) with the Powell gradient method and default settings (final RMS < 0.05 kcal/mol-Å).

X-Ray crystallography

Crystallography details for 17a and 10b. Crystals of **17a** were obtained by slow evaporation from ether at 0 °C. Crystals were mounted on glass fibers with Paratone-N oil (Exxon) and immediately cooled to -75 °C in a cold nitrogen gas stream on the diffractometer. Standard peak search and indexing procedures gave rough cell dimensions, and least squares refinement using 5344 reflections yielded the cell dimensions as given in Table 6.

Data were collected with an area detector by using the measurement parameters listed in Table 6. No systematic absences are noted for the P-1 space group. The measured intensities were reduced to structure factor amplitudes and their esds by correction for background, scan speed, and Lorentz and polarization effects. While corrections for crystal decay were unnecessary (the data were corrected for crystal decay), a Ψ -scan absorption correction was applied, the maximum and minimum transmission factors being 0.991 and 0.876. Systematically absent reflections were deleted and symmetry equivalent reflections were averaged to yield the set of unique data. All 5344 data were used in the least squares refinement.

The structure was solved using direct methods (SHELXTL). The correct positions for the C, N, O, S, and F atoms were deduced from an E-map. Subsequent least-squares refinement and difference Fourier calculations revealed the positions of the remaining non-hydrogen atoms. The quantity minimized by the least-squares program was $\sum w(F_o^2 - F_c^2)^2$, where $w = \{[\sigma(F_o)]^2 + (0.883P)^2\}^{-1}$ and $P = (F_o^2 + 2F_c^2)/3$. The analytical approximations to the scattering factors were used, and all structure factors were corrected for both real and imaginary components of anomalous dispersion. In the final cycle of least squares, independent anisotropic displacement factors were refined for the non-hydrogen atoms and the aromatic, methyl, and methine hydrogen atoms were fixed in 'idealized' positions with C-H=0.95 Å for the aromatic hydrogens, C-H=0.98 Å for the methyl hydrogens, and C-H=1.00 Å for the methine hydrogen. Successful convergence was indicated by the maximum shift/error of 0.001 for the last cycle. Final refinement parameters are given in Table 6. The largest peak in the final Fourier difference map (0.795 eÅ⁻³) was located 1.64 Å from C(18). A final analysis of variance between observed and calculated structure factors showed no apparent errors.

Single crystals of **10b** were grown from MeOH by slow evaporation at 23 °C in a partially sealed scintillation

Table 6. Crystal data and structure refinement for thiocarboxamide **17a** and carboxamide **10b**

| | 17a | 10b |
|--|--|---|
| Complex | | |
| Empirical formula | C ₁₈ H ₁₈ F ₃ NO ₂ S | C ₁₆ H ₁₇ NO ₃ |
| fw | 369.39 | 271.31 |
| Temperature | 198(2) K | 198(2) K |
| Wavelength | 0.71073 Å | 1.54178 Å |
| Cryst syst | triclinic | monoclinic |
| Space group | P-1 | P2 ₁ /n |
| Unit cell dimensions | a = 9.5099(7) Å b = 10.5351(8) Å c = 11.1127(8) Å 868.07(11) Å ³ | a = 18.248(4) Å b = 9.054(2) Å c = 18.248(4) Å 2916.4(10) Å ³ |
| Volume | | |
| Z | 2 | 8 |
| Density, calcd | 1.413 Mg/m ³ | 1.236 Mg/m ³ |
| Abs coeff | 0.228 mm ⁻¹ | 0.695 mm ⁻¹ |
| No. of indep reffs | 5344 [R(int) = 0.0293] | 4796 [R(int) = 0.0556] |
| Refinement method | full matrix least-squares on F ² | full matrix least-squares on F ² |
| No. of data/restraints/params | 3727/0/226 | 2727/0/362 |
| Goodness-of-fit (GooF) on F ² | 0.949 | 1.062 |
| Final R indices [I > 2σ(I)] | R1 = 0.0502, wR2 = 0.1393 | R1 = 0.0624, wR2 = 0.1662 |
| R indices (all data) | R1 = 0.0892, wR2 = 0.1533 | R1 = 0.0767, wR2 = 0.1881 |

vial. Crystals were mounted on glass fibers with Paratone-N oil (Exxon) and immediately cooled to -75°C in a cold nitrogen gas stream on the diffractometer. Standard peak search and indexing procedures gave rough cell dimensions. Initial inspection of the data suggested a C-centered orthorhombic cell, but no successful solution could be found in any orthorhombic space group. Eventually, a successful solution was found in a primitive monoclinic cell of half the volume in the space group $P2_1/n$. The refinement stalled at $wR_2=0.63$, despite having located all atoms and refining the non-hydrogen atoms anisotropically. The unusual equality in the lengths of the a and c axes, combined with the observation that $F_{\text{obs}} \gg F_{\text{calc}}$ for all the reflections in the 'most disagreeable reflections' list, suggested that the crystal was twinned. A twin law involving mirror reflection through the (101) plane was assumed, and a refinable parameter describing the relative volume fractions of the two twin individuals was added to the model. The intensities were calculated from the relation $F_{\text{TOT}}^2 = f F_{\text{hkl}}^2 + (1-f) F_{\text{h'k'l'}}^2$, where f is the volume fraction of twin individual one and F_{hkl}^2 and $F_{\text{h'k'l'}}^2$ are the contributions from the two twins (the twin law specifies that $h'k'l' = lkh$). The scale factor refined to 0.500(3), and the wR_2 factor dropped to an acceptable value of 0.185.

In the final cycle of least squares, independent anisotropic displacement factors were refined for the non-hydrogen atoms and the aromatic, methyl, and methine hydrogen atoms were fixed in 'idealized' positions with $\text{C-H}=0.95\text{ \AA}$ for the aromatic hydrogens, $\text{C-H}=0.98\text{ \AA}$ for the methyl hydrogens, and $\text{C-H}=1.00\text{ \AA}$ for the methine hydrogen. Successful convergence was indicated by the maximum shift/error of 0.001 for the last cycle. Final refinement parameters are given in Table 6. The largest peak in the final Fourier difference map (0.795 e\AA^{-3}) was located 1.64 \AA from C(18). A final analysis of variance between observed and calculated structure factors showed no apparent errors.

Chemical syntheses

4-Methoxyphenyl-4-methoxybenzene sulfonamide (3).⁸ To a mixture of 4-methoxybenzenesulfonylchloride (1.0 equiv) and pyridine (1.1 equiv) in CH_2Cl_2 (0.5 M) at 0°C was added dropwise to a solution of *p*-anisidine (1.5–5.0 equiv) in CH_2Cl_2 (1.5 M) over 30 min. The reaction mixture was warmed to rt and stirred until completion of reaction as indicated by TLC. Product isolation (H_2O , 2 N HCl) and recrystallized from EtOH afforded product as light red crystals (91%); mp $91\text{--}92.5^{\circ}\text{C}$, mp⁸ 93°C .

General procedure for phase transfer *N*-alkylation of sulfonamides.⁹ To a CH_2Cl_2 (0.06 M) solution of sulfonamide (1.0 equiv) was added an equal volume solution of NaOH (5 equiv) and (*n*-Bu)₄NSO₄H (0.1 equiv) in H_2O . Alkylhalide (2.0 equiv) was then added directly to the bi-phasic solution and stirred at rt. After 12 h the layers were separated. Product isolation (Na_2CO_3 , brine) followed by flash chromatography afforded the pure *N*-alkyl benzene sulfonamide.

***N*-(4-Methoxyphenyl)-*N*-(ethyl)-4-methoxybenzene sulfonamide (4a).**⁸ Purification by flash chromatography (20% EtOAc:hexane) afforded off-white powder (86%); mp $95\text{--}7^{\circ}\text{C}$, mp⁸ $100\text{--}104^{\circ}\text{C}$; ^1H NMR (CDCl_3) δ 1.06 (t, 3H, $J=7.1\text{ Hz}$), 3.52 (q, 2H, $J=7.0\text{ Hz}$), 3.81 (s, 3H), 3.84 (s, 3H), 6.82 (d, 2H, $J=8.8\text{ Hz}$), 6.94 (d, 2H, $J=8.0\text{ Hz}$), 6.96 (d, 2H, $J=8.0\text{ Hz}$), 7.54 (d, 2H, $J=8.8\text{ Hz}$).

***N*-(4-Methoxyphenyl)-*N*-(butyl)-4-methoxybenzene sulfonamide (4b).** Purification by flash chromatography (20% EtOAc:hexane) afforded transparent oil (81%); ^1H NMR (CDCl_3) δ 0.85 (t, 3H, $J=7.2\text{ Hz}$), 1.34 (m, 4H), 3.46 (t, 2H, $J=6.8\text{ Hz}$), 3.80 (s, 3H), 3.86 (s, 3H), 6.81 (d, 2H, $J=9.0\text{ Hz}$), 6.92 (app t, 4H, $J=9.1\text{ Hz}$), 7.51 (d, 2H, $J=9.0\text{ Hz}$); MS (EI, 70 eV) m/z 349 (M^+); HRMS calcd for ($\text{C}_{18}\text{H}_{23}\text{NO}_4\text{S}$, 349.1347, found 349.1348).

***N*-(4-Methoxyphenyl)-*N*-(benzyl)-4-methoxybenzene sulfonamide (4c).** Recrystallization from 20% EtOAc/hexane afforded flocculent white crystals (93%); mp $141\text{--}142^{\circ}\text{C}$; ^1H NMR (CDCl_3) δ 3.72 (s, 3H), 3.87 (s, 3H), 4.67 (s, 2H), 6.89 (d, 2H, $J=11\text{ Hz}$), 6.86 (d, 2H, $J=11.5\text{ Hz}$), 6.94 (d, 2H, $J=11\text{ Hz}$), 7.21 (m, 5H), 7.59 (d, 2H, $J=11\text{ Hz}$); ^{13}C NMR (CDCl_3) δ 55.1, 55.4, 55.8, 114.2, 127.7, 128.5, 128.7, 129.9, 130.4, 130.4, 131.7, 136.3, 158.9, 163.0; HRMS calcd for $\text{C}_{21}\text{H}_{21}\text{NSO}_4$, 383.1191, found 383.118.

General demethylating procedure using BBr_3 . To a solution of methyl ether compound in CH_2Cl_2 at -78°C was added a 1.0 M BBr_3 in CH_2Cl_2 (3 equiv) dropwise over 15 min. The reaction was allowed to reach rt and stir overnight or until disappearance of starting material as indicated by TLC. The mixture was then cooled to 0°C . Product isolation (H_2O , Et_2O , brine) and purification via radial or flash chromatography or recrystallization from an appropriate solvent afforded the desired phenolic compounds.

General demethylating procedure using EtSH. To a stirred DMF solution of NaH (6.2 equiv of a 60% w/w dispersion) at 0°C was added dropwise 6.0 equiv of EtSH. After 30 min the mixture was warmed to rt and a solution of the methyl ether protected compound in 5 mL DMF was added dropwise. The reaction mixture was heated to reflux for 4 h; then cooled in an ice-bath and acidified with 2 N HCl. Remaining product isolation (EtOAc, brine) and purification afforded the phenolic compounds.

***N*-(4-Hydroxyphenyl)-*N*-(ethyl)-4-hydroxybenzene sulfonamide (5a).** Deprotected according to BBr_3 procedure. SiO_2 plug (30% EtOAc/hexane) to afford off-white crystals (62%); ^1H NMR ($(\text{CD}_3)_2\text{SO}$) δ 0.98 (t, 3H, $J=7.2\text{ Hz}$), 3.43 (q, 2H, $J=6.8\text{ Hz}$), 6.67 (d, 2H, $J=8.7\text{ Hz}$), 6.76 (d, 2H, $J=8.4\text{ Hz}$), 6.86 (d, 2H, $J=8.5\text{ Hz}$), 7.34 (d, 2H, $J=8.7\text{ Hz}$); ^{13}C NMR ($(\text{CD}_3)_2\text{SO}$) δ 14.1 (CH_3), 45.2 (CH_2), 115.7 (ArCH), 115.8 (ArCH), 122.6 (ArC), 128.1 (ArC), 129.9 (ArCH), 130.1 (ArCH), 157.1 (ArC), 161.6 (ArC); MS (EI, 70 eV) m/z 293 (M^+); HRMS calcd for $\text{C}_{14}\text{H}_{15}\text{NSO}_4$, 293.0721, found 293.0722.

***N*-(4-Hydroxyphenyl)-*N*-(butyl)-4-hydroxybenzene sulfonamide (5b).** Deprotected according to BBr₃ procedure to afford tan crystals, recrystallized from EtOAc/hexane (71%); mp 137–138 °C; ¹H NMR (CDCl₃) δ 0.86 (t, 3H, *J* = 7.0 Hz), 1.35 (m, 4H), 3.48 (t, 2H, *J* = 7.0 Hz), 6.42 (d, 2H, *J* = 8.8 Hz), 6.87 (app t, 4H, *J* = 8.9 Hz), 7.47 (d, 2H, *J* = 9.0 Hz) ¹³C NMR (CD₃)₂SO δ 13.8 (CH₃), 19.2 (CH₂), 29.9 (CH₂), 49.7 (CH₂), 115.6 (ArCH), 115.7 (ArCH), 122.6 (ArCH), 128.0 (ArC), 129.9 (ArCH), 130.0 (ArC), 157.0 (ArC), 161.6 (ArC); MS (EI, 70 eV) *m/z* 321 (M⁺); HRMS calcd for C₁₆H₁₉NSO₄, 321.1034, found 321.1035. Anal. (C₁₆H₁₉N·0.3 H₂O): C, 58.81; H, 6.05; N, 4.29. Found: C, 58.60; H, 6.03; N, 4.13.

***N*-(4-Hydroxyphenyl)-*N*-(benzyl)-4-hydroxybenzene sulfonamide (5c).** Deprotected according to BBr₃ procedure to afford title compound after purification by radial chromatography (10%); ¹H NMR (CDCl₃) δ 4.65 (s, 2H), 6.66 (d, 2H, *J* = 8.5 Hz), 6.80 (d, 2H, *J* = 8.5 Hz), 6.96 (d, 2H, 8.8), 7.21 (br s, 5H), 7.59 (d, 2H, *J* = 8.9 Hz); MS (EI, 70 eV) *m/z* 355 (M⁺); HRMS calcd for C₁₉H₁₇NSO₄, 355.0878, found 355.0881.

***N*-(4-Methoxyphenyl)-4-methoxybenzamide (6).**³⁵ A CH₂Cl₂ solution of *p*-anisidine (1.3 equiv) was added dropwise to a stirring CH₂Cl₂ solution (2–5 mL) of pyridine (1.1 equiv) and *p*-anisoyl chloride (1.0 equiv) at 0 °C. Upon complete addition of amine (30 mm) mixture was allowed to reach rt, then re-cooled and vacuum filter to afford the crude carboxamide. Recrystallization from EtOH/benzene afforded the pure carboxamide as off-white crystals (72%); mp 199–200.5 °C, mp³² 202–203 °C.

***N*-(1-Phenethyl)-4-methoxyaniline (7).**⁷ To a 0 °C EtOH solution containing *p*-anisidine (1.0 equiv) and catalytic *p*-toluene sulfonic acid·H₂O (0.05 equiv) was added freshly distilled benzaldehyde dropwise. The mixture was allowed to reach rt and complete imine formation occurred within 0.5 h. The crude mixture was concentrated in vacuo, and product isolation followed (EtOAc, brine) to afford a dark brown powder. ¹H NMR confirmed imine which was directly used in the next step without further purification. **CH₃ addition:** Crude imine was dissolved in toluene and cooled to –78 °C. To this was added MeLi (1.0 M toluene solution, 3 equiv) dropwise over 15 min. After 60 min at –78 °C, the crude mixture was warmed to rt and stirred for an additional 2 h. The reaction was then cooled in an ice-bath and quenched with cold MeOH followed by addition of satd NH₄Cl until neutral pH. Concentration in vacuo followed by remaining workup (EtOAc, H₂O, brine) afforded amine as a red oil. Kugelrohr distillation provided pure product, which crystallized on standing as a red–orange powder (75%); ¹H NMR (CDCl₃) δ 1.50 (d, 3H, *J* = 7.0 Hz), 3.69 (s, 3H), 4.41 (q, 1H, *J* = 7.0 Hz), 6.47 (AA'BB', 2H, *J* = 9.0, 3.0 Hz), 6.69 (AA'BB', 2H, *J* = 9.0, 3.5 Hz), 7.29 (m, 5H); ¹³C NMR (CDCl₃) δ 25.4 (CH₃), 54.5 (CH), 55.9 (CH₃), 114.7 (ArCH), 114.9 (ArCH), 126.1 (ArCH), 127.0 (ArCH), 128.8 (ArCH), 141.7 (ArC), 145.7 (ArC), 152.1 (ArC); MS (EI, 70 eV) *m/z* 227 (M⁺); anal. (C₁₅H₁₇NO): C,

79.26; H, 7.54; N, 6.16. Found: C, 79.31; H, 7.54; N, 6.27.

***N*-[2-(3-Methyl)butane]-4-methoxyaniline (8).** To a THF solution at 0 °C containing *p*-anisidine (1 equiv), 3-methyl-2-butanone (1.0 equiv), and acetic acid (1.0 equiv) was added solid NaHB(OAc)₃. The mixture was allowed to reach rt and stirred for 15 h. The mixture was re-cooled to 0 °C; careful workup (H₂O, EtOAc, NaHCO₃, brine, MgSO₄) and concentration in vacuo afforded crude amine. Kugelrohr distillation provided pure product as light yellow oil (71%); bp 100 °C (0.3 mm); ¹H NMR (CDCl₃) δ 0.93 (d, 3H, *J* = 6.5 Hz), 1.00 (d, 3H, *J* = 6.5 Hz), 1.10 (d, 3H, *J* = 6.0 Hz), 1.86 (m, 1H, *J* = 6.5 Hz), 3.23 (br s, 1H, ArNH), 3.28 (dq, 1H, *J* = 7.0, 6.0 Hz), 3.77 (s, 3H), 6.58 (d, 2H, *J* = 7.0 Hz), 6.80 (d, 2H, *J* = 7.0 Hz); ¹³C NMR (CDCl₃) δ 16.5 (CH₃), 17.3 (CH₃), 19.3 (CH₃), 32.1 (CH), 54.5 (CH), 55.8 (CH₃), 114.6 (ArCH), 114.9 (ArCH), 142.1 (ArC), 151.7 (ArC); MS (EI, 70 eV) *m/z* 193 (M⁺); anal. (C₁₂H₁₉NO): C, 74.57; H, 9.91; N, 7.25. Found: C, 74.46; H, 9.76; N, 7.32.

General procedure for phase transfer *N*-alkylation of carboxamides.^{9,10} Alkylhalide (3 equiv) in benzene was added dropwise to a stirring mixture of carboxamide (1 equiv), finely powdered potassium hydroxide (2 equiv), and *n*-tetrabutylammonium bromide (0.05 equiv) in benzene (0.2 M) at rt. Reaction mixture was heated to 80 °C and maintained at this temperature until disappearance of starting material was observed by TLC (1–3 h). The reaction mixture was then cooled to rt and the salts removed by filtration. Product isolation (H₂O, brine), followed by flash chromatography (10–25% EtOAc/hexane) afforded product, usually as an oil.

General amidation procedures for anilines 7–8 and CF₃-containing anilines 14a–d. A 0.18 M benzene or toluene solution containing 1 equiv of aniline (14a, 14b, 7–8) in addition to 3 equiv of dry powdered K₂CO₃ and 1 equiv of pyridine was treated with 1.5 equiv of the corresponding acid chloride and heated between 80 and 110 °C. The reaction was monitored by TLC and the reaction cooled to rt upon completion. The crude mixture was filtered, concentrated in vacuo and taken up in Et₂O. Product isolation (H₂O, brine) and chromatographic purification afforded the protected carboxamide (15a–e and 9f and 9g).

Benzamides 15f and 15g were prepared from anilines 14c and 14d and the corresponding acid chloride (1.5 equiv) using 1,2-dichlorobenzene as solvent, 3 equiv of dry powdered K₂CO₃ and heated to 120–150 °C for 16 h or until disappearance of starting aniline. Reaction mixture was cooled to rt and eluted over silica with hexane to remove 1,2-dichlorobenzene. Gradient chromatography with 10, 20, and 30% EtOAc/hexane afforded the pure carboxamides 15f and 15g upon concentration.

***N*-(4-Methoxyphenyl)-*N*-(ethyl)-4-methoxybenzamide (9a).** Yellow oil (72%); ¹H NMR (CDCl₃) δ 1.12 (t, 3H, *J* = 7.2 Hz, CH₃), 3.62 (s, 3H, OCH₃), 3.65 (s, 3H, OCH₃), 3.84 (q, 2H, *J* = 7.0 Hz, CH₂), 6.57 (d, 2H,

$J=8.9$ Hz, ArH *ortho* OCH₃, *meta* RNCO), 6.68 (d, 2H, $J=8.9$ Hz, ArH *ortho* OCH₃, *meta* CONR), 6.87 (d, 2H, $J=8.9$ Hz, ArH *ortho* RNCO), 7.20 (d, 2H, $J=8.7$ Hz, ArH *ortho* CONR); ¹³C NMR (CDCl₃) δ 12.7 (CH₃), 45.5 (CH₂), 55.0 (OCH₃), 55.2 (OCH₃), 112.8 (ArCH), 114.2 (ArCH), 128.4 (ArC), 128.9 (ArCH), 130.7 (ArCH), 136.3 (ArC), 157.8 (ArC), 160.2 (ArC), 169.6 (C=O); MS (EI, 70 eV) m/z 285 (M⁺); HRMS calcd for C₁₇H₁₉NO₃, 285.1365, found 285.1364.

***N*-(4-Methoxyphenyl)-*N*-(2-propyl)-4-methoxybenzamide (9b).** Amber oil (43%): ¹H NMR (CDCl₃) δ 1.16 (d, 6H, $J=6.5$ Hz), 3.72 (s, 3H), 3.75 (s, 3H), 5.09 (br s, 1H), 6.63 (d, 2H, $J=8.5$ Hz), 6.74 (d, 2H, $J=9.0$ Hz), 6.93 (d, 2H, $J=8.5$ Hz), 7.21 (d, 2H, $J=8.5$ Hz); ¹³C NMR (CDCl₃) δ 21.2 (CH₃), 55.3 (CH₃), 55.5 (CH₃), 113.0 (ArCH), 113.9 (ArCH), 129.1 (ArC), 130.4 (ArCH), 131.8 (ArCH), 132.5 (ArC), 158.6 (ArC), 160.1 (ArC), 170.5 (C=O); MS (EI, 70 eV) m/z 299 (M⁺); HRMS calcd for C₁₈H₂₁NO₃, 299.1521, found 299.1521.

***N*-(4-Methoxyphenyl)-*N*-(butyl)-4-methoxybenzamide (9c).** Yellow oil (81%): ¹H NMR (CDCl₃) δ 0.84 (t, 3H, $J=7.3$ Hz, CH₃), 1.29 (sext, 2H, $J=7.0$ Hz, CH₂CH₂), 1.53 (quint, 2H, $J=7.8$ Hz, CH₂CH₂CH₂), 3.62 (s, 3H, OCH₃ *ortho* RNCO), 3.66 (s, 3H, OCH₃ *ortho* CONR), 3.78 (t, 2H, $J=7.7$ Hz, CH₂CH₂N), 6.58 (d, 2H, $J=8.8$ Hz, ArH *ortho* OCH₃, *meta* RNCO), 6.68 (d, 2H, $J=8.9$ Hz, ArH *ortho* OCH₃, and *meta* CONR), 6.88 (d, 2H, $J=8.9$ Hz, ArH *ortho* RNCO), 7.19 (d, 2H, $J=8.9$ Hz, ArH *ortho* CONR); ¹³C NMR (CDCl₃) δ 13.7 (CH₃), 20.0 (CH₂), 29.5 (CH₂), 50.3 (CH₂), 54.9 (OCH₃), 55.1 (OCH₃), 112.7 (ArCH), 114.1 (ArCH), 128.4 (ArC), 128.6 (ArCH), 130.5 (ArCH), 136.5 (ArC), 157.6 (ArC), 160.0 (ArC), 169.6 (ArC); MS (EI, 70 eV) m/z 313 (M⁺); HRMS calcd for C₁₉H₂₃NO₃, 313.7794, found 313.7879.

***N*-(4-Methoxyphenyl)-*N*-(benzyl)-4-methoxybenzamide (9e).** White flakes (82%): mp 104–106 °C; ¹H NMR (CDCl₃) δ 3.72 (s, 3H, OCH₃ *para* RNCO), 3.74 (s, 3H, OCH₃ *para* CONR), 5.09 (s, 2H, CH₂Ph), 6.68 (d, 2H, $J=9.2$ Hz, ArH *ortho* OCH₃, and *meta* RNCO), 7.31 (m, 9H, Ph and ArH); ¹³C NMR (CDCl₃) δ 54.3 (PhCH₂), 55.3 (OCH₃), 55.5 (OCH₃), 113.1 (ArCH), 114.3 (ArCH), 127.4 (ArCH), 128.6 (ArCH), 128.3 (ArC), 128.7 (ArCH), 128.9 (ArCH), 131.1 (ArCH), 137.0 (ArC), 138.0 (ArC), 158.0 (ArC), 160.6 (ArC), 170.2 (ArC); MS (EI, 70 eV) m/z 347 (M⁺); HRMS calcd for C₂₂H₂₁NO₃, 347.1521, found 347.1522.

***N*-(4-Methoxyphenyl)-*N*-(1-phenethyl)-4-methoxybenzamide (9f).** Prepared according to general procedure above using aniline 7 and *p*-anisoyl chloride. Purification by flash chromatography (2% (CH₃)₂CO/CH₂Cl₂) afforded product as clear oil (70%): ¹H NMR (CDCl₃) δ 1.48 (d, 3H, $J=6.8$ Hz), 3.67 (s, 3H), 3.69 (s, 3H), 6.38 (br q, 1H, $J=6.8$ Hz), 6.56 (br d overlapping br s, 4H), 6.62 (d, 2H, $J=8.8$ Hz), 7.23 (d, 2H, $J=8.5$ Hz), 7.29 (m, 5H); ¹³C NMR (CDCl₃) δ 16.9 (CH₃), 53.3 (CH), 55.2 (CH₃), 55.3 (CH₃), 112.9 (ArCH), 113.6 (ArCH), 127.5 (ArCH), 128.2 (ArCH), 128.3 (ArCH), 129.2 (ArC), 130.6 (ArCH), 131.5 (ArCH), 132.7 (ArC), 141.7

(ArC), 158.3 (ArC), 160.2 (ArC), 170.6 (C=O); MS (EI, 70 eV) m/z 361 (M⁺).

***N*-(4-Methoxyphenyl)-*N*-(1-methyl-2-methyl-1-propyl)-4-methoxybenzamide (9g).** Prepared according to general procedure above using aniline 8 and *p*-anisoyl chloride. Purification by flash chromatography (25% EtOAc/hexane) afforded product as light yellow oil (90%): ¹H NMR (CDCl₃) δ 0.93 (d, 6H, $J=6.7$ Hz), 1.90 (sept, 1H, $J=7.0$ Hz), 3.69 (s, 3H), 3.71 (s, 3H), 3.73 (d, 2H, $J=7.0$ Hz), 6.62 (d, 2H, $J=8.5$ Hz), 6.71 (d, 2H, $J=9.0$ Hz), 6.93 (d, 2H, $J=8.6$ Hz), 7.20 (d, 2H, $J=8.9$ Hz); ¹³C NMR (CDCl₃) δ 20.3 (CH₃), 27.0 (CH), 55.2 (CH₃), 55.4 (CH₃), 57.2 (CH₂), 113.0 (ArCH), 114.3 (ArCH), 128.7 (ArCH), 129.0 (ArC), 130.7 (ArCH), 137.1 (ArC), 157.8 (ArC), 160.3 (ArC), 170.3 (C=O); MS (EI, 70 eV) m/z 313 (M⁺).

***N*-(4-Hydroxyphenyl)-*N*-(ethyl)-4-hydroxybenzamide (10a).** Deprotected according to BBr₃ procedure to afford off-white powder, recrystallized from MeOH (70%): mp 208–209 °C; ¹H NMR ((CD₃)₂SO) δ 1.03 (t, 3H, $J=6.9$ Hz, CH₃), 3.72 (q, 2H, $J=7.1$ Hz, CH₂), 6.52 (d, 2H, $J=8.6$ Hz, ArH *meta* RNCO), 6.62 (d, 2H, $J=8.5$ Hz, ArH *meta* CONR), 6.86 (d, 2H, $J=8.6$ Hz, *ortho* RNCO), 7.06 (d, 2H, $J=8.5$ Hz, *ortho* CONR), 9.48 (s, 1H, OH), 9.71 (s, 1H, OH); ¹³C NMR ((CD₃)₂SO) δ 12.6 (CH₃), 39.1 (CH₂), 114.3 (ArCH), 115.7 (ArCH), 127.1 (ArC), 129.1 (ArC), 130.5 (ArCH), 134.7 (ArC), 155.7 (ArC), 158.3 (ArC), 168.9 (ArC); MS (EI, 70 eV) m/z 257 (M⁺); HRMS calcd for C₁₅H₁₅NO₃, 257.1052, found 257.1051.

***N*-(4-Hydroxyphenyl)-*N*-(2-propyl)-4-hydroxybenzamide (10b).** Deprotected according to BBr₃ procedure to afford powder, recrystallized from MeOH (77%): mp 210–212 °C; ¹H NMR (MeOD) δ 1.15 (d, 6H, $J=6.8$ Hz), 4.94 (br s, 1H), 6.56 (br s, 2H), 6.67 (d, 2H, $J=8.4$ Hz), 6.88; MS (EI, 70 eV) 271 (M⁺); anal. (C₁₆H₁₇NO₃·0.1 H₂O): C, 70.36; H, 6.36; N, 5.13. Found: C, 70.35; H, 6.37; N, 4.90.

***N*-(4-Hydroxyphenyl)-*N*-(butyl)-4-hydroxybenzamide (10c).** Deprotected according to BBr₃ procedure and purified by flash chromatography (25% EtOAc/hexane) to afford off-white crystals (95%): mp 174–175 °C; ¹H NMR ((CD₃)₂SO) δ 0.84 (s, 3H), 1.25 (sext, 2H, $J=7.6$ Hz), 1.43 (quint, 2H, $J=7.6$ Hz), 3.69 (t, 2H, $J=7.5$ Hz), 6.51 (d, 2H, $J=8.6$ Hz), 6.61 (d, 2H, $J=8.7$ Hz), 6.85 (d, 2H, $J=8.7$ Hz), 7.03 (d, 2H, $J=8.5$ Hz); ¹³C NMR ((CD₃)₂SO) δ 14.1 (CH₃), 19.9 (CH₂), 40.2 (CH₂), 114.5 (ArCH), 115.9 (ArCH), 127.4 (ArC), 129.2 (ArCH), 130.6 (ArCH), 135.1 (ArC), 155.8 (ArC), 158.4 (ArC); MS (EI, 70 eV) m/z 285 (M⁺); HRMS (EI) calcd for C₇H₁₉NO₃, 285.1365, found 285.1368; anal. (C₁₇H₁₉NO₃·0.5 H₂O): C, 69.37; H, 6.85; N, 4.76. Found: C, 69.30; H, 6.65; N, 4.57.

***N*-(4-Hydroxyphenyl)-*N*-(2-methyl-1-propyl)-4-hydroxybenzamide (10d).** Deprotected according to BBr₃ procedure and purified by flash chromatography (25% EtOAc/hexane) to afford white foam (quant): mp 166 °C dec.; ¹H NMR ((CD₃)₂SO) δ 0.93 (d, 6H, $J=6.5$ Hz),

1.82 (m, 1H, $J=6.5$ Hz), 3.66 (d, 2H, $J=7.5$ Hz), 6.59 (d, 2H, $J=8.5$ Hz), 6.68 (d, 2H, $J=9$ Hz), 6.94 (d, 2H, $J=8.5$ Hz), 7.10 (d, 2H, $J=8.5$ Hz); MS (EI, 70 eV) m/z 285 (M^+); anal. ($C_{17}H_{19}NO_3 \cdot 1.0 H_2O$): C, 67.31; H, 6.98; N, 4.62. Found: C, 67.45; H, 6.74; N, 4.41.

***N*-(4-Hydroxyphenyl)-*N*-(benzyl)-4-hydroxybenzamide (10e).** Deprotected according to EtSH procedure and purified by flash chromatography (25% EtOAc/hexane), which upon solvent concentration and recrystallization from $CHCl_3$ afforded title compound as off-white flakes (60%): mp 103–105 °C; 1H NMR ($(CD_3)_2SO$) δ 4.95 (s, 2H, CH_2), 6.53 (d, 2H, $J=6.3$ Hz, ArH *meta* RNCO), 6.56 (d, 2H, $J=6.2$ Hz, ArH *ortho* RNCO), 6.77 (d, 2H, $J=8.7$ Hz, ArH *meta* CONR), 7.13 (d, 2H, $J=8.7$ Hz, ArH *ortho* CONR), 7.25 (m, 5H, Ph), 9.67 (broad s, 2H, OH); ^{13}C NMR ($(CD_3)_2SO$) δ 53.1 (CH_2), 114.2 (ArCH), 115.5 (ArCH), 122.3 (ArC), 126.6 (ArC), 126.9 (ArCH), 127.9 (ArCH), 128.3 (ArCH), 128.7 (ArCH), 130.6 (ArCH), 134.9 (ArC), 137.9 (ArC), 155.5 (ArC), 158.5 (ArC), 169.4 (ArC); MS (EI, 70 eV) m/z 319 (M^+); HRMS (EI) calcd for $C_{20}H_{17}NO_3$, 319.1208, found 319.1206; anal. ($C_{20}H_{17}NO_3 \cdot 2.5 H_2O$): C, 65.92; H, 6.09; N, 3.84. Found: C, 65.58; H, 5.81; N, 3.53.

***N*-(4-Hydroxyphenyl)-*N*-(1-phenethyl)-4-hydroxybenzamide (10f).** Deprotected according to BBr_3 procedure recrystallized from MeOH/ CH_2Cl_2 to afford white powder (95%): mp 204–206 °C; 1H NMR (MeOD) δ 1.50 (d, 3H, $J=6.8$ Hz), 4.95 (s, under MeOH), 6.24 (br s, 2H), 6.49 (br s, 2H), 6.54 (br s, 2H), 6.54 (d, 2H, $J=8$ Hz), 7.10 (d, 2H, $J=8$ Hz), 7.28 (m, 5H); ^{13}C NMR (MeOD) δ 17.4 (CH_3), 49.0 (CH), 115.3 (ArCH), 115.9 (ArCH), 124.9 (ArCH), 128.6 (ArCH), 128.9 (ArC), 129.1 (ArCH), 129.3 (ArCH), 131.4 (ArCH), 132.4 (ArC), 132.7 (ArCH), 142.5 (ArC), 157.9 (ArC), 159.8 (C=O); MS (EI, 70 eV) m/z 333 (M^+); HRMS (EI) calcd for $C_{21}H_{19}NO_3$, 333.1365, found 333.1360; anal. ($C_{21}H_{19}NO_3$): C, 75.66; H, 5.74; N, 4.20. Found: C, 75.51; H, 5.80; N, 4.21.

General thionation procedure¹²

The carboxamide (1.01 mmol) and Lawesson's reagent (0.51 mmol) in 3 mL of HMPA were heated to 80–100 °C until the carboxamide had been consumed. After disappearance of carboxamide, the reaction mixture was allowed to cool to rt and then poured onto 5 mL of water. Product was extracted repeatedly with Et_2O , dried over Na_2SO_4 , rotary evaporated in vacuo and purified via flash chromatography. The protected thioamides were then directly used in the deprotection step with minimal purification.

***N*-(4-Hydroxyphenyl)-*N*-(ethyl)-4-hydroxythiobenzamide (11a).** Deprotected according to BBr_3 procedure and purified by flash chromatography (25% EtOAc/hexane) to afford yellow foam (63%): 1H NMR ($(CD_3)_2SO$) δ 1.16 (t, 3H, $J=6.8$ Hz, CH_3), 4.34 (q, 2H, $J=6.8$ Hz, CH_2), 6.44 (d, 2H, $J=8.4$ Hz, ArH *meta* RNCS), 6.59 (d, 2H, $J=8.9$ Hz, ArH *meta* CSNR), 6.87 (d, 2H, $J=8.7$ Hz, ArH *ortho* RNCS), 6.99 (d, 2H, $J=8.6$ Hz, ArH *ortho* CSNR); ^{13}C NMR ($(CD_3)_2SO$) δ 11.1 (CH_3), 52.1 (CH_2), 114.1 (ArH), 115.6 (ArH), 115.7 (ArH), 122.6 (ArH),

128.5 (ArH), 129.8 (ArH), 135.3 (ArC), 136.4 (ArC), 156.3 (ArC), 157.6 (ArC), 201.0 (CS); MS (EI, 70 eV) m/z 273 (M^+); HRMS (EI) calcd for $C_{15}H_{15}NSO_2$, 273.0824, found 273.0824; anal. ($C_{15}H_{15}NSO_2 \cdot 0.3 H_2O$): C, 64.63; H, 5.64; N, 5.02. Found: C, 64.51; H, 5.93; N, 4.64.

***N*-(4-Hydroxyphenyl)-*N*-(*i*-propyl)-4-hydroxythiobenzamide (11b).** Deprotected according to BBr_3 procedure and purified by flash chromatography (25% EtOAc/hexane) to afford yellow foam (98%): 1H NMR (MeOD, *i*-propyl rotamers 1:4:1 ratio) δ 1.15 (d, 1H, $J=6.5$ Hz), 1.20 (d, 4H, $J=6.5$ Hz), 1.27 (d, 1H, $J=6.5$ Hz), 6.00 (sept, 1H, $J=6.5$ Hz), 6.46 (d, 2H, $J=8.5$ Hz), 6.61 (d, 2H, $J=9$ Hz), 6.81 (d, 2H, $J=8.5$ Hz), 6.96 (d, 2H, $J=8.5$ Hz) additional minor ArCH resonances not listed; ^{13}C NMR (MeOD) δ 20.6 (CH_3), 21.9 (CH_3 minor), 54.8 (CH), 114.8 (ArCH), 115.9 (ArCH), 130.1 (ArCH), 131.7 (ArCH), 133.4 (ArC), 137.8 (ArC), 157.9 (ArC), 158.0 (ArC), 204.4 (C=S); MS (EI, 70 eV) m/z 287 (M^+); HRMS, $C_{16}H_{17}NSO_2$, 287.0980; found, 287.0971.

***N*-(4-Hydroxyphenyl)-*N*-(*n*-butyl)-4-hydroxythiobenzamide (11c).** Deprotected according to BBr_3 procedure and purified by radial chromatography (5% MeOH/ CH_2Cl_2) to afford yellow oil (10%): 1H NMR ($(CD_3)_2SO$) δ 0.84 (s, 3H, $J=7.5$ Hz, CH_3), 1.27 (sext, 2H, $J=6.8$ Hz, CH_2CH_2), 1.61 (quint, 2H, $J=8.0$ Hz, $CH_2CH_2CH_2$), 4.30 (t, 2H, $J=7.7$ Hz, CH_2NCS), 6.43 (d, 2H, $J=8.5$ Hz, ArH *meta* RNCS), 6.58 (d, 2H, $J=8.2$ Hz, ArH *meta* CSNR), 6.87 (d, 2H, $J=8.2$ Hz, ArH *ortho* RNCS), 6.97 (d, 2H, $J=8.5$ Hz, ArH *ortho* CSNR); ^{13}C NMR ($(CD_3)_2SO$) δ 14.2 (CH_3), 19.7 (CH_2), 27.9 (CH_2), 56.8 (CH_2), 114.1 (ArCH), 115.9 (ArCH), 128.5 (ArCH), 129.9 (ArCH), 135.2 (ArC), 136.8 (ArC), 156.2 (ArC), 157.7 (ArC), 201.0 (C=S); MS (EI, 70 eV), m/z 301 (M^+); HRMS calcd for $C_{17}H_{19}NO_2S$, 301.1136; found 301.1133.

***N*-(4-Hydroxyphenyl)-*N*-(*i*-butyl)-4-hydroxythiobenzamide (11d).** Deprotected according to BBr_3 procedure and purified by flash chromatography (35% EtOAc/hexane) to afford yellow foam (86%): 1H NMR ($CDCl_3$) δ 0.98 (d, 6H, $J=6.8$ Hz), 2.16 (m, 1H, $J=6.8$ Hz), 4.34 (d, 2H, $J=7.6$ Hz), 6.41 (d, 2H, $J=8.8$ Hz), 6.60 (d, 2H, $J=8.8$ Hz), 6.79 (d, 2H, $J=8.8$ Hz), 6.96 (d, 2H, $J=8.8$ Hz); ^{13}C NMR ($CDCl_3$) δ 20.3, 26.9, 27.2, 50.8, 63.9, 114.5, 116.1, 127.9, 129.5, 136.4, 137.7, 155.4, 156.5, 203.0; MS (EI, 70 eV) m/z 301 (M^+); HRMS calcd for $C_{17}H_{19}NO_2S$, 301.1136; found, 301.1144.

***N*-(4-Hydroxyphenyl)-*N*-(benzyl)-4-hydroxythiobenzamide (11e).** Deprotected according to EtSH procedure and purified by flash chromatography (35% EtOAc/hexane) to afford yellow foam (16%): 1H NMR ($(CDCl_3)$) δ 5.76 (s, 2H, CH_2), 6.59 (d, 2H, $J=8.4$ Hz, ArH *meta* RNCS), 6.61 (d, 2H, $J=8.3$ Hz, ArH *meta* CSNR), 6.77 (d, 2H, $J=8.8$ Hz, ArH *ortho* RNCS), 7.27 (m, 5H, Ph), 7.38 (d, 2H, $J=6.4$ Hz, ArH *ortho* CSNR); MS (EI, 70 eV) m/z 335 (M^+); HRMS calcd for $C_{20}H_{17}NO_2S$, 335.0980; found, 335.0984.

***N*-(4-hydroxyphenyl)-*N*-(1-phenethyl)-4-hydroxythiobenzamide (11f).** Deprotected according to BBr_3 procedure

and recrystallized from CHCl_3 to afford light yellow powder (quant): mp 174–175 °C; ^1H NMR (CDCl_3) δ 1.55 (d, 3H, $J=7.2$ Hz); 5.89 (br s, 1H); 6.27 (br s, 1H); 6.44 (d, 2H, $J=8.8$ Hz); 6.5 (br s, 1H); 6.71 (br s, 1H); 6.96 (d, 2H, $J=8.8$ Hz); 7.32 (m, 5H); 7.52 (q, 1H, $J=6.8$ Hz); MS (EI, 70 eV) m/z 349 (M^+); anal. ($\text{C}_{21}\text{H}_{19}\text{NO}_2\text{S}\cdot 0.4 \text{ H}_2\text{O}$): C, 70.72; H, 5.60; N, 3.93. Found: C, 70.88; H, 5.42; N, 3.98.

***N*-(4-Hydroxyphenyl)-*N*-[2-(3-methyl)-butyl]-4-hydroxythiobenzamide (11g).** Deprotected according to BBr_3 procedure and purified by flash chromatography (25% EtOAc/hexane) to afford foam (37%, two steps from carboxamide): ^1H NMR (CDCl_3) δ (major methyl rotamer) 0.95 (d, 3H, $J=6.6$ Hz), 1.14 (d, 3H, $J=6.9$ Hz), 1.21 (d, 3H, $J=6.3$ Hz), 1.82 (br m, 1H), 5.82 (quin, 1H, $J=7.4$ Hz), 6.30 (d, 2H, $J=8.5$ Hz), 6.60 (br m, 4H), 6.83 (d, 2H, $J=8.5$ Hz); ^{13}C NMR (CDCl_3) δ 17.1 (CH_3), 19.8 (CH_3), 20.9 (CH), 32.5 (CH), 114.7 (ArCH), 115.6 (ArCH), 128.8 (ArCH), 129.5 (ArCH), 133.2 (ArC), 137.2 (ArC), 155.2 (ArC), 155.3 (ArC), 204.4 ($\text{C}=\text{S}$); MS (EI, 70 eV) m/z 315 (M^+); anal. ($\text{C}_{18}\text{H}_{21}\text{NO}_2\text{S}\cdot 0.8 \text{ H}_2\text{O}$): C, 65.54; H, 6.91; N, 4.35. Found: C, 65.15; H, 6.67; N, 3.91.

Triphenylphosphine-4-methoxyphenylimine (12a).³⁶ *p*-Anisidine was diazotized in 50% H_2SO_4 and then added to a NaN_3 -sodium acetate buffered solution.¹⁵ The azide was extracted with diethyl ether and the phenolic side-product removed by Na_2CO_3 wash. Concentration in vacuo afforded the crude azide which was directly used in the next step. *Ylide formation*: to an ethereal solution of azide was added an equimolar solution of PPh_3 at rt. After the solution was heated under reflux for 2 h and N_2 evolution ceased, the solvent was concentrated and resulting $\text{Ph}_3\text{P}=\text{O}$ oxide removed. The crude imine was passed over SiO_2 plug (ether) to remove additional oxide. Final concentration and titration with hexanes afforded pure imine as orange crystals (53% from *p*-anisidine): mp 116–117.5 °C; mp³³ 119–120 °C.

Triphenylphosphine-phenylimine (12b).^{14,37} A cold aqueous solution of NaNO_2 (1.2 equiv) was added dropwise to a solution of aniline in 10% HCl at 0–5 °C with vigorous stirring. The mixture was kept below 5 °C for 30 min, and then a solution of NaN_3 in water was added dropwise while the temperature was kept below 5 °C. After 1 h the reaction was warmed to rt and extracted with diethyl ether. The extracts were dried over Na_2SO_4 and concentrated to afford the crude azide¹⁴ as an oil, which was directly used in the next step without additional purification. *Ylide formation*: same as described for **12a** to afford light yellow crystals upon solvent concentration (64% from aniline): mp 128–130 °C (mp³⁴ 131–132 °C).

***N*-(1,1,1-Trifluoro-2-propylidene)-4-methoxyaniline (13a).**⁶ Ylide **12a** and trifluoroacetone were heated to reflux in C_6H_6 for 12 h. The reaction was cooled to rt and concentrated in vacuo. The residue was triturated with Et_2O to remove Ph_3PO and the resulting filtrate concentrated followed by Kugelrohr distillation under

reduced pressure to afford product as light yellow oil (92%): bp 66 °C (0.1 mm); ^1H NMR (CDCl_3) δ 2.06 (s, 3H), 3.81 (s, 3H), 6.79, 6.92 (AA'BB', 4H, $J=8.8$, 4.0 Hz); ^{13}C NMR δ 14.6 (CH_3), 55.6 (CH_3), 114.5 (ArCH), 120.5 (q, CF_3 , $J=273$ Hz), 121.1 (ArCH), 121.5 (ArCH), 140.5 (ArC), 157.1 (q, CCF_3 , $J=33$ Hz), 157.6 (ArC); MS (EI, 70 eV) m/z 217 (M^+); anal. ($\text{C}_{10}\text{H}_{10}\text{NF}_3\text{O}$): C, 55.30; H, 4.64; N, 6.45. Found: C, 55.59; H, 4.99; N, 6.64.

***N*-(1,1,1-Trifluoro-2-propyl)-4-methoxyaniline (14a).**⁶ To a Et_2O solution of LiAlH_4 (0.5 equiv) at 0 °C was added a Et_2O solution of propylidene **13a** dropwise over 30 min. Upon complete addition the mixture was refluxed for 2 h. The mixture was then cooled to 0 °C and quenched using a 1:1:3 work up (H_2O :3M NaOH : H_2O). The resulting mixture was decanted into a separatory funnel, the aqueous layer separated and ether layer washed with brine, dried over MgSO_4 and concentrated. Purification by Kugelrohr distillation provided pure amine as light red oil (64%): bp 80 °C (0.2 mm); ^1H NMR (CDCl_3) δ 1.34 (d, 3H, $J=7.0$ Hz), 3.32 (br s, 1H), 3.72 (s, 3H), 3.87 (m, 1H), 6.61 (AA'BB', 2H, $J=8.8$, 4.0 Hz), 6.77 (AA'BB', 2H, $J=8.8$, 3.5 Hz); ^{13}C NMR (CDCl_3) δ 15.2 (CH_3), 52.7 (q, CHCF_3 , $J=30$ Hz), 55.8 (CH_3), 115.1 (ArCH), 115.4 (ArCH), 126.5 (q, CF_3 , $J=280$ Hz), 140.2 (ArC), 153.2 (ArC); MS (EI, 70 eV) m/z 219 (M^+).

***N*-(1,1,1-Trifluoro-2-phenethyl)-4-methoxyaniline (14b).** Prepared according to procedures outlined above from ylide **12a** and trifluoroacetophenone. The imine was isolated then used directly in reduction step to afford the title compound as a light yellow oil upon distillation (69%): bp 110 °C (0.1 mm); ^1H NMR (CDCl_3) δ 3.72 (s, 3H), 4.10 (br s, 1H), 4.81 (q, 1H, $J=7.0$ Hz), 6.61 (AA'BB', 2H, $J=8.8$, 4.0 Hz), 6.75 (AA'BB', 2H, $J=8.8$, 3.5 Hz), 7.40 (m, 5H); ^{13}C NMR (CDCl_3) δ 55.8 (CH_3), 62.0 (CHCF_3 , q, $J=30$ Hz), 115.0 (ArCH), 115.9 (ArCH), 125.5 (q, CF_3 , $J=280$ Hz), 128.2 (ArCH), 129.1 (ArCH), 129.3 (ArCH), 134.5 (ArC), 139.7 (ArC), 153.5 (ArC); MS (EI, 70 eV) m/z 281 (M^+); anal. ($\text{C}_{15}\text{H}_{14}\text{NF}_3\text{O}$): C, 64.05; H, 5.02; N, 4.98. Found: C, 63.90; H, 4.84; N, 5.05.

***N*-(1,1,1-Trifluoro-2-phenethyl)-aniline (14c).** Prepared according to procedures outlined above using ylide **12b** and trifluoroacetophenone. The imine was isolated then used directly in reduction to afford the title compound as a clear oil upon distillation (59%): bp 100 °C (0.5 mm); ^1H NMR (CDCl_3) δ 4.36 (d, 1H, $J=6.5$ Hz, NH), 4.96 (quint, 1H, $J=7.0$ Hz), 6.68 (d, 2H, $J=8.0$ Hz), 6.82 (t, 1H, $J=7.0$ Hz), 7.20 (d, 2H, $J=7.0$ Hz), 7.42 (m, 3H), 7.50 (d, 2H, $J=6.5$ Hz); ^{13}C NMR (CDCl_3) δ 60.7 (q, CHCF_3 , $J=29$ Hz), 114.1 (ArCH), 119.5 (ArCH), 122.5 (q, CF_3 , $J=278$ Hz), 128.1 (ArCH), 129.2 (ArCH), 129.4 (ArCH), 129.6 (ArCH), 134.3 (ArC), 145.8 (ArC); MS (EI, 70 eV) m/z 251 (M^+); anal. ($\text{C}_{14}\text{H}_{12}\text{F}_3\text{N}$): C, 66.93; H, 4.81; N, 5.57. Found: C, 66.79; H, 4.80; N, 5.54.

***N*-[1,1,1-Trifluoro-2-(3-methoxy)-phenethyl]-aniline (14d).** 2,2,2-Trifluoro-1-(3-methoxyphenyl)-ethanone precursor.¹³

Mg turnings (1.25 g, 50 mmol), 3-methoxyphenyl bromide (9.35 g, 50 mmol), and anhydrous THF (50 mL) were gingerly heated until a vigorous reaction took place. When all the Mg turnings were dissolved the reaction mixture was cooled to 0°C. A solution of *N*-trifluoroacetylpyridine³⁵ (7.52 g, 45 mmol) in anhydrous THF (10 mL) was added to the Grignard reagent dropwise over 0.5 h with stirring at 0°C. Upon complete addition, ice-bath was removed and the mixture stirred for 2 h. The reaction was quenched by the addition of satd aq NH₄Cl (5 mL), and the precipitates removed by filtration. The filtrate was dried over MgSO₄, evaporated in vacuo, and the crude ketone distilled to give 6.6 g (72%) of a colorless liquid: bp 50°C (0.5 mm) (bp⁹ 84–85°C (12 mm)).

The above prepared 2,2,2-trifluoro-1-(3-methoxyphenyl)-ethanone was then reacted with ylide **12a** as described previously. Imine isolation and LAH reduction afforded the title compound as a light green oil upon distillation (80%): bp 125°C (0.8 mm); ¹H NMR (CDCl₃) δ 3.79 (s, 3H), 4.31 (br s, 1H), 4.87 (q, 1H, *J* = 7.2 Hz), 6.63 (d, 2H, *J* = 7.6 Hz), 6.76 (td, 1H, *J* = 7.6, 0.8 Hz), 6.89 (dd, 1H, *J* = 8.5, 2.4 Hz), 6.99 (br s, 1H), 7.03 (d, 1H, *J* = 7.6 Hz), 7.15 (m, 2H), 7.28 (t, 1H, *J* = 8.0 Hz); ¹³C NMR (CDCl₃) δ 55.1 (CH₃), 60.3 (q, CHCF₃, *J* = 30 Hz), 113.8 (ArCH), 114.1 (ArCH), 119.1 (ArCH), 120.1 (ArCH), 124.9 (q, CF₃, *J* = 281 Hz), 128.7 (ArCH), 129.2 (ArCH), 129.8 (ArCH), 135.5 (ArC), 145.4 (ArC), 159.8 (ArC); MS (EI, 70 eV) *m/z* 281 (M⁺); anal. (C₁₅H₁₄F₃NO): C, 64.05; H, 5.02; N, 4.98. Found: C, 64.15; H, 4.99; N, 4.84.

***N*-(4-Methoxyphenyl)-*N*-(1,1,1-trifluoro-2-propyl)-4-methoxybenzamide (15a).**⁶ Prepared according to general procedure for CF₃-containing anilines and purified by flash chromatography (25% EtOAc/hexane) to afford product as white powder (68%): mp 85–86°C; ¹H NMR (CDCl₃) δ 1.21 (d, 3H, *J* = 7.0 Hz), 3.69 (s, 3H), 3.73 (s, 3H), 5.79 (sept, 1H, *J* = 6.5 Hz), 6.62 (d, 2H, *J* = 8.5 Hz), 6.75 (br s, 2H), 7.12 (br s, 2H), 7.22 (d, 2H, *J* = 8.5 Hz); ¹³C NMR (CDCl₃) δ 12.5 (CH₃), 55.2 (CH₃), 55.4 (CH₃), 113.1 (ArCH), 114.1 (ArCH), 125.2 (q, CF₃, *J* = 282 Hz), 128.0 (ArC), 130.6 (ArCH), 131.7 (ArC), 159.0 (ArC), 160.6 (ArC), 171.6 (C=O); MS (EI, 70 eV) *m/z* 353 (M⁺).

***N*-(4-Methoxyphenyl)-*N*-(1,1,1-trifluoro-2-phenethyl)-4-methoxybenzamide (15b).** Prepared according to general procedure for CF₃-containing anilines and purified by flash chromatography (25% EtOAc/hexane) to afford product as transparent oil (77%): ¹H NMR (CDCl₃) δ 3.68 (s, 3H), 3.69 (s, 3H), 6.05 (br s, 1H), 6.42 (br s, 1H), 6.61 (d overlapping br s, 3H, *J* = 8.5 Hz), 7.04 (br q, 1H, *J*_{HF} = 6.5 Hz), 7.25 (m, 8H); ¹³C NMR (CDCl₃) δ 55.1 (CH₃), 55.2 (CH₃), 58.8 (ArCHCF₃), 113.0 (ArCH), 113.6 (ArCH), 125.1 (q, CF₃, *J* = 281 Hz), 127.5 (ArC), 128.5 (ArCH), 129.0 (ArCH), 130.0 (ArCH), 130.7 (ArCH), 131.9 (ArC), 132.0 (ArCH), 132.9 (ArCH), 158.8 (ArC), 160.5 (ArC), 171.4 (C=O); MS (EI, 70 eV) *m/z* 415 (M⁺); HRMS calcd for C₂₃H₂₀F₃NO₃, 415.1395. Found, 415.1387.

***N*-(4-Methoxyphenyl)-*N*-(1,1,1-trifluoro-2-phenethyl)-benzamide (15c).** Prepared according to general procedure for CF₃-containing anilines and purified by flash chromatography (10% EtOAc/hexane) to afford product as light yellow oil (73%): bp 125°C (0.3 mm); ¹H NMR (CDCl₃) δ 3.61 (s, 3H), 6.01 (br s, 1H), 6.52 (2 overlapping br s, 3H), 7.12 (m, 4H), 7.26 (m, 6H); ¹³C NMR (CDCl₃) δ 55.4 (CH₃), 58.1 (CHCF₃), 113.6 (ArCH), 125.1 (q, CF₃, *J* = 282 Hz), 127.9 (ArCH), 128.7 (ArCH), 129.2 (ArCH), 129.6 (ArCH), 130.2 (ArCH), 131.4 (ArC), 131.9 (ArC), 132.4 (ArCH), 135.7 (ArC), 159 (ArC), 172.1 (C=O); MS (EI, 70 eV) *m/z* 385 (M⁺); anal. (C₂₂H₁₈F₃NO₂): C, 68.57; H, 4.71; N, 3.68. Found: C, 68.22; H, 5.03; N, 3.68.

***N*-(4-Methoxyphenyl)-*N*-(1,1,1-trifluoro-2-phenethyl)-3-methoxybenzamide (15d).** Prepared according to general procedure for CF₃-containing anilines and purified by flash chromatography (10% EtOAc/hexane) to afford product as transparent oil (79%): ¹H NMR (CDCl₃) δ 3.66 (2-s, 3H, ~1.2/1 ratio benzoyl rotamers), 3.88 (s, 3H), 6.78 (br d, 1H, *J* = 8.5 Hz), 6.8 (br s, 1H), 7.03 (q, 1H, *J* = 6.5 Hz, CHCF₃), 7.25 (m, 5H), 7.65 (dd, 1H, *J* = 8.5, 2.3 Hz), 7.75 (app dt, 1H, *J* = 7.6, 0.8 Hz); MS (EI, 70 eV) *m/z* 415 (M⁺).

***N*-(4-Methoxyphenyl)-*N*-(1,1,1-trifluoro-2-phenethyl)-2-methoxybenzamide (15e).** Prepared according to general procedure for CF₃-containing anilines and purified by flash chromatography (10% EtOAc/hexane) to afford product as transparent oil (36%, 84% corrected for recovered aniline); ¹H NMR (CDCl₃) δ 3.63 (s, 3H), 3.68 (s, 3H), 6.10 (br s, 1H), 6.43 (br s, 2H), 6.58 (d, 2H, *J* = 8.5 Hz), 6.72 (app t, 2H, *J* = 8.5 Hz), 7.21 (m, 7H); MS (EI, 70 eV) *m/z* 415 (M⁺).

***N*-(Phenyl)-*N*-(1,1,1-trifluoro-2-phenethyl)-4-methoxybenzamide (15f).** Prepared according to the general procedure for CF₃-containing anilines using 1,2-dichlorobenzene as solvent and purified by flash chromatography (10% EtOAc/hexane) to afford product as a transparent oil (54%): ¹H NMR (CDCl₃) δ 3.69 (s, 3H), 6.62 (d, 2H, *J* = 8.5 Hz), 7.11 (m, 3H), 7.25 (m, 9H); ¹³C NMR (CDCl₃) δ 55.1 (CH₃), 58.5 (CHCF₃), 113.0 (ArCH), 125.2 (q, CF₃, *J* = 282 Hz), 127.3 (ArC), 127.9 (ArCH), 128.6 (ArCH), 129.0 (ArCH), 129.9 (ArCH), 130.7 (ArCH), 130.9 (ArCH), 131.9 (ArC), 139.5 (ArC), 161.0 (ArC), 171.2 (C=O); MS (EI, 70 eV) *m/z* 385 (M⁺); anal. (C₂₃H₂₀NO₃F₃·1.1 CHCl₃): C, 52.95; H, 3.89; N, 2.56. Found: C, 52.84; H, 3.90; N, 2.65.

***N*-(Phenyl)-*N*-[1,1,1-trifluoro-2-(3-methoxy)-phenethyl]-4-methoxybenzamide (15g).** Prepared according to general procedure for CF₃-containing anilines using 1,2-dichlorobenzene as solvent and purified by flash chromatography (10–25% EtOAc/hexane) to afford product as transparent oil (51%): ¹H NMR (CDCl₃) δ 3.68 (s, 3H), 3.69 (s, 3H), 6.61 (d, 2H, *J* = 8.5 Hz), 6.77 (s, 1H), 6.88 (app td, 2H, *J* = 8.5, 3.5 Hz), 7.10 (m, 5H), 7.18 (app t, *J* = 8.0 Hz), 7.26 (d, 2H, *J* = 8.5 Hz); ¹³C NMR (CDCl₃) δ 55.3 (CH₃), 55.4 (CH₃), 58.7 (CHCF₃), 113.1

(ArCH), 115.0 (ArCH), 115.5 (ArCH), 122.5 (ArCH), 125.4 (q, CF₃, J = 281 Hz), 127.5 (ArC), 128.1 (ArCH), 128.7 (ArCH), 129.7 (ArCH), 130.9 (ArCH), 131.1 (ArCH), 133.3 (ArC), 139.7 (ArC), 159.6 (ArC), 160.9 (ArC), 171.4 (C=O); MS (EI, 70 eV) m/z 415 (M⁺).

***N*-(4-Hydroxyphenyl)-*N*-(1,1,1-trifluoro-2-propyl)-4-hydroxybenzamide (16a).**⁶ Deprotected according to BBr₃ procedure and recrystallized from EtOAc/hexane to afford white powder (62%): mp 203–205 °C (mp⁶ 207–207.5 °C); ¹H NMR (acetone-*d*₆) δ 1.24 (d, 3H, J = 6.5 Hz), 5.78 (q, 1H, J = 6.5 Hz), 6.62 (d, 2H, J = 8.8 Hz), 6.78 (br s, 2H), 7.05 (br s, 2H), 7.18 (d, 2H, J = 8.8 Hz), 8.61 (s, 1H), 8.70 (s, 1H); ¹³C NMR (acetone-*d*₆) δ 12.6 (CH₃), 51.3 (q, CH, $^3J_{\text{H-F}}$ = 30 Hz), 114.9 (ArCH), 115.0 (ArCH), 116.2 (ArCH), 126.8 (q, CF₃, $^1J_{\text{CF}}$ = 282 Hz), 128.2 (ArC), 131.4 (ArCH), 131.6 (ArC), 157.7 (ArC), 159.3 (ArC), 171.8 (C=O); MS (EI, 70 eV) m/z 325 (M⁺); anal. (C₁₆H₁₄NO₃F₃): C, 59.08; H, 4.34; N, 4.31. Found: C, 59.14; H, 4.37; N, 3.96.

***N*-(4-Hydroxyphenyl)-*N*-(1,1,1-trifluoro-2-phenethyl)-4-hydroxybenzamide (16b).** Deprotected according to BBr₃ procedure and purified by radial chromatography (25% EtOAc/hexane) to afford product as thick oil (53%): ¹H NMR (MeOD) δ 5.91 (br s, 1H), 6.32 (br s, 1H), 6.54 (d, 2H, J = 8.8 Hz), 6.62 (br s, 1H), 6.94 (q, 1H, $J_{\text{H-F}}$ = 9.2 Hz), 7.13 (d, 2H, J = 8.8 Hz), 7.23 (m, 6H); ¹³C NMR (MeOD) δ 60.2 (CH), 113.9 (ArCH), 114.5 (ArCH), 125.0 (q, CF₃, J = 282 Hz), 125.8 (ArC), 128.0 (ArCH), 128.7 (ArCH), 129.6 (ArCH), 130.0 (ArCH), 130.2 (ArC), 131.3 (ArC), 131.8 (ArC), 156.9 (ArC), 158.8 (ArC), 172.7 (C=O); MS (EI, 70 eV) m/z 387 (M⁺); anal. (C₂₁H₁₆F₃NO₃·0.1 H₂O): C, 64.81; H, 4.20; N, 3.60. Found: C, 64.68; H, 4.30; N, 3.45

***N*-(4-Hydroxyphenyl)-*N*-(1,1,1-trifluoro-2-phenethyl)-benzamide (16c).** Deprotected according to BBr₃ procedure and recrystallized from EtOAc/hexane to afford white powder (83%): mp 158–159 °C, ¹H NMR (CDCl₃) δ 5.91 (br s, 1H), 6.30 (br s, 1H), 6.61 (br s, 1H), 6.74 (s, 1H), 6.95 (q, 1H, J = 8.8 Hz), 7.24 (m, 9H); MS (EI, 70 eV) m/z 371 (M⁺); anal. (C₂₁H₁₆F₃NO₂): C, 67.92; H, 4.34; N, 3.77. Found: C, 68.05; H, 4.35; N, 3.63.

***N*-(4-Hydroxyphenyl)-*N*-(1,1,1-trifluoro-2-phenethyl)-3-hydroxybenzamide (16d).** Deprotected according to BBr₃ procedure and recrystallized from EtOAc/hexane to afford off-white powder (77%): mp 163–164 °C; ¹H NMR (CDCl₃) δ 5.92 (br s, 1H), 6.28 (br s, 1H), 6.64 (m, 2H), 6.96 (m, 3H), 7.31 (m, 7H); MS (EI, 70 eV) m/z 387 (M⁺); anal. (C₂₁H₁₆NO₃F₃·H₂O): C, 62.52; H, 4.48; N, 3.46. Found: C, 62.52; H, 4.17; N, 3.27.

***N*-(4-Hydroxyphenyl)-*N*-(1,1,1-trifluoro-2-phenethyl)-2-hydroxybenzamide (16e).** Deprotected according to BBr₃ procedure and recrystallized from EtOAc/hexane to afford off-white powder (59%): mp 191.5–193 °C; ¹H NMR (MeOD) δ 6.10 (br s, 2H), 6.59 (app q, 2H, J = 7.6, 7.2 Hz), 6.96 (m, 3H), 7.32 (m, 6H); MS (EI, 70 eV) m/z 387 (M⁺); anal. (C₂₁H₁₆F₃NO₃·0.7 H₂O): C, 63.06; H, 4.38; N, 3.50. Found: C, 63.04; H, 4.08; N, 3.50.

***N*-(Phenyl)-*N*-(1,1,1-trifluoro-2-phenethyl)-4-hydroxybenzamide (16f).** Deprotected according to BBr₃ procedure and recrystallized from EtOAc/hexane to afford off-white powder (quant): mp 114–116 °C; ¹H NMR (CDCl₃) δ 6.48 (d, 2H, J = 8.4 Hz), 7.0 (m, 4H), 7.15 (d, 2H, J = 8.4 Hz), 7.26 (d, 6H), 7.72 (s, 2H, exchange with D₂O); ¹³C NMR (MeOD) δ 50.8 (CH), 114.9 (ArCH), 125.0 (q, CF₃, J_{CF} = 281 Hz), 126.3 (ArC), 128.2 (ArCH), 128.6 (ArCH), 129.3 (ArCH), 130.0 (ArCH), 130.8 (ArCH), 131.0 (ArCH), 131.6 (ArC), 139.2 (ArC), 158.2 (ArC), 172.6 (C=O); MS (EI, 70 eV) m/z 371 (M⁺); anal. (C₂₁H₁₆F₃NO₂·0.5 H₂O): C, 66.31; H, 4.50; N, 3.68. Found: C, 66.19; H, 4.27; N, 3.57.

***N*-(Phenyl)-*N*-(1,1,1-trifluoro-2-(3-hydroxyphenethyl))-4-hydroxybenzamide (16g).** Deprotected according to BBr₃ procedure and recrystallized from CHCl₃ to afford small off-white crystals (95%): mp 163–165 °C; ¹H NMR (CDCl₃) δ 6.43 (d, 2H, J = 8.5 Hz), 6.67 (d, 1H, J = 8.0 Hz), 6.82 (dd, 1H, J = 8.5, 2 Hz), 6.91 (s, 1H), 7.08 (m, 8H), 7.62 (s, 1H); ¹³C NMR (CDCl₃) 114.9 (ArCH), 116.6 (ArCH), 117.0 (ArCH), 121.2 (ArCH), 124.6 (q, CF₃, J = 226 Hz), 126.1 (ArC), 128.3 (ArCH), 128.6 (ArCH), 129.8 (ArCH), 130.6 (ArCH), 132.6 (ArC), 138.8 (ArC), 156.3 (ArC), 157.8 (ArC), 173.0 (C=O); MS (EI, 70 eV) m/z 387 (M⁺); anal. (C₂₁H₁₆F₃NO₃): C, 65.12; H, 4.16; N, 3.62. Found: C, 64.78; H, 4.18; N, 3.38.

***N*-(4-Hydroxyphenyl)-*N*-(1,1,1-trifluoro-2-propyl)-4-hydroxythiobenzamide (17a).** Deprotected according to BBr₃ procedure and recrystallized from ether to afford yellow powder (93%): ¹H NMR (MeOD) δ 1.33 (d, 3H, J = 7.5 Hz), 6.47 (d, 2H, J = 8 Hz), 6.58 (d, 1H, J = 6.5 Hz), 6.64 (d, 1H, J = 6 Hz), 6.79 (d, 1H, J = 8.5 Hz), 6.96 (d, 1H, J = 8.0 Hz), 7.01 (d, 3H, J = 8.5 Hz; ArCH *ortho* C=O and CHCF₃); MS (EI, 70 eV) m/z 341 (M⁺); anal. (C₁₆H₁₄F₃NO₂S·0.1 H₂O): C, 56.00; H, 4.17; N, 4.08. Found: C, 55.76; H, 4.13; N, 3.74.

***N*-(4-Hydroxyphenyl)-*N*-(1,1,1-trifluoro-2-phenethyl)-4-hydroxythiobenzamide (17b).** Deprotected according to BBr₃ procedure and purified by chromatography (5% MeOH/CH₂Cl₂) to afford title compound as yellow foam (74%): ¹H NMR (CDCl₃) δ 5.47 (br s, 1H, OH), 5.58 (br s, 1H, OH), 5.86 (d, 1H, J = 5.5 Hz, ArH *ortho* to OH on aniline ring), 6.25 (d, 1H, J = 5.5 Hz, ArH *ortho* to OH on aniline ring), 6.36 (d, 2H, J = 8 Hz, ArH *ortho* to OH on benzamide ring), 6.57 (d, 1H, J = 6 Hz, ArH *ortho* to N=C=S), 6.93 (d, 2H, J = 9 Hz, ArH *ortho* to C=S), 6.98 (d, 1H, J = 6 Hz, ArH *ortho* to N=C=S), 8.39 (q, 1H, $J_{\text{H-F}}$ = 9 Hz); ¹³C NMR (CDCl₃) δ 63.8 (CHCF₃), 114.6 (ArCH), 115.0 (ArCH), 115.5 (ArCH), 125.1 (q, J = 163 Hz, CF₃), 129.0 (ArCH), 129.3 (ArCH), 129.8 (ArCH), 129.9 (ArCH), 131.4 (ArC), 133.4 (ArC), 136.3 (ArC), 155.3 (ArC), 155.7 (ArC), 208.3 (C=S); MS (EI, 70 eV) m/z 403 (M⁺); HRMS calcd for C₂₁H₁₆F₃NO₂S, 403.0853, found 403.0858; anal. (C₂₁H₁₆F₃NO₂S·0.3 H₂O): C, 61.70; H, 4.09; N, 3.43. Found: C, 61.68; H, 3.92; N, 3.25.

***N*-(4-Methoxyphenyl)-4-methoxyphenylacetamide (18).** To a 0 °C CH₂Cl₂ solution of *p*-anisidine (1.3 equiv) and pyridine (1.1 equiv) was added dropwise a CH₂Cl₂

solution (2–5 mL) of 4-methoxyphenylacetyl chloride (1.0 equiv). Upon complete addition (15 min) mixture was allowed to reach rt. Upon completion of the reaction, the mixture was diluted with CH_2Cl_2 followed by product isolation (H_2O , CuSO_4 , brine). Recrystallization from EtOAc/hexane afforded the title carboxamide as small white crystals (82%): mp 127–128 °C; ^1H NMR (CDCl_3) δ 3.65 (s, 2H), 3.76 (s, 3H), 3.82 (s, 3H), 6.80 (d, 2H, $J=9.0$ Hz), 6.92 (d, 2H, $J=8.5$ Hz), 7.07 (s, 1H), 7.23 (d, 2H, $J=9.0$ Hz), 7.30 (d, 2H, $J=8.5$ Hz); ^{13}C NMR (CDCl_3) δ 43.7 (CH_2), 55.3 (CH_3), 55.5 (CH_3), 114.1 (ArCH), 114.6 (ArCH), 121.8 (ArCH), 126.5 (ArC), 130.7 (ArCH), 130.8 (ArC), 156.5 (ArC), 159.0 (ArC), 169.7 (C=O); MS (EI, 70 eV) m/z 271 (M^+); anal. ($\text{C}_{16}\text{H}_{17}\text{NO}_3$): C, 70.83; H, 6.32; N, 5.16. Found: C, 70.87; H, 6.29; N, 5.29.

***N*-(4-Methoxyphenyl)-*N*-(ethyl)-4-methoxyphenylacetamide (19).** Prepared according to phase transfer catalysis conditions described above for carboxamides. Purification by either Kugelrohr distillation or flash chromatography (25% EtOAc/hexane) afforded product as red-orange oil (quant): bp 150 °C (0.2 mm); ^1H NMR (CDCl_3) δ 1.08 (t, 3H, $J=7.0$ Hz), 3.33 (s, 2H), 3.70 (q, 2H, $J=7.1$ Hz), 3.78 (s, 3H), 3.84 (s, 3H), 6.77 (d, 2H, $J=8.5$ Hz), 6.79 (d, 2H, $J=8.5$ Hz), 6.97 (d overlapping, 2H, $J=8.5$ Hz), 6.98 (d overlapping, 2H, $J=8.5$ Hz); ^{13}C NMR (CDCl_3) δ 13.2 (CH_3), 40.5 (CH_2), 44.4 (CH_2), 55.4 (CH_3O), 55.7 (CH_3O), 113.9 (ArCH), 114.8 (ArCH), 127.9 (ArC), 129.9 (ArCH), 130.2 (ArCH), 135.2 (ArC), 158.4 (ArC), 159.2 (ArC), 171.2 (C=O); MS (EI, 70 eV) m/z 299 (M^+); anal. ($\text{C}_{18}\text{H}_{21}\text{NO}_3 \cdot 0.1 \text{CHCl}_3$): C, 69.83; H, 6.83; N, 4.50. Found: C, 69.82; H, 6.98; N, 3.98.

***N*-(4-Methoxyphenyl)-*N*-(ethyl)- α -ethyl-4-methoxyphenylacetamide (20a).** *n*-BuLi in hexane (1.56 M, 2.0 equiv) was added dropwise to a -78°C THF (*i*-propyl) $_2\text{NH}$ (2.2 equiv) solution, then warmed to 0 °C. After 0.5 h at 0 °C the mixture was re-cooled to -78°C and a THF solution of acetamide **19** (1.0 equiv) added dropwise. After 20 min EtI (1.3 equiv) was added in one portion and the mixture allowed to reach rt. Product isolation (H_2O , Et_2O , Na_2SO_4) and purification by flash chromatography (25% EtOAc/hexane) as light yellow oil (95%): ^1H NMR (CDCl_3) δ 0.78 (t, 3H, $J=7.5$ Hz, CH_3 α -ethylacetamide), 1.05 (t, 3H, $J=7.0$ Hz, CH_3 *N*-ethyl), 1.60 (dq, 1H, $J=14.0$, 7.0 Hz, $\alpha\text{-CH}_2$), 2.04 (dq, 1H, $J=14.0$, 7.0 Hz, $\alpha\text{-CH}_2$), 3.27 (dd, 1H, $J=8.5$, 7.0 Hz, CH α -benzylic), 3.67 (m, 2H, $\text{-NCH}_2\text{CH}_3$), 3.77 (s, 3H), 3.85 (s, 3H), 6.75 (d, 2H, $J=8.8$ Hz), 6.87 (br s, 4H), 6.98 (d, 2H, $J=8.8$ Hz); ^{13}C NMR (CDCl_3) δ 12.5 (CH_3), 13.1 (CH_3), 28.5 (CH_2), 44.3 (CH_2), 55.2 (CH_3), 55.6 (CH_3), 113.7 (ArCH), 114.5 (ArCH), 129.2 (ArCH), 132.9 (ArC), 135.0 (ArC), 158.4 (ArC), 159.0 (ArC), 173.5 (C=O); MS (EI, 70 eV) m/z 327 (M^+); anal. ($\text{C}_{20}\text{H}_{25}\text{NO}_3$): C, 73.37; H, 7.70; N, 4.28. Found: C, 72.84; H, 7.56; N, 3.59.

***N*-(4-Methoxyphenyl)-*N*-(ethyl)- α -benzyl-4-methoxyphenylacetamide (20b).** Preparation as described in **20a** and purification by flash chromatography (15% EtOAc/hexane) afforded title compound as an oil (86%): ^1H

NMR (CDCl_3) δ 0.94 (t, 3H, $J=7.2$ Hz, NCH_2CH_3), 2.75 (dd, 1H, $J=12.8$, 4.8 Hz, methine H), 3.43 (m, 2H, NCH_2CH_3), 3.58 (dd, 1H, $J=10.2$, 5.1 Hz), 3.70 (dd, 1H, $J=13.3$, 7.1 Hz), 3.76 (s, 3H), 3.79 (s, 3H), 6.15 (br s, 1H), 6.75 (d, 2H, $J=8.3$ Hz), 6.78 (d, 2H, $J=6.7$ Hz), 7.09 (m, 4H), 7.24 (m, 3H); ^{13}C NMR (CDCl_3) δ 12.8 (CH_3), 41.5 (CH_2), 44.2 (CH_2), 50.3 (CH), 55.2 (OCH_3), 55.4 (OCH_3), 113.7 (ArCH), 114.3 (ArCH), 126.2 (ArCH), 128.2 (ArCH), 129.1 (ArCH), 129.4 (ArCH), 130.0 (ArCH), 132.4 (ArC), 134.6 (ArC), 140.1 (ArC), 158.5 (ArC), 158.9 (ArC), 172.5 (C=O); MS (EI, 70 eV) m/z 389 (M^+).

***N*-(4-Hydroxyphenyl)-*N*-(ethyl)-4-hydroxyphenylacetamide (21a).** Deprotected according to BBr_3 procedure and purified by chromatography (50% EtOAc/hexane) to afford tan foam (quant): mp 75 °C dec.; ^1H NMR ($(\text{CD}_3)_2\text{SO}$) δ 0.96 (t, 3H, $J=7.5$ Hz), 3.16 (s, 2H), 3.36 (q, 2H, $J=7.5$ Hz), 6.59 (d, 2H, $J=8.5$ Hz), 6.78 (m, 4H), 6.97 (d, 2H, $J=8.5$ Hz), 9.18 (br s, 1H), 9.62 (br s, 1H); MS (EI, 70 eV) m/z 271 (M^+); anal. ($\text{C}_{16}\text{H}_{17}\text{NO}_3 \cdot 0.9 \text{H}_2\text{O}$): C, 66.84; H, 6.59; N, 4.87. Found: C, 66.95; H, 6.20; N, 4.77.

***N*-(4-Hydroxyphenyl)-*N*-(ethyl)-4-hydroxyphenylthioacetamide (21b).** Deprotected according to BBr_3 procedure and purified by chromatography (50% EtOAc/hexane) to afford tan powder (84%): mp 156–157 °C; ^1H NMR ($(\text{CD}_3)_2\text{SO}$) δ 1.08 (t, 3H, $J=7.0$ Hz), 3.67 (s, 2H), 4.14 (q, 2H, $J=2$ Hz), 6.54 (d, 2H, $J=8.5$ Hz), 6.75 (app t, 4H, $J=8.0$ Hz), 6.87 (d, 2H, $J=8.5$ Hz), 9.17 (s, OH), 9.78 (s, OH); MS (EI, 70 eV) m/z 287 (M^+); HRMS calcd for $\text{C}_{16}\text{H}_{17}\text{NO}_2\text{S}$, 287.0980; found, 287.0977; anal. ($\text{C}_{16}\text{H}_{17}\text{NO}_2\text{S} \cdot 0.2 \text{H}_2\text{O}$): C, 66.04; H, 6.03; N, 4.81. Found: C, 65.97; H, 6.03; N, 4.78.

***N*-(4-Hydroxyphenyl)-*N*-(ethyl)- α -ethyl-4-hydroxyphenylacetamide (22a).** Deprotected according to BBr_3 procedure and purified by chromatography (50% EtOAc/hexane) to afford white foam (70%): ^1H NMR (CDCl_3) δ 0.76 (t, 3H, $J=7.5$ Hz), 1.04 (t, 3H, $J=7.0$ Hz), 1.54 (m, 1H, CH_2 β -amide), 1.94 (m, 1H, CH_2 β -amide), 3.27 (t, 1H, $J=7.0$ Hz, CH α -amide), 3.62 (m, 2H, $\text{-NCH}_2\text{CH}_3$), 6.63 (d, 2H, $J=8.8$ Hz), 6.79 (d, overlapping br s, 2H, $J=8.8$ Hz), 7.05 (br s, 4H); ^{13}C NMR (CDCl_3) δ 12.5 (CH_3), 13.0 (CH_3), 28.2 (CH_2), 44.8 (CH_2), 50.7 (CH), 116.1 (ArCH), 128.6 (ArCH), 129.3 (ArCH), 131.7 (ArCH), 133.7 (ArC), 155.4 (ArC), 156.8 (ArC), 174.7 (C=O); MS (EI, 70 eV) m/z 299 (M^+); HRMS calcd for $\text{C}_{18}\text{H}_{21}\text{NO}_3$, 299.1521, found 299.1520.

***N*-(4-Hydroxyphenyl)-*N*-(ethyl)- α -ethyl-4-hydroxyphenylthioacetamide (22b).** Deprotected according to BBr_3 procedure and purified by chromatography (25% EtOAc/hexane) to afford yellow residue (95%): ^1H NMR (MeOD) δ 0.73 (t, 3H, $J=7.3$ Hz), 1.14 (t, 3H, $J=7.2$ Hz), 1.76 (m, 1H, CH_2 β -amide), 2.17 (m, 1H, CH_2 β -amide), 3.62 (dd, 1H, $J=7.8$, 7.0 Hz, CH α -amide), 4.16 (m, 1H, CH_2 α -NCO), 4.30 (m, 1H, CH_2 α -NCO), 6.56 (dd, 1H, $J=8.4$, 2.6 Hz), 6.56 (AA'BB', 2H, $J=8.7$, 2.3 Hz), 6.75 (dd, 1H, $J=8.4$, 2.8 Hz), 6.91 (dd, 1H, $J=8.6$, 2.7 Hz), 6.94 (AA'BB', 2H, $J=8.5$, 1.9 Hz),

7.0 (dd, 1H, $J=8.7, 2.8$ Hz); ^{13}C NMR (CDCl_3) δ 11.4 (CH_3), 12.6 (CH_3), 13.9 (CH_2), 52.3 (CH_2), 56.2 (CH), 115.0 (ArCH), 116.3 (ArCH), 128.5 (ArCH), 129.1 (ArCH), 129.9 (ArCH), 133.5 (ArC), 136.5 (ArC), 154.6 (ArC), 155.9 (ArC), 207.5 ($\text{C}=\text{S}$); MS (EI, 70 eV) m/z 315 (M^+); HRMS calcd for $\text{C}_{18}\text{H}_{21}\text{NO}_2\text{S}$, 315.1293; found, 315.1301.

***N*-(4-Hydroxyphenyl)-*N*-(ethyl)- α -benzyl-4-hydroxyphenylthioacetamide (22c).** Deprotected according to BBr_3 procedure and purified by chromatography (15% EtOAc/hexane) to afford yellow residue (47%): ^1H NMR (MeOD) δ 1.05 (t, 3H, $J=7.2$ Hz), 2.90 (dd, 1H, $J=12.9, 4.9$ Hz, PhCH_2), 3.66 (dd, 1H, $J=12.9, 9.5$ Hz, PhCH_2), 3.95 (m, 1H, CH_3CH_2), 4.05 (dd, 1H, $J=9.3, 5.2$ Hz, PhCH_2CH), 4.30 (m, 1H, CH_3CH_2), 6.02 (dd, 1H, $J=8.4, 2.7$ Hz), 6.56 (d, 2H, $J=8.3$ Hz), 6.66 (overlapping dds, 2H, $J=9.2, 3.1$ Hz), 6.75 (dd, 1H, $J=8.8, 3.0$ Hz), 7.00 (d, 2H, $J=8.7$ Hz), 7.10 (m, 5H); HRMS calcd for $\text{C}_{23}\text{H}_{23}\text{NSO}_2$, 377.1449; found, 377.1443.

***N*-(4-Methoxyphenyl)-*N*-(1,1,1-trifluoro-2-propyl)-4-methoxyphenylacetamide (25).** Prepared according to general amidation procedure for CF_3 -containing anilines; product isolation and purification via flash chromatography (25% EtOAc/hexane) afforded title compound as light yellow oil (40%): ^1H NMR (CDCl_3) δ 1.16 (d, 3H, $J=7$ Hz), 3.32 (s, 2H), 3.76 (s, 3H), 3.84 (s, 3H), 5.61 (sept, 1H, $J=7.6$ Hz), 6.77 (d, 2H, $J=8.9$ Hz), 6.90 (m, 3H), 6.92 (d, 2H, $J=8.9$ Hz), 7.06 (m, 1H); ^{13}C NMR (CDCl_3) δ 12.5 (CH_3), 40.7 (CH_2), 50.1 (q, CHCF_3 , $J=31$ Hz), 55.3 (CH_3O), 55.6 (CH_3O), 113.9 (ArCH), 114.3 (ArCH), 114.6 (ArCH), 125.1 (q, CF_3 , $J=283$ Hz), 127.0 (ArC), 129.9 (ArC), 130.2 (ArCH), 132.0 (ArCH), 158.6 (ArC), 159.9 (ArC), 172.8 ($\text{C}=\text{O}$); HRMS calcd for $\text{C}_{19}\text{H}_{20}\text{NF}_3\text{O}_3$, 367.1395, found, 367.1394; anal. ($\text{C}_{19}\text{H}_{20}\text{NF}_3\text{O}_3$): C, 62.12; H, 5.49; N, 3.81. Found: C, 61.76; H, 5.58; N, 3.66.

***N*-(4-Methoxyphenyl)-*N*-(1,1,1-trifluoro-2-propyl)- α -methyl-4-methoxyphenylacetamide (26).** $n\text{-BuLi}$ in hexane (1.56 M, 2.0 equiv) was added dropwise to a -78°C THF (*i*-propyl) $_2\text{NH}$ (2.2 equiv) solution, then warmed to 0°C . After 0.5 h at 0°C the mixture was re-cooled to -78°C and a THF solution of *N*-(1,1,1-trifluoro-2-propyl) substituted acetamide **25** (1.0 equiv) was added dropwise. After 20 min MeI (1.3 equiv) was added in one portion and the mixture allowed to reach rt. Crude product isolation (H_2O , Et_2O , Na_2SO_4) afforded an amber oil (83%) which was determined by both ^1H NMR and HPLC to be an approx. 1:1 ratio of diastereomers for the expected product: ^1H NMR (CDCl_3) δ 1.05 (2-ds, 3H, $J=7.5$ Hz), 1.28 (2-ds, 3H, $J=7.5$ Hz), 3.42 (overlapping qs, 1H, $J=7.5$ Hz), 5.58 (m, 1H, CHCF_3), 6.44 (2-dds, 1H, $J=8.8, 2.8$ Hz), 6.68 (dd, 0.5 H, $J=8.8, 2.8$ Hz), 6.70 (m, 2.5H), 6.81 (m, 2H), 7.01 (2-dds, 1H, $J=8.4, 2.3$ Hz), 7.20 (2-dds, 1H, $J=8.4, 2.3$ Hz); HPLC (254 nm) 25% EtOAc/hexane, Micropac SiO_2 column: 5.82 min. (46.2%), 7.19 min. (53.7%), $\text{sd}\pm 5\%$.

***N*-(4-Hydroxyphenyl)-*N*-(1,1,1-trifluoro-2-propyl)- α -methyl-4-hydroxyphenylacetamide (27).** Deprotection using BBr_3 procedure and chromatography (35% EtOAc/hexane) afforded title compound as a white powder (95%) with a 1:1 ratio of diastereomers as found by ^1H NMR: mp $165\text{--}170^\circ\text{C}$; ^1H NMR (MeOD) δ 1.10 (overlapping ds, 3H, $J=7.5$ Hz), 1.25 (overlapping ds, 3H, $J=7.5$ Hz), 3.49 (overlapping qs, 1H, $J=7.5$ Hz), 5.52 (m, 1H, CHCF_3), 6.43 (2-dds, 1H, $J=8.8, 2.8$ Hz), 6.57 (dd, 0.5H, $J=8.8, 2.8$ Hz), 6.64 (m, 2.5H), 6.72 (m, 2.5H), 6.86 (app td, 1H, $J=8.4, 2.3$ Hz), 7.07 (2-dds, 1H, $J=8.4, 2.3$ Hz); MS (EI, 70 eV) m/z 353 (M^+); HRMS calcd for $\text{C}_{18}\text{H}_{18}\text{NF}_3\text{O}_3$, 353.1238; found, 353.1235.

***N*-(4-Hydroxyphenyl)-*N*-(1,1,1-trifluoro-2-propyl)-4-hydroxyphenylthioacetamide (28).** Carboxamide **25** (0.3 mmol, 100 mg) was treated with Lawesson's reagent as outlined in general procedure. Product isolation (H_2O , Et_2O , Na_2SO_4) and radial chromatography (20% EtOAc/hexane) afforded 5 mg of protected thiocarboxamide in low yield (5%). Subsequent deprotection using BBr_3 procedure afforded the title compound as a light yellow residue upon SiO_2 purification (30% EtOAc/hexane, quant): ^1H NMR (MeOD) δ 1.24 (d and m, 3H, $J=7.8$ Hz), 3.85 (ABq, 2H, $J=13$ Hz), 5.56 (sept, 1H, $J=7.8$ Hz), 6.72 (m, 4H), 6.85 (m, 4H); HPLC: Whatman C18 column, 90% MeOH:10% H_2O $R_t=3.123>98\%$ pure at 254 nm.

Acknowledgements

We are grateful for support of this research through grants from the US Army Breast Cancer Research Program (DAMD17-97-1-7076) and the National Institutes of Health (HHS 5R37 DK15556 and CA18119). We thank Kathryn E. Carlson for performing binding assays and Scott Wilson, Richard Cesati and Professor Greg Girolami for valuable assistance with X-ray data acquisition, structure determination and refinement. NMR spectra were obtained in the Varian Oxford Instrument Center for Excellence in NMR Laboratory. Funding for this instrumentation was provided in part from the W. M. Keck Foundation and the National Science Foundation (NSF CHE 96-10502). Mass spectra were obtained on instruments supported by grants from the National Institute of General Medical Sciences (GM 27029), the National Institute of Health (RR 01575), and the National Science Foundation (PCM 8121494).

References and Notes

1. Katzenellenbogen, J. A.; O'Malley, B. W.; Katzenellenbogen, B. S. *Mol. Endocrinol.* **1996**, *10*, 119.
2. Grese, T. A.; Dodge, J. A. *Curr. Pharm. Des.* **1998**, *4*, 71.
3. Gao, H.; Katzenellenbogen, J. A.; Garg, R.; Hansch, C. *Chem. Rev.* **1999**, *99*, 723.
4. Palkowitz, A. D.; Glasebrook, A. L.; Thrasher, K. J.; Hauser, K. L.; Short, L. L.; Phillips, D. L.; Muehl, B. S.; Sato, M.; Shetler, P. K.; Cullinan, G. J.; Pelt, T. R.; Bryant, H. U. *J. Med. Chem.* **1997**, *40*, 1407.

5. Fink, B. E.; Mortsensen, D. S.; Stauffer, S. R.; Aron, Z. D.; Katzenellenbogen, J. A. *Chem. Biol.* **1999**, *6*, 205.
6. Hartmann, R. W.; vom Orde, H.-D.; Heindl, A.; Schö-
nenberger, H. *Arch. Pharm.* **1988**, *321*, 497.
7. Hartmann, R. W.; vom Orde, H.-D.; Schö-
nenberger, H. *Arch. Pharm.* **1990**, *323*, 73.
8. Osawa, Y. *Nippon Kagaku Zasshi* **1963**, *84*, 137.
9. Zwierzak, A.; Gajda, T. *Synthetic, Communications* **1981**,
1005.
10. Diéz-Barra, E.; Loupy, A.; Sansoulet, J.; Carrillo, J. *Syn-
thetic Communications* **1992**, *22*, 1661.
11. Tomioka, K.; Inoue, I.; Shindo, M.; Koga, K. *Tetrahedron
Lett.* **1991**, *32*, 3095.
12. Scheibye, S.; Pedersen, B. S.; Lawesson, S.-O. *Bull. Soc.
Chim. Belg.* **1978**, *87*, 229.
13. Hatanaka, Y.; Hashimoto, M.; Kurihara, H.; Nakayama,
H.; Kanaoka, Y. *J. Org. Chem.* **1994**, *59*, 383.
14. Tanno, M.; Sueyoshi, S.; Kamiya, S. *Chem. Pharm. Bull*
1982, *30*, 3125.
15. Dyll, L. K.; Suffolk, P. M.; Dehaen, W.; L'abbe, G. J. *J.
Chem. Soc. Perkin Trans. 2* **1994**, 2115.
16. Stewart, W. E.; Siddall III, T. H. *Chem. Rev.* **1970**, *70*, 517.
17. Bourn, A. J. R.; Gillies, D. G.; Randall, E. W. *Tetrahedron*
1966, *22*, 3132.
18. Wiberg, K. B.; Breneman, C. L. *J. Am. Chem. Soc.* **1992**,
117, 831.
19. Lauvergnat, D.; Hiberty, P. C. *J. Am. Chem. Soc.* **1997**,
119, 9478.
20. Hadad, C. M.; Rablen, P. R.; Wiberg, K. B. *J. Org. Chem.*
1998, *63*, 8668.
21. Neugebauer Crawford, S. M.; Taha, A. N.; True, N. S.;
LeMaster, C. B. *J. Phys. Chem. A* **1997**, *101*, 4699.
22. Laidig, K. E.; Cameron, L. M. *J. Am. Chem. Soc.* **1996**,
118, 1737.
23. Minick, D.; Frenz, J.; Patrick, M.; Brent, D. *J. Med.
Chem.* **1988**, *31*, 1923.
24. Erber, S.; Ringshandl, R.; von Angerer, E. *Anti-Cancer
Drug Des.* **1991**, *6*, 414.
25. von Angerer, E.; Erber, S. *J. Steroid. Biochem. Mol. Biol.*
1992, *41*, 557.
26. Brzozowski, A. M.; Pike, A. C.; Dauter, Z.; Hubbard, R.
E.; Bonn, T.; Engstrom, O.; Öhman, L.; Greene, G. L.; Gus-
tafsson, J.-A.; Carlquist, M. *Nature* **1997**, *389*, 753.
27. O'Hagan, D.; Rzepa, H. S. *Chem. Commun.* **1997**, 645.
28. Anstead, G. M.; Wilson, S. R.; Katzenellenbogen, J. A. *J.
Med. Chem.* **1989**, *32*, 2163.
29. Shiau, A. K.; Barstad, D.; Loria, P. M.; Cheng, L.;
Kushner, P. J.; Agard, D. A.; Greene, G. L. *Cell* **1998**, *95*,
927.
30. Anstead, G. M.; Peterson, C. S.; Katzenellenbogen, J. A. *J.
Steroid Biochem.* **1989**, *33*, 877.
31. Sun, J.; Meyers, M. J.; Fink, B. E.; Rajendran, R.; Katzen-
ellenbogen, J. A.; Katzenellenbogen, B. S. *Endocrinology* **1999**,
140, 800.
32. Katzenellenbogen, J. A.; Johnson, Jr., H. J.; Myers, H. N. *Biochemistry* **1973**, *12*, 4085.
33. Carlson, K. E.; Choi, I.; Gee, A.; Katzenellenbogen, B. S.;
Katzenellenbogen, J. A. *Biochemistry* **1997**, *36*, 14897.
34. Williams, D.; Gorski, J. *Biochem.* **1974**, *13*, 5537.
35. Chapman, Fidler *J. Chem. Soc.* **1936**, 448.
36. Johnson, A. W.; Wong, S. C. K. *Can. J. Chem.* **1966**, *44*,
2793.
37. Staudinger, H.; Meyer, J. *Helv. Chim. Acta* **1919**, *2*, 643.

Solid-Phase Synthesis of Tetrasubstituted Pyrazoles, Novel Ligands for the Estrogen Receptor

Shaun R. Stauffer and John A. Katzenellenbogen

Department of Chemistry, University of Illinois,
Urbana, Illinois 61801

JOURNAL OF
combinatorial
CHEMISTRY

Reprinted from
Volume 2, Number 4, Pages 318-329

Solid-Phase Synthesis of Tetrasubstituted Pyrazoles, Novel Ligands for the Estrogen Receptor

Shaun R. Stauffer and John A. Katzenellenbogen*

Department of Chemistry, University of Illinois, Urbana, Illinois 61801

Received January 11, 2000

Most ligands for the estrogen receptor (ER) are not well suited for synthesis by combinatorial means, because their construction involves a series of carbon–carbon bond forming reactions that are not uniformly high yielding. In previous work directed to overcoming this limitation, we surveyed various phenol-substituted five-membered heterocycles, hoping to find a system that would afford both high ER binding affinity and whose synthesis could be adapted to solid-phase methods (Fink et al. *Chem. Biol.* **1999**, 6, 206–219.) In this report, we have developed a reliable and efficient solid-phase method to prepare the best of these heterocycles, the tetrasubstituted pyrazoles, and we have used this methodology to produce small, discrete libraries of these novel ER ligands. We used a combination of FT-IR and nanoprobe ^1H NMR-MAS to characterize intermediates leading up to the final pyrazole products directly on the bead. We also developed a scavenging resin, which enabled us to obtain products free from inorganic contaminants. We prepared a 12-member test library, and then a 96-member library, and in both cases we determined product purity and ER binding affinity of all of the library members. Several interesting binding affinity patterns have emerged from these studies, and they have provided us with new directions for further exploration, which has led to pyrazoles having high affinity and potency as agonists and antagonists toward the ER α subtype.

Introduction

In recent years, combinatorial chemistry, with its ability to generate a large set of structurally related analogues, has become a bona fide tool for increasing productivity in the functional assessment of compound libraries and the rapid development of structure–activity relationships.¹ Combinatorial techniques for preparing peptide libraries are well established, but methods for the combinatorial synthesis of small-molecule libraries for the development of useful pharmaceuticals remains a formidable challenge. Small molecules are generally not oligomeric, and a diverse range of chemical transformations may be required for their synthesis. Therefore, the development of an appropriate parallel synthesis format is not always straightforward. This limitation is increasingly encountered in the quest for chemical diversity, because the fidelity of a given library member can be compromised when the building block components are not uniformly reactive. Consequently, there has been an active quest to develop the sort of truly general, high yielding transformations necessary to maintain high quality in the preparation of small-molecule libraries.

Novel estrogens having tissue selective action suitable for menopausal hormone replacement or the treatment and prevention of breast cancer are actively being sought by the pharmaceutical industry.² These agents, often referred to as selective estrogen receptor modifiers or SERMs, generally consist of a nonsteroidal core structure onto which is

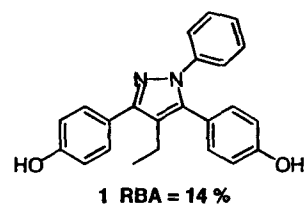
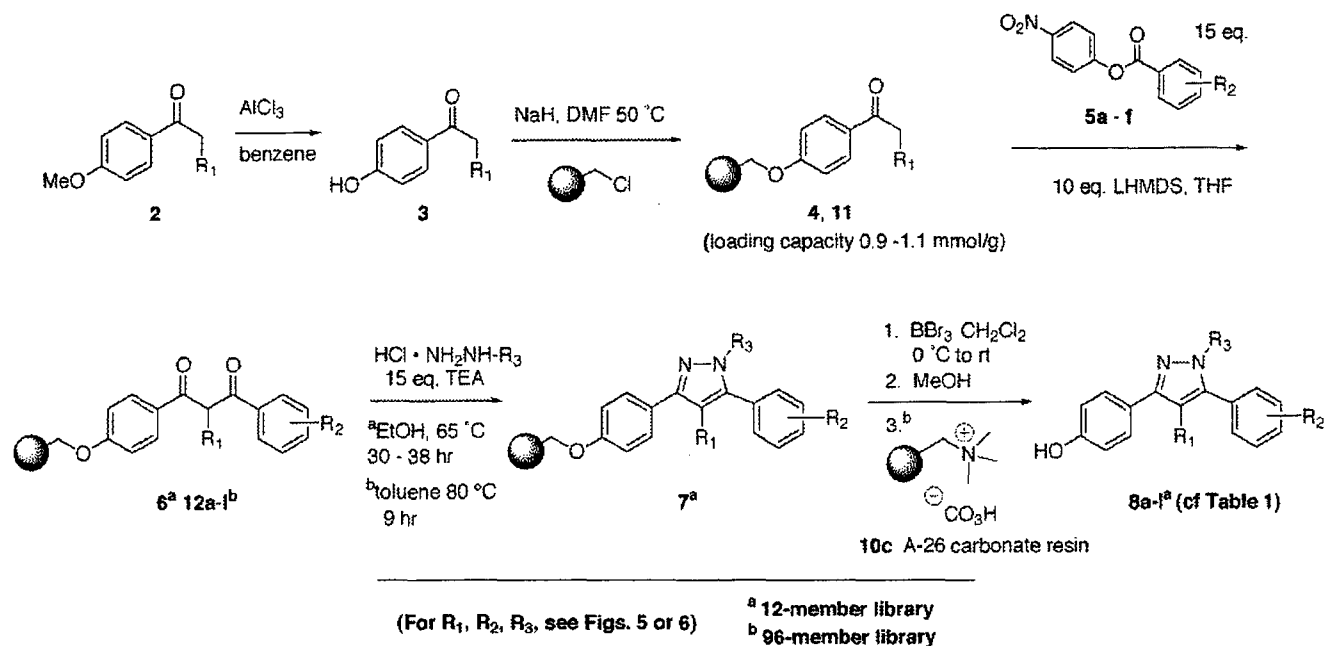


Figure 1. Estrogen receptor- α selective pyrazole discovered from a solution-phase study. RBA is relative binding affinity for the estrogen receptor; for estradiol, RBA = 100%.

appended a basic or polar function.³ Most ligands for the estrogen receptor (ER), however, are not well suited for synthesis by combinatorial means, because their construction generally involves a series of carbon–carbon bond forming reactions that are not uniformly high yielding, nor necessarily easily adaptable to solid-phase synthesis methods. Two small combinatorial libraries of nonsteroidal ER ligands have been reported,^{4,5} but these efforts produced either low affinity ligands or ones of limited structural diversity.

To circumvent these current limitations and to expand the possible combinatorial approaches to ER ligands, we have proposed a novel modular ER pharmacophore consisting of a *variable* core structure, onto which are linked four independent substituents of defined variability. Using this paradigm, we have investigated core structures consisting of five-membered heterocycles, as well as other functionalities.⁶ Among the five-membered systems that we have studied to date, we found that 1,3,5-triaryl-4-alkyl-pyrazoles, such as compound **1** (Figure 1), showed high binding affinity for the estrogen receptor, and intriguingly this compound had 100-fold higher potency as an agonist in a cell-based transcription assay through ER α than through ER β .⁷ Com-

* Address correspondence to: John A. Katzenellenbogen, Department of Chemistry, University of Illinois, 600 South Mathews Avenue, Urbana, Illinois 61801; 217 333 6310 (phone); 217 333 7325 (fax); jkatzene@uiuc.edu (e-mail).

Scheme 1. Routes for the Preparation of the 12-Member and the 96-Member Pyrazole Libraries

pounds that show high ER subtype selectivity are in great demand as agents to define the biological roles of these subtypes⁸ and as potential tissue-selective estrogens for the uses noted above.

Because of these interesting initial findings, we wished to use a combinatorial approach to explore this pyrazole template further, to gain a better understanding of its structure–binding affinity pattern with the ER and to discover additional compounds with ER subtype selectivity. In particular, we hoped that such an expanded study would enable us to determine the preferred binding orientation for these pyrazoles in the ER, an issue that was not settled by our initial investigations.⁶ We required this information to guide our future placement of pharmacophore elements in the design of selective antiestrogens (Stauffer, S. R., Huang, Y., Aron, Z., Coletta, C. J., Sun, J., Katzenellenbogen, B. S., Katzenellenbogen, J. A., unpublished).

As we had noted in their original conception,⁶ the tetrasubstituted pyrazoles offer an attractive template for the combinatorial development of ligands for the estrogen receptor. Their heterocyclic nucleus provides a core upon which several common substructural motifs found in high affinity ER ligands can adequately be displayed in several possible configurations, and their synthesis involves simple condensation reactions, some of which have already been demonstrated on solid phase, although mostly for trisubstituted pyrazole derivatives.^{9–12}

This work describes our efforts in the design and preparation of libraries of tetrasubstituted pyrazoles as ER ligands and our evaluation of the binding affinities of the library members. These studies have led us to a new series of high affinity compounds that display very high ER α agonist selectivity in cell-based transactivation assays, the details of which will be reported elsewhere (Stauffer, S. R., Sun, J., Katzenellenbogen, B. S., Coletta, C. J., Katzenellenbogen, J. A., unpublished).

Results and Discussion

Library Strategy. It was our intention to prepare discrete analogues (96-member libraries) of our tetrasubstituted pyrazole pharmacophore, noted above, in a parallel split-split format to produce material for ER binding affinity assays. Synthetically, the classical 1,3-dione-hydrazine condensation route (illustrated in Scheme 1) seemed attractive, because it is well preceded and can be accomplished under conditions that are potentially adaptable to solid-phase synthesis.⁶ Also, the β -diketone component can be readily generated from a crossed-Claisen condensation reaction.

Using this route, we can introduce molecular diversity in the target pyrazole in either the alkylphenone, the ester, or the hydrazine component. Our choice to introduce the C-4 alkyl group early on within the ketone, rather than by alkylating the β -diketone intermediate, was based on solution feasibility studies; in contrast to the pyrazole synthesis strategy reported by Marzinzik and Felder,⁹ we found that alkylation was not general for the preparation of 1,3-diarylpropane-1,3-diones. Our approach is also attractive because many of the 4'-methoxy-alkylphenone precursors are commercially available or can be produced in one step via Friedel–Crafts acylation reactions.

Linker. We selected the phenol component as the site for attachment of the pyrazole to the polymer support because it is convenient and it is the one functional group that is present in all of the pyrazoles. Merrifield's resin was used as the solid support, so the tethered phenol became attached to the resin as a *p*-substituted benzyl ether.

Our overall linker strategy is advantageous for two reasons: First, we knew from solution studies for tetrasubstituted pyrazoles of this type that a robust linker would be required to withstand the conditions for pyrazole formation (DMF/THF 120 °C).⁶ Thus, we expected that the stable benzyl ether link would be more satisfactory than other more labile linkers. Second, we anticipated that the strong acidic

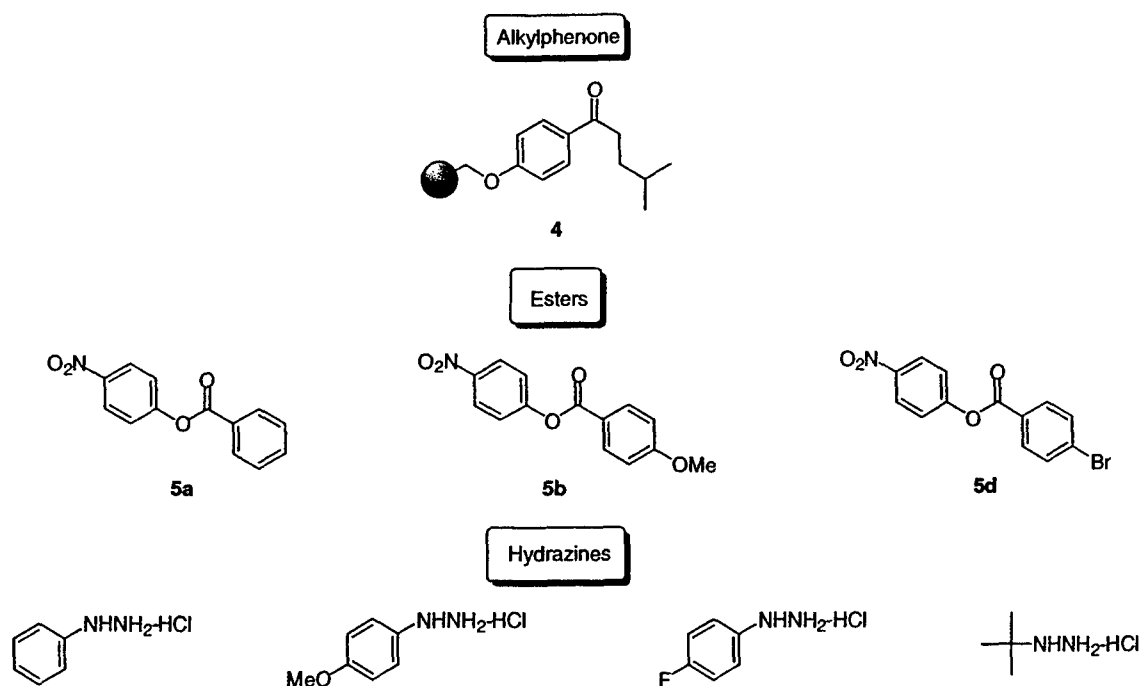


Figure 2. Components for 12-member library.

conditions required for product cleavage from the resin (i.e., BBr_3) could be adjusted to cleave, as well, any methyl ethers protecting other phenolic components. This approach is similar to that reported by Green for the preparation of lavendustin analogues,¹³ but different in that our linker is a benzyl ether rather than a benzyl ester.

Method Development. The adaptation of the pyrazole synthesis from solution phase to solid phase required extensive optimization and later modification. Our initial route is shown in Scheme 1, and it was used for the preparation a small 12-member library, which was intended to serve as a standard for later, larger library design. In addition, this smaller library was developed to evaluate the generality of the reaction conditions by using various electronically demanding building blocks (Figure 2). The conditions described below were initially developed using our original lead compound **1** as a model.

Few starting alkylphenones (**2**, Scheme 1) are available commercially, but they were readily prepared via Friedel–Crafts acylation, using anisole and the desired acid chloride. Thus, the protected *p*-methoxy-alkylphenone **2** was obtained and then demethylated using AlCl_3 to afford **3**, which was subsequently loaded onto Merrifield's resin (Novabiochem Inc., 1.39 mmol/g), according to the method of Ellman and co-workers.¹⁴ Formation of the resin-bound ketone **4** was ascertained using standard techniques (FT-IR, null %Cl combustion analysis), and a portion was cleaved with $\text{BF}_3\text{--SMe}_2$ to determine the loading capacity based on mass recovery. After minimal workup, the expected ketone was cleanly observed by ^1H NMR and HPLC (purity >99%), and the loading capacity was found to be between 0.9 and 1.1 mmol/g.

Following ketone immobilization, we used a crossed-Claisen condensation reaction to form the requisite β -diketones (**6**). This transformation proceeds satisfactorily using excess lithium hexamethyldisilazide (LHMDS) and activated

p-nitrophenyl esters (**5a,b,d**) in THF. Other bases, such as NaNH_2 or KO^tBu , were less effective, particularly with higher alkylphenones (e.g., propiophenone and higher). In addition, *p*-nitrophenyl activated esters proved to be most general in providing high yields of the dione. In most cases, the active ester could be present in the reaction vessel during the addition of base. However, esters with electron withdrawing groups, such as compound **5d** (Figure 2), required preformation of the resin-bound enolate prior to the addition of the ester, because of competing nucleophilic addition of the disilamide anion to the activated ester.

We found nanoprobe ^1H NMR-MAS to be an indispensable tool for following β -dione formation on solid-phase and for optimizing reaction conditions. Although FT-IR was useful for monitoring ketone immobilization, we did not find it satisfactory for evaluating the progress of dione formation. We had expected that a shift in the C=O stretch of the alkylphenone at 1675 cm^{-1} would occur as the dione formed and equilibrated with its intramolecularly hydrogen bonded enol tautomer. We were surprised, however, when the ^1H NMR spectrum of 1,3-bis(4-methoxyphenyl)-2-ethyl-1,3-propanedione showed that these α -substituted β -diketones exist exclusively in the diketo tautomeric form in solution. We presume that this is due to the A-strain present in these substituted molecules, because ^1H NMR analysis shows that the less hindered 1,3-diaryl-1,3-propanediones, which do not bear a 2-alkyl substituent, exist as mixtures of both enol and diketo tautomers. In most cases FT-IR revealed a C=O doublet for the dione. However, the intensity of this signal was often weak and variable, and thus was not a reliable indicator of reaction progress. In contrast, by using ^1H NMR-MAS and nanoprobe technology, we were able to conveniently and quickly ascertain the level of β -diketone formation.

Shown in Figure 3 panel A (top) is the spectrum for the starting resin-bound 4-hydroxy-butyrophenone, and in panel

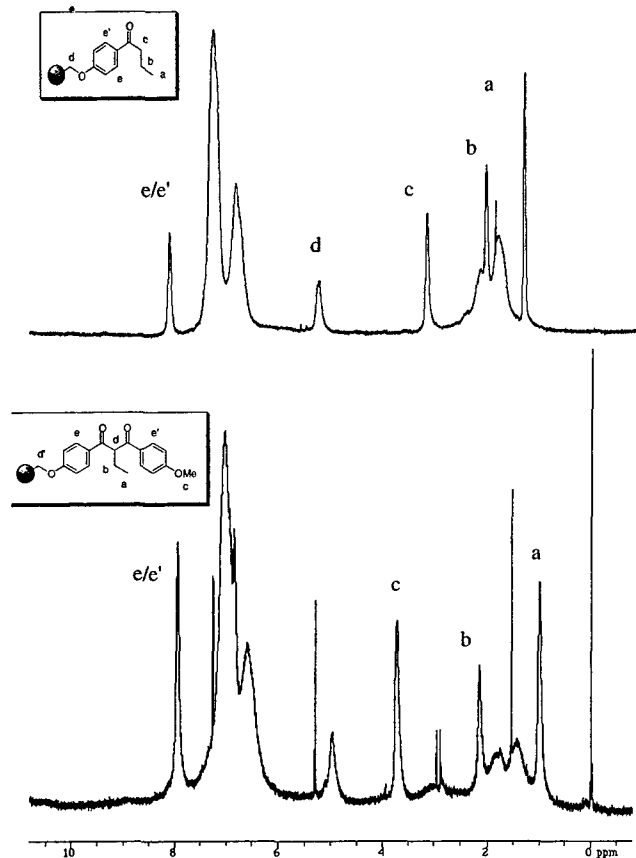
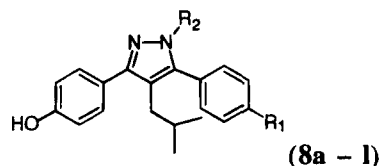


Figure 3. Panel A (top): ^1H NMR-MAS of polymer-bound butyrophenone derivative **11**. Panel B (bottom): ^1H NMR-MAS of β -diketone product **12b** after Claisen condensation reaction.

B (bottom) is the spectrum for the expected dione product after Claisen condensation with 4-methoxy-(4'-nitrophenyl)-benzoate. Because we are using a short linker, which holds these molecular segments close to the rigid polystyrene backbone, the line widths for these signals remain fairly large (20 Hz), and as a result, coupling information is unavailable. Despite this limitation, however, we can readily discern diagnostic chemical shift differences between the product and starting material, so that we confidently assess the success or failure of the reaction.

To form the tetrasubstituted pyrazole on solid phase, we first tried conditions that had been successfully used for the solution-phase synthesis (heating the dione and hydrazine hydrochloride salt to 110–120 °C in DMF/THF solutions for up to 16 h), as well as conditions developed by Marzinzik and Felder for solid-phase pyrazole synthesis (DMA as a solvent at 80 °C).⁹ Unfortunately, even with extended heating, neither of these methods gave the desired heterocycle. When we used triethylamine (TEA) to neutralize the hydrazine hydrochloride and DMF as solvent, we obtained low yields of the desired product, but purity after cleavage/deprotection was less than 35%. Ultimately, we found that toluene as solvent with the addition of TEA was effective, affording the pyrazole product **1** in >90% purity after cleavage/deprotection. One should note that subsequently we found that these reaction conditions, which involved heating toluene to 80 °C for 9 h, were not compatible with our 96-well reaction plate (Polyfiltronics 96-well Unifilter plate). Nevertheless, at the time we used these conditions to prepare

Table 1. HPLC Purity Determination and Estrogen Receptor Binding Affinities (RBA Values) of C(4) *i*-Butyl Pyrazole Library



| compd | R ₁ | R ₂ | HPLC purity ^a (%) | % RBA ^b |
|-----------|----------------|---|------------------------------|------------------------|
| 8a | H | Ph | 80 | 0.38/0.13 ^c |
| 8b | H | <i>p</i> -OHC ₆ H ₄ | 67 | 9.3/0.86 ^c |
| 8c | H | <i>p</i> -FC ₆ H ₄ | 92 | 0.04 |
| 8d | H | <i>t</i> -Bu | 29 | 0.47 |
| 8e | OH | Ph | 62 | 5.4 |
| 8f | OH | <i>p</i> -OHC ₆ H ₄ | >99 | 7.6 |
| 8g | OH | <i>p</i> -FC ₆ H ₄ | 90 | 4.0 |
| 8h | OH | <i>t</i> -Bu | 23 | 3.8 |
| 8i | Br | Ph | 75 | 0.76/0.01 ^c |
| 8j | Br | <i>p</i> -OHC ₆ H ₄ | >85 | 3.3 |
| 8k | Br | <i>p</i> -FC ₆ H ₄ | >80 | 0.17 |
| 8l | Br | <i>t</i> -Bu | 28 | 0.90 |

^a RP-HPLC, 80% MeOH:H₂O, flow rate of 1.0 mL/min, detection at 254 nm (performed before purification by radial chromatography).

^b Relative Binding Affinity (RBA) values determined by a modification of our standard competitive binding assay using only three concentrations of ligand; all compounds tested were at >80% purity.

^c Independent assays performed on the two individual regioisomers.

a 12-member library of pyrazoles and then later modified the pyrazole-forming step to make it compatible with our 96-well reaction plate (see below).

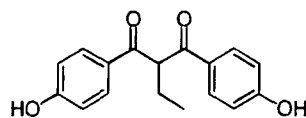
The diones (**6**) needed for this (and the larger library) were prepared in a single batch, using a homemade reaction block capable of holding 16–20 mL scaled conical polypropylene tubes as reaction vessels. The block was rotated in an oven at 40 °C for 4 h, using a modified rotary evaporator motor. After washing the resins and drying them overnight, we verified dione formation by nanoprobe ^1H NMR-MAS. Each dione resin was then split into the appropriate number of portions and reacted with the appropriate hydrazine, the cyclization products then being cleaved/deprotected with BBr₃. For this smaller 12-member library, the cleaved material was collected, treated to a minimal workup (MeOH, passage through a SiO₂ plug), and analyzed for purity by HPLC.

Shown in Table 1 are the HPLC-evaluated purities and the ER binding affinities for the C-(4)-*iso*-butyl pyrazoles (**8a–l**) in the 12-membered library. The HPLC purity values listed were obtained on the pyrazoles after only minimal workup, yet some of these are quite high (>90%). The pyrazoles derived from *tert*-butylhydrazine were of the lowest quality. The major byproduct in those having lower purity was the corresponding β -diketone intermediate, and in some cases small amounts of the starting ketone. Prior to binding affinity determination, all compounds were purified by radial chromatography, so that their purities were at least 80%. The molecular ions of all purified pyrazoles in the C(4) *i*-butyl series were also verified by ES-MS.

The binding affinities of these pyrazoles were determined in a competitive radiometric binding assay (for details see Experimental Section), using [³H]estradiol as tracer and lamb

uterine cytosol as a source of ER, and they are expressed as relative binding affinity values (RBA), with estradiol having an RBA of 100%. In the past, we have found that repeat determinations of binding affinities by this assay have a coefficient of variation of 0.3.

We were concerned that even small amounts of contaminants in the purified pyrazoles might be affecting the RBA determinations. To test this, we examined the effect of dihydroxyphenyl dione **9** on the affinity determination of pyrazole **1**. This dione (**9**) itself binds to the ER only very weakly (RBA = 0.012%), and when it was added to pyrazole **1** at 10, 20, and 30%, we noted no effect on the RBA value obtained for pyrazole **1**. Thus, we believe that the binding affinity values we have determined for all of these pyrazoles (Table 1) are valid.



9 RBA = 0.012 %

Overall, the *i*-butyl pyrazoles bind to ER with reasonable affinity (Table 1), and even within this small set of compounds some structure–affinity trends are apparent. Clearly, there is a primary preference for hydroxy substitution at R₁, as in most cases, and the pyrazoles in the **8e–h** series bind better than those in the **8a–d** and **8i–l** series. Bromine substitution (series **8i–l**) is unusual for nonsteroidal ligands, but pyrazole **8j** (1.4:1 ratio of regioisomers) has a reasonable affinity of 3.3%. The reasonable affinity of the *tert*-butyl pyrazole **8h** suggests that bulky substituents other than phenyl are tolerated at R₂. The highest affinity members of this small pyrazole library, **8b** and **8f**, contain two and three hydroxyl substituents, respectively. The similar but lower affinity diphenolic pyrazole **8e** suggests that two distinct binding orientations may exist for **8e** and **8b**.

In those cases where more than one regioisomer was expected and they could be separated by HPLC, two RBA values are indicated. In three cases where we could do this, one regioisomer showed a higher affinity: In both the monohydroxy pyrazole **8a** and dihydroxy pyrazole **8b**, a 3–10-fold preference was found for one regioisomer, and in the case of pyrazole **8i**, this preference is much greater.

At this point, we could not make a definitive assignment of the structure of these regioisomers, but these results suggest that only one of them is providing an effective mimic of the A-ring of estradiol. In other work, we have carried out independent, regioselective syntheses of single pyrazole regioisomers in a related series, and we have conducted molecular graphics modeling studies of how these isomers might fit into the ligand binding domain of ER (Stauffer, S. R., Huang, Y., Coletta, C. J., Katzenellenbogen, J. A., unpublished). These studies suggest that there are indeed preferred orientations of these regioisomers within the ER binding pocket. However, it appears that the preferred orientation may switch, depending on the substituent display.

Adaptation to a 96-Well Format. To prepare the 96-member library, we used the Polyfilteronics 96-well Unifilter plate. The Unifilter plate contains a single underlying

membrane which is designed to hold back most organic solvents, except when a vacuum is applied. Unfortunately, the Polyfilteronics plate did not withstand our conditions for pyrazole formation, using prolonged heating with toluene at 80 °C.

In our search for alternate conditions for pyrazole formation which the Polyfilteronics plate would withstand, we used pyrazole **1** as a model, and we explored a greater number of solvents and solvent mixtures for pyrazole formation (THF, BuCN, HC(OMe)₃, CH₃NO₂, and alcohols) with and without various additives (TiCl₄, Na₂SO₄, and 4 Å molecular sieves), at room temperature and at elevated temperatures. Ultimately, only alcohol solvents proved to be effective in forming the pyrazole product and were compatible with the Unifilter plate.

In this larger library, we also wanted to develop an expedited method for product isolation, whereby we could quench the cleavage/deprotection reagent BBr₃ and neutralize the HBr generated without introducing water, thereby avoiding cumbersome liquid–liquid phase extractions. Our approach was to develop a scavenger resin to neutralize the HBr and remove the inorganic contaminants by sequestration. Our initial efforts were based on work by Cardillo and co-workers,¹⁵ involving the use of macroreticular carbonate resin as a reagent in the hydrolysis of alkyl halides.

Resin **10a** (Scheme 2), which is readily prepared from the chloride form of the ion exchange Amberlyst A-26 resin, was effective in quenching the BBr₃, but not surprisingly the final product was contaminated with NaBr. However, by modifying the resin to a sodium-free, bicarbonate form, we could still neutralize the HBr, but now with the liberation of only CO₂ and H₂O. Moreover, the polymer-bound quaternary ammonium groups sequestered any bromide ions from solution. Thus, by treating the crude cleaved/deprotected product with this bicarbonate resin, we could remove all of the inorganic contaminants, leaving the desired pyrazole remaining in solution together with only MeOH (bp 65 °C), B(OMe)₃ (bp 58 °C), and a small amount of H₂O, so that solvent removal gave the product free from any reagent contamination.

Two methods were used to prepare the bicarbonate form of A-26 resin (Scheme 2). Both resins (**10b** and **10c**) afford the product pyrazole in reasonable purity, but the bicarbonate resin which was prepared using NaHCO₃ (**10b**) still contained small amounts of Na ions, risking product contamination with NaBr. The preferred method to prepare Na ion-free resin was first to convert the chloride form of the A-26 resin to the hydroxide form and then generate the bicarbonate resin by bubbling CO₂ through an aqueous suspension of the resin. This ensured that there was no Na ion contamination, and this material (**10c**) afforded the pyrazole product with somewhat better purity. Shown in Scheme 1 is the overall optimized solid-phase synthesis route to the 96-member pyrazole library. The notable modifications from the original route used to prepare the 12-member library are the conditions for the pyrazole-forming step and final workup procedure involving the bicarbonate resin **10c**.

The individual components chosen for the 96-member library are shown in Figure 4. The components used to

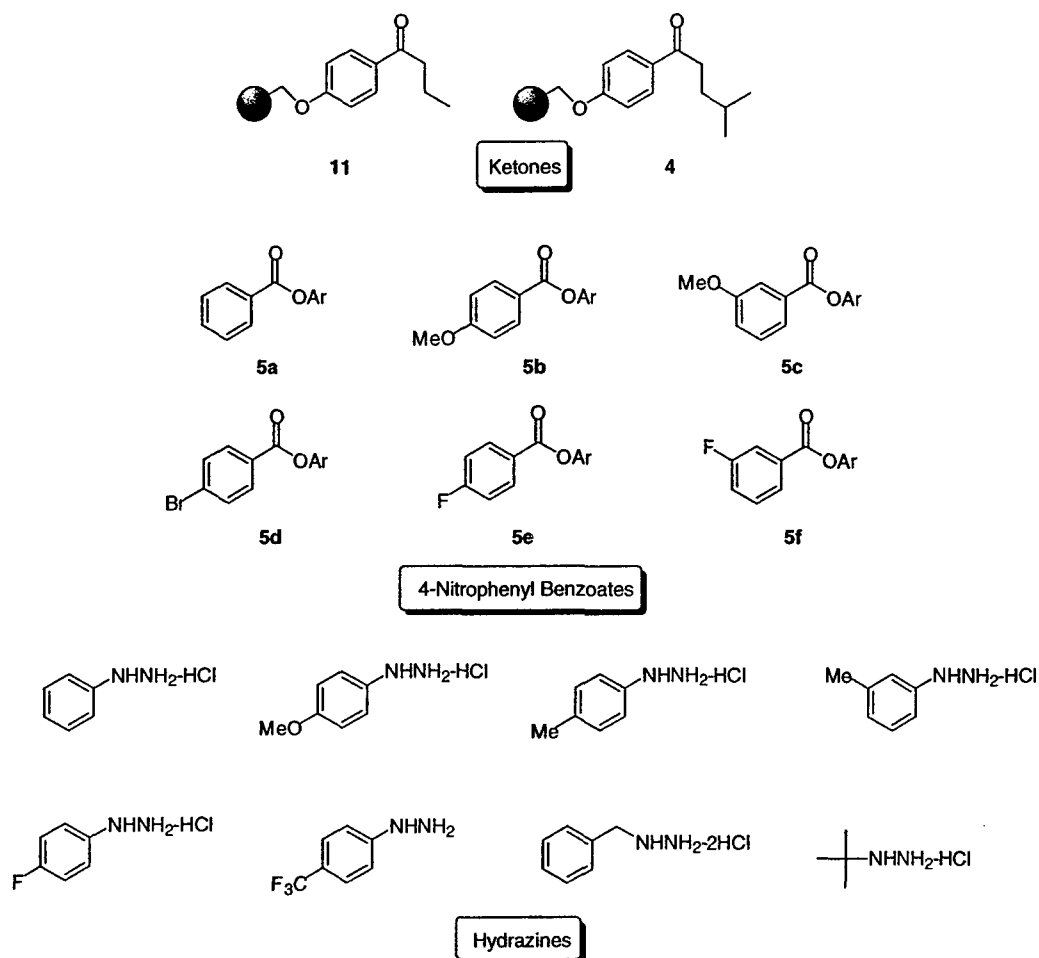
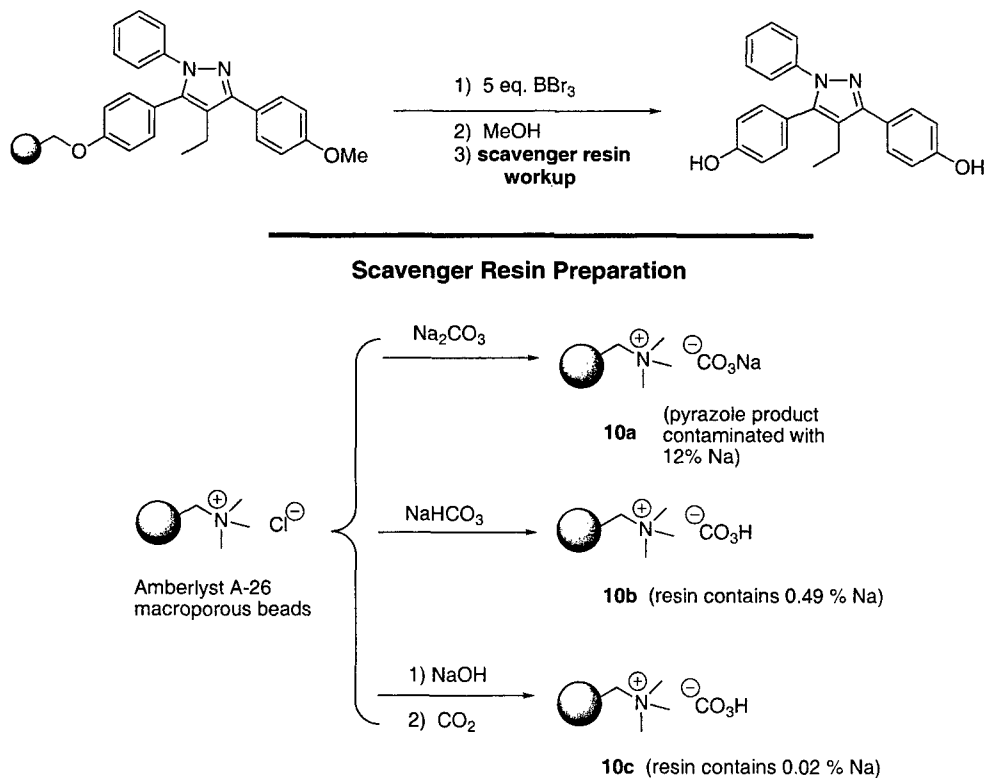


Figure 4. Components for 96-member pyrazole library.

Scheme 2. Development and Use of Bicarbonate Resin for HBr Neutralization



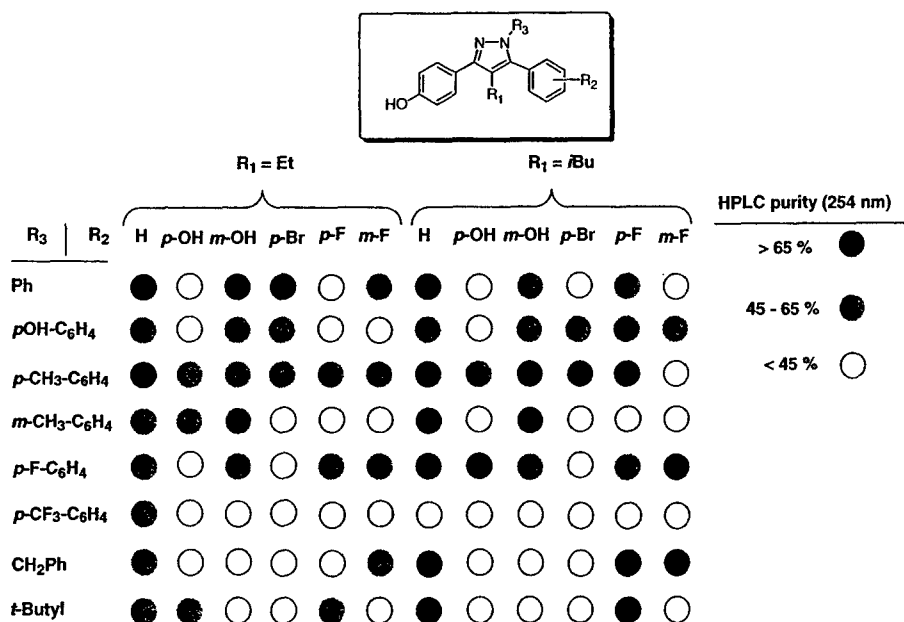


Figure 5. HPLC purities for 96-member ER library.

prepare the *i*-butyl library (Figure 2, Table 1) were again included as standards to measure the success and reproducibility of the synthesis and to verify the RBA assays. The progress of pyrazole formation for suspected "worst-case" combinations, such as CF₃-phenyl and *tert*-butyl hydrazines reacting with halogen-substituted diones, was monitored using FT-IR. The disappearance of the C=O signal at 1670 cm⁻¹ was a reliable marker for determining the progress of individual reactions. Unfortunately, for several CF₃-substituted hydrazines we were unable to drive the reaction to completion, even after subjecting these resins to fresh reagent and heating for an additional 20 h. In any event, cleavage/deprotection with BBr₃ followed, and reactions were carefully quenched with MeOH and then incubated with bicarbonate resin **10c** for 1 h at 50–60 °C to ensure complete HBr neutralization and bromide ion sequestration. After being cooled, the pyrazole products were collected and concentrated, then reconstituted in 1 mL MeOH and analyzed using a standard, steep gradient elution on a high throughput reverse-phase HPLC column. Because the pyrazoles are uniformly fluorescent, we used fluorescence detection in tandem with UV detection to identify which of the eluted peaks was the pyrazole. This proved to be a robust approach to characterizing product purity. After obtaining the purity for each member, we determined the ER binding affinity in a simplified, three-point assay (see Experimental Section for details).

Purity and ER Binding Affinity Relationships. A summary of the HPLC purities for the final pyrazoles is shown in Figure 5, according to gray scale coded ranges. The average purity for the library was 50% (±15%). This is not an unreasonable level of purity when you consider that this library included components, such as *tert*-butyl hydrazine hydrochloride, which we have found to be less reactive than the aromatic hydrazines. As before, the principal impurities could be identified as the unreacted dione precursors, which we had previously shown did not affect the results of the binding assay (see above). On the basis of product yields,

p-CF₃-substituted phenyl hydrazines appear to be even less reactive than *t*-butyl hydrazine hydrochloride, because this group of pyrazoles had the lowest overall purity of the whole library. Where regioisomers were expected within this series (see above), it was difficult to assign the product peaks, even with the help of fluorescence as a marker. In these cases, we assumed the purity to be 30%.

Shown in Figure 6 are the relative binding affinity (RBA) values for the 96-member library, indicated as ranges according to a gray scale coded legend. Several members of the library showed appreciable affinity for the ER. Particularly gratifying was the fact that most members of the 12-member *i*-butyl control library (Table 1) had RBA values which were reproduced quite well in the larger library (i.e., within 30%, relative), with the exception of **8f** (7.6%) vs **B-8** (23%). A repeat assay **8f** showed that its determination in the original 12-member library was low. The binding affinity of 16 additional select members was also re-tested after chromatographic purification (>80%), and the RBA values for these members also agreed quite well with the original determinations on the crude isolated products.

The use of an affinity array chart in Figure 6 permits a rapid, visual assessment of binding affinity patterns. For example, it is readily apparent that, for pyrazoles in both the R_1 ethyl and *i*-butyl series (column 2 and 8), those with HO substituents at R_2 have, overall, the highest affinity. Within these two series (columns 2 and 8), a number of substituents are tolerated at R_3 , the best being *p*-HO- C_6H_4 , for which the two highest affinity pyrazoles are represented, pyrazole **B-2** (14%) and **B-8** (23%). For pyrazoles with $R_3 = p\text{-HO-C}_6\text{H}_4$ (row B), a number of substituents are tolerated to varying degrees; those with fluorine substituents on R_2 for both the ethyl and *i*-butyl series bind moderately well (RBA = 1–5%). For members with $R_1 = i\text{-butyl}$ and $R_3 = p\text{-HO-C}_6\text{H}_4$, even more polar substituents appear to bind well. Particularly noteworthy is the *m*-HO analogue **B-9**, which has a relative binding affinity of 6.8%, and the fluoro derivative **B-11**. By contrast, few other R_3 substituents are

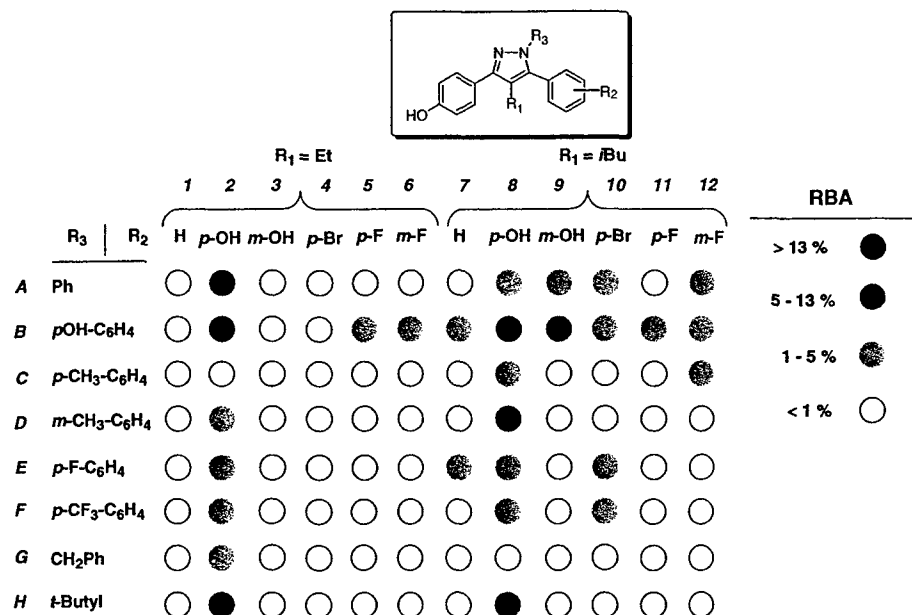


Figure 6. ER binding affinity for 96-member pyrazole library. (In unsymmetrical systems, i.e., $R_2 \neq p\text{-OH}$, the average regioisomer ratio was 1.4 to 1.)

well tolerated by the ER, one exception, however, being the *tert*-butyl pyrazoles **H-2** and **H-8**, which each have affinities of 6–7%. As was the case with pyrazole **8j** from the 12-member *i*-butyl library, several pyrazoles with *p*-bromo substituents at R_2 have reasonable affinity (~2–3%). However, these affinities are much lower when R_1 = ethyl (RBA < 1%), than when R_1 = *i*-butyl.

In investigations to be reported elsewhere (Stauffer, S. R., Coletta, C. J., Sun, J., Katzenellenbogen, B. S., Katzenellenbogen, J. A., unpublished), we have made other analogues based on the high affinity 1,3,5-*p*-hydroxyphenyl-pyrazole template, and we have found a compound with an RBA of 30% that shows very high affinity and potency selectivity for ER α . We have also prepared other pyrazoles that act as ER α potency selective antagonists (Stauffer, S. R., Huang, Y., Aron, Z. D., Coletta, C. J., Sun, J., Katzenellenbogen, B. S., Katzenellenbogen, J. A., unpublished).

Conclusions

We have developed a consistent and efficient method to prepare and isolate tetrasubstituted pyrazoles using a solid-phase strategy, and we have used this approach for the production of small, discrete libraries of estrogen receptor (ER) ligands. A combination of FT-IR and nanoprobe ^1H NMR-MAS allowed us to characterize intermediates leading up to the final pyrazole products directly on the bead. We also developed a scavenging resin to afford the cleaved/deprotected products free from inorganic contaminants. Using this approach, we prepared a 12-member test library, and then a more extensive 96-member library, and we determined product purity and ER binding affinity of all the library members. Several interesting binding affinity patterns emerged from these studies, and they have provided us with clear directions for further exploration of these tetrasubstituted pyrazoles, through which we have found a high affinity and high potency agonist with excellent selectivity for ER α and pyrazoles that selectivity antagonize ER α .

Experimental Methods

General. Melting points were determined on a capillary apparatus and are uncorrected. All reagents and solvents were obtained from Aldrich, Fisher, or Mallinckrodt. Tetrahydrofuran was freshly distilled from sodium/benzophenone. Dimethylformamide was vacuum distilled prior to use and was stored over 4 Å molecular sieves. Et_3N was stirred with phenylisocyanate, filtered, distilled, and stored over 4 Å molecular sieves. All reactions were performed under a dry N_2 atmosphere unless otherwise specified. Radial preparative-layer chromatography was performed on a Chromatotron instrument (Harrison Research, Inc., Palo Alto, CA) using EM Science silica gel Kieselgel 60 PF₂₅₄ as adsorbent. Flash column chromatography¹⁶ was performed using Woelm 32–63 μm silica gel packing. Resin bound ketone **11** was prepared according to procedure outlined in Scheme 1 from commercially available 4'-methoxybutyrophenone or from anisole and the acid chloride.

^1H and ^{13}C NMR spectra were recorded on 400 or 500 MHz spectrometers, using CDCl_3 or MeOD as solvent. Chemical shifts were reported as parts per million downfield from an internal tetramethylsilane standard ($\delta = 0.0$ for ^1H) or from solvent references. NMR coupling constants are reported in hertz. ^{13}C NMR data were determined using either the Attached Proton Test (APT) experiment or standard ^{13}C pulse settings. Low resolution electrospray mass spectrometry was performed using a VG Quattro (quadrupole-hexapole-quadrupole, QHQ) mass spectrometer system (Fisons Instruments, VG Analytical; Manchester, U.K.).

FT-IR Analysis and Nanoprobe ^1H NMR-MAS Spectra. FT-IR analysis was performed on an FTIR spectrometer, and absorption bands are reported in cm^{-1} . Infrared analysis was accomplished by placing approximately 1–2 mg of resin between two NaCl plates, swelling the beads in CHCl_3 , and immediately recording an FT-IR spectrum. Solid-phase NMR spectra were obtained on a Varian 500 MHz wide-bore spectrometer using a nanoprobe. The polystyrene-bound

dione intermediates **12a–1** were characterized using 2 mg or less of resin in a pre-swollen CDCl_3 solution (nanotube, approximately 40 μL total volume). The sample was spun about the magic angle (54.7 °C) at 2.3–2.5 kHz, and four scans were collected for each ^1H experiment, using a pulse width of 15 μs and delay time of 4 ms. Tetramethylsilane was used as an internal reference.

Relative Binding Affinity Assay. Ligand binding affinities (RBAs) using lamb uterine cytosol as a receptor source were determined by a competitive radiometric binding assay. This assay is conducted in 96-well microtiter plates in a total volume of 70 μL , using ca. 1 nM of estrogen receptor binding equivalents, 10 nM [^3H]estradiol as tracer, and dextran-coated charcoal as an adsorbent for free ligand.¹⁷ On the basis of interspecies comparison, lamb uterus is thought to contain predominantly estrogen receptor subtype α .^{18,19} All incubations were done at 0 °C for 18–24 h. Binding affinities are expressed relative to estradiol (RBA = 100%) and are reproducible with a coefficient of variation of 0.3. RBA determinations for the 96-member library were performed using a three-point assay, at ligand concentrations of 10^{-4} , 10^{-6} , and 10^{-8} M and were corrected for individual purity level.

Chemical Syntheses. 4'-Methoxy-4-methyl-valerylphenone (2). To a stirred solution of AlCl_3 (6.4 g, 48 mmol) in 1,2-dichloroethane at 0 °C was added 4-methyl-valeryl chloride (5.3 g, 39.0 mmol) dropwise over approximately 10 min. The resulting solution was warmed to room temperature, stirred for 0.5 h, then re-cooled to 0 °C, and a 1,2-dichloroethane solution of anisole (5.1 mL, 46 mmol in 20 mL) was added dropwise. The reaction was stirred at room temperature for 9 h, then cooled to 0 °C, quenched with H_2O , and extracted with CH_2Cl_2 . The organic layer was washed with saturated NaHCO_3 and brine, then dried over MgSO_4 , and concentrated to afford product as a pale yellow oil (6.0 g, 75%): ^1H NMR (CDCl_3) δ 0.94 (d, 6H, J = 6.0), 1.60 (m, 3H, overlapping methine and β - CH_2), 2.90 (t, 2H, J = 6.8), 3.87 (s, 3H), 6.92 (d, 2H, J = 8.8), 7.90 (d, 2H, J = 8.8); ^{13}C NMR (CDCl_3) δ 22.6, 28.5, 33.9, 36.4, 55.2, 113.5, 130.2, 163.6, 198.7; MS (EI, 70 eV) m/z 206.1 (M^+). Anal. ($\text{C}_{13}\text{H}_{18}\text{O}_2$): C, 75.69; H, 8.80. Found: C, 75.63; H, 8.59.

4'-Hydroxy-4-methyl-valerylphenone (3). To a stirred solution of AlCl_3 (19.4 g, 145 mmol) in benzene (300 mL) at 0 °C was added a benzene solution (60 mL) of ketone **2** over 20 min. The reaction mixture was then brought to reflux for 2 h. After cooling to room temperature the mixture was poured over 400 mL of water, and then the organic layer washed with saturated NaHCO_3 and brine. The organic layer was then dried over NaSO_4 and concentrated to afford the phenolic product as a tan solid which was then used directly in the next step to functionalize Merrifield's resin (8.97 g, 96%): ^1H NMR (CDCl_3) δ 0.94 (d, 6H, J = 6.0) 1.27 (m, 3H, overlapping methine and β - CH_2), 2.90 (t, 2H, J = 8), 6.87 (d, 2H, J = 8.5), 7.91 (d, 2H, J = 9.0).

Alkylphenone Loading onto Merrifield Resin (4, 11). To a solution of the phenolic ketone (28.0 mmol, either **3** or 4'-hydroxy-butyrophenone) in DMF (144 mL) at 0 °C was added NaH as a 60% oil dispersion (1.05 g, 26.4 mmol). The reaction mixture was returned to room temperature;

Merrifield resin (5.74 g, 1.39 mmol/g Novabiochem, Inc.) was added, and the reaction was heated to 55 °C for 22 h. The solution was then cooled to room temperature and quenched by addition of methanol (150 mL). The resin-bound product was then isolated via vacuum filtration and rinsed with methanol/DMF 1:1 (1 \times 300 mL), DMF (3 \times 350 mL), CH_2Cl_2 (3 \times 350 mL), and methanol (3 \times 350 mL). The resulting salmon-colored resin was then dried in vacuo for 18 h to afford >6 g of immobilized ketone. FT-IR analysis revealed the C=O stretch at 1670 cm^{-1} , which verified that the resin-bound ketone was produced. In addition, %Cl analysis was performed to verify the absence of halogen, indicating that most of the chloromethyl sites were substituted. Loading capacity, which ranged from 0.9 to 1.1 mmol/g, was determined from the mass recovery of expected product by cleaving a small portion of the ketone resin using $\text{BF}_3\text{--SMe}_2$.

General Procedure for Preparation of *p*-Nitrophenyl Benzoate Esters (5a–f). To a mechanically stirred solution of the substituted benzoic acid (52.6 mmol), *p*-nitrophenol (22.2 g, 157.8 mmol), and DMAP (3.2 g, 26.3 mmol) in 100 mL CH_2Cl_2 at 0 °C was added diisopropylcarbodiimide (57.9 mmol) dissolved in CH_2Cl_2 (100 mL) dropwise over 10 min. The resulting solution was allowed to stir for 18 h at room temperature. The reaction mixture was filtered, and the filtrate was concentrated under reduced pressure. The crude esters were recrystallized from EtOH or EtOAc to afford the desired ester (55–95%). Products were judged pure by comparison to literature melting points²⁰ and then used in the next step of the synthesis.

2-Ethyl-1,3-bis-(4-hydroxyphenyl)-propane-1,4-dione (9). The methoxy-protected derivative of **1** (prepared in 95% yield from 4-methoxybutyrophenone and the *p*-nitrophenylbenzoate ester using LHMDs, under the same conditions used for the solid-phase synthesis; see **12a–1**, and purified by flash chromatography (ethyl acetate/hexanes)) was treated with 5 equiv of 1.0 M BBr_3 in CH_2Cl_2 at 0 °C. The mixture was allowed to reach room temperature and stir for 5 h. The reaction was then re-cooled to 0 °C and carefully quenched with water and repeatedly extracted with Et_2O . The combined organic layers were dried over Na_2SO_4 , and upon solvent removal the title compound was afforded as a tan foam: ^1H NMR (MeOD) δ 0.99 (t, 3H, J = 7.5), 2.01 (q, 2H, J = 7.5) 5.32 (t, 1H, J = 1.5), 6.81 (AA'BB', 2H, J = 7.0, 3.0), 7.90 (AA'BB', 2H, J = 6.5, 3.0); ^{13}C NMR (MeOD) δ 11.4, 23.0, 56.6, 115.1, 128.0, 130.9, 162.8, 195.9; MS (EI, 70 eV) m/z 284 (M^+). Anal. ($\text{C}_{12}\text{H}_{16}\text{O}_4$): C, 71.28; H, 5.67. Found: C, 70.90; H, 5.57.

Preparation of Bicarbonate Form of Amberlyst A-26 Resin Using NaOH/CO₂ (10c). A medium sintered glass filter containing 15 g of Amberlyst A-26 resin in the chloride form (average capacity ~3.7 mequiv/g) was treated portionwise with 1 L of an aqueous 1.0 M NaOH solution. The resin in the hydroxide form was then dried under aspirator vacuum and suspended in a 150 mL water solution. A flow of CO_2 gas was bubbled into the aqueous solution for approximately 30 min with gentle mixing. The resin was then washed sequentially with MeOH, acetone, and ether,

and then extensively dried in vacuo. Elemental analysis indicated essentially no Na ion contamination (0.02%).

Solid-Phase Conditions Used To Prepare 12-Member Pyrazole Library (8a–l). A THF suspension for each of the six dione resins (50 mg, loading capacity 0.92–0.98 mmol/g, prepared according to procedure below), one of the four appropriate hydrazine hydrochlorides (15 equiv), and triethylamine (15 equiv) in toluene (2 mL) were heated to 80 °C for 9 h in a glass cell culture tube with a Teflon-lined screwed cap. Mixing was achieved using a rotating reaction block via a modified rotary evaporator motor. The reaction mixtures were cooled to room temperature and then isolated via vacuum filtration in coarse sintered glass frits. The product resins were rinsed with methanol/DMF 1:1 (2 × 5 mL), DMF (3 × 5 mL), CH₂Cl₂ (3 × 10 mL), and methanol (2 × 5 mL). The resulting resins were dried in vacuo for 18 h and then pre-swollen in a 2 mL CH₂Cl₂ solution under N₂ at –78 °C, using 10 mL conical vials, each containing a magnetic stir bar. Pyrazole cleavage/deprotection was followed by addition of 1 M BBr₃ (5 equiv, 0.7 mL) in CH₂Cl₂. The reaction was allowed to warm to room temperature and stir for 6 h and was quenched at 0 °C by the addition of CH₃OH (2 mL). The resins were isolated by vacuum filtration and rinsed twice with 5 mL portions of CH₃OH. The individual filtrates were concentrated in vacuo, dissolved in MeOH, and concentrated once again. This procedure was repeated twice, prior to RP-HPLC analysis. Pyrazoles 8a–l were then purified to >80% HPLC purity by radial chromatography (10–20% MeOH/CH₂Cl₂) and submitted for ES-MS and RBA analysis. The expected molecular ion pattern by electrospray was observed in all cases: (8a) ES-MS calcd for C₂₅H₂₄N₂ 368.4, found MH²⁺ 370.1 (individual isomers separately measured); (8b) ES-MS calcd for C₂₅H₂₄N₂O₂ 384.5, found MH⁺ 385.2 (individual isomers separately measured); (8c) ES-MS calcd for C₂₅H₂₃FN₂O 386.5, found MH⁺ 387.2; (8d) ES-MS calcd for C₂₃H₂₈N₂O 348.5, found MH⁺ 349.1; (8e) ES-MS calcd for C₂₅H₂₄N₂O₂ 384.5, found MH²⁺ 386.2; (8f) ES-MS calcd for C₂₅H₂₄N₂O₃ 400.5, found MH⁺ 401.1; (8g) ES-MS calcd for C₂₅H₂₃FN₂O₂ 402.5, found MH⁺ 403.1; (8h) ES-MS calcd for C₂₃H₂₈N₂O₂ 364.5, found MH⁺ 365.2; (8i) ES-MS calcd for C₂₅H₂₃BrN₂O 446.1, found MH⁺ 447.0 (individual isomers separately measured); (8j) ES-MS calcd for C₂₅H₂₃BrN₂O₂ 462.1, found MH⁺ 463.1; (8k) ES-MS calcd for C₂₅H₂₂BrFN₂O 464.1, found MH⁺ 465.1; (8l) ES-MS calcd for C₂₃H₂₇BrN₂O 426.1, found MH⁺ 427.2.

General Procedure for Batch Dione Synthesis (12a–l). Twelve conical polypropylene cell culture tubes (20 mL) were charged with 400 mg of ketone resin (4 and 11, approximately 0.38 mmol, six tubes per ketone), *p*-nitrophenyl esters (5.76 mmol, 5a–c), and 15 mL of THF. Each tube was then purged with a nitrogen atmosphere using a 14/20 septa and then chilled in an ice bath. A 1.0 M THF solution of LHMDS (3.84 mmol) was added dropwise via syringe to each tube; the reaction was then sealed with a screw cap and shaken vigorously. Esters 5d–f could not be present during enolate formation due to their reactivity toward LHMDS and thus were added in one portion 30 min after addition of LHMDS. All 12 reaction tubes were then

loaded into a homemade reaction block, which was slowly rotated within a 40 °C oven using a modified rotary evaporator motor. After 5 h, the resins were transferred to coarse sintered glass filters using CH₂Cl₂. A rinse procedure followed involving methanol/DMF 1:1 (1 × 30 mL), DMF (3 × 20 mL), CH₂Cl₂ (3 × 20 mL), and methanol (2 × 20 mL). The resins were then dried in vacuo, and the level of product formation was determined by nanoprobe ¹H NMR-MAS. In all 12 cases, disappearance of the ketone α-protons occurred, and a new signal at approximately δ 5–5.3 was observed for the α/α' methine proton, indicating successful dione formation. Diagnostic chemical shifts are reported below (note: aromatic resonances from dione which overlap with polystyrene backbone in addition to the resin backbone signals themselves are not listed; for purposes of naming, polystyrene is abbreviated "PS"; integration values are approximately ±15%).

1-PS-(4-Benzyloxyphenyl)-2-ethyl-3-phenyl-propane-1,3-dione (12a): δ 1.02 (3H, CH₃CH₂), 2.15 (2H, CH₃CH₂), 4.95 and 5.05 (two overlapping s, 3H, PS-ArCH₂O and α/α'-CH), 7.95 (4H, ArCH *ortho*-C=O).

1-PS-(4-Benzyloxyphenyl)-2-ethyl-3-(4-methoxyphenyl)-propane-1,3-dione (12b): δ 1.01 (3H, CH₃CH₂), 2.15 (2H, CH₃CH₂), 3.74 (3H, OCH₃), 4.98 (s, 3H, ArCH₂ and α/α'-CH), 7.95 (4H, ArCH *ortho*-C=O).

1-PS-(4-Benzyloxyphenyl)-2-ethyl-3-(3-methoxyphenyl)-propane-1,3-dione (12c): δ 1.02 (3H, CH₃CH₂), 2.14 (2H, CH₃CH₂), 3.72 (3H, OCH₃), 5.05 (two overlapping s, 3H, PS-ArCH₂O and α/α'-CH), 7.51 (2H, ArCH), 7.96 (2H, ArCH).

1-PS-(4-Benzyloxyphenyl)-2-ethyl-3-(4-bromophenyl)-propane-1,3-dione (12d): δ 1.01 (3H, CH₃CH₂), 2.13 (2H, CH₃CH₂), 4.97 (s, PS-ArCH₂O and α/α'-CH), 7.50 (ArCH), 7.79 (ArCH), 7.95 (ArCH).

1-PS-(4-Benzyloxyphenyl)-2-ethyl-3-(4-fluorophenyl)-propane-1,3-dione (12e): δ 1.01 (3H, CH₃CH₂), 2.14 (2H, CH₃CH₂), 4.97 (s, PS-ArCH₂O and α/α'-CH), 7.97 (4H, ArCH).

1-PS-(4-Benzyloxyphenyl)-2-ethyl-3-(3-fluorophenyl)-propane-1,3-dione (12f): δ 1.01 (3H, CH₃CH₂), 2.13 (2H, CH₃CH₂), 4.97 (s, PS-ArCH₂O and α/α'-CH), 7.64, 7.69, 7.95 (three s, 4H, ArCH).

1-PS-(4-Benzyloxyphenyl)-2-iso-butyl-3-phenyl-propane-1,3-dione (12g): δ 0.96 (6H, (CH₃)₂), 2.01 (β-CH₂), 4.95 (2H, PS-ArCH₂O), 5.24 (1H, α/α'-CH), 7.39 (3H, ArCH), 7.48 (ArCH), 7.97 (3H, ArCH).

1-PS-(4-Benzyloxyphenyl)-2-iso-butyl-3-(4-methoxyphenyl)-propane-1,3-dione (12h): δ 0.95 (6H, (CH₃)₂), 2.02 (β-CH₂), 3.76 (3H, OCH₃), 4.93 (2H, PS-ArCH₂O), 5.17 (1H, α/α'-CH), 7.97 (4H, ArCH).

1-PS-(4-Benzyloxyphenyl)-2-iso-butyl-3-(3-methoxyphenyl)-propane-1,3-dione (12i): δ 0.96 (6H, (CH₃)₂), 2.00 (β-CH₂), 3.74 (3H, OCH₃), 4.95 (2H, PS-ArCH₂O), 5.23 (1H, α/α'-CH), 7.29 (ArCH), 7.52 (2H, ArCH), 7.97 (2H, ArCH).

1-PS-(4-Benzyloxyphenyl)-2-iso-butyl-3-(4-bromophenyl)-propane-1,3-dione (12j): δ 0.95 (6H, (CH₃)₂), 1.97 and 2.05 (overlapping s, β-CH₂), 4.95 (2H, PS-ArCH₂O), 5.14 (1H, α/α'-CH), 7.51 (2H, ArCH), 7.81 (2H, ArCH), 7.96 (3H, ArCH).

1-PS-(4-Benzyloxyphenyl)-2-iso-butyl-3-(4-fluorophenyl)-propane-1,3-dione (12k): δ 0.95 (6H, $(\text{CH}_3)_2$), 1.99 and 2.05 (overlapping s, β - CH_2), 4.95 (2H, PS- ArCH_2O), 5.16 (1H, α/α' -CH), 7.98 (4H, ArCH).

1-PS-(4-Benzyloxyphenyl)-2-iso-butyl-3-(3-fluorophenyl)-propane-1,3-dione (12l): δ 0.95 (6H, $(\text{CH}_3)_2$), 1.95 and 2.07 (overlapping s, β - CH_2), 4.97 (2H, PS- ArCH_2O), 5.18 (1H, α/α' -CH), 7.66 (ArCH), 7.73 (ArCH), 7.97 (4H, ArCH).

General Solid-Phase Conditions Used To Prepare 96-Member Pyrazole Library. Pyrazole Formation: Each of the above diones (12a–l) were divided into eight approximately 50 mg portions and distributed across each row of an 8 \times 12 Polyfiltronics Unifilter plate. After charging each well with the appropriate dione, the 12 commercially available hydrazine components (Figure 4) were carefully added as preweighed solids to the appropriate wells while carefully blocking off neighboring wells in order to avoid cross-contamination. The bottom of the plate was then secured in a reaction clamp (Polyfiltronics Combiclamp) with two Viton gaskets. To each well was added 1.5 mL of EtOH and approximately 100 μL of TEA. The top of the plate was sealed and the assembly agitated and heated to 65 $^\circ\text{C}$ in an oscillating cell culture oven. The reaction was monitored by FT-IR using several suspected "worst-case" scenarios (H-2, F-2, and E-5 and our lead compound, A-2) by observing the diminishing intensity of the C=O signal at 1670 cm^{-1} . After 38 h, the plate was cooled to room temperature, and the crude mixtures were filtered within the reaction block by vacuum aspiration (Polyfiltronics filter/collection vacuum manifold). The resin-bound pyrazoles were then rinsed with methanol/DMF 1:1 (2 \times 2 mL), DMF (3 \times 2 mL), CH_2Cl_2 (3 \times 2 mL), and methanol (3 \times 2 mL) and then dried in vacuo overnight in a desiccator.

Deprotection/Cleavage: In a N_2 -charged glovebag at room temperature, the resins were suspended in 0.5 mL of CH_2Cl_2 and treated dropwise with a 1.0 M CH_2Cl_2 solution of BBr_3 (500 μL). The reaction block was sealed as before and allowed to stand at room temperature with occasional mixing. After 8 h, the resins were carefully quenched with cold MeOH (0.5 mL), and then approximately 100 mg of bicarbonate resin 10c was added to each well. After 20 min, when most of the CO_2 evolution ceased, the reaction top was resealed and the block heated to 50–60 $^\circ\text{C}$ for 1 h. Upon cooling to room temperature, the released library members were collected in a 96-well 2 mL collection plate, and the solvent evaporated to dryness (a 96-pin manifold capable of providing a gentle overhead stream of N_2 to each well in addition to gentle warming using a hot plate allowed for the removal of most of the MeOH; the remaining residual volatiles were removed in vacuo). Each member was then reconstituted in 1 mL of MeOH and analyzed by RP-HPLC.

Characterization of 96-Member Pyrazole Library. RP-HPLC analysis was performed on an analytical HPLC system with an autosampler. UV detection was performed at 254 nm and a flow rate of 1.0 mL/min using a C-18 CombiScreen analytical column (YMC, Inc., 4.6 mm \times 50 mm) with a MeOH:H₂O gradient solvent system (40–90% MeOH, 0–5 min, total run time = 10 min). A fluorometer HPLC flow

detector was used to aid in identification of the expected pyrazole peak. An excitation wavelength of 306 nm and emission wavelength of 364 nm were used, based on the fluorescence properties of pyrazole 1. After RP-HPLC analysis, the library members were transferred from autosampler vials to tared 7 \times 40 mm flat bottom vials (8 mm crimp tops), and the solvent was then removed using a Savant vacuum centrifuge. After further drying in vacuo the sample weight was recorded, and a modified three-point competitive binding assay was then performed. Authentic HPLC traces obtained for 8a–l (Table 1) were used to help confirm their later synthesis in the 96-member library. These controls represent 13% of the total library members produced. The RBA values of these "controls" from this library were equivalent to those obtained for the same compounds in the 12-membered library, within the statistical limits of the binding assay (coefficient of variation is 0.3).

Acknowledgment. We are grateful for support of this research through grants from the U.S. Army Breast Cancer Research Program (DAMD17-97-1-7076) and the National Institute of Health (HHS 5R37 DK1556). We thank Kathryn E. Carlson for performing binding assays. NMR spectra were obtained in the Varian Oxford Instrument Center for Excellence in NMR Laboratory. Funding for this instrumentation was provided in part from the W. M. Keck Foundation and the National Science Foundation (NSF CHE 96-10502). Mass spectra were obtained on instruments supported by grants from the National Institute of General Medical Sciences (GM 27029), the National Institute of Health (RR 01575), and the National Science Foundation (PCM 8121494).

References and Notes

- (1) Dolle, R. E.; Nelson, K. H. J. Comprehensive Survey of Combinatorial Library Synthesis. *J. Comb. Chem.* **1999**, *1*, 235–282.
- (2) Grese, T. A.; Dodge, J. A. Selective Estrogen Receptor Modulators (SERMS) [Review]. *Curr. Pharm. Des.* **1998**, *4*, 71–92.
- (3) Grese, T. A.; Sluka, J. P.; Bryant, H. U.; Cullinan, G. J.; Glasebrook, A. L.; Jones, C. D.; Matsumoto, K.; Palkowitz, A. D.; Sato, M.; Termine, J. D.; Winter, M. A.; Yang, N. N.; Dodge, J. A. Molecular determinants of tissue selectivity in estrogen receptor modulators. *Proc. Natl. Acad. Sci. U.S.A.* **1997**, *94*, 14105–14110.
- (4) Willard, R.; Jammalamadaka, V.; Zava, D.; Benz, C. C.; Hunt, C. A.; Kushner, P. J.; Scanlan, T. S. Screening and characterization of estrogenic activity from hydroxystilbene library. *Chem. Biol.* **1995**, *2*, 45–51.
- (5) Brown, D. S.; Armstrong, R. W. Synthesis of tetrasubstituted ethylenes on solid support via resin capture. *J. Am. Chem. Soc.* **1996**, *118*, 6331–6332.
- (6) Fink, B. E.; Mortensen, D. S.; Stauffer, S. R.; Aron, Z. D.; Katzenellenbogen, J. A. Novel structural templates for estrogen-receptor ligands and prospects for combinatorial synthesis of estrogens. *Chem. Biol.* **1999**, *6*, 205–219.
- (7) Sun, J.; Meyers, M. J.; Fink, B. E.; Rajendran, R.; Katzenellenbogen, J. A.; Katzenellenbogen, B. S. Novel ligands that function as selective estrogens or antiestrogens for estrogen receptor- α or estrogen receptor- β . *Endocrinology* **1999**, *140*, 800–804.
- (8) Nilsson, S.; Kuiper, G.; Gustafsson, J. A. ER beta: a novel estrogen receptor offers the potential for new drug development [Review]. *Trends Endocrinol. Metab.* **1998**, *9*, 387–395.
- (9) Marzinek, A. L.; Felder, E. R. Solid support synthesis of highly functionalized pyrazoles and isoxazoles; scaffolds for molecular diversity. *Tetrahedron Lett.* **1996**, *37*, 1003–1006.
- (10) Marzinek, A. L.; Felder, E. R. Key intermediates in combinatorial chemistry: access to various heterocycles from α,β -unsaturated ketones on the solid phase. *J. Org. Chem.* **1998**, *63*, 723–727.

- (11) Watson, S. P.; Wilson, R. D.; Judd, D. B.; Richards, S. A. Solid-phase synthesis of 5-aminopyrazoles and derivatives. *Tetrahedron Lett.* **1997**, *38*, 9065–9068.
- (12) Wilson, R. D.; Watson, S. P.; Richards, S. A. Solid-phase synthesis of 5-aminopyrazoles and derivatives. *Tetrahedron Lett.* **1998**, *39*, 2827–2830.
- (13) Green, J. Solid-Phase synthesis of lavendustin analogues. *J. Org. Chem.* **1995**, *60*, 4287–4290.
- (14) Boojamra, C. G.; Burow, K. M.; Ellman, J. A. An Expedient and High-Yielding Method for the Solid-Phase Synthesis of Diverse 1,4-Benzodiazepine-2,5-Diones. *J. Org. Chem.* **1995**, *60*, 5742–5743.
- (15) Cardillo, G.; Orena, M.; Porzi, G.; Sandri, S. Carbonate ion on a polymeric support: hydrolysis of alkyl halides and cyclic iodocarbonates. *Synthesis* **1981**, 793–794.
- (16) Still, W. C.; Kahn, M.; Mitra, A. Rapid chromatographic technique for preparative separations with moderate resolution. *J. Org. Chem.* **1978**, *43*, 2923–2926.
- (17) Katzenellenbogen, J. A.; Johnson, H. J., Jr.; Myers, H. N. Photo-affinity labels for estrogen binding proteins of rat uterus. *Biochemistry* **1973**, *12*, 4085–4092.
- (18) Kuiper, G. G. J. M.; Carlsson, B.; Grandien, K.; Enmark, E.; Häggblad, J.; Nilsson, S.; Gustafsson, J.-Å. Comparison of the ligand binding specificity and transcript tissue distribution of estrogen receptor α and β . *Endocrinology* **1997**, *138*, 863–870.
- (19) Mosselman, S.; Polman, J.; Dijkema, R. ER β : identification and characterization of a novel human estrogen receptor. *FEBS* **1996**, *392*, 49–53.
- (20) O'Connor, C. J.; Lomax, T. D. The reactivity of *p*-nitrophenyl esters with surfactants in apolar solvents. VII* substituent effects on the reactivity of 4'-nitrophenyl 4-substituted benzoates in benzene solutions of dodecylammonium propionate and butane-1,4-diamine bis(dodecanoate). *Aust. J. Chem.* **1983**, *36*, 917–925.

CC0000040

**PYRAZOLE LIGANDS: STRUCTURE-AFFINITY/ACTIVITY RELATIONSHIPS OF
ESTROGEN RECEPTOR- α SELECTIVE AGONISTS**

Shaun R. Stauffer^a, Christopher J. Coletta^a, Rosanna Tedesco^a, Jun Sun^b, Benita S.
Katzenellenbogen^{b,c}, and John A. Katzenellenbogen^{a*}

^aDepartment of Chemistry

^bDepartment of Physiology

^cDepartment of Cell and Structural Biology

University of Illinois and University of Illinois College of Medicine,
Urbana, IL 61801

Submitted to: *Journal of Medicinal Chemistry*

*Address Correspondence to:
John A. Katzenellenbogen
Department of Chemistry
University of Illinois
600 South Mathews Avenue
Urbana IL 61801
217 333 6310 (phone)
217 333 7325 (fax)
e-mail: jkatzene@uiuc.edu

Abstract

We have found that certain tetrasubstituted pyrazoles are high affinity ligands for the estrogen receptor (ER) (Fink, et al., *Chem. Biol.*, **1999**, 6, 205-219) and that one pyrazole is considerably more potent as an agonist on the ER α than on the ER β subtype (Sun, et al., *Endocrinol.*, **1999**, 140, 800-804). To investigate what substituent pattern provides optimal ER binding affinity and the greatest enhancement of potency as an ER α agonist, we prepared a series of tetrasubstituted pyrazole analogs with defined variations at certain substituent positions. Analysis of their binding affinity pattern shows that a C(4)-propyl substituent is optimal and that a *p*-hydroxyl group on the N(1)-phenyl group also enhances affinity. The best compound in this series, a propylpyrazole triol (PPT, compound **4g**), binds to ER α with high affinity (ca. 50% that of estradiol), and it has a 410-fold binding affinity preference for ER α . It also activates gene transcription only through ER α . Thus, this compound represents the first *ER α -specific agonist*. The exceptional ER α binding affinity selectivity of pyrazole **4g**, which underlies its potency selectivity, can be interpreted by molecular modeling; the ER α binding selectivity appears to result from differences in the interaction of the pyrazole core and C(4)-propyl group with portions of the receptor where ER α has a smaller residue than ER β . These ER-subtype specific interactions should prove useful in defining biological activities in estrogen target cells that are selectively mediated by ER α .

Introduction

The estrogen receptor (ER) displays a remarkable capacity for binding non-steroidal ligands with high affinity.¹ Many of these non-steroidal ligands have been developed into hormonal agents having mixed agonist-antagonist and tissue-selective activities that are useful in menopausal hormone replacement, infertility treatment, and in the treatment and prevention of breast cancer. Because of their unusual pharmacology, these agents have been termed Selective Estrogen Receptor Modulators (SERMs).² To understand the molecular basis of the tissue selectivity of these SERMs, it would be helpful to know details about how they are interacting with the ER. However, short of performing X-ray crystallographic analysis of ER complexes with each ligand, it can be a challenge to obtain such information.

If the non-steroidal ligand bears a reasonable structural relationship with steroidal estrogens, it is generally quite easy to imagine the orientation that it is likely to adopt when it is bound by ER.^{3,4} ER mutagenesis studies,⁵ and the recent X-ray crystallographic structures of ER complexed with both estradiol and three non-steroidal ligands (raloxifene, hydroxytamoxifen, and diethylstilbestrol) provide additional guidance in the selection of reasonable binding orientations for ligands of this type.^{4,6} However, when the non-steroidal estrogens have structures that are more divergent from those of steroidal estrogens, and particularly when they are non-symmetrical, it becomes a greater challenge to predict ligand-binding orientation.⁷

The recent characterization of a second estrogen receptor gene, encoding ER β , places a further premium on our understanding of the details of ligand-receptor interaction,^{8,9} because it would be especially interesting to have ligands that could activate or inhibit each of the ER subtypes with high selectivity. Such ligands would be valuable tools to define the biological effects that are mediated by ER α and ER β . So far, however, there have been only a few reports of ER subtype-selective estrogens, and in many cases, the selectivity has been relatively modest.¹⁰

Recently, we investigated various heterocyclic diazole structures as core elements for non-steroidal estrogens of novel design.^{11,12} Our aim was to identify systems that would be amenable

to combinatorial assembly and library synthesis. From among the several systems we studied that included imidazoles, oxazoles, thiazoles, and isoxazoles, we found that high affinity ER ligands could be obtained by appropriate substitution on a pyrazole core. Subsequently, we used a parallel, solid-phase synthesis approach to prepare some combinatorial pyrazole libraries of moderate size.¹³ In the cases we investigated, high affinity binding required tetra-substitution of the pyrazole core and an appropriate display of aromatic, phenolic and aliphatic groups.^{11,12} An example of this optimal pattern of substitution that we have thus far delineated for pyrazoles includes three aromatic groups at the 1,3 and 5-positions, specifically phenols at the 3 and 5 positions, and an alkyl group at the 4-position (Figure 1). Initial studies on one of these compounds (Fig. 1, X=H, R=Et) showed that it acted as an agonist on both ER subtypes, but it was considerably more potent on ER α than on ER β .¹⁴ Thus, this pyrazole was termed an ER α potency-selective agonist.¹⁴

[Figure 1]

In this report, we have investigated structure-activity relationships in these tetrasubstituted pyrazoles to delineate two aspects of their behavior: (1) The C(4)-alkyl substituent and phenol hydroxyl pattern that provide optimal ER subtype selectivity and (2), the extent to which the ER α -selective potency of these pyrazoles can be understood in the context of crystal structures of the ER α ligand binding domain and models for ER β derived from these structures. Our studies provide new and definitive information on these issues, and, in the process, we have identified a pyrazole that shows complete ER α selectivity in transcription activation by the receptor.

Results and Discussion

Chemical Syntheses

The compounds we have studied have various C(4) alkyl substituents, and have either a phenyl or 4-hydroxyphenyl substituent on N(1). Shown in Scheme 1 is the route used for the synthesis of the pyrazoles (**4a-i**). The starting alkylphenones (**1a-f**) were readily prepared in good yields by Friedel-Crafts acylation of anisole. The requisite β -diketones (**2a-e**) were then produced in moderate to good yields by acylation of the corresponding lithium enolates with 4-nitrophenyl 4-methoxybenzoate. Because the pyrazoles are sterically crowded, rather harsh conditions were required for their formation (>16 h at reflux at 110-120 °C in DMF/THF solution). Nonetheless, these conditions served quite well for pyrazole formation in solution. Several of the pyrazole intermediates protected as methyl ethers were isolated in good yield. However, with the trimethoxy pyrazoles (**3g-i**), it was difficult to separate the protected product from traces of the diketone precursor by chromatography. So, in these cases the crude material was passed through a short silica gel column and, without further purification, was then deprotected using BBr₃. Pyrazoles **3d-e** were also treated in this manner. The final phenolic pyrazoles (**4a-i**) were isolated in 30 to 98% yield after purification by recrystallization and/or chromatography.

[Scheme 1]

In addition to the final pyrazole products **4a-i**, we wished to prepare the *iso*-propyl analog derived from ketone **1f**. However, we encountered difficulties in the preparation of this hindered dione because of significant O-acylation that occurred during the Claisen condensation. Separation of the O-acylated by-product from the desired dione proved to be difficult. Moreover, once the dione was isolated, the pyrazole condensation failed using the conditions described above, which had been optimized for solution phase synthesis. To avoid these problems, we utilized a solid phase synthesis according to the methodology that we had previously developed,¹³ and in this manner we were able to obtain the *i*-propyl pyrazole **6** starting from the resin bound ketone **5**, as shown in Scheme 2, although the overall yield was relatively low.

[Scheme 2]

ER Binding Affinity of Tetrasubstituted Pyrazoles

The ER binding affinity of pyrazoles **4a-i** and **6** was determined in a competitive radiometric binding assay using purified full length human ER α and ER β , as previously described,^{15,16}. The affinities are expressed as relative binding affinity (RBA) values and are presented in Table 1.

A number of interesting trends are notable in these binding affinity data. In both the diphenol series (X = H, **4a-e**, **6**) and the triphenol series (X = OH, **4f-i**), optimal binding affinity for ER α requires a C(4) alkyl substituent that is not too long (*n*-Bu: **4e,i**) or too short (Me: **4a**), the highest affinity being found with the intermediate size substituents Et (**4b,f**), *n*-Pr (**4c,g**), and *i*-Bu (**4d,h**). Thus, it appears that the subpocket that is accommodating this group has a limited size and relatively narrow shape. Another significant trend observed for RBA values for ER α is that in all cases, binding affinities for the triphenols (X = OH, **4f-i**) are greater than for the corresponding diphenols (X = H, **4b-e**). This is not expected, because additional polar substituents are generally poorly tolerated in the center of the ligand binding pocket of ER, at least in most non-steroidal ligand systems that have been examined, such as the benzo[b]thiophenes¹⁷ and 2,3-diarylindanes.⁷ One exception is found with certain triphenylacrylonitriles, where addition of a third hydroxyl increases binding affinity.¹⁸

[Table 1]

In all cases, the affinity of these pyrazoles for ER β is much lower than for ER α . In fact, some of the members show a remarkable selectivity in their binding affinity for ER α vs. ER β , which is 30-40 fold for some of the pyrazole diols (**4c,d**) and as high as 200-400 fold for some of the pyrazole triols (**4f,g**).

We have previously reported binding affinities for one of these pyrazoles (**4b**), using receptor preparations containing only the *ligand binding domains* of human ER α and ER β , rather than *full length* human ER α and ER β .¹⁴ The values obtained previously were higher but less ER α selective (60 \pm 16 for ER α and 18 \pm 4 for ER β). At this point, the reasons for these affinity differences between full length ER and the ER ligand binding domain are not clear, although they

have been seen, as well, in a structurally different class of ER ligands.¹⁶ However, it is of note that the higher ER α /ER β affinity ratio that we obtain for pyrazole **4b** with the full length ERs is more consistent with the 120-fold potency ratio we described in transcription assays than was the 3-fold ER α /ER β affinity ratio obtained with ERs containing only the ligand binding domains.¹⁴

Transcriptional Activity and Potency of Tetrasubstituted Pyrazoles

For investigation of transcription activation ability, we selected two compounds, the pyrazole having the highest ER α /ER β affinity selectivity (410 fold, the propylpyrazole triol **4g**, called PPT for convenience), and the corresponding pyrazole in the diol series (**4c**, called propylpyrazole diol or PPD). These two pyrazoles were assayed for estrogen agonist activity in transactivation assays using human endometrial cancer (HEC-1) cells transfected with expression plasmids for ER α and ER β and an estrogen-responsive reporter gene plasmid. The dose-response curves for these compounds are shown in Figure 2.

Both compounds are potent in activating gene transcription through ER α , but the PPD (**4c**) is weak in transcriptional activation through ER β , and PPT(**4g**) is completely inactive in stimulating transcription via ER β . Thus, PPT (**4g**) is an ER α -specific agonist. This pharmacological profile is reminiscent of the behavior of the C(4)-ethyl analog of pyrazole **4c** (namely, pyrazole, **4b**), that we have previously described as an agonist that is more potent on ER α -than on ER β . This compound (**4b**) had an EC₅₀ of ca. 1 nM on ER α and showed a 120-fold potency selectivity for this ER subtype.¹⁴ However, in cell tranfection assays both PPT and PPD are nearly 10-fold more potent than the original pyrazole **4b** on ER α , and they are much more ER α selective.

As we had noted in our earlier study on pyrazole **4b**,¹⁴ and is clearly evident here as well, the ER α selectivity of these pyrazoles in terms of their *potency* in transcription assays is substantially greater than their *affinity* selectivity in binding assays. For example, the ER α affinity-selectivity of PPD (**4c**) is 32, yet its potency selectivity is ca. 1000 (Cf., Fig. 2). Likewise, the ER α affinity selectivity of PPT (**4g**) is 410, and its potency selectivity, which although is difficult to accurately evaluate (Cf., Fig. 2), is probably greater than 10,000. Such a discordance between

affinity and potency might be explained in the context of “tripartite receptor pharmacology”, a concept that we advanced some time ago.¹⁹ Binding measured in vitro with purified ERs involves only the interaction between ligand and receptor, whereas transcription measured in cells involves the additional interaction of the ligand-receptor complex with coactivators and other cell components. Thus, compared to their relative affinities for ER α and ER β , the relative potency of two ligands can be modulated by differences in the strength with which their respective ligand-receptor complexes bind to coactivators or are modified by other cellular elements, although other factors, as well, might be involved. In this case, it appears that the pyrazole complexes with ER α are better able to bind coactivators than are the ER β -pyrazole complexes, as we have documented in a recent study.²⁰

[Figure 2]

A Model for the Binding of Pyrazoles with the ER Subtypes

The high affinity, and particularly the high selectivity, with which these pyrazoles bind to ER α raises the important issue of what molecular features underlie the differences in their interaction with ER α vs ER β . Without crystal structures available for the comparison of any of these pyrazoles complexed with both ER α and ER β , we are currently limited to investigating this issue by molecular modeling.

Orientation of Pyrazole Ligands in the Ligand Binding Pocket of ER α – We have previously done modeling of the pyrazole ligands in the ER ligand binding domains (LBDs), first in our initial study on these ligands,¹¹ and, more recently, in connection with a study of the orientation of these ligands in the binding pocket.²¹ As a result of our more recent and more extensive modeling,²¹ we have come to appreciate that there are some ambiguities in how polyphenolic ligands such as these pyrazoles can be accommodated by ER, at least at the level at which we are currently able to model. For the purposes of this paper, we have chosen to illustrate a binding mode for these pyrazoles in which the C(3) phenyl group is placed in the ER-LBD pocket that normally binds the A-ring of estradiol. As will be described elsewhere in more detail,²¹ pyrazole orientations with the N(1) phenol in the A-ring pocket appear unlikely on the basis of

binding energy considerations and binding affinity measurements. Orientations in which the C(5) phenol is in the A-ring pocket appear to be reasonable, but are considered less likely on the basis of structure-affinity considerations.²¹

The two possible ways that the pyrazoles can be bound with the C(3) phenol in the A-ring binding pocket are illustrated in Figure 3 (Mode A and Mode A'). Both of these modes have the C(3) phenol oriented so that it is congruent with the A-ring of estradiol; they differ simply in the orientation of the remainder of the pyrazole structure, and they are related by rotation of the pyrazole core around the darkened bond. This rotation has the effect of interchanging the positions of the C(4) alkyl group and N(2).

[Figure 3]

We conducted a ligand docking/binding minimization routine by placing PPT (**4g**) in ER α in both orientations Mode A and Mode A' (Flexidock routine within SYBYL; see Experimental Section, Molecular Modeling). During the course of the ligand docking routine, the PPT that began in orientation Mode A' became reoriented into Mode A, whereas the one in Mode A remained in Mode A. Therefore, Mode A' was not considered further. After the docking/minimization routine, the PPT in Mode A was nicely accommodated in this orientation, with only minimal changes in the side chain conformations of some of the residues that line the ligand binding pocket. We also modeled the four other possible orientations of this pyrazole using the same routine (not shown), but we found that none of them gave a fit as good as that of the pyrazole orientation illustrated as Mode A in Figure 3.

In Figure 4, we show a crossed-stereo skeletal model view illustrating PPT (**4g**) in the ER α -estradiol structure, oriented in binding Mode A, after the ligand docking/minimization routine. For clarity and for the ER α and ER β comparison below, only selected residues from ER are shown. In this orientation, the N(1) phenyl group of PPT (**4g**) projects into a region of the binding pocket which represents the C/D subpocket that is normally occupied by portions of the C- and D-rings and the 18-methyl substituent on estradiol (E₂). The N(1)- and the C(5)-phenols of PPT project somewhat more deeply into the C/D subpocket than does estradiol. However, this region is known

to tolerate a variety of substituents,³ and certain residues have been re-positioned by the docking/minimization routine to make additional space for the pyrazole ligand. It is of note that these residue conformational changes, which allow for PPT binding in this mode, involve relatively minimal alteration in the total protein energy.

Analysis of Interactions Between Pyrazole Substituents and Amino Acid Residues in ER α and ER β – We have used this model to try to understand the origins of the high ER α affinity selectivity of PPT (**4g**), and to do this, we have constructed a model for ER β that is derived from ER α -LBD-diethylstilbestrol (DES), structure (See Experimental for details).⁶ Although the ligand binding domains of ER α and ER β have only 56% amino acid identity, the residues that line the ligand binding pocket are nearly identical.²² In fact, of the 22-24 residues that are considered to be in contact with the ligand (i.e., within 4Å), all but two are identical in ER α and ER β .²² The only differences are at ER α position 384, where ER α has a leucine but ER β has a methionine, and at ER α position 421, where ER α has a methionine but ER β has an isoleucine. It has been speculated that these sequence differences, in particular, may underlie the differences in the ER α and ER β binding affinities of ligands that have been studied so far.²² For clarity, we have distinguished these residues in Figure 4 by color: The residues common to ER α and ER β are illustrated in yellow, but at the two positions where the ER β residues are different, the ER β residues, colored in red, are superimposed over the ER α residues in yellow (See, Figure 4 and legend).

[Figure 4]

In this model with the most ER α potency-selective ligand, PPT (**4g**), we can see that the pyrazole core itself has the closest contact with Leu384 in the case of ER α and Met in the case of ER β . For the Met/Ile discriminating residues at ER α position 421, the C(4)-propyl group as well as the C(5)-phenol appear to have close contacts, although this interaction seems less severe.

A model for PPT (**4g**) binding to ER β was generated by changing the two residues in the ER α ligand binding pocket to those found in ER β , inserting the ligand according to Mode A, and then conducting the ligand docking/minimization routine as was done before with ER α (See Experimental). The comparative fit of this pyrazole in the ligand binding pocket of ER α and ER β

can be appreciated by the composite receptor surface model shown in Figure 5 in crossed stereo. In this figure, we have displayed the pyrazoles in both of the receptors as skeletal structures, and the two pockets as colored surfaces. The ligand in the ER α model is shown with standard atom colors and the ER α surface in yellow; both the ligand and receptor in the ER β model are shown in red. In this figure, the view has been rotated, twisting the C(3) phenol away from the viewer; this orientation allows differences between the models to be seen most clearly.

[Figure 5]

The principal difference in the surface of the ligand binding pocket is at the site where ER α has a smaller residue (Leu384) than ER β (Met). This is illustrated by the sharp red interpenetrating surface in the middle left region of the pocket. The increased steric bulk in ER β at this site makes contact with the pyrazole core of this ligand, displacing it relative to the pyrazole position in the ER α model. Because the C(3) phenol remains relatively fixed in the rather rigid A-ring binding pocket, this pyrazole core displacement causes a large shift in the position of N(1) phenol, and a significant but somewhat smaller shift of the C(5) phenol and the propyl group. The shift of the propyl group forces this substituent to adopt a gauche conformation in ER β (vs an anti orientation in ER α); this is a change that would most likely increase ligand internal energy and reduce binding affinity. The shift of the pyrazole position in the ER β model moves the C(5) phenol towards the site where the smaller Ile residue in ER β replaces the bulkier Met421 in ER α . Thus, the different shape of the ligand binding pocket in ER β , in particular the increased bulk of the ER β Met residue where ER α has a Leu, appears to interfere with the optimal binding of the pyrazole ligand and is therefore thought to account for its lowered binding affinity. It is interesting to note that even after extensive minimization, there is a substantial energy difference between the two complexes, with the ER α complex having greater stabilization by ca. 30 Kcal/mole.

Conclusions

A series of C(4) tetra-substituted pyrazole analogs have been prepared and their relative binding affinity determined for the ER. These compounds show an interesting binding affinity

pattern, including high affinity selectivity for ER α , which for the propylpyrazole triol (PPT, **4g**) reaches 410 fold. This compound also has very high potency selectivity for ER α in reporter gene transcription assays in cells, and it is the first ER α -specific agonist. A model of PPT (**4g**) docked in the ER α -LBD-E₂ crystal structure in the most likely binding orientation suggests that the very high ER α binding selectivity of this pyrazole derives from particular interactions between the pyrazole core and the C(4)-propyl group with a region on the ligand binding pocket where ER α has a smaller residue (Leu384) than ER β (Met). These interactions may serve as the basis for future structure-based design of ER α and ER β specific ligands.

Experimental Methods

General

All reagents and solvents were obtained from Aldrich, Fisher or Mallinckrodt. Tetrahydrofuran was freshly distilled from sodium/benzophenone. Dimethylformamide was vacuum distilled prior to use, and stored over 4 Å molecular sieves. Melting points were determined on a Thomas-Hoover UniMelt capillary apparatus and are uncorrected. All reactions were performed under a dry N₂ atmosphere unless otherwise specified. Reaction progress was monitored by analytical thin-layer chromatography using GF silica plates purchased from Analtech. Visualization was achieved by short wave UV light (254 nm) or potassium permanganate stain. Radial preparative-layer chromatography was performed on a Chromatotron instrument (Harrison Research, Inc., Palo Alto, CA) using EM Science silica gel Kieselgel 60 PF₂₅₄ as adsorbent. Flash column chromatography was performed using Woelm 32-63 μ m silica gel packing.²³ Synthetic procedures for **1a-f** and spectral data for **1d** and **1f** are described below. Compounds **1a**,²⁴ **1b**,²⁵ **1c**,²⁶ and **1e**²⁷ were spectroscopically identical to the reported compounds.

¹H and ¹³C NMR spectra were recorded on either a Varian Unity 400 or 500 MHz spectrometers using CDCl₃, or MeOD-*d*₄ as solvent. Chemical shifts were reported as parts per million downfield from an internal tetramethylsilane standard (δ 0.0 for ¹H) or from solvent references. NMR coupling constants are reported in Hertz. ¹³C NMR were determined using

either the Attached Proton Test (APT) or standard ^{13}C pulse sequence parameters. Low resolution and high resolution electron impact mass spectra were obtained on Finnigan MAT CH-5 or 70-VSE spectrometers. Low and high resolution fast atom bombardment (FAB) were obtained on a VG ZAB-SE spectrometer. Elemental analyses were performed by the Microanalytical Service Laboratory of the University of Illinois. Those final components that did not give satisfactory combustion analysis (i.e., **4b**, **c**, **d**, **6**) were found to be at least 98% pure by HPLC analysis under normal and reversed phase conditions.

Relative Binding Affinity Assays

Purified ER α and ER β binding affinities were determined using a competitive radiometric binding assay using 10 nM [^3H]estradiol as tracer, commercially available ER α and ER β preparations (PanVera Inc. Madison, WI), and hydroxylapatite (HAP) to adsorb bound receptor-ligand complex.^{15,16} HAP was prepared following the recommendations of Williams and Gorski.²⁸ All incubations were done at 0 °C for 18-24h. Binding affinities are expressed relative to estradiol (RBA = 100%) and are reproducible within $\pm 30\%$.

Transcription Activation Assays

Human endometrial cancer (HEC-1) cells were maintained in culture and transfected as described previously.²⁹ Transfection of HEC-1 cells in 60 mm dishes used 0.4 mL of a calcium phosphate precipitate containing 2.5 μg of pCMV β Gal as internal control, 2 μg of the reporter gene plasmid, 100 ng of the ER expression vector, and carrier DNA to a total of 5 μg DNA. CAT activity, normalized for the internal control β -galactosidase activity, was assayed as previously described.²⁹

Molecular Modeling for Pyrazole 4g.

The starting conformation for **4g** used for receptor docking studies was generated from a random conformational search performed using the MMFF94 force field as implemented in Sybyl 6.6. The resulting lowest energy conformer was then used for docking studies. Charge

calculations were determined using the MMFF94 method and molecular surface properties displayed using MOLCAD module in Sybyl 6.6.

Pyrazole **4g**, generated as noted above, was pre-positioned in the DES-ER α -LBD crystal structure (Protein Data Bank ID No. 3ERD)⁶ using a least squares multfitting of select atoms within the DES ligand. Once pre-positioned, DES was deleted and ligand **4g** optimally docked in the ER α binding pocket using the Flexidock routine within Sybyl (Tripos). Both hydrogen-bond donors and acceptors within the pocket surrounding the ligand (Glu₃₅₃, Arg₃₉₄, and His₅₂₄), the ligand itself and select torsional bonds were defined. The best docked receptor ligand complex from Flexidock then underwent a three step minimization: first non-ring torsional bonds of the ligand were minimized in the context of the receptor using the torsmin command, followed by minimization of the side chain residues within 8 Å of the ligand while holding the backbone and residues Glu₃₅₃ and Arg₃₉₄ fixed. A final third minimization of both the ligand and receptor was conducted using the Anneal function (hot radius 8 Å, interesting radius 16Å from pyrazole **4g**) to afford the final model.

The ER- β molecular model was generated within Sybyl by first modifying residues Leu384 to Met and Met421 to Ile in the DES-ER α -LBD crystal structure⁶ and conducting an initial minimization of these two residues while holding the remaining atoms fixed. This was followed by a final minimization using the Anneal function (hot radius 4 Å, interesting radius 8 Å from Met384 and Ile421) using conditions similar to above. The pyrazole **4g** was introduced into this ER β model and the Flexidock routine implemented as for the ER α model (see above). All minimizations were done using the MMFF94 Forcefield with the Powell gradient method (final RMS <0.02 kcal/mol·Å).

Chemical Syntheses

General procedure for preparation of alkylphenones using AlCl₃ (1a-c, f), method A. To a stirred solution of AlCl₃ (46.8 mmol) in 1,2-dichloroethane (10 mL) at 0 °C was added the commercial acid chloride (39.0 mmol) dropwise over 10 minutes. The resulting solution was

allowed to come to rt for 20 minutes until all of the AlCl_3 had dissolved. The reaction mixture was cooled to $0\text{ }^\circ\text{C}$ and a solution of anisole (5.1 mL, 46.8 mmol) in 1,2-dichloroethane (20 mL) was then added dropwise over 30 minutes. Upon completion the reaction was allowed to reach rt and stir for 8-15h. The mixture was then quenched by pouring over 100g of ice and extracted with CH_2Cl_2 (3 x 25 mL). The combined organic layers were washed with water, NaHCO_3 (sat.), brine, then dried over MgSO_4 and concentrated under reduced pressure. Excess anisole was removed in vacuo and then the ketone product distilled.

General procedure for preparation of alkylphenones using PPA (1d-e), method B.

A mechanically stirred mixture consisting of carboxylic acid (1.0 eq), anisole (1.1 eq) and polyphosphoric acid (PPA, 6.15g/mL of anisole) was heated to $90\text{--}100\text{ }^\circ\text{C}$ for 1.5h. Upon cooling to near rt the dark mixture was poured over ice (100g/0.1mol) and extracted repeatedly with EtOAc. The organic layers were then washed with sat. NaHCO_3 followed by brine. After drying the extract over Na_2SO_4 and removal of solvent, a crude oil was afforded. The final products were purified by bulb-to-bulb distillation.

1-(4-Methoxyphenyl)-4-methyl-pentan-1-one (1d). Prepared according to method B outlined above to afford the title compound as a pale yellow oil (75%): ^1H NMR (CDCl_3 , 500 MHz) δ 0.94 (d, 6H, $J = 6.0$), 1.60 (m, 3H, overlapping methine and $\beta\text{-CH}_2$), 2.90 (t, 2H, $J = 6.8$), 3.87 (s, 3H), 6.92 (d, 2H, $J = 8.8$), 7.90 (d, 2H, $J = 8.8$); ^{13}C NMR (CDCl_3 , 125 MHz) δ 22.6, 28.5, 33.9, 36.4, 55.2, 113.5, 130.2, 163.6, 198.7; MS (EI, 70 eV) m/z 206.1 (M^+); Anal ($\text{C}_{13}\text{H}_{18}\text{O}_2$) C, H.

1-(4-Methoxyphenyl)-3-methyl-butan-1-one (1f). Prepared according to general method A outlined above to afford the title compound as a pale yellow oil (84%): ^1H NMR (CDCl_3 , 500 MHz) δ 0.95 (d, 6H, $J = 6.7$), 2.24 (sept, 1H, $J = 6.6$), 2.73 (d, 2H, $J = 6.7$), 3.81 (s, 3H), 6.88 (d, 2H, $J = 8.9$), 7.90 (d, 2H, $J = 9.2$); ^{13}C NMR (CDCl_3 , 125 MHz) δ 22.6, 25.2, 46.2, 55.2, 113.5, 130.2, 130.3, 163.1, 198.7; HRMS (EI, M^+) calcd for $\text{C}_{12}\text{H}_{16}\text{O}_2$: 192.1150. Found: 192.1153.

2-Methyl-1,3-bis-(4-methoxyphenyl)-propane-1,3-dione (2a). To a solution of **1a** (160 mg, 0.97 mmol) and 4-nitrophenyl 4-methoxybenzoate (prepared from *p*-nitrophenol and 4-methoxybenzoic acid using DIC and DMAP) in THF (35 mL) at 0 °C was added a 1.0 M solution of LHMDS (3.03 mL, 3.03 mmol) dropwise over 5 minutes. The reaction was warmed to room temperature and allowed to stir for 1.5 h. At this time the reaction was quenched by the addition of H₂O (25 mL). The mixture was then repeatedly extracted with diethyl ether. The organic layers were combined and washed with H₂O, then dried over Na₂SO₄ and concentrated under reduced pressure to afford a crude solid. Unreacted ester was removed by adding a solution of 40% ethyl acetate/hexanes and filtering off the insoluble ester. The remaining filtrate was concentrated and subjected to flash chromatography (40% ethyl acetate/hexanes) to afford the title compound as a light yellow oil (266 mg, 92%): ¹H NMR (CDCl₃, 500 MHz) δ 1.58 (d, 3H, *J* = 7.3), 3.85 (s, 3H), 5.13 (q, 1H, *J* = 7.2), 6.92 (d, 2H, *J* = 6.8), 7.93 (d, 2H, *J* = 7.0).

2-Ethyl-1,3-bis-(4-methoxyphenyl)-propane-1,3-dione (2b).¹¹ Prepared according to procedure outlined above from **1b** and purified by flash chromatography (ethyl acetate/hexanes) to afford a viscous oil (95%): ¹H NMR (CDCl₃, 500 MHz) δ 1.01 (t, 3H, *J* = 7.4), 2.12 (quint, 2H, *J* = 7.1), 3.80 (s, 6H), 4.98 (t, 1H, *J* = 6.6), 6.87 (AA'XX', 2H, *J* = 8.8, 2.1), 7.94 (AA'XX', 2H, *J* = 8.5, 2.3); APT ¹³C NMR (CDCl₃, 125 MHz) δ 12.9 (CH₃), 23.2 (CH₂), 55.6 (CH), 58.8 (CH₃O), 114.0 (ArCH), 129.3 (ArC), 131.0 (ArCH), 163.8 (ArC), 195.0 (C=O); MS (EI, 70 eV) *m/z* 312.3 (M⁺).

2-Propyl-1,3-bis-(4-methoxyphenyl)-propane-1,3-dione (2c). Prepared according to procedure outlined above from **1c** and purified by flash chromatography (ethyl acetate/hexanes) to afford product as a clear viscous oil (76%): ¹H NMR (CDCl₃, 500 MHz) δ 0.95 (t, 3H, *J* = 7.4), 1.36-1.47 (m, 2H), 2.06- 2.11 (m, 2H), 3.83 (s, 6H), 5.05 (t, 1H, *J* = 6.7) 6.90 (AA'XX', 2H, *J* = 9.0, 2.5), 7.95 (AA'XX', 2H, *J* = 9.0, 2.5); ¹³C NMR (CDCl₃, 125 MHz) δ 14.0, 21.5, 31.6, 55.4, 57.1, 113.8, 129.0, 130.8, 163.5, 194.8; HRMS (EI, M⁺) calcd. for C₂₀H₂₂O₄: 326.1518. Found: 326.1512.

2-*i*-Butyl-1,3-bis-(4-methoxyphenyl)-propane-1,3-dione (2d). Prepared according to procedure outlined above from **1d** and purified by flash chromatography (ethyl acetate/hexanes) to afford product as a clear viscous oil (77%): ^1H NMR (CDCl_3 , 500 MHz) δ 0.96 (d, 3H, $J = 6.5$), 1.70 (m, 1H, $J = 6.7$), 2.00 (br t, 2H, $J = 6.9$), 3.82 (s, 6H), 5.18 (t, 1H, $J = 6.5$), 6.89 (d, 2H, $J = 8.6$), 7.97 (d, 2H, $J = 9.0$); ^{13}C NMR (CDCl_3 , 125 MHz) δ 22.8 (CH_3), 27.2 (CH), 38.5 (CH_2), 55.7 (CH_3O), 55.8 (CH), 114.2 (ArCH), 129.4 (ArC), 131.2 (ArCH), 163.2 (C=O); HRMS (EI, M^+) calcd for $\text{C}_{13}\text{H}_{18}\text{O}_4$: 340.1674. Found: 340.1679; Anal ($\text{C}_{21}\text{H}_{24}\text{O}_4$) C, H.

2-*n*-Butyl-1,3-bis-(4-methoxyphenyl)-propane-1,3-dione (2e). Prepared according to procedure outlined above from **1e** and purified by flash chromatography (ethyl acetate/hexanes) to afford product as a light yellow oil (69%): ^1H NMR (CDCl_3 , 500 MHz) δ 0.89 (t, 3H, $J = 7.0$), 1.37 (m, 4H), 2.11 (q, 2H, $J = 7.1$), 3.85 (s, 6H), 6.91 (d, 4H, $J = 9.0$), 7.98 (d, 4H, $J = 9.0$); ^{13}C NMR (CDCl_3 , 125 MHz) δ 14.0 (CH_3), 22.9 (CH_2), 22.7 (CH_2), 30.7 (CH_2), 55.7 (CH_3O), 57.7 (CH), 114.2 (ArCH), 129.5 (ArC), 131.2 (ArCH), 163.2 (C=O); HRMS (EI, M^+) calcd for $\text{C}_{13}\text{H}_{18}\text{O}_4$: 340.1674. Found: 340.1675; Anal ($\text{C}_{13}\text{H}_{18}\text{O}_4$) C, H.

General procedure for pyrazole synthesis. To a DMF (30 mL) and THF (10 mL) solution containing diketone (1.0 mmol) was added phenylhydrazine hydrochloride (3-5 equiv). The mixture was brought to reflux (oil bath temperature 120 $^\circ\text{C}$) until disappearance of diketone as evident by TLC (8-20h). The reaction mixture was then allowed to cool to room temperature and diluted with H_2O (30 mL). The product was extracted repeatedly with ethyl acetate (3 X 25 mL) and the organic layers combined and washed sequentially with a sat. LiCl solution (25 mL), sat. NaHCO_3 (25 mL), and brine (25 mL). The organic layer was dried over Na_2SO_4 and concentrated under reduced pressure to afford the crude product in the form of an oil, which was purified by flash chromatography or by passage through a short silica plug eluting with an ethyl acetate/hexane solvent system.

3,5-Bis-(4-methoxyphenyl)-4-methyl-1-phenyl-1H-pyrazole (3a). The diketone **2a** (250 mg, 0.84 mmol) was reacted with phenylhydrazine hydrochloride (423 mg, 2.94 mmol) according to the general procedure above. Upon purification by flash chromatography (40% ethyl

acetate/hexanes) the title compound was obtained as a tan solid (220 mg, 71 %): mp 142-143 °C; ¹H NMR (CDCl₃, 500 MHz) δ 2.21 (s, 3H), 3.83 (s, 3H), 3.86 (s, 3H), 6.89 (AA'XX', 2H, *J* = 8.9, 2.5), 6.99 (AA'XX', 2H, *J* = 8.9, 2.5), 7.15 (AA'XX', 2H, *J* = 8.8, 2.5), 7.19 - 7.32 (m, 5H), 7.74 (AA'XX', 2H, *J* = 8.9, 2.5); ¹³C NMR (CDCl₃, 125 MHz) δ 10.2, 55.2, 55.3, 113.6, 113.9, 113.9, 123.1, 124.7, 126.5, 126.6, 128.7, 129.1, 131.3, 140.4, 141.2, 150.9, 159.2, 159.4; MS (EI, 70 eV) *m/z* 370 (M⁺); Anal. (C₂₄H₂₂N₂O₂) C, H, N.

4-Ethyl-3,5-Bis-(4-methoxyphenyl)-1-phenyl-1*H*-pyrazole (3b).¹¹ Diketone **2b** and phenyl hydrazine hydrochloride were reacted as outlined above to afford **3b** as an orange solid after flash chromatography purification (87%): ¹H NMR (CDCl₃, 400 MHz) δ 1.04 (t, 3H, *J* = 7.6), 2.63 (q, 2H, *J* = 7.6), 3.83 (s, 3H), 3.86 (s, 3H), 6.90 (AA'XX', 2H, *J* = 8.8, 2.4), 6.99 (AA'XX', 2H, *J* = 8.8, 2.6), 7.17 (AA'XX', 2H, *J* = 8.8, 2.4), 7.20 (m, 2H), 7.24 (m, 3H), 7.72 (AA'XX', 2H, *J* = 9.0, 2.4); ¹³C NMR (CDCl₃, 100 MHz) δ 15.8, 17.3, 55.4, 55.5, 114.1, 114.2, 120.7, 123.5, 124.8, 126.8, 127.0, 128.8, 129.3, 131.5, 140.5, 141.2, 150.8, 159.4, 159.6; HRMS (EI, M⁺) calcd for C₂₅H₂₄N₂O₂: 384.1835. Found: 384.1837.

3,5-Bis-(4-methoxyphenyl)-1-phenyl-4-propyl-1*H*-pyrazole (3c). Diketone **2c** (200 mg, 0.61 mmol) was reacted with phenylhydrazine hydrochloride (444 mg, 3.07 mmol) according to general procedure to afford **3c** as an orange oil after purification by flash chromatography (40% ethyl acetate/hexanes, 130 mg, 53 %): ¹H NMR (CDCl₃, 500 MHz) δ 0.79 (t, 3H, *J* = 7.4), 1.42 (sext, 2H, *J* = 7.7), 2.57 (t, 2H, *J* = 8.0), 3.83 (s, 3H), 3.86 (s, 3H), 6.90 (AA'XX', 2H, *J* = 8.6, 2.5), 6.99 (AA'XX', 2H, *J* = 8.8, 2.5), 7.18 - 7.32 (m, 5H), 7.15 (AA'XX', 2H, *J* = 8.6, 2.5), 7.72 (AA'XX', 2H, *J* = 8.8, 2.5); ¹³C NMR (CDCl₃, 125 MHz) δ 14.05, 23.79, 25.86, 55.09, 55.15, 113.74, 113.85, 118.87, 118.86, 122.86, 124.60, 126.52, 129.49, 131.17, 139.66, 141.31, 150.36, 159.14, 159.33; HRMS (EI, M⁺) calcd. for C₂₆H₂₆N₂O₂: 398.1994. Found: 398.2000.

4-Isobutyl-3,5-bis-(4-methoxyphenyl)-1-phenyl-1*H*-pyrazole (3d). Diketone **2d** was reacted with phenylhydrazine hydrochloride according to general procedure to afford **3d** as an orange oil after a short silica plug (20% ethyl acetate/hexanes, 86%). The purified material was then directly used in the subsequent deprotection step.

4-Butyl-3,5-bis-(4-methoxyphenyl)-1-phenyl-1H-pyrazole (3e). Diketone **2e** was reacted with phenylhydrazine hydrochloride according to general procedure to afford **3e** as a reddish oil after purification by flash chromatography (20% ethyl acetate/hexanes, 86%). This material was then directly used in the subsequent deprotection step.

4-Ethyl-1,3,5-tris-(4-methoxyphenyl)-1H-pyrazole (3f). Diketone **2b** (400 mg, 1.28 mmol) was reacted with 4-methoxyphenylhydrazine hydrochloride (1.11 g, 6.40 mmol) according to general procedure. The crude product was purified by flash chromatography (2% acetone/CH₂Cl₂) to afford **3f** as an oil (351 mg, 66 %): ¹H NMR (CDCl₃, 500 MHz) δ 1.06 (t, 3H, *J* = 7.5), 2.65 (q, 2H, *J* = 7.5), 3.73 (s, 3H), 3.79 (s, 3H), 3.83 (s, 3H), 6.78 (AA'XX', 2H, *J* = 9.0, 2.8) 6.89 (AA'XX', 2H, *J* = 8.8, 2.4), 6.69 (AA'XX', 2H, *J* = 8.8, 2.4), 7.16 (AA'XX', 2H, *J* = 8.8, 2.4), 7.21 (AA'XX', 2H, *J* = 9.0, 2.7), 7.74 (AA'XX', 2H, *J* = 8.7, 2.4); ¹³C NMR (CDCl₃, 125 MHz) δ 15.52, 17.09, 55.05, 55.10, 55.22, 113.65, 113.80, 113.83, 119.78, 123.11, 125.96, 126.78, 128.95, 131.18, 133.45, 140.84, 149.94, 158.99, 157.97, 159.22; HRMS (EI, M⁺) calcd. for C₂₆H₂₆N₂O₃: 414.1943. Found: 414.1942.

1,3,5-Tris-(4-methoxyphenyl)-4-propyl-1H-pyrazole (3g). Diketone **2c** (500 mg, 1.52 mmol) was reacted with 4-methoxyphenylhydrazine hydrochloride (800 mg, 4.59 mmol) according to general procedure to afford 362 mg of **3g** as a red oil after a short silica plug (20% ethyl acetate/hexanes, 67%). This material was then directly used in the subsequent deprotection step.

4-Isobutyl-1,3,5-tris-(4-methoxyphenyl)-1H-pyrazole (3h). Diketone **2d** was reacted with 4-methoxyphenylhydrazine hydrochloride according to general procedure to afford **3h** as a light orange oil after a short silica plug (20% ethyl acetate/hexanes, 85%). The purified material was then directly used in the subsequent deprotection step.

4-Butyl-1,3,5-tris-(4-methoxyphenyl)-1H-pyrazole (3i). Diketone **2e** was reacted with 4-methoxyphenylhydrazine hydrochloride according to the general procedure to afford **3i** as a light orange oil after a short silica plug (20% ethyl acetate/hexanes, 87%). The purified material was then directly used in the subsequent deprotection step.

General demethylation procedure. To a stirred solution of methyl protected pyrazole (1 equiv) in CH_2Cl_2 at -78°C was added dropwise a 1M BBr_3 solution in CH_2Cl_2 (3-5 equiv). Upon complete addition of BBr_3 , the reaction was maintained at -78°C for 1h and then allowed to reach rt and stir for an additional 16h. The mixture was cooled to 0°C and carefully quenched with H_2O (15-25 mL). The product was then repeatedly extracted with EtOAc and the organic layers dried over Na_2SO_4 . Upon solvent removal the crude phenolic products were purified by flash chromatography and/or recrystallization from $\text{MeOH}/\text{CH}_2\text{Cl}_2$ mixtures.

3,5-Bis-(4-hydroxyphenyl)-4-methyl-1-phenyl-1H-pyrazole (4a). A stirred CH_2Cl_2 solution of **3a** (200 mg, 0.54 mmol) was deprotected using BBr_3 according to the general demethylation procedure. Purification by flash chromatography (5% $\text{CH}_3\text{OH}/\text{CH}_2\text{Cl}_2$) afforded the title compound as a tan solid (54 mg, 30%): mp $225\text{--}230^\circ\text{C}$; ^1H NMR ($\text{MeOD}-d_4$, 500 MHz) δ 2.13 (s, 3H), 6.76 (AA'XX', 2H, $J = 8.4$, 2.7), 6.93 (AA'XX', 2H, $J = 8.7$, 2.5), 7.01 (AA'XX', 2H, $J = 8.8$, 2.5), 7.54 (AA'XX', 2H, $J = 8.6$, 2.4), 7.35 – 7.22 (m, 5H); ^{13}C NMR ($\text{MeOD}-d_4$, 125 MHz) 8.7, 112.8, 114.7, 114.8, 120.9, 124.4, 124.8, 126.7, 128.3, 128.9, 130.9, 139.8, 151.4, 157.1, 157.4; MS (EI, 70 eV) m/z 342. Anal. ($\text{C}_{22}\text{H}_{18}\text{N}_2\text{O}_2 \cdot \text{H}_2\text{O}$) C, H, N.

4-Ethyl-3,5-bis-(4-hydroxyphenyl)-1-phenyl-1H-pyrazole (4b).¹¹ A stirred CH_2Cl_2 solution of **3b** (100 mg, 0.26 mmol) was deprotected using BBr_3 according to the general demethylation procedure. Purification by flash chromatography (5% $\text{CH}_3\text{OH}/\text{CH}_2\text{Cl}_2$) afforded the title compound as a white solid (50 mg, 54%): mp $247\text{--}248^\circ\text{C}$; ^1H NMR ($\text{MeOD}-d_4$, 400 MHz) δ 0.98 (t, 3H, $J = 7.4$), 2.60 (q, 2H, $J = 7.5$), 6.78 (AA'XX', 2H, $J = 8.8$, 2.4), 6.88 (AA'XX', 2H, $J = 8.7$, 2.5), 7.05 (AA'XX', 2H, $J = 8.8$, 2.4), 7.24 – 7.42 (m, 5H), 7.51 (AA'XX', 2H, $J = 8.7$, 2.5); HRMS (EI, M^+) calcd for $\text{C}_{23}\text{H}_{21}\text{N}_2\text{O}_2$: 357.1611. Found: 357.1603.

3,5-Bis-(4-hydroxyphenyl)-1-phenyl-4-propyl-1H-pyrazole (4c). A stirred CH_2Cl_2 solution of **3c** (107 mg, 0.27 mmol) was deprotected using BBr_3 according to the general demethylation procedure. The crude product was purified by flash chromatography (10% $\text{CH}_3\text{OH}/\text{CH}_2\text{Cl}_2$) to afford **4c** as a tan solid (85 mg, 86%): mp: $240\text{--}245^\circ\text{C}$; ^1H NMR ($\text{MeOD}-d_4$, 500 MHz) δ 0.72 (t, 3H, $J = 7.4$), 1.35 (sext, 2H, $J = 7.5$), 2.55 (t, 2H, $J = 7.7$), 6.77 (AA'XX', 2H,

$J = 8.7, 2.5$), 6.88 (AA'XX', 2H, $J = 8.5, 2.4$), 7.03 (AA'XX', 2H, $J = 8.5, 2.4$), 7.32 – 7.27 (m, 5H), 7.50 (AA'XX', 2H, $J = 8.8, 2.5$); ^{13}C NMR (MeOD- d_4 , 400 MHz) δ 12.73, 13.28, 25.28, 114.75, 114.89, 118.26, 121.13, 124.78, 124.82, 126.69, 128.26, 128.99, 131.02, 139.71, 142.12, 151.30, 157.08, 157.49; HRMS (EI, M^+) calcd for $\text{C}_{24}\text{H}_{22}\text{N}_2\text{O}_2$: 370.1681. Found: 370.1676.

4-Isobutyl-3,5-bis-(4-hydroxyphenyl)-1-phenyl-1H-pyrazole (4d). A stirred CH_2Cl_2 solution of **3d** (100 mg, 0.24 mmol) was deprotected using BBr_3 according to the general demethylation procedure. The crude product was purified by flash chromatography (10% $\text{CH}_3\text{OH}/\text{CH}_2\text{Cl}_2$) to afford **4d** as a tan powder (70 mg, 76%): mp 225 °C dec; ^1H NMR (MeOD- d_4 , 500 MHz) δ 0.63 (d, 6H, $J = 6, 5$), 1.51 (m, 1H, $J = 7.0$), 2.51 (d, 2H, $J = 7.5$), 6.76 (AA'XX', 2H, $J = 9.0, 2.3$), 6.87 (AA'XX', 2H, $J = 8.9, 2.3$), 7.02 (AA'XX', 2H, $J = 8.5, 2.4$), 7.26 (m, 5H), 7.49 (AA'XX', 2H, $J = 8.0, 2.3$); ^{13}C NMR (MeOD- d_4 , 125 MHz) δ 22.8, 29.9, 33.8, 116.4, 116.6, 119.1, 123.0, 126.6, 126.8, 128.4, 129.9, 130.9, 132.9, 141.5, 144.2, 153.4, 158.8, 159.2; FAB-HRMS ($\text{M}+1$) calcd for $\text{C}_{25}\text{H}_{25}\text{N}_2\text{O}_2$: 385.1916. Found: 385.1916.

4-Butyl-3,5-bis-(4-hydroxyphenyl)-1-phenyl-1H-pyrazole (4e). A stirred CH_2Cl_2 solution of **3e** (100 mg, 0.24 mmol) was deprotected using BBr_3 according to the general demethylation procedure. The crude product was purified by flash chromatography (30% EtOAc/hexanes) to afford a tan solid. This material was subsequently recrystallized from 5-10% MeOH/ CH_2Cl_2 to afford the title compound as small off-white crystals (59 mg, 64%): mp 205.5–207.5 °C; ^1H NMR (MeOD- d_4 , 400 MHz) δ 0.72 (t, 3H, $J = 7.2$), 1.16 (sext, 2H, $J = 7.2$), 1.34 (quint, 2H, $J = 7.2$), 2.60 (t, 2H, $J = 7.2$), 4.95 (br s, 2H exchange with D_2O), 6.78 (d, 2H, $J = 9.0$), 6.91 (d, 2H, $J = 8.0$), 7.02 (d, 2H, $J = 8.8$), 7.26 (m, 5H), 7.53 (d, 2H, $J = 8.4$); ^{13}C NMR (MeOD- d_4 , 125 MHz) δ 14.6, 23.9, 24.8, 34.3, 116.8, 116.9, 120.5, 123.2, 126.8, 128.7, 130.3, 131.0, 131.1, 133.1, 141.7, 144.0, 153.3, 159.0, 159.4. Anal. ($\text{C}_{25}\text{H}_{24}\text{N}_2\text{O}_2 \cdot 0.1 \text{H}_2\text{O}$) C, H, N.

4-Ethyl-1,3,5-tris-(4-hydroxyphenyl)-1H-pyrazole (4f). A stirred CH_2Cl_2 solution of **3f** (200 mg, 0.48 mmol) was deprotected using BBr_3 according to the general demethylation procedure. A crude oil was isolated which was triturated with a 10% $\text{CH}_3\text{OH}/\text{CH}_2\text{Cl}_2$ solution from which the desired product precipitated. The white powder was collected by filtration and

recrystallized from CH₃OH/CH₂Cl₂ to afford the title compound **4f** (175 mg, 98%): mp 210-215 °C; ¹H NMR (MeOD-*d*₄, 400 MHz): δ 0.96 (t, 3H, *J* = 7.5) 2.58 (q, 2H, *J* = 7.5) 6.70 (AA'XX', 2H, *J* = 8.8, 2.6), 6.77 (AA'XX', 2H, *J* = 8.6, 2.3), 6.87 (AA'XX', 2H, *J* = 8.8, 2.3), 7.10 (m, 4H), 7.48 (AA'XX', 2H, *J* = 8.6, 2.4); ¹³C NMR (MeOD-*d*₄, 100 MHz) δ 14.5, 16.6, 114.8, 114.9, 114.9, 119.2, 121.4, 125.0, 126.8, 129.1, 131.2, 131.9, 142.1, 150.5, 156.7, 157.1, 157.5. Anal. (C₂₃H₂₀N₂O₃ · 0.7 H₂O) C, H, N.

1,3,5-Tris-(4-hydroxyphenyl)-4-propyl-1H-pyrazole (4g). A stirred CH₂Cl₂ solution of **3g** (200 mg, 0.48 mmol) was deprotected using BBr₃ according to the general demethylation procedure. A crude oil was isolated which was triturated with a 10% CH₃OH/CH₂Cl₂ solution from which the desired product precipitated. The white powder was collected by filtration and recrystallized from CH₃OH/CH₂Cl₂ to afford the title compound **4g** (125 mg, 68%): mp 230 °C dec.; ¹H NMR (MeOD-*d*₄, 400 MHz) δ 0.72 (t, 3H, *J* = 7.2), 1.33 (sext, 2H, *J* = 7.6), 2.54 (t, 2H, *J* = 8), 6.70 (AA'XX', 2H, *J* = 8.8, 2.4), 6.76 (AA'XX', 2H, *J* = 6.8, 2.0), 6.87 (AA'XX', 2H, *J* = 8.8, 2.4), 7.02 (AA'XX', 2H, *J* = 8.8, 2.4), 7.05 (AA'XX', 2H, *J* = 9.2, 2.4), 7.47 (AA'XX', 2H, *J* = 8.8, 2.0); ¹³C NMR (MeOD-*d*₄, 100 MHz) δ 25.8 (CH₃), 36.4 (CH₂), 38.4 (CH₂), 127.0 (C), 128.0 (C), 128.5 (C), 130.5 (CH), 134.3 (CH), 137.9 (CH), 138.9 (C), 140.3 (C), 141.3 (C), 142.8 (C), 143.3 (C), 144.1 (C), 144.7 (CH), 155.3 (CH), 163.6 (CH), 169.5 (CH), 170.3 (CH). Anal. (C₂₄H₂₂N₂O₃ · 0.6 H₂O) C, H, N.

4-Isobutyl-1,3,5-tris-(4-hydroxyphenyl)-1H-pyrazole (4h). A stirred CH₂Cl₂ solution of **3h** (250 mg, 0.56 mmol) was deprotected using BBr₃ according to the general demethylation procedure. Recrystallization from CH₃OH/CH₂Cl₂ afforded the title compound **4h** as an off-white powder (80 mg, 37%): mp 226-228 °C; ¹H NMR (MeOD-*d*₄, 500 MHz) δ 0.61 (d, 6H, *J* = 6.5), 1.50 (m, 1H, *J* = 7.0), 2.50 (d, 2H, *J* = 7.5), 4.87 (s, 3H, OH), 6.70 (AA'XX', 2H, *J* = 8.5, 2.0), 6.75 (AA'XX', 2H, *J* = 8.5, 2.3), 6.85 (AA'XX', 2H, *J* = 9.0, 2.3), 7.01 (AA'XX', 2H, *J* = 9.0, 2.3), 7.05 (AA'XX', 2H, *J* = 9.0, 2.3), 7.45 (AA'XX', 2H, *J* = 8.5, 2.3); ¹³C NMR (MeOD-*d*₄, 125 MHz) δ 22.9, 29.9, 33.9, 116.4, 116.5, 116.6, 118.3, 123.2, 126.9, 128.3, 130.9, 132.9, 133.5, 144.3, 152.7, 158.2, 158.6, 158.9. Anal. (C₂₅H₂₄N₂O₃ · 0.7 H₂O) C, H, N.

4-Butyl-1,3,5-tris-(4-hydroxyphenyl)-1H-pyrazole (4i). A stirred CH_2Cl_2 solution of **3i** (200 mg, 0.45 mmol) was deprotected using BBr_3 according to the general demethylation procedure. Recrystallization from $\text{CH}_3\text{OH}/\text{CH}_2\text{Cl}_2$ afforded the title compound **4i** as an off-white powder (90 mg, 50%): mp 214-230 °C dec., ^1H NMR ($\text{MeOD}-d_4$, 500 MHz) δ 0.71 (t, 3H, $J = 7.5$), 1.13 (sext, 2H, $J = 7.0$), 1.30 (quint, 2H, $J = 8.5$), 2.57 (t, 2H, $J = 8.0$), 6.70 (AA'XX', 2H, $J = 9.0, 2.4$), 6.76 (AA'XX', 2H, $J = 8.5, 2.3$), 6.86 (AA'XX', 2H, $J = 9.0, 2.5$), 7.02 (AA'XX', 2H, $J = 8.5, 2.3$), 7.05 (AA'XX', 2H, $J = 8.5, 2.3$), 7.46 (AA'BB', 2H, $J = 8.5, 2.3$); ^{13}C NMR ($\text{MeOD}-d_4$, 400 MHz) δ 14.1, 23.5, 24.4, 33.9, 116.3, 116.4, 116.5, 119.3, 123.0, 126.7, 128.3, 130.7, 132.8, 133.5, 143.9, 152.4, 158.3, 158.7, 159.0. Anal. ($\text{C}_{25}\text{H}_{24}\text{N}_2\text{O}_3 \cdot 0.3 \text{H}_2\text{O}$) C, H, N.

4-Isopropyl-3,5-bis-(4-methoxy-phenyl)-1-phenyl-1H-pyrazole (6).¹³ Upon solid support cleavage and solvent removal the crude solid was recrystallized from 25% ethyl acetate/hexane to afford **6** as small cubic crystals (30 mg, 11 % over three steps): mp: 225-230 °C; ^1H NMR ($\text{MeOD}-d_4$, 400 MHz) δ 1.09 (d, 6H, $J = 7.0$ Hz) 2.98 (septet, 1H, $J = 7.11$ Hz), 6.76 (AA'XX', 2H, $J = 9.1, 2.6$), 6.88 (AA'XX', 2H, $J = 9.0, 2.6$), 7.1 (AA'XX', 2H, $J = 8.7, 2.5$), 7.20 -7.30 (m, 5H), 7.39 (AA'XX', 2H, $J = 8.8, 2.40$); ^{13}C NMR ($\text{MeOD}-d_4$, 100 MHz) δ 22.5, 24.5, 114.5, 114.6, 121.6, 124.6, 125.0, 126.7, 128.2, 130.2, 131.8, 139.6, 141.3, 151.3, 157.2, 157.6; HRMS (EI, M^+) calcd for $\text{C}_{24}\text{H}_{22}\text{N}_2\text{O}_2$: 370.1681. Found: 370.1674.

Acknowledgments

We are grateful for support of this research through grants from the U. S. Army Breast Cancer Research Program (DAMD17-97-1-7076 to J.A.K.) and the National Institutes of Health (PHS 5R37 DK15556 to J.A.K. and PHS 5R37 CA18119 to B.S.K.). We thank Kathryn E. Carlson for her advice and for performing binding assays. NMR spectra were obtained in the Varian Oxford Instrument Center for Excellence in NMR Laboratory. Funding for this instrumentation was provided in part from the W.M. Keck Foundation and the National Science Foundation (NSF CHE 96-10502). Mass spectra were obtained on instruments supported by grants from the National Institute of General Medical Sciences (GM 27029), the National Institute of Health (RR 01575), and the National Science Foundation (PCM 8121494).

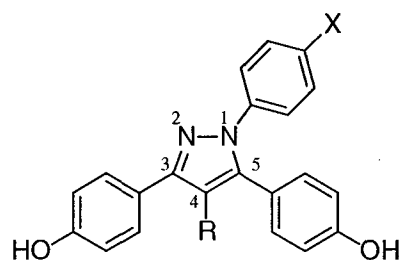


Table 1. Relative Binding Affinity (RBA) data for C(4) pyrazole analogs^a

| Cpd. No. | R | X | RBA ER α ^b | RBA ER β ^b | ER α /ER β RBA ratio |
|----------|--------------|----|------------------------------|-----------------------------|-----------------------------------|
| 4a | Me | H | 0.76 \pm 0.18 | 0.28 \pm 0.16 | 2.7 |
| 4b | Et | H | 30.6 \pm 15 | 1.1 \pm 0.2 | 28 |
| 6 | <i>i</i> -Pr | H | 5.6 \pm 2 | 0.86 \pm 0.11 | 6.5 |
| (PPD) 4c | <i>n</i> -Pr | H | 16.8 \pm 0.3 | 0.52 \pm 0.03 | 32 |
| 4d | <i>i</i> -Bu | H | 56.4 \pm 5.5 | 1.41 \pm 0 | 40 |
| 4e | <i>n</i> -Bu | H | 8.7 \pm 2 | 0.47 \pm 0.1 | 19 |
| 4f | Et | OH | 35.7 \pm 5.8 | 0.15 \pm 0.014 | 240 |
| (PPT) 4g | <i>n</i> -Pr | OH | 48.8 \pm 12 | 0.12 \pm 0.04 | 410 |
| 4h | <i>i</i> -Bu | OH | 75.1 \pm 6.1 | 0.89 \pm 0.06 | 84 |
| 4i | <i>n</i> -Bu | OH | 13.9 \pm 4 | 0.18 \pm 0.09 | 77 |

^a Relative Binding Affinity (RBA), where estradiol is 100%. Values are the mean of at least 2 and more typically 3 or more independent determinations (\pm SD).³⁰

^b Competitive radiometric binding assays were done with purified full-length human ER α and ER β (PanVera Inc), using 10nM [³H]E₂ as tracer and hydroxylapatite for adsorption of the receptor-tracer complex.^{15,16}

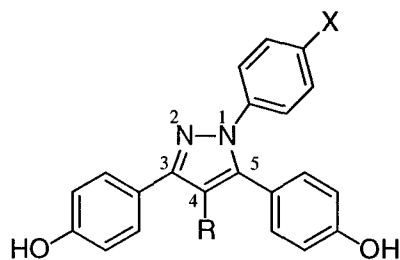


Figure 1. A pyrazole core optimized for high affinity ER binding. (X = H, OH; R = alkyl)

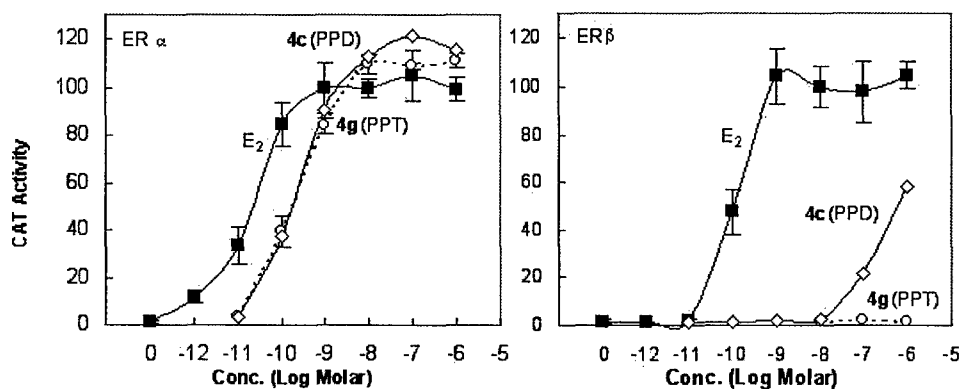


Figure 2. Transcription activation by ER α (left) and ER β (right) in response to pyrazoles **4c** (PPD) and **4g** (PPT). Human endometrial cancer (HEC-1) cells were transfected with expression vectors for ER α or ER β and an (ERE)3-pS2-CAT reporter gene and were treated with indicated concentrations of ligand for 24h. CAT activity was normalized for β -galactosidase activity from an internal control plasmid. Values are expressed as a percent of the ER α or ER β response with 1 nM E₂, which is set at 100%.²⁹

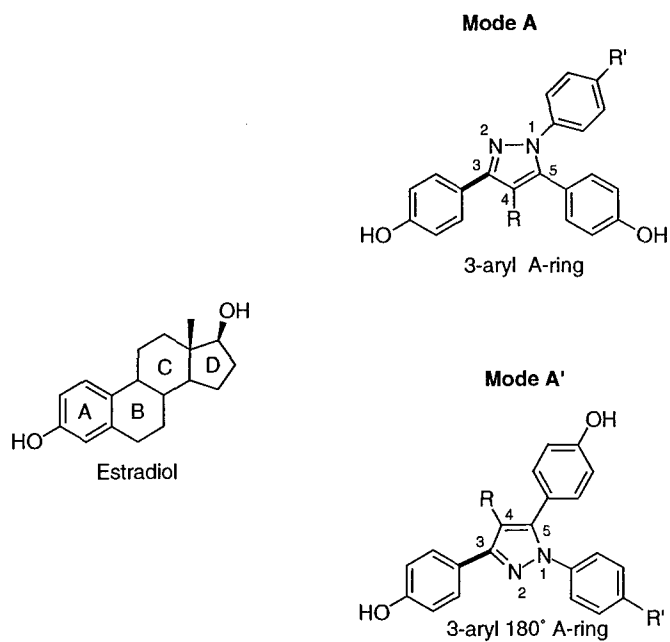
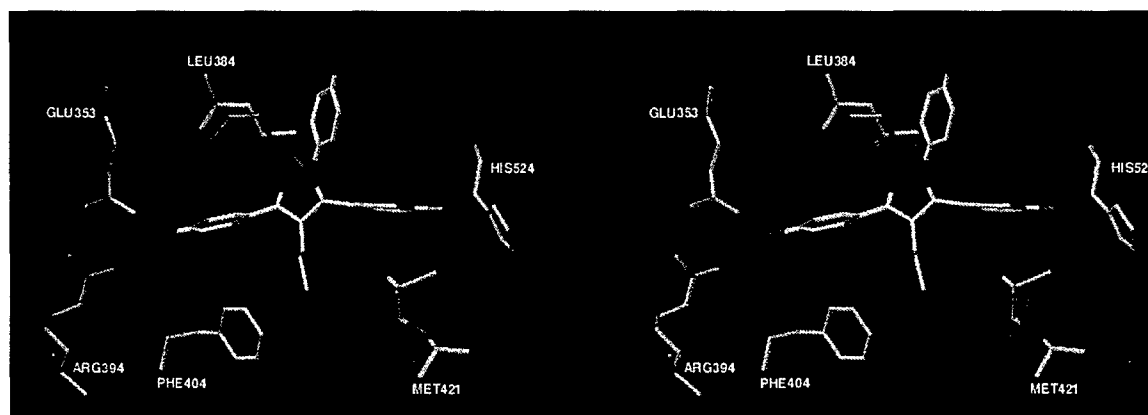
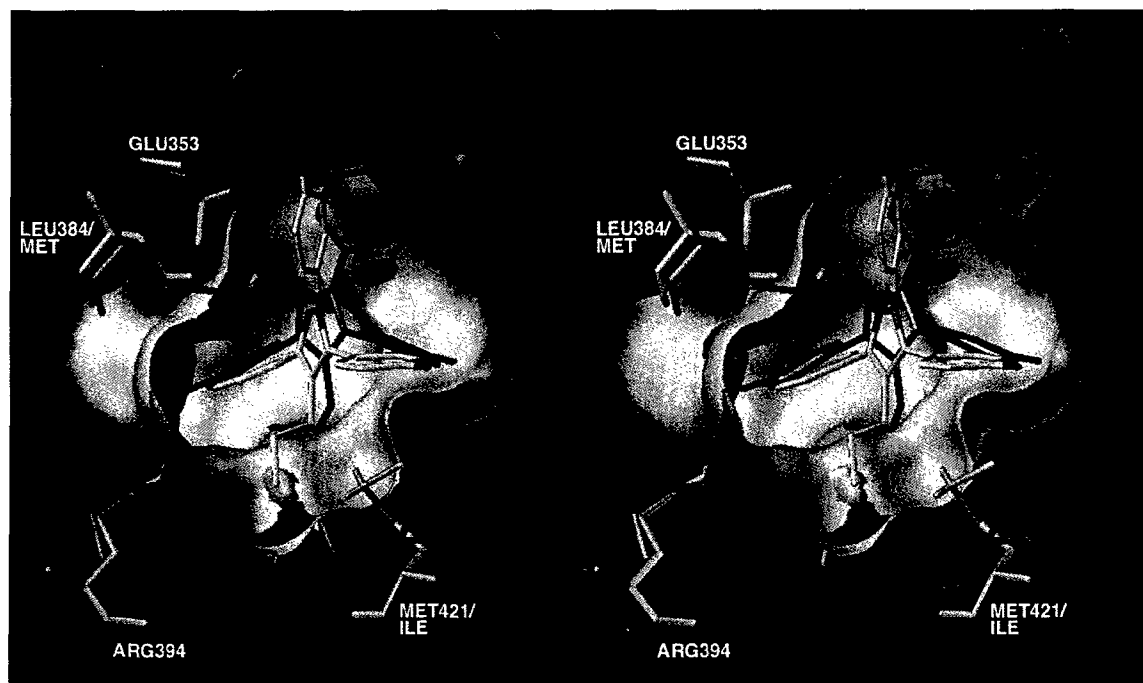


Figure 3. Potential pyrazole binding Modes relative to estradiol. Both Modes A and A' have the C(3) phenol oriented to project in to the estradiol A-ring binding pocket. Modes A and A' are related to one another by rotation of the pyrazole core around the darkened bond.



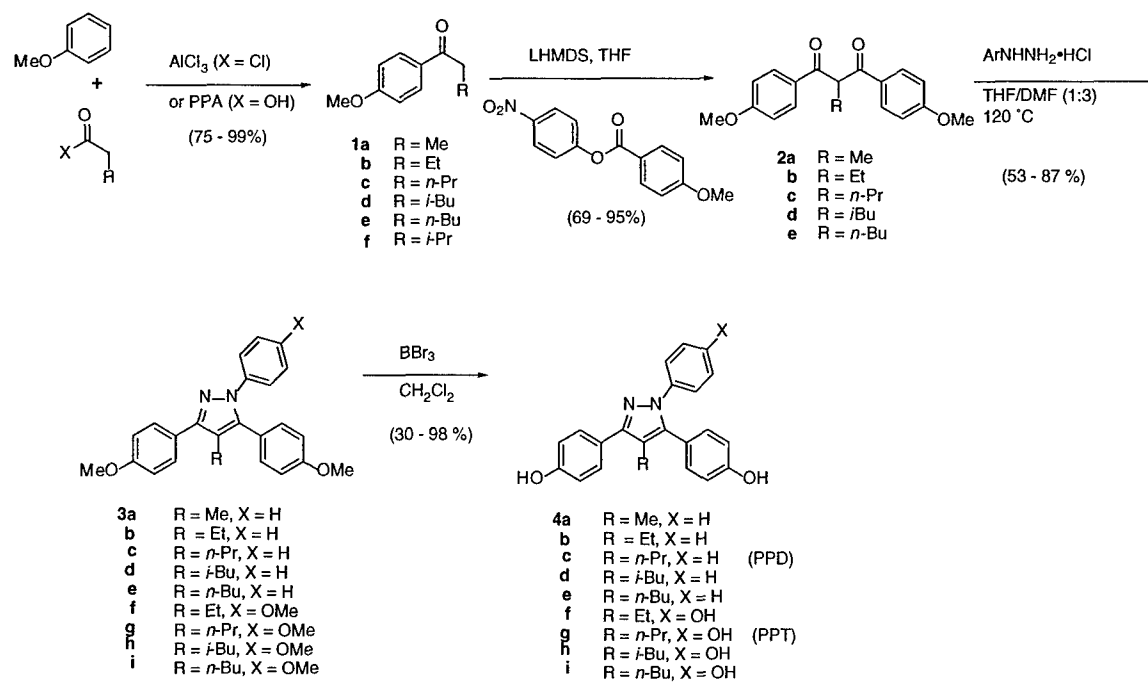
[in color]

Figure 4. Crossed-stereo view of propylpyrazole triol (PPT, **4g**) docked and minimized in ER α -LBD binding pocket according to binding Mode A, showing selected residues close to the ligand. The pyrazole ligand is shown with standard atom colors. The residues in ER α are identified and shown in yellow. At the two positions where the ER β sequence differs from ER α , the ER β residues are shown in red (methionine in ER β in place of ER α L384 and isoleucine in ER β in place of ER α M421).

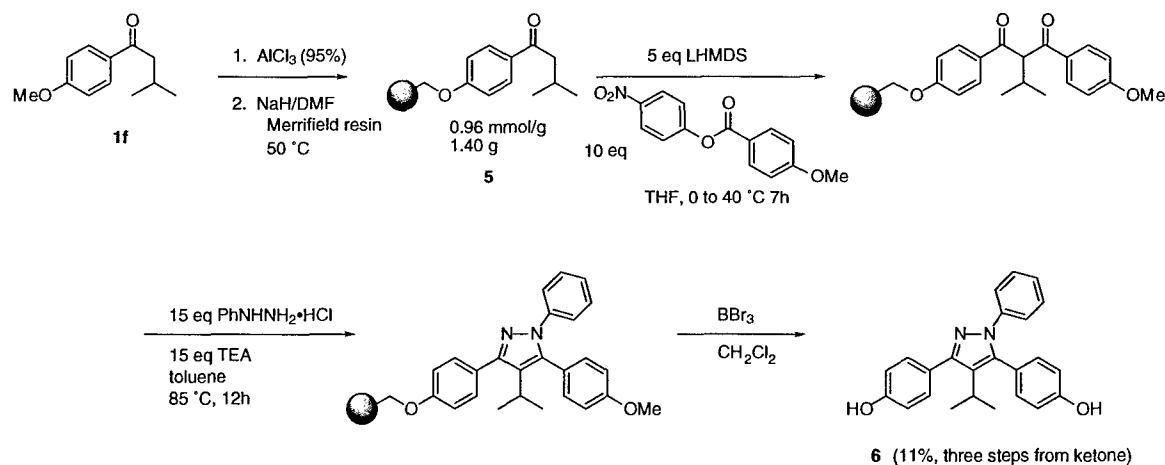


[in color]

Figure 5. Crossed stereo view of ligand skeletal structures and receptor molecular surfaces for the ER α - and ER β -propylpyrazole triol (PPT, **4g**) complexes. The PPT in ER α is shown with standard atom colors, and the ER α receptor surface is shown in yellow; in the ER β -PPT complex, both the ligand and receptor surface are shown in red. For further details, see text.



Scheme 1. Synthesis of C(4) alkyl pyrazole analogs.



Scheme 2. Synthesis of C(4)-*iso*-propyl pyrazole (**6**) by solid phase methodology.¹³

References

- (1) Gao, H.; Katzenellenbogen, J. A.; Garg, R.; Hansch, C. Comparative QSAR Analysis of Estrogen Receptor Ligands. *Chem. Rev.* **1999**, *99*, 723-744.
- (2) Grese, T. A.; Dodge, J. A. Selective Estrogen Receptor Modulators (SERMs) [Review]. *Current Pharmaceutical Design* **1998**, *4*, 71-92.
- (3) Anstead, G. M.; Carlson, K. E.; Katzenellenbogen, J. A. The estradiol pharmacophore: ligand structure-estrogen receptor binding affinity relationships and a model for the receptor binding site. *Steroids* **1997**, *62*, 268-303.
- (4) Brzozowski, A. M.; Pike, A. C.; Dauter, Z.; Hubbard, R. E.; Bonn, T. et al. Molecular basis of agonism and antagonism in the oestrogen receptor. *Nature* **1997**, *389*, 753-758.
- (5) Ekena, K.; Weis, K. E.; Katzenellenbogen, J. A.; Katzenellenbogen, B. S. Different residues of the human estrogen receptor are involved in the recognition of structurally diverse estrogens and antiestrogens. *J. Biol. Chem.* **1997**, *272*, 5069-5075.
- (6) Shiau, A. K.; Barstad, D.; Loria, P. M.; Cheng, L.; Kushner, P. J. et al. The structural basis of estrogen receptor/coactivator recognition and the antagonism of this interaction by tamoxifen. *Cell* **1998**, *95*, 927-937.
- (7) Anstead, G. M.; Peterson, C. S.; Katzenellenbogen, J. A. Hydroxylated 2,3-diarylindenes: Synthesis, estrogen receptor binding affinity, and binding orientation considerations. *J. Steroid Biochem.* **1989**, *33*, 877-887.
- (8) Kuiper, G. G. J. M.; Enmark, E.; Peltö-Huikko, M.; Nilsson, S.; Gustafsson, J. Å. Cloning of a novel receptor expressed in rat prostate and ovary. *Proc. Natl. Acad. Sci. U.S.A.* **1996**, *93*, 5925-5930.
- (9) Mosselman, S.; Polman, J.; Dijkema, R. ER β : identification and characterization of a novel human estrogen receptor. *FEBS* **1996**, *392*, 49-53.
- (10) Kuiper, G. G. J. M.; Carlsson, B.; Grandien, K.; Enmark, E.; Häggblad, J. et al. Comparison of the ligand binding specificity and transcript tissue distribution of estrogen receptor α and β . *Endocrinology* **1997**, *138*, 863-870.

- (11) Fink, B. E.; Mortensen, D. S.; Stauffer, S. R.; Aron, Z. D.; Katzenellenbogen, J. A. Novel Structural Templates for Estrogen-Receptor Ligands and Prospects for Combinatorial Synthesis of Estrogens. *Chem. Biol.* **1999**, *6*, 205-219.
- (12) Katzenellenbogen, J. A.; Katzenellenbogen, B. S.; Fink, B. S.; Stauffer, S. R.; Mortensen, D. S. et al. Estrogen Receptor Ligands, 2000.
- (13) Stauffer, S. R.; Katzenellenbogen, J. A. Solid-Phase Synthesis of Tetrasubstituted Pyrazoles, Novel Ligands for the Estrogen Receptor. *J. Combinat. Chem.* **2000**, *In Press*.
- (14) Sun, J.; Meyers, M. J.; Fink, B. E.; Rajendran, R.; Katzenellenbogen, J. A. et al. Novel Ligands that Function as Selective Estrogens or Antiestrogens for Estrogen Receptor- α or Estrogen Receptor- β . *Endocrinology* **1999**, *140*, 800-804.
- (15) Carlson, K. E.; Choi, I.; Gee, A.; Katzenellenbogen, B. S.; Katzenellenbogen, J. A. Altered ligand binding properties and enhanced stability of a constitutively active estrogen receptor: Evidence that an open pocket conformation is required for ligand interaction. *Biochemistry* **1997**, *36*, 14897-14905.
- (16) Meyers, M. J.; Sun, J.; Carlson, K. E.; Katzenellenbogen, B. S.; Katzenellenbogen, J. A. Estrogen receptor subtype-selective ligands: Asymmetric synthesis and biological evaluation of cis- and trans-5,11-dialkyl- 5,6,11,12- tetrahydrochrysenes. *J. Med. Chem.* **1999**, *42*, 2456-2468.
- (17) Grese, T. A.; Cho, S.; Finley, D. R.; Godfrey, A. G.; Jones, C. D. et al. Structure-activity relationships of selective estrogen receptor modulators: Modifications at the 2-arylbenzothiophene core of raloxifene. *J. Med. Chem.* **1997**, *40*, 146-167.
- (18) Pons, M.; Michel, F.; Crastes de Paulet, A.; Gilbert, J.; Miquel, J.-F. et al. Influence of new hydroxylated triphenylethylene (TPE) derivatives on estradiol binding to uterine cytosol. *J. Steroid Biochem.* **1984**, *20*, 137-145.
- (19) Katzenellenbogen, J. A.; O'Malley, B. W.; Katzenellenbogen, B. S. Tripartite steroid hormone receptor pharmacology: Interaction with multiple effector sites as a basis for the cell- and promoter-specific action of these hormones. *Mol. Endocrinol.* **1996**, *10*, 119-131.

- (20) Sun, J.; Kraichley, D. M.; Meyers, M. J.; Katzenellenbogen, J. A.; Katzenellenbogen, B. S. Novel Selective Estrogen Receptor-Beta Antagonists Block Transcriptional Activation and Abolish Coactivator Recruitment. *Keystone Symposium, Nuclear Receptors 2000* **2000**, In Press.
- (21) Stauffer, S. R.; Huang, Y.; Coletta, C. J.; Katzenellenbogen, J. A. Estrogen Pyrazoles: Defining the Pyrazole Core Structure and Orientation of Substituents in the Ligand Binding Pocket of the Estrogen Receptor. *Bio. Med. Chem.* **2000**, Submitted.
- (22) Pike, A. C.; Brzozowski, A. M.; Hubbard, R. E.; Bonn, T.; Thorsell, A. G. et al. Structure of the ligand-binding domain of oestrogen receptor beta in the presence of a partial agonist and a full antagonist. *EMBO J.* **1999**, *18*, 4608-4618.
- (23) Still, W. C.; Kahn, M.; Mitra, A. Rapid chromatographic technique for preparative separations with moderate resolution. *J. Org. Chem.* **1978**, *43*, 2923-2926.
- (24) Hachiya, I.; Moriwaki, M.; Kobayashi, S. Hafnium (IV) Trifluoromethanesulfonate, An Efficient Catalyst for the Friedel-Crafts Acylation and Alkylation Reactions. *Bull. Chem. Soc. Jpn.* **1995**, *68*, 2053-2060.
- (25) Wang, D.; Chen, D.; Haberman, J.; Li, C. J. Ruthenium-Catalyzed Isomerization of Homoallylic Alcohols in Water. *Tetrahedron* **1998**, *54*, 5129-5142.
- (26) Horiuchi, Y.; Oshima, K.; Utimoto, K. Titanium Tetrachloride-Induced Three-Component Coupling Reaction of α -Haloacylsilane, Allylsilane, and Carbonyl Compound. *J. Org. Chem.* **1996**, *61*, 4483-4486.
- (27) Narasaka, K.; Kusama, H. Friedel-Crafts Acylation of Arenes Catalyzed by Bromopentacarbonylrhenium (I). *Bull. Chem. Soc. Jpn.* **1995**, *68*, 2379-2383.
- (28) Williams, D.; Gorski, J. Equilibrium binding of estradiol by uterine cell suspensions and whole uteri *in vitro*. *Biochemistry* **1974**, *13*, 5537-5542.
- (29) McInerney, E. M.; Tsai, M. J.; O'Malley, B. W.; Katzenellenbogen, B. S. Analysis of estrogen receptor transcriptional enhancement by a nuclear hormone receptor coactivator. *Proc. Natl. Acad. Sci. U. S. A.* **1996**, *93*, 10069-10073.

- (30) Katzenellenbogen, J. A.; Johnson, H. J., Jr.; Myers, H. N. Photoaffinity labels for estrogen binding proteins of rat uterus. *Biochemistry* **1973**, *12*, 4085-4092.

**Estrogen pyrazoles: Defining the pyrazole core structure and the orientation of
substituents in the ligand binding pocket of the estrogen receptor**

Shaun R. Stauffer, Ying Huang, Christopher J. Coletta, Rosanna Tedesco, and John A.
Katzenellenbogen*

Department of Chemistry, University of Illinois, Urbana IL 61801

Submitted to: *Bioorganic and Medicinal Chemistry*

Address Correspondence to:
John A. Katzenellenbogen
Department of Chemistry
University of Illinois
600 South Mathews Avenue
Urbana IL 61801
217 333 6310 (phone)
217 333 7325 (fax)
jkatzene@uiuc.edu

Abstract

Previously, we reported that certain tetrasubstituted (1,3,5-triaryl-4-alkyl) pyrazoles bind to the estrogen receptor (ER) with high affinity [Fink, et al., *Chem. Biol.*, **1999**, 6, 205-219; Stauffer, et al., *J. Combinat. Chem.* **2000**, *In Press*; Stauffer, et al., *J. Med. Chem.* **2000**, *Submitted*]. To investigate how cyclic permutation of the two nitrogen atoms of a pyrazole might affect ER binding affinity, we prepared a new pyrazole core isomer, namely a 1,3,4-triaryl-5-alkyl-pyrazole (**2**), to compare it with our original pyrazole (**1**). We also prepared several peripherally matched core pyrazole isomer sets to investigate whether the two pyrazole series share a common binding orientation. Our efficient, regioselective synthetic route to these pyrazoles relies on the acylation of a hydrazone anion, followed by cyclization, halogenation, and Suzuki coupling. We found that the ER accommodates 1,3,4-triarylpyrazoles of the isomeric series only somewhat less well than the original 1,3,5-triaryl series, and it appears that both series share a common binding mode. This preferred orientation for the 1,3,5-triaryl-4-alkyl-pyrazoles is supported by binding affinity measurements of analogs in which the phenolic hydroxyl groups were systematically removed from each of the three aryl groups, and the orientation is consistent, as well, with molecular modeling studies. These studies provide additional insight into the design of heterocyclic core structures for the development of high affinity ER ligands by combinatorial methods.

Introduction

The estrogen receptor (ER) binds a remarkably wide range of non-steroidal ligands,¹ and the diverse core structures of these ligands span a wide range of synthetic accessibility.² We have been intrigued, in particular, by the design of non-steroidal ligand cores that might be easily prepared and thus would be well suited to combinatorial expansion. As part of this investigation, we identified pyrazoles as favorable heterocyclic core building blocks,³ and we found that by attaching a sufficient number of appropriate substituents onto this core system, we could obtain high affinity ligands for the ER.³⁻⁵

An issue which had interested us initially about these systems was whether the heterocyclic core structure itself plays an active role in ligand-receptor interaction, or whether it acts merely as an inert scaffold, simply displaying groups in a geometry appropriate for filling the various subpockets that make up the ligand cavity of ER.³ Interestingly, we found that there were large differences in binding affinity (up to 50 fold) for ligands that had identical peripheral substitution patterns but different core structures (e.g., the two diazoles, imidazoles vs. pyrazoles; Figure 1).³ Clearly, our initial thought that the ligand core structure might be acting as a passive entity—simply to position peripheral substituents—was not true. In the case shown below, the lower ER binding affinity for the imidazoles compared to the pyrazoles was attributed, at least in part, to the significantly greater dipole moment of the imidazoles.³

[Figure 1]

In further consideration, we wondered whether the distribution of heteroatoms within the *same* heterocyclic system would also have a significant effect on ER binding affinity. In the two *imidazoles* shown in Figure 1, the different position of the nitrogen atoms had little effect on their binding affinity. However, we were curious whether the related cyclic permutation of the two nitrogen atoms of a *pyrazole* might have a more significant effect on ER binding affinity.

To investigate this issue, we have prepared a new pyrazole core isomer, namely a 1,3,4-triaryl-5-alkyl-pyrazole (**2**), to compare it with our original 1,3,5-triaryl-4-alkyl-pyrazole (**1**) (Figure 2). This new compound (**2**) represents the only other possible pyrazole system capable of

displaying the same relative substitution pattern of aryl, alkyl, aryl, and phenyl groups as does our original pyrazole **1**. To extend this investigation further, we synthesized several other peripherally matched core pyrazole isomer sets, in which some of the phenolic hydroxyl groups are systematically deleted, to establish more definitively which core isomer is most favored and to investigate whether they share a common binding orientation.

[Figure 2]

Results and Discussion

Synthesis of 1,3,4-triaryl-5-alkyl-pyrazoles

Our initial attempts to synthesize the pyrazole isomer **2** involved conditions similar to those used in previous studies (Scheme 1).³ We first prepared diketone **3** in high yield, starting from the deoxybenzoin and propionic anhydride. However, our attempts to generate the pyrazole by condensation of the dione with 4-methoxyphenylhydrazine were unsuccessful and resulted in a complex mixture that contained the two possible retro-Claisen condensation products from cleavage of the 1,3-dione.

[Scheme 1]

Because of these difficulties and the fact that this route was not likely to be regioselective, we investigated an alternative, potentially regioselective approach that involved a one-pot acylation and cyclization procedure starting from an appropriate hydrazone, as illustrated in Figure 3. Unfortunately, we could not isolate the hydrazone (**4**), because it rapidly underwent Fischer indole cyclization to the 2,3-diaryl-indole product (**5**). Even under mild conditions, we obtained only starting material or indole product, but no hydrazone. Apparently, the 4-methoxyphenyl substituent in the deoxybenzoin starting material facilitates the [3,3]-sigmatropic cyclization of the ene-phenylhydrazone intermediate by stabilizing the transition state through a stilbene-like structure (Figure 3).

[Figure 3]

We wondered whether we could avoid this competing cyclization by omitting the 4-methoxyphenyl substituent during the synthesis of the pyrazole (Figure 4). Of course, this approach would entail adding an aryl group later to the completed heterocycle, but this could presumably be done using an appropriate Pd(0)-mediated coupling reaction. This synthetic strategy was also attractive because it allows for the introduction of additional structural diversity into these systems at a late stage, just before phenol deprotection, an attractive feature for combinatorial library expansion.⁵

[Figure 4]

According to this approach, we were able to successfully synthesize pyrazole **2** as well as analogs **10a-d** (Scheme 2). Initial formation of hydrazones **6a-c** by reaction of the acetophenone compounds with either the hydrochloride salt of 4-methoxyphenylhydrazine or phenylhydrazine occurred in moderate yields, and as we had hoped, no competing cyclization to the indole occurred with this less stabilized system. Hydrazones **6a-c** were then treated with butyl lithium to form the corresponding dianion, which was acylated with an alkyl anhydride and then cyclized upon addition of HCl.⁶ The yields shown for pyrazole formation are based on the anhydride and are typical for this reaction.

[Scheme 2]

To introduce the last aromatic substituent, the tri-substituted pyrazoles **7a-d** were iodinated by treatment with a solution of KI and I₂,⁷ and then subjected to Suzuki coupling conditions with either phenylboronic acid or *p*-methoxyphenylboronic acid. Initial conditions involved using Pd(PPh₃)₄ as a Pd(0) catalyst and DME/H₂O as solvent (**9c** 52%, 72h); however, by using Pd(OAc)₂ as a pre-catalyst and a *n*-PrOH/H₂O solvent mixture, we were able to obtain the tetra-substituted pyrazoles (**9a,b,d,e**) with slightly improved yields (60-71%) and shorter reaction times (1-14h).⁸ The protected pyrazole isomers were subsequently demethylated using BBr₃ to afford the desired phenolic products **10a-d** and **2**.

Comparison of the estrogen receptor binding affinities of the isomeric 1,3,4-triaryl-pyrazoles (Series II) and the original 1,3,5-triaryl pyrazoles (Series I)

The binding affinities of the pyrazoles for ER were assayed in a competitive radiometric binding assay; this assay has been described previously,⁹ and affinities are expressed as relative binding affinity (RBA) values, where estradiol has an affinity of 100% (Table 1). The 1,3,4-triaryl-pyrazole **2**, which is the nitrogen ring isomer of our original 1,3,5-triaryl-pyrazole **1**, has a very significant affinity of 5.8%, but is 2.6-fold less than the original pyrazole **1**. To determine whether the 1,3,4-triaryl pyrazole binds to ER in the same mode as pyrazole **1**, we investigated the binding

affinity of several other 1,3,4-triaryl-pyrazoles (**10a-d**) and compared their affinities with that of their corresponding 1,3,5-triaryl-pyrazole isomers (**11a-b**⁴ and **11c-d**¹⁰).

[Table 1]

When examining the first three sets of isomeric pyrazoles (the other two are discussed below), the pyrazoles in the new isomeric Series II (1,3,4-triarylpyrazoles) have somewhat lower affinity than those in the original Series I (1,3,5-triarylpyrazoles), but only by an average of 2 fold. Within the original pyrazole series (Series I), certain changes to the peripheral substituents resulted in an increase in RBA. For example, when a hydroxyl group is added to the N(1)-phenyl substituent (i.e., from pyrazole **1** to **11a**), a slight increase in affinity occurs. A similar increase in RBA upon hydroxyl substitution is observed in the isomeric Series II, going from pyrazole **2** to **10a**.

Previously, we also showed that modification of the alkyl chain at C(4)-position of the initial pyrazole Series I from an ethyl **1** to a propyl substituent **11b** results in a 1.6-fold increase in affinity, indicating a more favorable hydrophobic interaction. However, this favorable interaction ended at propyl, as the *n*-butyl isomer experienced a significant drop in binding affinity.⁴ In Series II, going from R₃ = Et (**2**) to *n*-propyl (**10b**) results in a similar but somewhat larger increase in affinity than it does in Series I (2.7-fold vs. 1.6 fold).

Because the structure-binding affinity pattern observed for both pyrazole isomers (Series I and II) are quite similar, we postulated that these distinct core structure pyrazole isomers would be binding in the same orientation in the ER binding pocket.

Elucidation of the aryl group in the pyrazole that mimics the A-ring of estradiol: Inferring pyrazole orientation in the ligand binding pocket from the binding affinity of isomeric monophenols

To further support the hypothesis that both pyrazole isomers have the same binding mode and to more confidently establish which phenolic group is playing the role of the A-ring phenol in estradiol, we prepared the individual *mono*-phenolic derivatives of pyrazole **1** (Table 1, Series I, **11c**

and **11d**) and pyrazole **2** (Table 1, Series II, **10c** and **10d**). Systematic phenol deletion is a standard approach that has been used in the past to determine which phenol in an unsymmetrical bisphenolic non-steroidal ER ligand mimics the crucial A-ring phenol of estradiol (E_2).^{11,12} The mono-phenolic analog having the highest affinity is then presumed to have preserved the phenol that is acting as the estradiol A-ring mimic, because the hydroxyl substituent at this position is known to be essential for high affinity binding to the ER.¹³ (At the outset, it is of note that removal of one of the phenols from the R1 position (pyrazole **1** vs **11a** in Series I, and pyrazole **2** vs **10a** in Series II) has little effect on binding affinity, suggesting that these rings are not the ones that corresponds to the A-ring of estradiol.)

The route in Scheme 2 was used to prepare both the N(1) and the C(4) monophenolic pyrazole Series II analogs **10c** and **10d**, regioselectively and in good yield. The RBA of pyrazole isomer **10c** is 0.43%, whereas that of pyrazole isomer **10d** is only 0.008%. When these affinities are compared to that of the bisphenolic pyrazole **2** (5.8%) (Table 1), one can see that removal of the phenolic hydroxyl from the N(1) phenyl ring results in a 725-fold decrease in affinity, whereas removal of the hydroxyl from the C(4) phenyl group results in only a 13-fold decrease. Thus, the 56-fold greater decrease in affinity that results from deleting the phenolic hydroxyl from the N(1) phenyl group vs. from the C(4) phenyl group strongly suggests that the N(1)-phenolic substituent in the Series II pyrazoles is acting as the A-ring mimic (Figure 5).

[Figure 5]

Initial attempts to prepare the C(3) and C(5) monophenol pyrazole analogs for Series I (**11c** and **11d**) regioselectively using the acylation-cyclization strategy were unsuccessful. However, these compounds could successfully be prepared via the corresponding pyrazolines by a new regioselective route (not shown) that will be described elsewhere.¹⁰ The binding affinities for the Series I monophenolic isomers **11d** and **11c** are 0.007% and 0.46%, respectively. Compared to the corresponding bisphenolic pyrazole **1** (15.3%) (Table 1), a much greater decrease in binding affinity results when the hydroxyl group is removed from C(3) phenol (2185-fold, **11d**) than from the C(5) phenol (33-fold, **11c**). The difference in affinity loss that result from the alternative

hydroxy group deletion in this series (i.e., 2185/33 or 66 fold) is comparable to that found in Series II (56 fold). This result indicates that in Series I the C(3) phenol is mimicking the A-ring of E₂. Thus, because the C(3) phenol in Series I and the N(1) phenol in Series II are positioned in a congruent fashion, we believe that the pyrazoles of both Series I and II share a single common binding mode, as illustrated in Figure 5. According to this mode, the other two aryl groups are displayed within a region of the binding pocket resembling the C/D region of E₂ which is known to tolerate a large number of substituents.¹³

Modeling pyrazole orientation in the ligand binding pocket

In our original study of pyrazole **1**, we used molecular modeling to show that this compound could bind in an orientation in which the C(5) phenol mimicked the A-ring of estradiol;³ this is different from that shown in Figure 5. However, in this earlier study, we had based our model on the ER α crystal structure with the *antagonist* ligand raloxifene.¹⁴ Upon further consideration, we now think that the ER α crystal structure we used previously was not an appropriate one for modeling ligands like pyrazole **1**, because unlike raloxifene, these pyrazoles are ER α *agonists*, not antagonists.^{4,15}

We have recently completed a more extensive modeling of a pyrazole *triphenol* that corresponds to pyrazole *diphenol* **11b**,⁴ using as a starting point an X-ray structure of ER α complexed with the *agonist* diethylstilbestrol, a non-steroidal estrogen agonist with an RBA of 98%.¹⁶ In this study, we considered six possible starting orientations (the three phenols placed in the A-ring pocket and in each case the two alternative orientations of the remaining two phenols that come from rotation about the bond linking the A-ring phenol and the pyrazole core.) From this recent study,⁴ the orientation in which the C(3) phenol of the Series I pyrazole mimics the A-ring of estradiol gave the lowest energy structure and appeared to be quite reasonable on steric grounds, although it is difficult to rigorously eliminate some of the other possible orientations. This is the orientation shown in Figure 5 for the Series I pyrazole.

In the present study, we have used this approach to examine the six possible binding orientations of the ethyl triphenol Series II pyrazole **10a**. Again, the orientation in which the N(1) phenol is the mimic of the A-ring of estradiol (cf. Figure 5) is well accommodated by the structure and has a reasonable binding energy, although an alternative orientation with the C(4) phenol in this position cannot be ruled out by binding energy considerations. Nevertheless, this latter orientation seems unlikely, given the much higher experimental binding affinity of monophenol **10c** vs **10d** (Table 1).

Thus, on the basis of the experimental determinations of monophenol binding affinities and molecular modeling, we suggest that the preferred binding modes of the pyrazoles in the estrogen receptor corresponds to those illustrated in Figure 5. A pictorial representation of pyrazole **10a** in this orientation is shown in Figure 6.

[Figure 6]

Conclusions

To explore the effect of core structure on the ability of pyrazole ligands to bind to ER, we developed an efficient, regioselective, and flexible route to a new isomeric series of pyrazoles (1,3,4-triaryl-5-alkyl-pyrazoles), and we evaluated their binding affinity to ER. The synthesis relies on the acylation of a hydrazone anion, followed, after cyclization and halogenation, by a Pd(0) Suzuki coupling strategy. We found that the ER accommodates 1,3,4-triarylpyrazoles of the new isomeric series (Series II) only slightly less well than the original 1,3,5-triaryl series (Series I), and on the basis of the binding affinity of the corresponding monophenols and molecular modeling studies, both isomers appear to share a common binding mode. In this binding mode, the putative A-ring mimic is the C(3) phenol in Series I and the N(1) phenol in Series II. Thus, as in the case of the imidazoles discussed earlier (Fig. 1), it does appear possible to permute the position of heteroatoms in the azole ring without having a major effect on the ER binding affinity, provided that the peripheral substituents remain disposed with the same geometry and provided that one remains in the same azole series (i.e., 1,2-azoles [pyrazoles] not 1,3-azoles [imidazoles]), so that compounds

with equivalent dipole moments and polarities are being compared. These studies provide additional insight into the design of heterocyclic core structure for the development of high affinity ER ligands by combinatorial methods.

Experimental Methods

General

Melting points were determined on a Thomas-Hoover UniMelt capillary apparatus and are uncorrected. All reagents and solvents were obtained from Aldrich, Fisher or Mallinckrodt. Tetrahydrofuran was freshly distilled from sodium/benzophenone. Dimethylformamide was vacuum distilled prior to use, and stored over 4 Å molecular sieves. *n*-Butyllithium and *t*-butyllithium were titrated with *N*-pivaloyl-*o*-toluidine. Et₃N was stirred with phenylisocyanate, filtered, distilled, and stored over 4 Å molecular sieves. All reactions were performed under a dry N₂ atmosphere unless otherwise specified. Reaction progress was monitored by analytical thin-layer chromatography using GF silica plates purchased from Analtech. Visualization was achieved by short wave UV light (254 nm) or potassium permanganate. Flash column chromatography was performed using Woelm 32-63 µm silica gel packing.¹⁷

¹H and ¹³C NMR spectra were recorded on either a Varian Unity 400 MHz or 500 MHz spectrometer using CDCl₃, MeOD or (CD₃)₂SO as solvent. Chemical shifts were reported as parts per million downfield from an internal tetramethylsilane standard (δ = 0.0 for ¹H) or from solvent references. NMR coupling constants are reported in Hertz. ¹³C NMR were determined using either the Attached Proton Test (APT) or standard ¹³C pulse sequence parameters. Low resolution and high resolution electron impact mass spectra were obtained on Finnigan MAT CH-5 or 70-VSE spectrometers. Elemental analyses were performed by the Microanalytical Service Laboratory of the University of Illinois. Hydrazones **6a-c** are prone to decomposition and therefore could only be stored for 2-3 days at 0 °C. Once the hydrazone products were confirmed by ¹H NMR they were typically used directly in the acylation-cyclization step without further characterization.

Biological Procedures: Relative Binding Affinity Assay

Ligand binding affinities (RBAs) using lamb uterine cytosol as a receptor source were determined by a competitive radiometric binding assay using 10 nM [³H]estradiol as tracer and dextran-coated charcoal as an adsorbent for free ligand.⁹ All incubations were done at 0 °C for 18-24h. Binding affinities are expressed relative to estradiol (RBA = 100%) and are reproducible with a coefficient of variation of 0.3.

Molecular Modeling of Pyrazole 10a

The protocol for modeling followed that recently described for a related pyrazole triphenol.⁴ The starting conformation for pyrazole **10a** used for receptor docking studies was generated from a random conformational search performed using the MMFF94 force field as implemented in Sybyl 6.6. The resulting lowest energy conformer was then used for docking studies. Charge calculations were determined using the MMFF94 method and molecular surface properties displayed using MOLCAD module in Sybyl 6.6.

Pyrazole **10a**, generated as noted above, was pre-positioned in the DES-ER α -LBD crystal structure¹⁶ using a least squares multifitting of select atoms within the DES ligand. Once pre-positioned, DES was deleted and ligand **10a** was optimally docked in the ER α binding pocket in six orientations (as specified in the text) using the Flexidock routine within Sybyl (Tripos). Both hydrogen-bond donors and acceptors within the pocket surrounding the ligand (Glu₃₅₃, Arg₃₉₄, and His₅₂₄), the ligand itself and select torsional bonds were defined. The docked receptor ligand complexes from Flexidock then underwent a three step minimization. First, non-ring torsional bonds of the ligand were minimized in the context of the receptor using the torsmin command. This was followed by minimization of the side chain residues within 8 Å of the ligand, while holding the backbone and residues Glu₃₅₃ and Arg₃₉₄ fixed. A final third minimization of both the ligand and receptor was conducted using the Anneal function (hot radius 8 Å, interesting radius 16Å from pyrazole **10a**) to afford the final model.

Chemical Syntheses

5-Ethyl-1,4-bis-(4-methoxy-phenyl)-3-phenyl-1H-pyrazole (2). A stirred solution of **9e** (46 mg, 0.16 mmol) in CH_2Cl_2 (15 mL) was treated with BBr_3 (1.62 mL, 1.62 mmol) according to the general demethylation procedure. After workup and a SiO_2 plug (30% EtOAc/hexanes) a white solid was isolated (40 mg, 94%): mp: 220–225 °C; ^1H NMR ($\text{MeOD-}d_4$, 400 MHz) δ 0.90 (t, 3H, $J = 7.5$), 2.62 (q, 2H, $J = 7.5$), 6.79 (XX' of AA'XX', 2H, $J_{\text{AX}} = 8.3$, $J_{\text{XX'}} = 2.3$), 6.94 (XX' of AA'XX', 2H, $J_{\text{AX}} = 8.6$, $J_{\text{XX'}} = 2.7$), 7.04 (AA' of AA'XX', 2H, $J_{\text{AX}} = 8.2$, $J_{\text{AA'}} = 2.4$), 7.20 – 7.27 (m, 2H), 7.34 (AA' of AA'XX', 2H, $J_{\text{AX}} = 8.8$, $J_{\text{AA'}} = 2.6$), 7.37 – 7.44 (m, 3H); ^{13}C NMR ($\text{MeOD-}d_4$, 100 MHz) δ 12.4, 17.2, 114.8, 115.2, 118.5, 124.3, 126.9, 127.4, 127.5, 127.6, 131.0, 131.0, 132.9, 144.1, 148.9, 156.2, 157.8; MS (EI, 70 eV) m/z (relative intensity, %): 356 (M+, 100); Anal calcd for $\text{C}_{23}\text{H}_{20}\text{N}_2\text{O}_2 \cdot \text{H}_2\text{O}$: C, 73.78; H, 5.92; N, 7.48. Found: C, 73.82; H, 5.95; N, 7.69.

4'-methoxyacetophenone-4-methoxyphenylhydrazone (6a). An EtOH (40 mL) solution of 4-methoxyacetophenone (1 g, 6.67 mmol), sodium acetate (1.09 g, 13.34 mmol), and 4-methoxyphenylhydrazine hydrochloride (1.74 g, 10.0 mmol) was heated to 80 °C for 3.0 h. The reaction mixture was cooled to room temperature and concentrated under reduced pressure. The residue was dissolved in ethyl acetate (30 mL) and washed with water (40 mL) and brine (2 X 40 mL). After drying over MgSO_4 , and solvent concentration a red and white heterogeneous solid formed. The product was collected by filtration and rinsed with cold ethanol (20 mL) to afford **6a** as a white solid (1.18 g, 66%) which was used directly in the next step.

Acetophenone-4-methoxyphenylhydrazone (6b). A solution of acetophenone (250 mg, 2.00 mmol), 4-methoxyphenylhydrazine hydrochloride (349 mg, 2.00 mmol) was reacted similarly to conditions used for **6a** to afford a red and white heterogeneous solid. Cold ethanol (20 mL) was added and the remaining solid collected via vacuum filtration to afford **6b** as a white solid (1.41 g, 59%) which was used directly in the next step.

Acetophenonephenylhydrazone (6c). A solution of acetophenone (1.8 g, 15 mmol), phenylhydrazine hydrochloride (2.17 g, 15 mmol), and sodium acetate (1.23 g, 15.0 mmol), in

anhydrous ethanol (40 ml) was reacted similarly to conditions used for **6a** to afford a yellow and white heterogeneous solid. Cold ethanol (20 mL) was added to the solid, and the product collected via vacuum filtration to afford **6c** as a white solid (1.67 g, 53%) which was used directly in the next step.

General acylation-cyclization procedure (7a-d). To a stirred solution of hydrazone (3.05 mmol) in THF (10 mL) at 0 °C was added 1.29 M BuLi (4.73 mL, 6.10 mmol) dropwise. The resulting deep red solution was allowed to stir at 0 °C for 0.25 h, then room temperature for 0.25 h, and re-cooled to 0 °C whereupon a THF solution (2.0 mL) of the appropriate alkyl anhydride (1.53 mmol) was added dropwise. This mixture was stirred at 0 °C for 0.25 h, then treated with 3 M HCl (6 mL, 18 mmol) and refluxed for 1.5 h. The biphasic mixture was cooled to room temperature and the aqueous layer separated and neutralized with saturated NaHCO₃. The neutralized solution was extracted with ethyl acetate (3 X 20 mL) and the organic layers combined with the THF layer from the reaction mixture. The final organic layers were washed with sat. NaHCO₃ (3 X 20 mL), dried over MgSO₄, and concentrated to afford a red oil. The crude oil was purified by flash chromatography.

5-Ethyl-1,3-bis-(4-methoxy-phenyl)-1H-pyrazole (7a). Following the general procedure above hydrazone **6a** (824 mg, 3.05 mmol) was acylated with propionic anhydride (198 mg, 0.20 mL, 1.53 mmol) and cyclized with HCl. Flash chromatography (25% EtOAc/hexanes) afforded an inseparable mixture of 4-methoxyacetophenone and **7a** (474 mg). The phenone was reduced by the dropwise addition of a solution of NaBH₄ (27.3 mg, 0.72) in H₂O (5 mL) to a solution of the product mixture in ethanol (5 mL). The solution was stirred for 18 h at room temperature and poured over 1 M HCl (20 mL). Upon product isolation (EtOAc, sat NaHCO₃, brine) and solvent removal under reduced pressure an orange oil was isolated, which upon addition of 25% EtOAc/hexanes resulted in selective crystallization of pyrazole **7a** as fine white crystals (200 mg, 44%): ¹H NMR (CDCl₃, 400 MHz) δ 1.24 (t, 3H, *J* = 7.6), 2.64 (q, 2H, *J* = 7.5), 3.83 (s, 3H) 6.45 (s, 1H), 3.85 (s, 3H), 6.98 (XX' of AA'XX', 2H, *J*_{AX} = 8.9, *J*_{XX'} = 2.4), 7.09 (XX' of AA'XX', 2H, *J*_{AX} = 9.0, *J*_{XX'} = 2.7), 7.39 (AA' of AA'XX', 2H, *J*_{AX} = 8.9, *J*_{AA'} = 2.7), 7.79 (AA'

of AA'XX', 2H, $J_{AX} = 8.9$, $J_{AA'} = 2.8$); ^{13}C NMR (CDCl_3 , 100 MHz) δ 13.0, 19.6, 55.1, 55.4, 101.2, 113.7, 114.1, 126.2, 126.8, 126.8, 133.0, 146.5, 150.8, 158.9, 159.1.

1-(4-Methoxy-phenyl)-3-phenyl-5-propyl-1H-pyrazole (7b). Following the general procedure above hydrazone **6a** (1.37 g, 5.71 mmol) was acylated with butyric anhydride (452 mg, 0.47 mL, 2.86 mmol) and cyclized with HCl. Flash chromatography (30% EtOAc/hexanes) afforded the title compound as a yellow oil (710 mg, 42 %): ^1H NMR (CDCl_3 , 400 MHz) δ 0.96 (t, 3H, $J = 7.5$) 1.66 (sext, 2H, $J = 7.5$), 2.61 (t, 2H, $J = 7.7$), 3.85 (s, 3H), 6.54 (s, 1H), 6.99 (XX' of AA'XX', 2H, $J_{AX} = 8.7$, $J_{XX'} = 2.7$), 7.31 (app tt, 1H, $J = 7.3$, 1.5), 7.38 – 7.43 (m, 4H), 7.89 (AA' of AA'XX', 2H, $J_{AX} = 7.2$, $J_{AA'} = 1.3$); ^{13}C NMR (CDCl_3 , 100 MHz) δ 13.7, 21.9, 27.1, 55.4, 102.2, 114.1, 125.5, 126.9, 127.5, 128.4, 132.9, 133.4, 145.2, 150.9, 159.1; HRMS (EI, M+) calcd for $\text{C}_{19}\text{H}_{20}\text{N}_2\text{O}$: 292.1576. Found: 292.1569.

5-Ethyl-1-(4-mthoxyphenyl)-3-phenylpyrazole (7c). Following the general procedure above hydrazone **6b** (4.50 g, 18.75 mmol) was acylated with propionic anhydride (1.22 g, 1.20 mL, 9.38 mmol) and cyclized with HCl. Upon solvent removal a crude orange solid was isolated. The crude solid was recrystallized from 20% ethyl acetate/hexanes to afford the title compound as pale yellow needles (1.82 g, 35%): mp 70-75 °C; ^1H NMR (CDCl_3 , 400 MHz) δ 1.25 (t, 3H, $J = 7.5$), 2.65 (q, 2H, $J = 7.5$), 6.53 (s, 1H), 3.86 (s, 3H), 6.99 (AA'XX', 2H, $J = 8.6$, 2.6), 7.28 - 7.33 (m, 1H), 7.37 – 7.43 (m, 4H), 7.85 – 7.90 (m, 2H); ^{13}C NMR (CDCl_3 , 125 MHz) δ 13.0, 19.6, 55.4, 101.6, 114.2, 125.5, 126.8, 127.5, 128.4, 132.9, 133.3, 146.6, 151.0, 159.0; MS (EI, 70 eV) m/z (relative intensity, %): 278 (M+, 100); Anal calcd for $\text{C}_{18}\text{H}_{18}\text{N}_2\text{O}$: C, 77.67; H, 6.52; N, 10.06. Found: C, 77.62; H, 6.49; N, 10.05.

1,3-Diphenyl-5-propyl-1H-pyrazole (7d). Following the general procedure above hydrazone **6c** (1.30 g, 6.19 mmol) was acylated with propionic anhydride (403 mg, 0.40 mL, 3.10 mmol) and cyclized with HCl. Flash chromatography (20% diethyl ether/hexanes) afforded the title compound as a yellow oil (600 mg, 40 %): ^1H NMR (CDCl_3 , 500 MHz) δ 1.28 (t, 3H, $J = 7.4$), 2.72 (q, 2H, $J = 7.4$), 6.58 (s, 1H), 7.32 – 7.53 (m, 8H), 7.91 (d, 2H, $J = 7.5$); ^{13}C NMR (CDCl_3 ,

100 MHz) δ 13.2, 19.9, 102.3, 125.7, 127.8, 127.9, 128.8, 129.1, 133.4, 140.0, 146.7, 151.5; HRMS (EI, M+) calcd for C₁₇H₁₆N₂: 248.1313. Found: 248.1312.

General iodination procedure (8a-d). To a refluxing solution of pyrazole (0.59 mmol) and sodium acetate (107 mg, 1.13 mmol) in H₂O (4.00 mL) was added a solution of KI (591 mg, 3.56 mmol) and I₂ (301 mg, 1.19 mmol) in H₂O (4 mL) dropwise. The resulting dark brown solution was allowed to reflux for 3 h and then was cooled to room temperature and the product extracted with diethyl ether (3 X 25 mL). The organic layers were combined, washed with NaS₂O₂ (3 X 20 mL), NaHCO₃ (2 X 20 mL), brine (2 X 20 mL) and then dried over MgSO₄ and concentrated under reduced pressure to afford the crude iodo-pyrazoles. The products were purified by recrystallization from hexanes or by flash chromatography on silica gel.

5-Ethyl-4-iodo-1,3-bis-(4-methoxy-phenyl)-1H-pyrazole (8a). Pyrazole **7a** (153 mg, 0.59 mmol) was iodinated according to the general procedure above. A crude tan solid was isolated and recrystallized from hexanes to afford the title compound as a white solid (224 mg, 87%): ¹H NMR (CDCl₃, 400 MHz) δ 1.13 (t, 3H, *J* = 7.4), 2.73 (q, 2H, *J* = 7.5), 3.84 (s, 3H), 3.85 (s, 3H), 6.94 - 7.02 (m, 4H), 7.36 (AA'XX', 2H, *J* = 9.0, 2.7), 7.83 (AA'XX', 2H, *J* = 8.8, 2.5); ¹³C NMR (CDCl₃, 125 MHz) δ 13.1, 20.1, 55.1, 55.4, 60.1, 113.4, 114.2, 125.4, 126.9, 129.4, 132.6, 147.2, 151.4, 159.4, 159.5.

4-Iodo-1-(4-methoxyphenyl)-3-phenyl-5-propylpyrazole (8b). Pyrazole **7b** (660 mg, 2.26 mmol) was iodinated according to the general procedure above. A crude oil was isolated and purified by flash chromatography (25% ethyl acetate/hexanes) to afford a mixture of unreacted pyrazole **7b** and product **8b** as a pale yellow oil (yield as determined by NMR: 65%; resonances listed for product only): ¹H NMR (CDCl₃, 400 MHz) δ 0.90 (t, 3H, *J* = 7.4) 1.56 (sext, 2H, *J* = 7.6), 2.70 (t, 2H, *J* = 7.8), 3.86 (s, 3H), 6.99 (XX' of AA'XX', 2H, *J*_{AX} = 8.7, *J*_{XX'} = 2.8), 7.90 (AA' of AA'XX', 2H, *J*_{AX} = 8.3, *J*_{AA'} = 1.6), 7.26 - 7.46 (m, 5H); ¹³C NMR (CDCl₃, 100 MHz) δ 13.8, 21.9, 28.4, 55.4, 60.9, 114.2, 127.1, 128.0, 128.0, 128.2, 132.8, 146.2, 151.5, 159.5; HRMS (EI, M+) calcd for C₁₉H₁₉N₂OI: 418.0542. Found: 418.0550.

5-Ethyl-4-iodo-1-(4-methoxy-phenyl)-3-phenyl-1H-pyrazole (8c). Pyrazole **7c** (500 mg, 1.80 mmol) was iodinated according to the general procedure above to afford the title compound as a white solid (603 mg, 83%): mp 70-73 °C; ¹H NMR (CDCl₃, 500 MHz) δ 1.14 (t, 3H, *J* = 7.5), 2.74 (q, 2H, *J* = 7.5), 3.86 (s, 3H), 6.99 (AA'XX', 2H, *J* = 8.6, 2.9), 7.34 – 7.47 (m, 5H), 7.86 – 7.92 (m, 2H); MS (EI, 70 eV) *m/z* (relative intensity, %): 404 (M⁺, 100); Anal calcd for C₁₈H₁₇N₂OI: C, 53.48; H, 4.24; N, 6.93. Found: C, 53.66; H, 4.24; N, 6.89.

5-Ethyl-4-iodo-1,3-diphenyl-1H-pyrazole (8d). Pyrazole **7d** (248 mg, 1.13 mmol) was iodinated according to the general procedure above to afford a crude orange solid. Recrystallization from hexanes afforded **8d** as small white crystals (312 mg, 74%): mp 82-85 °C; ¹H NMR (CDCl₃, 500 MHz) δ 1.61 (t, 3H, *J* = 7.5), 2.78 (q, 2H, *J* = 7.5), 7.35 – 7.55 (m, 8H), 7.86 – 7.91 (m, 2H); ¹³C NMR (CDCl₃, 125 MHz) δ 13.3, 20.3, 61.1, 125.6, 128.2, 128.3, 128.4, 128.6, 129.3, 132.9, 139.9, 147.3, 152.1; HRMS (EI, M⁺) calcd for C₁₇H₁₅N₂I: 374.0280. Found: 374.0277.

General procedure for Suzuki coupling (9a,b,d,e). To a stirred solution of iodo-pyrazole (0.43 mmol) in *n*-propanol (2 mL) was added the appropriate boronic acid (0.45 mmol), Pd(OAc)₂ (3 mg, 0.013 mmol), PPh₃ (10 mg, 0.039 mmol), 2 M Na₂CO₃ (0.47 mL, 0.95 mmol), and H₂O (0.5 mL). The heterogeneous solution was heated to reflux for 5 h, cooled to room temperature, and filtered through Celite (EtOAc 4 x 5mL). The filtrate was concentrated and partitioned in diethyl ether and water and the aqueous layer separated and extracted twice more with ether. The combined organic layers were washed with brine, dried over MgSO₄ and concentrated under reduced pressure. The tetrasubstituted pyrazoles were subsequently purified by flash chromatography.

5-Ethyl-1,3,4-tris-(4-methoxy-phenyl)-1H-pyrazole (9a). Iodo-pyrazole **8a** (187 mg, 0.43 mmol) was coupled with 4-methoxyphenylboronic acid (68 mg, 0.45 mmol) according to the general procedure above to afford a crude brown oil. Flash chromatography (40% ethyl acetate/hexanes) furnished the title compound as a clear oil (124 mg, 70%): ¹H NMR (CDCl₃, 400 MHz) δ 0.93 (t, 3H, *J* = 7.5), 2.63 (q, 2H, *J* = 7.5), 3.77 (s, 3H), 3.85 (s, 3H), 3.87 (s, 3H), 6.78 (AA'XX', 2H, *J* = 8.9, 2.5), 6.93 (AA'XX', 2H, *J* = 8.7, 2.5), 7.01 (AA'XX', 2H, *J* = 8.9, 2.6), 7.20

(AA'XX', 2H, $J = 8.6, 2.5$), 7.43 (AA'XX', 2H, $J = 8.8, 2.4$), 7.46 (AA'XX', 2H, $J = 8.9, 2.6$); ^{13}C NMR (CD_3OD , 100 MHz) δ 13.7, 17.8, 54.9, 55.0, 55.4, 113.3, 113.8, 114.1, 125.9, 126.4, 127.1, 127.4, 128.9, 131.3, 133.1, 143.5, 148.7, 158.3, 158.7, 159.1; HRMS (EI, M^+) calcd for $\text{C}_{26}\text{H}_{26}\text{N}_2\text{O}_3$: 414.1943. Found: 414.1937.

1,4-Bis-(4-methoxy-phenyl)-3-phenyl-5-propyl-1H-pyrazole (9b). Iodo-pyrazole **8b** (300 mg, 0.72 mmol) was coupled with 4-methoxyphenylboronic acid (115 mg, 0.75 mmol) according to the general procedure above. Flash chromatography (25% EtOAc/hexanes) afforded the title compound as a glassy solid (203 mg, 71%): ^1H NMR (CDCl_3 , 500 MHz) δ 0.70 (t, 3H, $J = 7.4$), 1.31 (sext, 2H, $J = 7.6$), 2.59 (t, 2H, $J = 7.9$), 3.84 (s, 3H), 3.86 (s, 3H), 6.92 (AA'XX', 2H, $J = 8.4, 2.4$), 7.00 (AA'XX', 2H, $J = 8.5, 2.5$), 7.16 – 7.27 (m, 5H), 7.45 (AA'XX', 2H, $J = 8.7, 2.4$), 7.48 – 7.54 (m, 2H); ^{13}C NMR ($\text{MeOD}-d_4$, 100 MHz) δ 13.8, 22.2, 26.5, 55.2, 55.5, 113.9, 114.3, 114.6, 126.4, 127.2, 127.3, 127.9, 128.1, 131.5, 133.3, 133.4, 142.6, 149.0, 158.5, 159.3; HRMS (EI, M^+) calcd for $\text{C}_{26}\text{H}_{27}\text{N}_2\text{O}_2$: 398.1994. Found: 398.1991.

5-Ethyl-1,4-bis-(4-methoxy-phenyl)-3-phenyl-1H-pyrazole (9c). To a degassed solution of 2M Na_2CO_3 (0.55 mL, 1.09 mmol; 0.5 mL H_2O), and DME (3.0 mL) was added 4-methoxyphenylboronic acid (83 mg, 0.55 mmol) and pyrazole **8c** (200 mg, 0.45 mmol). To this solution $\text{Pd}(\text{Ph}_3\text{P})_4$ (27 mg, 0.025 mmol) was added and the mixture heated to 80 °C for 72 h. The reaction mixture was then cooled to room temperature and filtered through Celite. The filtrate was transferred to a separatory funnel and the aqueous layers extracted with Et_2O (3 X 5 mL). The organic layers were combined and concentrated under reduced pressure. Flash chromatography (25% EtOAc/hexanes) afforded **9c** as a white solid (100 mg, 53 %): ^1H NMR (CDCl_3 , 400 MHz) δ 0.93 (t, 3H, $J = 7.5$), 2.64 (q, 2H, $J = 7.6$), 3.85 (s, 3H), 3.86 (s, 3H), 6.93 (AA'XX', 2H, $J = 8.7, 2.4$), 7.00 (AA'XX', 2H, $J = 9.2, 2.7$), 7.18 – 7.27 (m, 5H), 7.46 (AA'XX', 2H, $J = 9.0, 2.7$), 7.49 – 7.53 (m, 2H); HRMS (EI, M^+) calcd for $\text{C}_{25}\text{H}_{24}\text{N}_2\text{O}_3$: 384.1834. Found: 384.1838.

5-Ethyl-1-(4-methoxy-phenyl)-3,4-diphenyl-1H-pyrazole (9d). Iodo-pyrazole **8c** (400 mg, 0.99 mmol) was coupled with phenylboronic acid (144 mg, 1.04 mmol) according to the general procedure above to afford a crude brown oil. Flash chromatography (15% THF/Hexanes)

furnished the product and a mixture of the product and unreacted starting material. The mixture was treated to a second column under the same conditions to afford additional **9d** (50 mg combined, 14% isolated yield; 217 mg for remaining mixture, 60% total yield as determined by NMR): ^1H NMR (MeOD- d_4 , 500 MHz) δ 0.94 (t, 3H, $J = 7.4$), 2.66 (q, 2H, $J = 7.5$), 7.02 (AA'XX', 2H, $J = 8.9, 2.7$), 7.17 – 7.53 (m, 12H); ^{13}C NMR (MeOD- d_4 , 100 MHz) δ 13.7, 17.8, 55.4, 114.1, 118.7, 126.6, 127.2, 127.9, 127.9, 128.3, 130.2, 132.8, 133.1, 133.9, 143.7, 148.8, 159.3.

5-Ethyl-4-(4-methoxy-phenyl)-1,3-diphenyl-1H-pyrazole (9e). Iodo-pyrazole **8d** (244 mg, 0.65 mmol) was coupled with 4-methoxyphenylboronic acid (105 mg, 0.69 mmol) according to the general procedure above to afford a yellow oil. Flash chromatography (15% EtOAc/hexanes) was performed to afford a pale yellow oil which was then recrystallized from hexanes to afford the title compound as white crystals (160 mg, 70%): ^1H NMR (MeOD- d_4 , 500 MHz) δ 0.94 (t, 3H, $J = 7.5$), 2.70 (q, 2H, $J = 7.5$), 3.85 (s, 3H), 6.94 (AA'XX', 2H, $J = 8.8, 2.6$), 7.19 – 7.28 (m, 5H), 7.43 (app tt, 1H, $J = 7.4, 1.7$), 7.48 – 7.55 (m, 4H), 7.55 – 7.60 (m, 2H); ^{13}C NMR (MeOD- d_4 , 125 MHz) δ 13.7, 17.9, 55.1, 113.8, 118.8, 125.7, 126.1, 127.2, 127.8, 127.9, 129.0, 131.3, 133.2, 140.0, 143.6, 149.3, 158.4.

General procedure for demethylation using BBr_3 (2, 10a-d). To a stirred solution of pyrazole (**9a-e**, 0.28 mmol) in CH_2Cl_2 (10 mL) -78°C was added BBr_3 (2.82 mL, 2.82 mmol) dropwise as a 1M solution in CH_2Cl_2 . The mixture was allowed to warm to room temperature and stir for 3 h. The reaction was quenched at 0°C by the addition of H_2O (10 mL). The resulting solid was solublized by the addition of ethyl acetate and the resulting biphasic solution transferred to a separatory funnel and the aqueous layer isolated. The aqueous layer was acidified with 3 M HCl (3 mL) and extracted with ethyl acetate (2 X 15 mL). The combined organic layers were washed with brine and dried over MgSO_4 . The solvent was removed under reduced pressure and the phenolic products purified by flash chromatography and/or crystallization.

5-Ethyl-1,3,4-tris-(4-hydroxy-phenyl)-1H-pyrazole (10a). A stirred solution of **9a** (46 mg, 0.11 mmol) in CH_2Cl_2 (5 mL) was treated with BBr_3 (1.10 mL, 1.10 mmol) according to

the general demethylation procedure. After workup a reddish brown oil isolated. The oil was dissolved in methanol and concentrated under reduced pressure. No effort was made to remove trace amounts of methanol remaining in the sample. The residue was triturated by adding CH_2Cl_2 dropwise until a precipitate formed. The precipitate was isolated by vacuum filtration to afford **10a** as a white solid (40 mg, 93%): ^1H NMR ($\text{MeOD}-d_4$, 400 MHz) δ 0.89 (t, 3H, $J = 7.6$) 2.59 (q, 2H, $J = 7.5$), 6.65 (d, 2H, $J = 8.4$), 6.79 (d, 2H, $J = 8.4$), 6.93 (d, 2H, $J = 8.8$), 7.03 (d, 2H, $J = 8.8$), 7.21 (d, 2H, $J = 8.4$), 7.32 (d, 2H, $J = 8.8$); ^{13}C NMR ($\text{MeOD}-d_4$, 100 MHz) δ 12.4, 17.2, 114.3, 114.8, 115.1, 118.0, 124.2, 124.6, 127.4, 128.9, 131.0, 131.2, 143.9, 149.1, 156.0, 156.6, 157.7; HRMS (EI, M^+) calcd for $\text{C}_{23}\text{H}_{20}\text{N}_2\text{O}_3$: 372.1474. Found: 372.1468.

1,4-Bis-(4-hydroxy-phenyl)-3-phenyl-5-propyl-1H-pyrazole (10b). A stirred solution of **9b** (100 mg, 0.25 mmol) in CH_2Cl_2 (10 mL) was treated with BBr_3 (2.50 mL, 2.50 mmol) according to the general demethylation procedure. After workup a red solid was isolated. The solid was recrystallized from 10% $\text{CH}_3\text{OH}/\text{CHCl}_3$ to afford **10b** as small white crystals (75 mg, 81%): mp 233-236 °C; ^1H NMR ($\text{MeOD}-d_4$, 400 MHz) δ 0.67 (t, 3H, $J = 7.3$), 1.29 (sext, 2H, $J = 7.5$), 2.59 (t, 2H, $J = 7.9$), 6.79 (AA'XX', 2H, $J = 8.4$, 2.2), 6.94 (AA'XX', 2H, $J = 8.6$, 2.5), 7.03 (AA'XX', 2H, $J = 8.3$, 2.1), 7.20 – 7.26 (m, 3H), 7.31 – 7.43 (m, 4H); ^{13}C NMR ($\text{MeOD}-d_4$, 100 MHz) δ 12.4, 21.5, 25.9, 114.9, 115.2, 119.1, 124.4, 127.0, 127.4, 127.5, 127.6, 131.1, 131.2, 132.9, 142.8, 148.9, 156.2, 157.8; HRMS (EI, M^+) calcd for $\text{C}_{24}\text{H}_{22}\text{N}_2\text{O}_2$: 370.1681. Found: 370.1685.

5-Ethyl-1-(4-hydroxy-phenyl)-3,4-diphenyl-1H-pyrazole (10c). A stirred solution of **9c** (37 mg, 0.10 mmol) in CH_2Cl_2 (5 mL) was treated with BBr_3 (1.00 mL, 1.00 mmol) according to the general demethylation procedure. After workup a brown oil was afforded. The crude oil was purified by flash chromatography (5% $\text{CH}_3\text{OH}/\text{CH}_2\text{Cl}_2$) to afford **10c** as a white solid (30 mg, 86%): mp 210-220 °C; ^1H NMR ($\text{MeOD}-d_4$, 400 MHz) δ 0.90 (t, 3H, $J = 7.60$ Hz), 2.65 (q, 2H, $J = 7.4$), 6.95 (AA'XX', 2H, $J = 9.1$, 2.7), 7.19 – 7.26 (m, 5H), 7.31 – 7.42 (m, 7H); ^{13}C NMR ($\text{MeOD}-d_4$, 100 MHz) δ 13.8, 17.8, 116.5, 118.8, 126.8, 127.5, 127.6, 128.1, 128.1, 128.5, 130.3, 132.1, 132.9, 133.9, 144.2, 149.1, 156.5; HRMS (EI, M^+) calcd for $\text{C}_{23}\text{H}_{20}\text{N}_2\text{O}$: 340.1576. Found: 340.1576.

5-Ethyl-4-(4-hydroxy-phenyl)-1,3-diphenyl-1H-pyrazole (10d). A stirred solution of **9e** (100 mg, 0.28 mmol) in CH₂Cl₂ (10 mL) was treated with BBr₃ (2.82 mL, 2.82 mmol) according to the general demethylation procedure. After workup a crude brown solid was isolated. The solid was purified by flash chromatography (5% CH₃OH/CH₂Cl₂) to afford **10d** as a white solid (89 mg, 93%): ¹H NMR (MeOD-*d*₄, 500 MHz) δ 0.93 (t, 3H, *J* = 7.5), 2.68 (q, 2H, *J* = 7.6), 6.78 (XX' of XX'AA', 2H, *J*_{AX} = 8.4, *J*_{XX'} = 2.5), 7.10 (AA' of AA'XX', 2H, *J*_{AX} = 8.4, *J*_{AA'} = 2.5), 7.21 – 7.28 (m, 3H), 7.40 – 7.52 (m, 6H), 7.53 – 7.58 (m, 2H); ¹³C NMR (MeOD-*d*₄, 100 MHz) δ 13.7, 17.9, 115.6, 119.1, 125.8, 125.9, 127.4, 128.0, 128.1, 128.2, 129.2, 131.5, 133.0, 139.8, 143.9, 149.5, 154.9; HRMS (EI, M+) calcd for C₂₃H₂₀N₂O: 340.1576. Found: 340.1571.

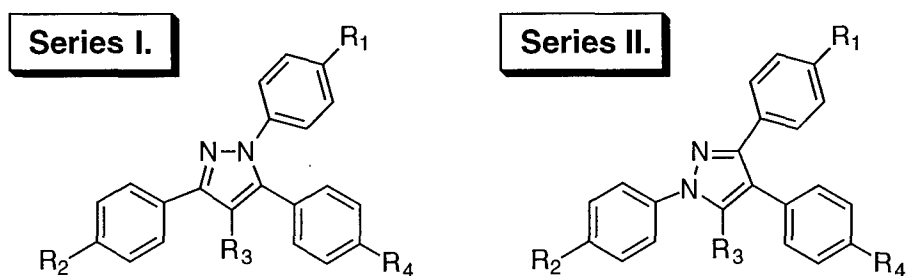
Acknowledgments

We are grateful for support of this research through grants from the U. S. Army Breast Cancer Research Program (DAMD17-97-7076) and the National Institutes of Health (PHS 5R37 DK15556 and T32 CA 09067 (Training Grant for Y. H.). We thank Kathryn E. Carlson for performing binding assays and for helpful comments. NMR spectra were obtained in the Varian Oxford Instrument Center for Excellence in NMR Laboratory. Funding for this instrumentation was provided in part from the W.M. Keck Foundation and the National Science Foundation (NSF CHE 96-10502). Mass spectra were obtained on instruments supported by grants from the National Institute of General Medical Sciences (GM 27029), the National Institute of Health (RR 01575), and the National Science Foundation (PCM 8121494).

References

- (1) Gao, H.; Katzenellenbogen, J. A.; Garg, R.; Hansch, C. *Chem. Rev.* **1999**, *99*, 723-744.
- (2) Magarian, R. A.; Overacre, L. B.; Singh, S.; Meyer, K. L. *Curr. Med. Chem.* **1994**, *1*, 61-104.
- (3) Fink, B. E.; Mortensen, D. S.; Stauffer, S. R.; Aron, Z. D.; Katzenellenbogen, J. A. *Chem. Biol.* **1999**, *6*, 205-219.
- (4) Stauffer, S. R.; Coletta, C. J.; Sun, J.; Tedesco, R.; Katzenellenbogen, B. S.; Katzenellenbogen, J. A. *J. Med. Chem.* **2000**, *Submitted*.
- (5) Stauffer, S. R.; Katzenellenbogen, J. A. *J. Comb. Chem.* **2000**, *In Press*.
- (6) Foote, R. S.; Beam, C. F.; Hauser, C. R. *Heterocycle Chem.* **1970**, *7*, 589-592.
- (7) Holzer, W.; Gruber, H. *Heterocycle Chem.* **1995**, *32*, 1351-1354.
- (8) Huff, B. E.; Koenig, T. M.; Staszak, M. A. *Org. Synth.* **1998**, *75*, 53-60.
- (9) Katzenellenbogen, J. A.; Johnson, H. J., Jr.; Myers, H. N. *Biochemistry* **1973**, *12*, 4085-4092.
- (10) Huang, Y.; Katzenellenbogen, J. A. *Organic Letters* **2000**, *Submitted*.
- (11) Anstead, G. M.; Wilson, S. R.; Katzenellenbogen, J. A. *J. Med. Chem.* **1989**, *32*, 2163-2171.
- (12) Anstead, G. M.; Peterson, C. S.; Katzenellenbogen, J. A. *J. Steroid Biochem.* **1989**, *33*, 877-887.
- (13) Anstead, G. M.; Carlson, K. E.; Katzenellenbogen, J. A. *Steroids* **1997**, *62*, 268-303.
- (14) Brzozowski, A. M.; Pike, A. C.; Dauter, Z.; Hubbard, R. E.; Bonn, T.; Engström, O.; Öhman, L.; Greene, G. L.; Gustafsson, J.-A.; Carlquist, M. *Nature* **1997**, *389*, 753-758.
- (15) Sun, J.; Meyers, M. J.; Fink, B. E.; Rajendran, R.; Katzenellenbogen, J. A.; Katzenellenbogen, B. S. *Endocrinology* **1999**, *140*, 800-804.
- (16) Shiau, A. K.; Barstad, D.; Loria, P. M.; Cheng, L.; Kushner, P. J.; Agard, D. A.; Greene, G. L. *Cell* **1998**, *95*, 927-937.
- (17) Still, W. C.; Kahn, M.; Mitra, A. *J. Org. Chem.* **1978**, *43*, 2923-2926.

Table 1. Binding affinity data for pyrazole isomers and original pyrazole series.



| R ₁ | R ₂ | R ₃ | R ₄ | Cmpd. (I) | RBA (I) ^a | Cmpd. (II) | RBA (II) ^a |
|----------------|----------------|----------------|----------------|------------|----------------------|------------|-----------------------|
| H | OH | Et | OH | 1 | 15.3±3 | 2 | 5.8±0.3 |
| OH | OH | Et | OH | 11a | 20.3±3 | 10a | 7.8±4 |
| H | OH | <i>n</i> -Pr | OH | 11b | 25±0.01 | 10b | 16.0±1 |
| H | OH | Et | H | 11c | 0.46 | 10c | 0.43±0.07 |
| H | H | Et | OH | 11d | 0.007 | 10d | 0.008±0.005 |

^aCompetitive radiometric binding assays were done using 10nM [³H]E₂ as tracer and lamb uterine cytosol as receptor source; for details, see Experimental. Compounds **11a-d** were prepared as described elsewhere.^{5,10}

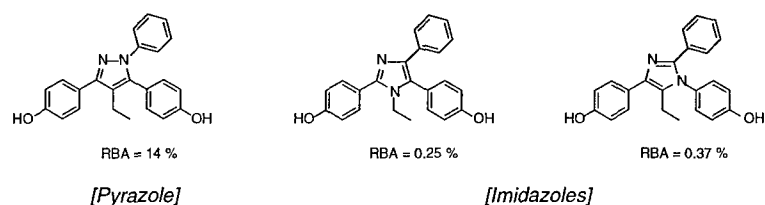


Figure 1. Effect of different core structures of selected five-member heterocycles (diazoles) on their estrogen receptor relative binding affinity (RBA).

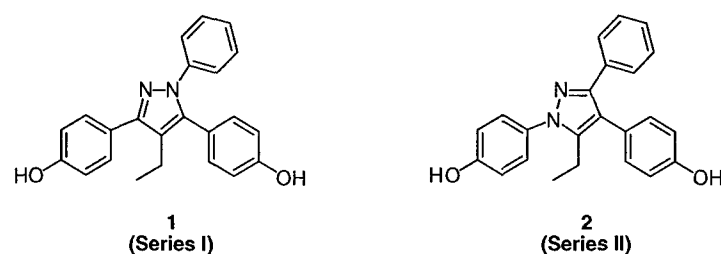


Figure 2. Original 1,3,5-triaryl-pyrazole **1** (the basis of Series I) and the new 1,3,4-triaryl-pyrazole isomer **2** (the basis of Series II).

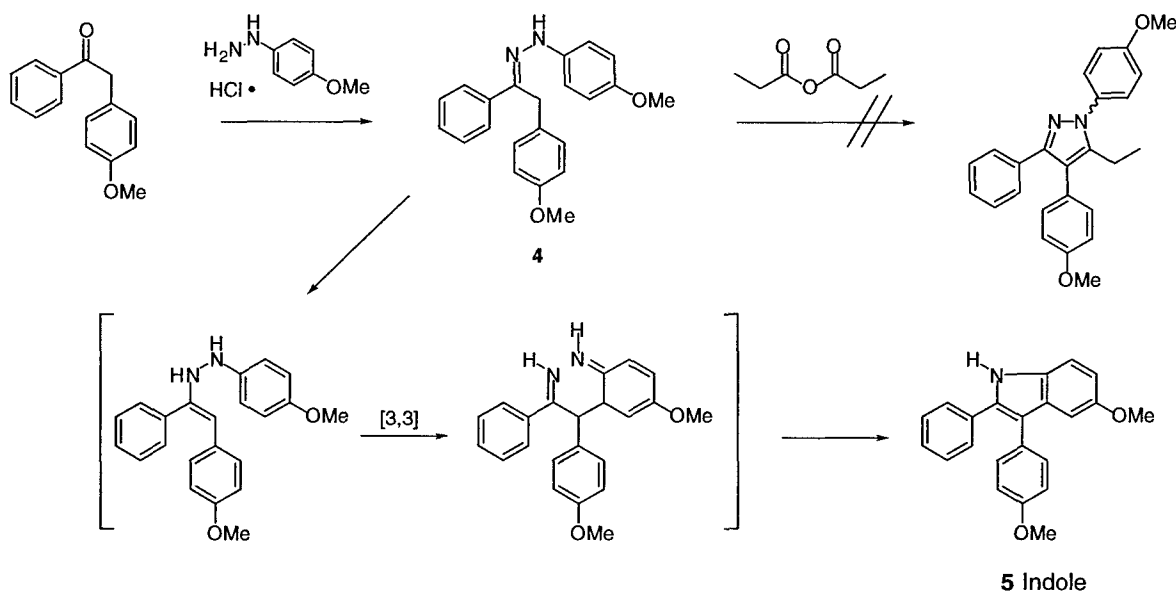


Figure 3. Attempted synthesis of pyrazole isomer using an acylation-cyclization.

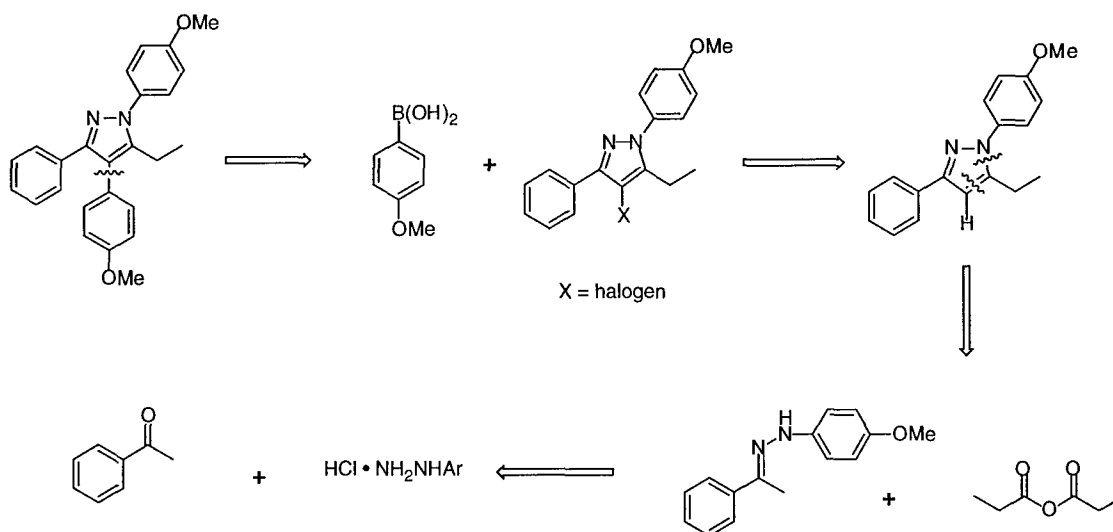


Figure 4. Retro-synthetic strategy for Pd(0)-mediated coupling approach to pyrazoles.

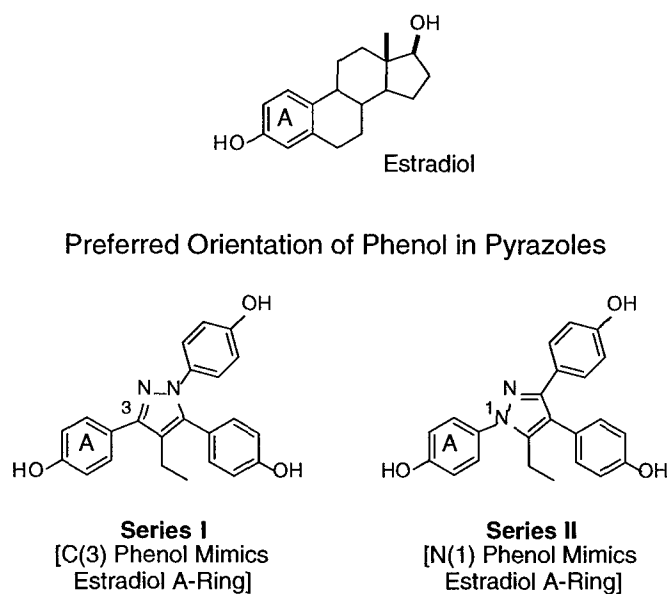


Figure 5. Preferred orientation and proposed A-ring mimic for Series I and Series II Pyrazoles

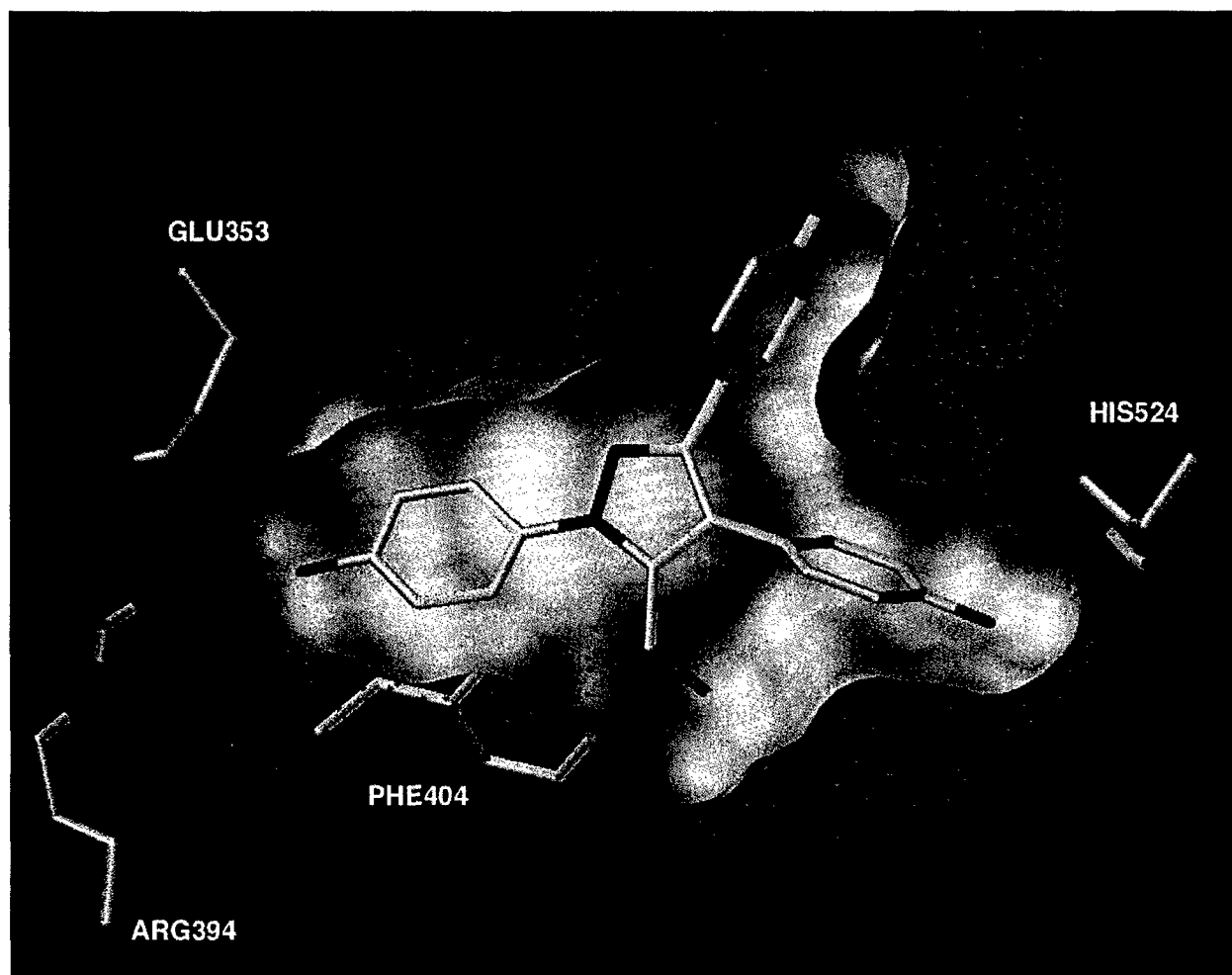
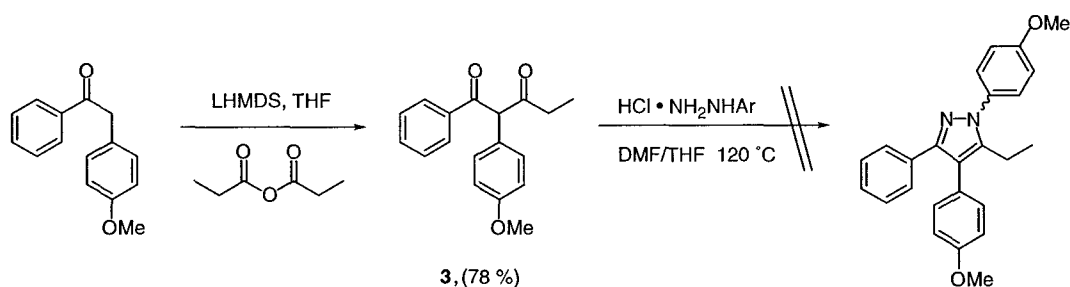
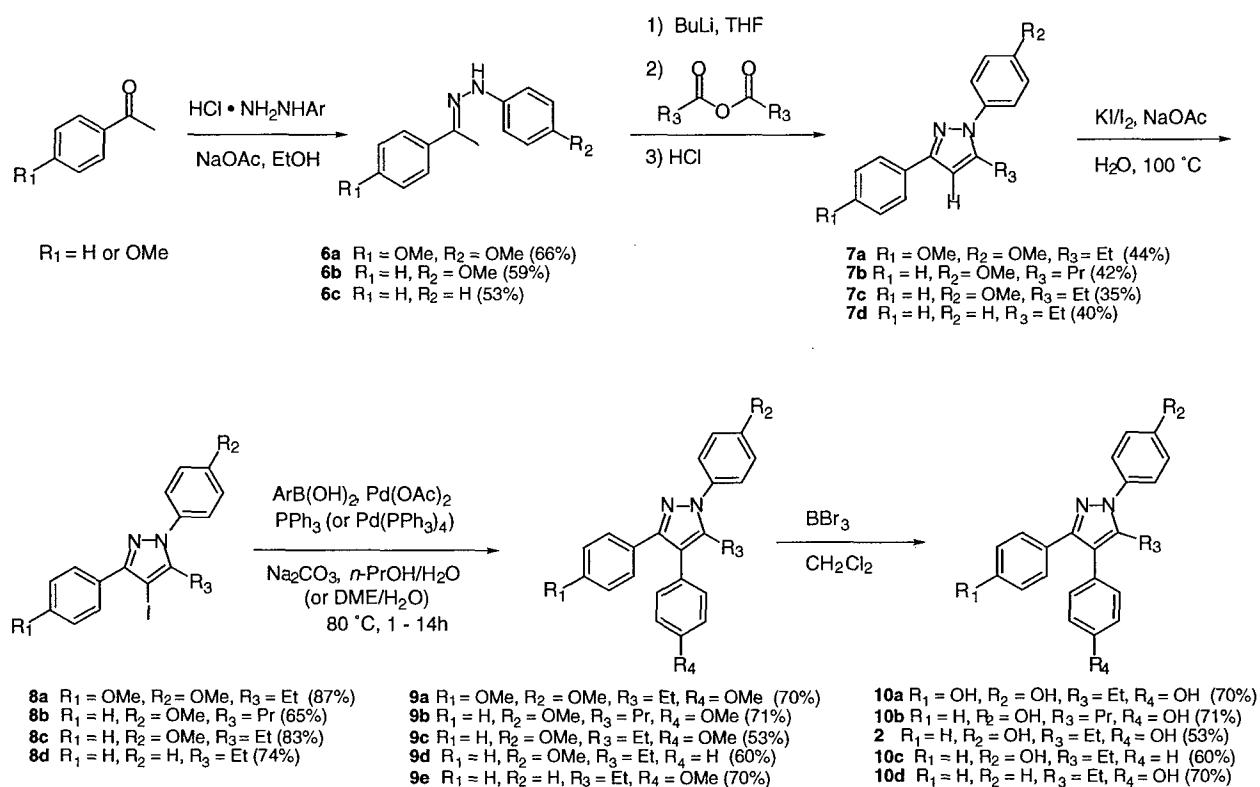


Figure 6. A model for pyrazole **10a** docked and minimized in the DES-ER α -LBD. The surface of the ligand is shown in yellow, and the solvent accessible surface of ER as purple dots.



Scheme 1. Attempted synthesis of MeO-protected pyrazole isomer.



Scheme 2. Synthesis of 1,3,4-triaryl-5-alkylpyrazoles.

7
11
12
13

MS No: BF/2000/000063

Revised: August 14, 2000

**Triarylpyrazoles with basic side chains: Development of pyrazole-based estrogen
receptor antagonists**

Shaun R. Stauffer^a, Ying R. Huang^a, Zachary D. Aron^a, Christopher J. Coletta^a, Jun Sun^b,
Benita S. Katzenellenbogen^{b,c}, and John A. Katzenellenbogen^{a*}

^a*Department of Chemistry*

^b*Department of Physiology*

^c*Department of Cell and Structural Biology
University of Illinois and University of Illinois College of
Medicine, Urbana IL 61801*

Submitted to: *Bioorganic and Medicinal Chemistry*

Address Correspondence to:

John A. Katzenellenbogen
Department of Chemistry
University of Illinois
600 South Mathews Avenue
Urbana IL 61801
217 333 6310 (phone)
217 333 7325 (fax)
jkatzene@uiuc.edu

Keywords: estrogen receptors; pyrazole estrogens; pyrazole antiestrogens; antiestrogens;
non-steroidal estrogens

Abstract - Recently, we developed a novel triaryl-substituted pyrazole ligand system that has high affinity for the estrogen receptor (ER)(Fink, et al., *Chem. Biol.* **1999**, *6*, 205). Subsequent work has shown that some analogs in this series are very selective for the ER α subtype in terms of binding affinity and agonist potency.(Stauffer et al., *J. Med. Chem.*, **2000**, submitted). We now investigate how this pyrazole ER agonist system might be converted into an antagonist or a selective estrogen receptor modifier (SERM) by incorporating a basic or polar side chain like those typically found in antiestrogens and known to be essential determinants of their mixed agonist/antagonist character. We selected an N-piperidinyl-ethyl chain as a first attempt, and introduced it at the four possible sites of substitution on the pyrazole core structure to determine the orientation that the pyrazole might adopt in the ER ligand binding pocket. Of these four, the C(5) piperidinyethoxy-substituted pyrazole **5** had by far the highest affinity. Also, it bound to the ER subtype alpha (ER α) with 20-fold higher affinity than to ER β . In cell-based transcription assays, pyrazole **5** was an antagonist on both ER α and ER β , and it was also more potent on ER α . Based on structure-binding affinity relationships and on molecular modeling studies of these pyrazoles in a crystal structure of the ER α -raloxifene complex, we propose that pyrazoles having a basic substituent on the C(5) phenyl group adopt a binding mode that is different from that of the pyrazole agonists that lack this group. The most favorable orientation appears to be one which places the N(1) phenol in the A-ring binding pocket so that the basic side chain can adopt an orientation similar to that of the basic side chain of raloxifene.

Introduction

The term SERM, or selective estrogen receptor modifier, is used to describe ligands for the estrogen receptor (ER) that display an interesting balance of agonist and antagonist activity that can vary from tissue to tissue.¹ SERMs have particular utility in menopausal hormone replacement and in the treatment and prevention of breast cancer, although the pharmacological profiles of the currently available agents are not optimal.

SERMs typically consist of a non-steroidal core structure onto which is attached a side chain bearing a basic or polar function. X-ray crystal structures of the ER ligand binding domain (LBD) complexed with the SERMs raloxifene² or hydroxytamoxifen³ show that the large side chains of these ligands displace the C-terminal helix (helix-12) from the position it normally occupies in ER-LBD complexes with agonists. In this antagonist conformation, helix-12 moves into a position where it occludes a hydrophobic groove on the surface of the receptor that normally functions as a tethering site for the interaction of ER with coactivator proteins, an interaction that is important in mediating agonist activity.^{3,4}

It is clear, however, that more subtle changes in the conformation of ER must underlie some of the pharmacological differences among various SERMs.^{5,6} Recently, conformation-sensitive peptides have been used to discriminate among these different ligand-induced ER conformations.⁷⁻⁹ Nevertheless, it is not completely clear how the ligand structure of the various SERMs determines ER conformation, at least at this level of detail. In addition, differential interaction of SERMs with the two ER subtypes, ER α and ER β , might also underlie certain aspects of their tissue-selectivity activity.¹⁰⁻¹²

In recent studies of novel, heterocyclic non-steroidal estrogens amenable to combinatorial assembly and library synthesis, we identified tetrasubstituted pyrazoles as a system that afforded high affinity ligands for ER.¹³ Subsequently, we used parallel synthesis, as well as directed synthesis, to characterize structure-affinity relationships in this series.^{14,15} In the process, we found several high affinity compounds, and in

particular, some that show very high binding affinity and transcriptional efficacy for the ER alpha subtype (ER α).¹⁵ Although some of these compounds were also agonists on the ER beta subtype (ER β), their potency and binding affinity on this ER subtype was much lower.¹⁵ The high difference in ER-subtype binding affinities shown by some of these pyrazoles raised an interesting prospect that this system might be a favorable starting point for the development of ER α potency-selective antagonists or SERMs. This would depend, of course, on whether these ligands could be converted to antagonists by appropriate substitution of basic or polar side chains.

In this report, we describe the preparation of several analogs of an ER α high-affinity pyrazole which embody the type of basic or polar side chain that is typically found in SERMs. We evaluate how this substitution is tolerated in terms of ER binding affinity, and in some selected cases, we show it affects the transcriptional efficacy and potency of these ligands. We also develop a model for how these basic side chain-substituted pyrazoles are likely to be orientated in the ligand-binding pocket of ER.

Results and Discussion

An example of a favorable pattern of substitution for high affinity ER pyrazoles ligands consists of three phenols at the 1,3 and 5-positions and an alkyl group at the 4-position, and is shown below in Figure 1 (pyrazole **1**).¹³⁻¹⁶ The piperidinyethyl substituent, which is widely represented in many SERM classes (See, for example, Raloxifene, Fig. 1),^{1,17} was chosen in this study as a typical basic side chain that might be expected to confer the characteristic mixed agonist/antagonist activity of these compounds. The question at hand, however, is at which position on a pyrazole such as **1** should this basic substituent be attached. Molecular modeling studies using the LBD crystal structures provided a starting point towards answering this question.

[Figure 1]

From published crystal structures, it is known that the ER-LBD adopts a different conformation when complexed with agonists (E_2 , DES) versus antagonists (hydroxytamoxifen, raloxifene).^{2,3} In our initial molecular modeling studies, we examined various binding modes for the pyrazole core structure (i.e., without a basic side chain) based on the larger ligand binding pocket in the ER-LBD-raloxifene (antagonist) complex.¹³ However, in a subsequent publication,¹⁵ knowing now that these pyrazoles were agonists, we reexamined our initial predictions, this time using the ER-LBD-DES (agonist) structure. As a result of this additional modeling work, as well as further structure-activity relationship studies we have done in this series of compounds,¹⁵ we now believe that these core pyrazoles, which behave as agonists, bind in an orientation in which the C(3) phenol plays a role analogous to the critical A-ring of estradiol.¹⁵ We have illustrated this binding orientation with the relative positions we have chosen for pyrazole **1** and estradiol in Figure 1. The orientation of the SERM raloxifene relative to estradiol, known from X-ray crystallography,² is also displayed in Figure 1. In this orientation, the benzothiophene ring system of raloxifene mimics the AB ring system of

estradiol, so that the basic side chain is directed roughly in the estradiol 11 β direction (Fig. 1), where it extends outward to displace helix-12, as noted above.²

On the basis of our current model, we might have considered it unlikely that the pyrazole ligand could even accommodate a basic side-chain. When bound with the ER-LBD in the agonist conformation, there is no position on the pyrazole analog where such a side chain could be disposed so as to occupy a region of the ligand binding pocket that is normally occupied by this group in other SERMs (i.e., the estradiol 11 β region, Fig. 1).^{2,3} However, because of the near symmetry of these triaryl pyrazoles and the known flexibility of the ligand-binding pocket of the ER,^{2,3} we were not convinced that the binding orientation preferences of the smaller core pyrazole agonist ligands would be retained. The additional bulk and polarity of the basic side chain that we were adding to engender antagonist activity might cause the ligand to adopt a entirely different orientation in the binding pocket.

Therefore, as an initial effort to develop pyrazole-based SERMs, we prepared four pyrazoles in which the basic piperidinylethyl side chain is attached at four different positions (**2-5**, Figure 1), and we determined the binding affinity of these derivatives for the ER. Each of these isomers serves as a model to determine which position on the heterocycle scaffold can best accommodate the SERM-defining basic side chain in the ER-LBD. Once identified, such a site would obviously be a prime target for further study through a series of pyrazoles in which the structure of this basic substituent is varied.¹⁸

The four basic side chain-containing pyrazoles (**2-5**) shown in Figure 1 are designed to probe several potential ligand orientations within the binding pocket. For example, pyrazole **2** was proposed on the basis of our initial docking study of the N-aryl pyrazole **1** in the ER α -raloxifene X-ray crystal structure,¹³ (now revised, as noted above¹⁵) which placed the C(5) phenol in the subpocket corresponding to the A-ring of E₂. In this mode, the N(1) basic side chain group resides in what would be the estradiol 11 β direction. Pyrazole **3** was envisioned to undergo a ligand "flipping" around the bond

between the pyrazole core and the C(3) phenol, to place the C(4)-linked basic side chain in the estradiol 11 β direction. Pyrazoles **4** and **5** are regioisomers that have the basic side chain at the 3 and 5-positions, respectively. Pyrazole **5**, a C(5)-substituted analog, was predicted to have a potentially favorable interaction with ER by way of a ca. 120° counterclockwise rotation about an axis perpendicular to the pyrazole ring, resulting in a binding mode that would make the N(1) phenol the mimic of the A-ring in estradiol. Pyrazole **4**, a regioisomer of pyrazole **5**, was considered unlikely to have a favorable interaction with the ER, because the phenols and the basic side chain groups are displayed in a “long” orientation. This leaves the remaining two free phenols too close to one another for proper interaction with the A-ring and D-ring subpockets in ER. Nevertheless, it was prepared for the sake of completeness.

Chemical Syntheses

The synthesis of pyrazole **2** is shown in Scheme 1. For the preparation of the required piperidinylethoxy-substituted phenylhydrazine, we initially investigated the classical diazotization-reduction route, starting from the corresponding substituted aniline **6**. However, we had difficulty isolating the desired hydrazine precursor. Fortunately, we found the approach of Demers and Klaubert,¹⁹ involving metallation of the corresponding aromatic bromide (**7**) followed by reaction with an azodicarboxylate ester, conveniently afforded the di-Boc protected hydrazine **8**. Because isolation of the free hydrazine proved to be problematic, we performed the Boc deprotection and pyrazole cyclization in one-pot, which gave pyrazole **9** in 65% yield. Selective demethylation using either AlCl₃-EtSH or BBr₃ afforded pyrazole **2** in 55-75% yield.

[Scheme 1]

The synthesis of the C(4) basic side chain-containing pyrazole **3** is shown in Scheme 2. Introduction of a basic side chain into the pyrazole structure at the 4-position

was done early in the synthesis, starting with Freidel-Crafts acylation of anisole with 6-bromohexanoyl chloride. For this transformation, the temperature had to be carefully maintained at -10 °C to avoid reaction of the product ketone **10** with a second equivalent of anisole, a side reaction that results in the formation of a 1,1-diaryl-alkene by-product upon dehydration. The bromoketone **10** was then aminated with excess piperidine in DMF to afford amino-ketone **11** in high yield. Condensation with the *p*-nitrophenyl benzoate furnished the β -diketone **12**, which was cyclized with phenyl hydrazine hydrochloride to give the desired protected pyrazole **13**. Deprotection using $\text{AlCl}_3\text{-EtSH}$ yielded the final pyrazole **3**.

[Scheme 2]

The final pyrazoles **4** and **5** were initially prepared as an approx. 1:1 mixture of regioisomers by the route shown Scheme 3. Starting from 4-hydroxybutyrophenone, we used a Mitsunobu reaction to prepare the piperidinylethoxy-substituted ketone **14**. Claisen condensation afforded the requisite β -diketone **15**. Treatment with phenylhydrazine hydrochloride followed by BBr_3 deprotection afforded the desired pyrazoles **4** and **5** as a 1:1 mixture that could be separated by chromatography. Pyrazole **4** was further purified by recrystallization from MeOH, and definitive regiochemical assignment of this isomer was made on the basis of a single crystal X-ray analysis. An ORTEP diagram of this compound is shown in Figure 2.

[Scheme 3] [Figure 2]

Isolation of the last pyrazole (**5**) proved to be more problematical because we found that the basic side chain of these pyrazoles undergoes partial cleavage when BBr_3 is used as a deprotection reagent. This is a significant problem, because the triphenolic by-product resulting from this cleavage was difficult to separate from the desired C(5) basic side chain isomer by chromatography and it has distinctly different biological

activity.¹⁵ Later, we found that we could do this deprotection selectively, without this side reaction, using the milder $\text{AlCl}_3\text{-EtSH}$ reagent. Ultimately, however, we used a regioselective route (described elsewhere in detail¹⁸) to produce the desired pyrazole **5**.

Estrogen Receptor Binding Affinity of Pyrazoles 2-5

The binding affinity of pyrazoles **2-5** for ER was assayed in a competitive radiometric binding assay as described previously,^{20,21} and affinities are expressed as relative binding affinity (RBA) values, where the affinity of estradiol is considered to be 100% (Table 1). The affinity of all compounds was tested both in a natural ER preparation from lamb uterine cytosol,²¹ which is predominantly $\text{ER}\alpha$,^{10,11} as well as with purified recombinant human $\text{ER}\alpha$ and $\text{ER}\beta$ (See Experimental).²⁰

When uterine cytosol was used as a source of estrogen receptor, pyrazole **2** had a relatively low binding affinity, just 1.5% that of estradiol, a value which is 10-fold lower than that of the parent N(1) aryl pyrazole (**1**).^{13,15} Pyrazole **3** with the basic side chain on C(4) also displayed very low affinity for the receptor. Apparently, even with the reorientation proposed above, this analog, in which the basic side chain is attached to the pyrazole core solely through aliphatic linkages, does not fit well in the ligand binding pocket of ER. More intriguing are the two regioisomeric pyrazoles **4** and **5**; they display very distinctive preferences for binding to the ER, pyrazole **5** having a 65-90-fold higher affinity than pyrazole **4** in all three test systems. As noted previously, the higher affinity of isomer **5** vs. **4** was expected.

[Table 1]

Pyrazole **5** has the highest affinity of all basic side-chain pyrazoles investigated thus far, and, in fact, is among the highest affinity of all pyrazoles we have reported as ER ligands.¹³⁻¹⁵ When we evaluated the binding affinity of these pyrazoles with pure human $\text{ER}\alpha$ and $\text{ER}\beta$ (Table 1),²⁰ pyrazole **5** showed a distinctive preference for binding

to ER α (ca. 20 fold), a characteristic that it shares with the parent pyrazole triol **1** (ca. 230 fold).¹⁵ Pyrazole **2** shows only a 5-fold affinity preference for ER α . Pyrazoles **3** and **4** had very low affinity for both ER α and ER β , and they were not investigated further either for binding affinity or transcriptional activity.

Transcription Activity of Pyrazole 5

Based on the promising ER α binding selectivity of pyrazole **5** and because of its piperidine side chain, we were interested in whether this compound had antagonistic properties, and in particular, whether it might function as an antagonist on one or both of the ER subtypes in a potency selective manner. Figure 3 shows the transcriptional activity profiles of pyrazole **5** assayed in HEC-1 cells with either ER α or ER β . Cells were transfected with an expression plasmid for ER α or ER β , together with an estrogen-responsive reporter gene construct ((ERE)₃-pS2-CAT), and reporter gene expression was determined at different concentrations of ligand. Antagonism was assayed at different concentrations of ligand in the presence of 10⁻⁹ M E₂.

[Figure 3]

Pyrazole **5** showed no stimulation of transcriptional activity of ER α or ER β , and it was a full antagonist on ER α and ER β , completely antagonizing activity stimulated by estradiol (Fig. 3). Thus, introduction of the type of basic side chain typically found in the mixed agonist/antagonist SERMs at the proper site on the parent pyrazole **1**, which is an agonist, converts this pyrazole system into an antagonist (pyrazole **5**). The relatively good ER α binding affinity selectivity of pyrazole **5** (ca. 20 fold; cf., Table 1) is preserved to a considerable degree in its potency as a transcriptional antagonist. Its IC₅₀ value is ca. 20 nM on ER α and ca. 160 nM on ER β , which gives an ER α antagonist potency selectivity of ca. 10 fold (Fig. 3).

In work to be presented elsewhere, we have prepared additional analogs of pyrazole **5** having other basic and polar side chains as substituents on the C(5) phenyl

group.¹⁸ Some of these have very high affinity selectivity for ER α over ER β , and they act as ER α potency selective antagonists. (J. Sun et al., in preparation)

Binding Models for Pyrazoles 2 and 5 in the ER α -Raloxifene Crystal Structure

As previously mentioned, the low binding affinity of pyrazole **4** was not surprising. The low affinity of pyrazole **3**, however, was unexpected, because, as mentioned earlier, when the pyrazole core is flipped, the basic side chain attached to C(4) appears to be orientated properly for this substituent to project through the 11 β channel.

Pyrazole **2**, in which the basic side chain is substituted on the N(1) phenyl group, was initially believed to be the most favorable candidate for interacting with ER. However, this turned out not to be the case; pyrazole **5** has the highest affinity. These two pyrazoles have somewhat related structures (cf., Fig. 1); the three aryl groups (two unsubstituted and one side chain-substituted) can be superimposed in a congruent fashion, as illustrated in Figure 4. When oriented in this fashion, the only difference between these two isomers is the position of the two ring nitrogen atoms and the C(4) ethyl substituent.

[Figure 4]

In an attempt to understand the 16-fold higher affinity of pyrazole **5** than pyrazole **2**, we performed some docking studies of these two ligands with the ER α -raloxifene crystal structure.² Both ligands were docked in the ER α -raloxifene crystal structure in a similar manner, and they were subjected to a three-step minimization protocol to generate the final receptor-ligand model complexes shown (see Experimental Methods, Molecular Modeling for details). Residue side chains that were close to each ligand in its initial position were allowed to undergo torsional movement during the docking operation, in order to obtain an optimal fit, prior to minimization. A crossed-stereo view of pyrazoles **2** and **5** is shown in Figure 5A and B. The final models have similar energies, which at

least at this level of refinement, simply indicates that they have no bad contacts or unfavorable conformations.

[Figure 5]

In both of the views shown in Figure 5, the three aryl groups displayed peripherally from the pyrazole core are accommodated comfortably and in a very similar manner within the ligand binding pocket. This was achieved with only minimal and energetically favorable movement of a few residues that were initially in close contact with the ligand.

The most significant difference between the complexes with pyrazole **2** and **5** is the position of the ethyl group (cf., Fig. 4). In Figure 5B, the C(4) ethyl group of pyrazole **5** projects into a region of ER that accommodates the 18-methyl of estradiol in the ER-E₂ complex.² In this subpocket, the favorable van der Waals interaction that normally occurs between Leu525 and the 18-methyl group of E₂ is conveniently replaced by a similar interaction with the ethyl substituent of pyrazole **5** (Fig 5B).

By contrast, in the complex with pyrazole **2**, the ethyl substituent is oriented in a different position (downward), where it no longer benefits as much from a favorable hydrophobic-hydrophobic interaction, as was the case in the complex with pyrazole **5**. Leu525 is somewhat closer to the pyrazole core, where it interacts with the N(1) phenyl ring. The closest residue for interaction with the C(4) ethyl of pyrazole **2** (Fig. 5A) is Met388. This residue is a somewhat “softer” partner for interaction than Leu525, and may be less stabilizing. Other differences between the ER complexes with pyrazoles **2** and **5** which could account for their differing binding affinity may have to do with electronic effects and are not considered in these models. As noted earlier (Fig. 4), the positions of the nitrogen atoms are different between the two binding modes, so the

electronic molecular surfaces that are presented to the receptor are predicted to be quite different.

Conclusions

We have prepared a series of basic side chain-substituted pyrazoles as potential selective antagonists for ER subtypes. The initial four analogs were designed to explore the four possible orientations that the pyrazole core structure might adopt in the ER ligand binding pocket, and thereby to identify which site on the pyrazole could best accommodate the rather large, basic side chain substituent. Of the four analogs, the C(5) piperidinyl ethoxy-substituted pyrazole **5** was found to have the highest affinity for ER α , with an affinity among the highest observed for all ER ligands of the pyrazole type. It also shows considerable affinity selectivity for ER α vs ER β . Through cell-based transfection assays, we found that pyrazole **5** was an antagonist on both ER α and ER β , and that its potency on ER α was somewhat higher, reflecting its ER α affinity selectivity. Modeling studies using the crystal structure of the ER α -raloxifene complex were used to compare potential binding modes for pyrazoles **2** and **5**. The binding modes appear to be quite similar, and the origin of the higher affinity for pyrazole **5** vs. **2** may result from a more favorable positioning of the ethyl group in the binding pocket in the complex with pyrazole **5**. In work to be presented elsewhere, we have prepared additional analogs of pyrazole **5** having other basic and polar side chains as substituents on the C(5) phenyl group.¹⁸ Some of these have very high affinity selectivity for ER α over ER β , and they act as ER α potency selective antagonists (J. Sun, et al. In preparation). This work is the first effort towards developing a novel SERM based on a pyrazole core structure.

Experimental Methods

General

Melting points were determined on a Thomas-Hoover UniMelt capillary apparatus and are uncorrected. All reagents and solvents were obtained from Aldrich, Fisher or Mallinckrodt. Tetrahydrofuran was freshly distilled from sodium/benzophenone. Dimethylformamide was vacuum distilled prior to use, and stored over 4 Å molecular sieves. *n*-Butyllithium was titrated with *N*-pivaloyl-*o*-toluidine. Et₃N was stirred with phenylisocyanate, filtered, distilled, and stored over 4 Å molecular sieves. All reactions were performed under a dry N₂ atmosphere unless otherwise specified. Reaction progress was monitored by analytical thin-layer chromatography using GF silica plates purchased from Analtech. Visualization was achieved under illumination with short wave UV light (254 nm) or with a potassium permanganate indicator spray. Radial preparative-layer chromatography was performed on a Chromatotron instrument (Harrison Research, Inc., Palo Alto, CA) using EM Science silica gel Kieselgel 60 PF₂₅₄ as adsorbent. Flash column chromatography was performed using Woelm 32-63 µm silica gel packing. The preparation of pyrazole **5** by a regioselective route is described elsewhere.¹⁸

¹H and ¹³C NMR spectra were recorded on either a Varian Unity 400 or 500 MHz spectrometers using CDCl₃, or MeOD-*d*₄ as solvent. Chemical shifts were reported as parts per million downfield from an internal tetramethylsilane standard (δ 0.0 for ¹H) or relative to solvent peaks. NMR coupling constants are reported in Hertz. ¹³C NMR were determined using either the Attached Proton Test (APT) or standard ¹³C pulse sequence parameters. Low resolution and high resolution electron impact mass spectra were obtained on Finnigan MAT CH-5 or 70-VSE spectrometers. Elemental analyses were performed by the Microanalytical Service Laboratory of the University of Illinois. Single crystal X-ray analysis on pyrazole **4** was performed to determine connectivity. A rigorous analysis was not performed because of the presence of a disordered solvent molecule in the unit cell. However, for the purposes of regiochemical assignment, the analysis was satisfactory.

Biological Procedures

Relative Binding Affinity Assay. Ligand binding affinities (RBAs) using lamb uterine cytosol as a receptor source were determined by a competitive radiometric binding assay using 10 nM [3 H]estradiol as tracer and dextran-coated charcoal as an adsorbent for free ligand, as previously described.²¹ Binding affinities with purified recombinant human ER α and ER β were determined by a competitive radiometric binding assay using 10 nM [3 H]estradiol as tracer, commercially available ER α and ER β preparations (PanVera Inc. Madison, WI), and hydroxylapatite (HAP) to adsorb bound receptor-ligand complex.²⁰ HAP was prepared following the recommendations of Williams and Gorski.²² All incubations were done at 0 °C for 18-24h. Binding affinities are expressed relative to estradiol (RBA = 100%) and are reproducible with a coefficient of variation of 0.3.

Transcriptional Activation Assay Human endometrial cancer (HEC-1) cells were maintained in culture and transfected as described previously.^{23,24} Transfection of HEC-1 cells in 60 mm dishes used 0.4 mL of a calcium phosphate precipitate containing 0.5 μ g of pCMV β Gal as internal control, 2 μ g of the reporter gene plasmid, 100 ng of the ER expression vector, and carrier DNA to a total of 5 μ g DNA. Compounds were added to the cell culture media as ethanol solutions so as to yield a final ethanol concentration of 0.1%. CAT activity, normalized for the internal control β -galactosidase activity, was assayed as previously described.^{23,24}

Molecular Modeling

Small molecule modeling. The starting structures of pyrazoles **2** and **5** used for the ER-LBD docking studies were generated from random conformational searches using the TRIPOS force field as implemented in Sybyl 6.5.2. Low energy conformers then underwent full minimization until a convergence criterion of 0.001 kcal/mol was met

using the AM1 semi-empirical force field. Charge calculations were done using Gasteiger-Huckel method and molecular surface properties displayed using MOLCAD module in Sybyl 6.5.2.

Receptor docking studies. The lowest energy conformers for pyrazoles **2** and **5**, generated as indicated above, were used for docking studies. Prior to docking, a +1 formal charge and a proton were added to each piperidinyll nitrogen. Ligands were then pre-positioned in the crystal structure of the ER α -raloxifene complex,² using a least squares multifitting of the most congruent atoms of the pyrazole and raloxifene. In raloxifene this included the A-ring carbon atoms and the 1,4-carbon atoms in both the 2 and 3-substituted phenyl groups. The same fitting strategy was used in the pyrazoles, all six carbon atoms in the ring corresponding to the A-ring and the 1,4-carbon atoms of the other two aryl rings. Once pre-positioned, the raloxifene structure was deleted and then the pyrazole ligand was optimally docked in the ER α binding pocket using the TRIPOS Flexidock routine. Hydrogen bond donors (Arg394, His524) and hydrogen bond acceptors (Glu353, His524, and Asp351) in ER were indicated in Flexidock, as well as the hydrogen bond donors and acceptors in the ligand. Side chains that were allowed to rotate during docking of the pyrazoles **2** and **5** included Met543, Leu539, Leu536, Leu354, Asp351, Trp383, all of which are near the basic side chain group; Phe404, Leu387, and Met388, which are near the A-ring mimic; Leu384, Leu346, Leu428, and Trp383, which are near the B/C ring region; and Ile424, His524, and Leu525, which are near the D-ring subpocket. Arg394 and Glu353, the hydrogen bonding partners of the critical A-ring phenol mimic, were kept fixed during the entire docking and minimization.

The best docked ligand ER-LBD complex from the Flexidock routine then underwent a three-step minimization: First, non-ring torsional bonds of the ligand were minimized in the context of the receptor, using the torsmin command. This was followed by minimization of the side chain residues within 8 Å of the ligand while holding the

backbone and residues Glu353 and Arg394 fixed. A final, third minimization of both the ligand and receptor was conducted using the Anneal function (hot radius 8 Å, interesting radius 16 Å), again holding residues Glu353 and Arg394 fixed. The result of this was considered to be the final model. Minimizations were done using the TRIPOS Forcefield (MAXIMIN) with the Powell gradient method and default settings (final RMS <0.05 kcal/mol·Å). The total energy for the ER α complex with pyrazole **2** was -806 kcal/mol and for the complex with pyrazole **5** was -868 kcal/mol. At this level of refinement, these numbers cannot be used to predict relative binding affinities. However, they indicate that there are no serious errors or unfavorable contacts in the ER-LBD ligand models.

Chemical Synthesis

1-[4-(2-*N*-piperidinyl-ethoxy)-phenyl]-3,5-di-(4-hydroxyphenyl)-4-ethyl-pyrazole (2**).**

To a stirred solution of the protected pyrazole **9** (100 mg, 0.19 mmol) in CH₂Cl₂ (1.0 mL) at 0 °C was added BBr₃ (1.0 M CH₂Cl₂, 5 equiv, 0.95 mL) dropwise. The reaction was kept at 0 °C for 4h and then quenched with water. The solution was neutralized with sat. NaHCO₃ and then repeatedly extracted with EtOAc. The combined organic layers were washed with brine, dried over Na₂SO₄ and concentrated to afford a tan residue. Purification by flash chromatography (5% TEA and 5% MeOH in CH₂Cl₂) afforded **2** as an off-white powder (75%): mp 125-130 °C (decomposed); ¹H NMR (CDCl₃, 400 MHz) δ 0.98 (t, 3H, *J* = 7.3), 1.51 (br s, 2H), 1.62 (quint, 4H, *J* = 5.5), 2.58 (q, 2H, 7.5), 2.67 (br s, 4H), 2.89 (t, 2H, *J* = 5.5), 4.13 (t, 2H, *J* = 5.5), 6.76 (d, 2H, *J* = 8.5), 6.87 (d, overlapping, 2H, *J* = 8.5), 6.88 (d, overlapping, 2H, *J* = 9), 7.03 (d, 2H, *J* = 8.5), 7.16 (d, 2H, *J* = 9.0), 7.49 (d, 2H, *J* = 8.5); APT ¹³C NMR (CDCl₃, 100 MHz) δ 9.9 (CH₃), 18.5 (CH₂), 24.8 (CH₂), 26.2 (CH₂), 54.1 (CH₂), 56.1 (CH₂), 58.8 (CH₂), 116.1 (CH), 116.8 (CH), 116.9 (CH), 121.4 (C), 123.1 (C), 126.8 (C), 128.5 (CH), 130.9 (CH), 133.0 (CH), 135.2 (C), 144.0 (C), 152.6 (C), 159.1 (C), 159.4 (C), 159.5 (C); MS (EI, 70 eV) *m/z* 483.3 (M⁺); HRMS (EI) calcd for C₃₀H₃₃N₃O₂ (M⁺-HBr): 483.2522. Found: 481.2365 (M⁺-

HBr-2)

4-(4-*N*-Piperdiny-butyl)-3,5-di-(4-hydroxyphenyl)-1-phenylpyrazole hydrochloride

(3). To a stirred CH₂Cl₂ (1.0 mL) solution of the protected pyrazole **13** (72 mg, 0.15 mmol) was added AlCl₃ (116 mg, 0.87 mmol). The mixture was cooled to 0 °C and EtSH (55 µL, 0.73 mmol) added dropwise. The mixture was then allowed to reach room temperature and stir for an additional 0.5 h. At this time the reaction was concentrated under a stream of nitrogen in a fume hood, brought up in CH₂Cl₂ and concentrated once again. The crude mixture was re-dissolved in CH₂Cl₂ and a mixture of THF (1 mL), water (1 mL), and 6 M HCl (0.25 mL) added. The resulting precipitate was isolated by vacuum filtration and was washed with four 5 mL portions of water followed by four 5 mL portions of ether to afford pyrazole **3** as a white solid (37 mg, 54%): ¹H NMR (MeOD-*d*₄, 500 MHz) δ 1.30-1.60 (m, 6H), 1.75 (br s, 6H), 2.73 (t, 2H, *J* = 7.2), 2.78 (t, 4H, *J* = 8.1), 6.90 (XX' of AA'XX', 2H, *J*_{AX} = 8.8, *J*_{XX''} = 2.5), 7.07 (AA' of AA'XX', 2H, *J*_{AX} = 8.8, *J*_{AA'} = 2.5), 7.23-7.36 (m, 5H), 7.32 (XX' of AA'XX', 2H, *J*_{AX} = 8.6, *J*_{XX''} = 2.4), 7.52 (AA' of AA'XX', 2H, *J*_{AX} = 8.6, *J*_{AA'} = 2.2); ¹³C NMR (MeOD-*d*₄, 125 MHz) δ 21.5, 22.5, 22.3, 23.0, 27.0, 52.8, 56.6, 115.1, 115.2, 117.4, 121.1, 124.8, 124.9, 127.0, 127.3, 128.5, 131.2, 139.8, 142.4, 151.5, 157.5, 157.9; MS (EI, 70 eV) *m/z* (relative intensity, %): 467 (M⁺-HCl, 21); HRMS (EI, M⁺) calcd for C₃₀H₃₃N₃O₂: 467.2573. Found: 467.2579.

1-(4-hydroxyphenyl)-3-[4-(2-*N*-piperidinyl-ethoxy)-phenyl]-4-ethyl-5-(4-hydroxy-phenyl)-1*H*-pyrazole (4). A CH₂Cl₂ solution (10 mL) of the crude protected pyrazole isomers (300 mg, 0.60 mmol) prepared from the 1,3-dione **15** was cooled to 0 °C and treated dropwise with BBr₃ (1M in hexane, 5 equiv, 3 mmol). The reaction was allowed to reach temperature and stir overnight. The mixture was re-cooled to 0 °C and quenched with 5 mL H₂O and the solvent removed under reduced pressure. To the crude mixture 8

mL of H₂O was added and the aqueous layer neutralized with a sat. aqueous NaHCO₃ solution and extracted repeatedly with EtOAc (5 X 20 mL). The organic layers were washed with brine, dried over Na₂SO₄ and concentrated in vacuo to afford a brown residue. Pyrazole **4** was cleanly separated from the regioisomer **5** and other byproducts by flash chromatography (7% Et₃N and 7% MeOH in CH₂Cl₂). It was further purified by recrystallization from MeOH to afford the C(3) isomer (**4**) as small white crystals whose structure was verified by X-ray analysis (23%): Pyrazole **4**-mp 151–153 °C; ¹H NMR ((CD₃)₂SO, 400 MHz) δ 1.01 (t, 3H, *J* = 7.6), 1.43 (m, 2H), 1.55 (m, 4H), 2.49 (br s, 4H), 2.59 (q, 2H, *J* = 7.6), 2.72 (t, 2H, *J* = 5.6), 4.15 (t, 2H, *J* = 6.0), 6.74 (d, 2H, *J* = 8.4), 6.83 (d, 2H, *J* = 8.4), 7.08 (apparent triplet due to three overlapping doublets, 6H, *J* = 7.6), 7.67 (d, 2H, *J* = 8.4), 9.71 (br s, 2H, OH exchangeable with D₂O); APT ¹³C NMR ((CD₃)₂SO, 100 MHz) δ 15.4 (CH₃), 16.8 (CH₂), 23.9 (CH₂), 25.6 (CH₂), 54.5 (CH₂), 57.5 (CH₂), 65.6 (CH₂), 114.5 (CH), 115.1 (CH), 115.4 (CH), 118.7 (C), 120.9 (C), 126.1 (CH), 126.5 (C), 128.5 (CH), 131.2 (CH), 131.8 (C), 141.2 (C), 148.5 (C), 156.2 (C), 157.4 (C), 157.9 (C); HRMS (EI, M⁺) calcd for C₃₀H₃₃N₃O₃: 483.2521. Found: 483.2516.

As was noted in the text, isolation of the other regioisomer (pyrazole **5**) from this reaction mixture was complicated by the fact that it could not be separated effectively from the triphenolic byproduct that resulted from partial cleavage of the basic side chain during the BBr₃ deprotection. This compound was prepared in a regioselective fashion by another route that is described elsewhere.¹⁸

1-Bromo-4-(2-*N*-piperidinyl-ethoxy)benzene (7). In 250 mL flask charged with Ph₃P (35 mmol) in 60 mL of THF at 0 °C was added di-*iso*-propyl-azodicarboxylate (DIAD, 35 mmol) reagent dropwise. The solution was kept at 0 °C and stirred for 50 min. At this time *N*-(2-hydroxyethyl)-piperidine was added dropwise via syringe. After 10 min, *p*-bromophenol (35 mmol) and TEA (86.7 mmol) in 20 mL THF was added dropwise via

an addition funnel. After 1h at 0 °C the reaction was warmed to rt and stirred for 6 h. The crude mixture was then concentrated in vacuo and the Ph₃PO byproduct removed by vacuum filtration. The filtrate was again concentrated and the product purified by gradient flash chromatography using 5% TEA and 30% EtOAc in hexanes up to 5% TEA and 50% EtOAc in hexanes to afford **7** as a clear oil:²⁵ ¹H NMR (CDCl₃, 500 MHz) δ 1.41 (m, 2H), 1.58 (m, 4H), 2.47 (br s, 4H), 2.72 (d, 2H, *J* = 7.2), 4.05 (d, 2H, *J* = 7.6), 6.79 (d, 2H, 8.3), 7.82 (d, 2H, *J* = 8.1); ¹³C NMR (CDCl₃, 125 MHz) δ 22.1, 38.0, 67.5, 113.0, 116.5, 121.8, 123.8, 132.3, 136.6, 149.6, 158.0, 158.3; MS (EI, 70 eV) *m/z* 284 (M⁺).

***N,N'*-di-*tert*-Butoxycarbonyl-*N*-[4-(2-*N*-piperidinyl-ethoxy)phenyl]hydrazine (**8**)**. To a THF solution at -70 °C containing the substituted bromobenzene **7** (10.56 mmol) was added *n*-BuLi (1.3 equiv) dropwise over 10 min. After 30 min, *tert*-butoxycarbonylazodicarboxylate (15.84 mmol) was added as a solid in one portion. The mixture was then slowly warmed to rt and 1 equiv of dilute AcOH acid added. After stirring the quenched mixture for 30 min, the reaction was partitioned between water (30 mL) and Et₂O (50 mL). The layers were separated and the aqueous layer extracted twice more with Et₂O (2 X 50 mL). The combined organic layers were washed with brine and dried over Na₂SO₄. Subsequent solvent removal afforded 6.8 g of a crude red oil. Flash chromatography (5% TEA and 25% EtOAc in hexanes) produced **8** as a white solid (75%): mp 50–55 °C; (Note: spectrum complicated by Boc rotamers) ¹H NMR (CDCl₃, 400 MHz) δ 1.38 (s, 9H), 1.40 (overlapping s, 11H), 1.61 (m, 4H), 2.45 (m, 4H), 2.73 (t, 2H, *J* = 5.6), 4.05 (t, 2H, *J* = 5.3), 6.82 (d, 2H, *J* = 7.8), 7.25 (br s, 2H); ¹³C NMR (CDCl₃, 100 MHz) δ 24.2 (CH₂), 24.8 (CH₂), 28.2 (CH₃), 28.3 (CH₃), 36.8 (CH₂), 46.0 (CH₂), 46.7 (CH₂), 55.1 (CH₂), 57.8 (CH₂), 60.4 (CH₂), 65.7 (CH₂), 66.0 (CH₂), 81.0 (CH₂), 81.8 (CH₂), 113.9 (CH), 114.6 (CH), 120.7 (CH), 129.4 (CH), 156.7 (C), 158.7

(C), 171.2 (C); MS (EI, 70 eV) m/z 435.4 (M^+ , 35%); Anal. ($C_{23}H_{37}N_3O_5$): C, 63.42; H, 8.56; N, 9.65. Found: C, 63.20; H, 8.72; N, 9.47.

1-[4-(2-*N*-Piperidinyl-ethoxy)-phenyl]-3,5-bis-(4-methoxyphenyl)-4-ethyl-1*H*-

pyrazole (9). To a stirred solution of DMF (14 mL), THF (6 mL), and 1,3-bis-(4-methoxyphenyl)-2-ethyl-propane-1,3-dione (500 mg, 1.52 mmol)¹⁵ was added hydrazine **8** in 3-fold excess (800 mg, 4.59 mmol). The mixture was brought to reflux for 5h and then recooled to rt. The THF was removed under reduced pressure and the remaining residue diluted with H₂O (30 mL) and extracted repeatedly with EtOAc. The organic layers were washed with brine, dried over Na₂SO₄ and concentrated to produce a crude red-orange oil. Flash chromatography using 10% TEA and 20% EtOAc in hexanes afforded the pure product **9** as an orange oil (65%): ¹H NMR (CDCl₃, 400 MHz) δ 1.03 (t, 3H, J = 8.1), 1.42 (m, 2H), 1.58 (quin, 4H, J = 6); 2.47 (br s, 2H), 2.61 (q, 2H, J = 6.2), 2.72 (t, 2H, J = 6), 3.79 (s, 3H), 3.82 (s, 3H), 4.04 (t, 2H, J = 6.2), 6.76 (d, 2H, J = 9.0), 6.86 (d, 2H, J = 9.0), 6.96 (d, 2H, J = 9.1), 7.13 (d, 2H, J = 9.1), 7.16 (d, 2H, J = 9.1), 7.69 (d, 2H, J = 9.0); ¹³C NMR (CDCl₃, 100 MHz) δ 15.6 (CH₃), 17.2 (CH₂), 24.3 (CH₂), 26.0 (CH₂), 55.1 (CH₃), 55.2 (CH₃), 57.9 (CH₂), 66.2 (CH₂), 113.8 (CH), 113.9 (CH), 114.5 (CH), 119.9 (C), 123.3 (C), 126.0 (CH), 126.9 (C), 129.0 (CH), 131.3 (CH), 133.6 (C), 141.0 (C), 150.1 (C), 157.4 (C), 159.1 (C), 159.4 (C); HRMS (EI, M^+) calcd for C₃₂H₃₇N₃O₂: 511.2834. Found: 511.2825.

6-Bromo-1-(4-methoxy-phenyl)-hexan-1-one (10). To a stirred solution of AlCl₃ (12.40 g, 92.75 mmol) in 1,2-dichloroethane (30 mL) at 0 °C was added 6-bromohexanoyl chloride (23.70 g, 17 mL, 111.30 mmol) dropwise over 10 minutes. The resulting solution was stirred at room temperature for 0.5 h, cooled to -15 °C and a solution of anisole (10.00 g, 10.05 mL, 92.75 mmol) in 1,2-dichloroethane (10 mL) was added dropwise over 20 minutes. The reaction mixture was allowed to stir at -15 °C for 1

h, then quenched with H₂O (50 mL). The aqueous layer was isolated and extracted with CH₂Cl₂ (2 X 50 mL), and the organic layers were combined and washed with H₂O (2 X 50 mL), saturated NaHCO₃ (2 X 50 mL), and brine (2 X 50 mL). Subsequent drying over Na₂SO₄ and solvent removal in vacuo afforded a crude orange oil. Upon standing at room temperature, large crystals formed after 48h. The crystals were isolated and rinsed with cold hexane to afford **10** (23 g, 87%): mp 50-52 °C; ¹H NMR (CDCl₃, 400 MHz) δ 1.52 (quint, 2H, *J* = 7.6), 1.76 (quint, 2H, *J* = 7.5), 1.91 (quint, 2H, *J* = 7.1), 2.94 (t, 2H, *J* = 7.3), 3.42 (t, 2H, *J* = 6.7), 3.87 (s, 3H), 6.93 (d, 2H, *J* = 8.8), 7.94 (d, 2H, *J* = 9.0); ¹³C NMR (CDCl₃, 100 MHz) δ 23.39, 27.79, 32.51, 33.59, 37.80, 55.34, 113.56, 129.88, 130.13, 163.24, 198.48; HRMS (EI, M⁺) calcd for C₁₃H₁₇O₂Br: 286.0391. Found: 286.0394.

1-(4-Methoxy-phenyl)-6-(*N*-piperidinyl)-hexan-1-one (11). To a stirred solution of ketone **10** (248 mg, 1.00 mmol) in DMF (30 mL) at 0 °C was added piperidine (170 mg, 0.20 mL, 2.00 mmol) dropwise over 5 min. The solution was placed in a 70 °C oil bath for 4h and then cooled to room temperature. The crude mixture was concentrated under reduced pressure to remove a majority of the DMF and excess piperidine to afford an orange residue. The residue was taken up in CH₂Cl₂ (30 mL), washed with brine (2 X 20 mL), dried over MgSO₄ and concentrated under reduced pressure to afford **11** as a white solid (227 mg, 79%): mp 163-165 °C; ¹H NMR (CDCl₃, 500 MHz) δ 1.35-1.45 (m, 2H), 1.65-2.00 (m, 8H), 2.26 (br q, 2H, *J* = 8), 2.59 (br q, 2H, *J* = 7), 2.88-2.96 (m, 4H), 3.51 (br d, 2H), 3.88 (s, 3H), 6.93 (d, 2H, *J* = 8.9), 7.93 (d, 2H, *J* = 8.9); ¹³C NMR (CDCl₃, 100 MHz) δ 22.1, 22.3, 23.3, 23.4, 26.4, 37.5, 53.1, 55.5, 57.2, 113.8, 129.9, 130.3, 163.5, 198.5; MS (EI, 70 eV) *m/z* (relative intensity, %): 289 (M⁺, 3); HRMS (EI, M⁺) calcd. for C₁₉H₂₇NO₂: 289.2042. Found: 289.2060.

1,3-Bis-(4-methoxy-phenyl)-2-(4-*N*-piperidinyl-butyl)-propane-1,3-dione (12). To a solution of ketone **11** (350 mg, 1.21 mmol) and TMEDA (140.6 mg, 0.18 mL, 1.21 mmol) in THF (15 mL) at 0 °C was added a 1.0 M solution of LiHMDS (3.02 mL, 3.02 mmol) dropwise. The solution was allowed to stir at room temperature for 0.5 h, then was cooled back to 0 °C. At this time a solution of 4-nitrophenyl 4-methoxybenzoate (990 mg, 3.63 mmol; prepared from *p*-nitrophenol and 4-methoxybenzoic acid using DIC and DMAP coupling conditions) in THF (5 mL) was added dropwise. The resulting solution was allowed to stir for 15 h at room temperature and 4 h at reflux (oil bath temperature of 70 °C). At this time the mixture was allowed to come to room temperature and quenched by the addition of H₂O (10 mL). The organic layer was isolated and washed with H₂O (3 X 15 mL), dried over Na₂SO₄, and concentrated under reduced pressure to afford a yellow solid. The remaining ester was removed by warming the crude mixture in 15% ethyl acetate/hexanes and filtering off the excess crystalline ester. The filtrate was concentrated under reduced pressure and purified by flash chromatography (10% TEA and 55% EtOAc in hexanes) to afford **12** as a yellow oil (227 mg, 51%): ¹H NMR (CDCl₃, 400 MHz) δ 1.22-1.48 (m, 4H), 1.50-1.75 (m, 6H), 2.10 (q, 2H, *J* = 7.5), 2.34 (t, 2H, *J* = 9.8), 2.42 (br s, 4H), 3.83 (s, 6H), 5.05 (t, 1H, *J* = 6.6), 6.89 (d, 4H, *J* = 8.9), 7.94 (d, 4H, *J* = 8.9); ¹³C NMR (CDCl₃, 100 MHz) δ 24.0, 25.3, 26.1, 26.3, 29.3, 54.3, 55.4, 57.0, 58.7, 113.9, 128.9, 128.9, 130.8, 130.8, 163.6, 194.6.

3,5-Bis-(4-methoxyphenyl)-4-(4-*N*-piperidinyl-butyl)-1-phenyl-1*H*-pyrazole (13). To a stirred solution of DMF (45 mL), THF (20 mL), and β-diketone **12** (170 mg, 0.40 mmol) was added phenylhydrazine hydrochloride (289 mg, 2.00 mmol). The solution was brought to reflux (oil bath temperature between 110 - 120 °C) for 22 h. The reaction mixture was allowed to cool to room temperature, and the THF was evaporated under reduced pressure. The remaining mixture was diluted with H₂O (40 mL) and extracted with EtOAc (3 X 40 mL). The organic layers were combined and washed with saturated

LiCl (3 X 40 mL), saturated NaHCO₃ (2 X 40 mL), H₂O (2 X 40 mL), and brine (2 X 40 mL). The organic layer was dried over MgSO₄ and concentrated under reduced pressure to afford a crude brown oil. Purification by flash chromatography (10% TEA and 55% EtOAc in hexanes) afforded **13** as a reddish oil (79 mg, 40 %). Compound **13** was verified by ¹H NMR and used in the next step of the reaction scheme without further characterization.

1-[4-(2-*N*-Piperidinyl-ethoxy)-phenyl]-butan-1-one (14). To a solution of PPh₃ (10.05 g, 38.31 mmol) in THF (150mL) at 0 °C was added diisopropyl azodicarboxylate (7.5 mL, 38.31 mmol) dropwise. After stirring at 0 °C for 50 min. *N*-piperidineethanol (5.09 mL, 38.31 mmol) was added followed 10 min later by addition of a solution of 4-hydroxy-butyrophenone (5.24 g, 31.9 mmol) in Et₃N (13.4mL, 95.8 mmol) and THF (30 mL). The mixture was allowed to warm to rt and stir overnight and then concentrated in vacuo. To the crude residue were added Et₂O (150 mL) and the insoluble Ph₃PO by-product removed by filtration. The filtrate was concentrated once again and the residue purified by flash chromatography (10% TEA and 25% EtOAc in hexanes) to afford an oil. This material was dissolved in Et₂O (60 mL) and acidified with HCl (4M in dioxane, 6.3 mL). The precipitate that formed was collected by vacuum filtration and partitioned between saturated NaHCO₃ (35 mL) and ether (50 mL). The organic layer was washed with brine, dried over Na₂SO₄ and concentrated under reduced pressure to give **14** as pale yellow crystals (3.05 g, 35%). An analytically pure sample was obtained by recrystallization from hexane: mp 48-50 °C; ¹H NMR (CDCl₃, 400 MHz) δ 0.99 (t, 3H, *J* = 7.5), 1.43-1.49 (m, 2H), 1.64 (quint, 4H, *J* = 5.9), 1.75 (sext, 2H, *J* = 7.6), 2.55 (br s, 4H), 2.87 (t, 2H, *J* = 5.9), 2.90 (t, 2H, *J* = 7.2), 4.19 (t, 2H, *J* = 6.0), 6.93 (XX' of AA'XX', 2H, *J*_{AX} = 8.9, *J*_{XX'} = 2.5), 7.93 (AA' of AA'XX', 2H, *J*_{AX} = 9.0, *J*_{AA'} = 2.5); ¹³C NMR δ 14.1, 18.2, 24.2, 26.0, 40.4, 55.3, 57.9, 66.3, 114.4, 130.5, 162.7, 199.2; HRMS calcd for C₁₇H₂₆NO₂: 276.1963. Found: 276.1964.

2-Ethyl-1-(4-methoxyphenyl)-3-[4-(2-*N*-piperidinyl-ethoxy)-phenyl]-propane-1,3-dione (15). To a THF (25 mL) solution of ketone **14** (500 mg, 1.82 mmol) and 4-nitrophenyl 4-methoxybenzoate (745.3 mg, 2.73 mmol) at 0 °C was added LiHMDS (1M solution in hexane, 4.55 ml, 4.55 mmol) dropwise. Upon complete addition of LiHMDS the solution was allowed to warm to rt and stir overnight. The reaction mixture was concentrated to near dryness and EtOAc (35 mL) added. The crude mixture was washed sequentially with saturated NaHCO₃ and brine. The solvent was dried over Na₂SO₄, removed in vacuo and the resulting oil purified via flash chromatography (10% TEA and 50% EtOAc in hexanes) to give **15** as a viscous red oil (465 mg, 63%): ¹H NMR (CDCl₃, 400 MHz) δ 1.03 (t, J=7.31), 1.49 (br s, 2H), 1.70 (br s, 4H), 2.16 (quint, J=7.29Hz, 2H), 2.63 (br s, 4H), 2.90 (br s, 2H), 3.85 (s, 3H), 4.25 (br s, 2H), 4.96 (t, J=6.76Hz, 1H), 6.91 (d, J=9.05Hz, 4H), 7.95(d, J=8.96Hz, 2H), 7.96 (d, J=8.85Hz, 2H); ¹³C NMR (CDCl₃, 125 MHz) δ 12.8, 23.1, 24.0, 25.8, 55.0, 55.4, 57.6, 59.0, 66.2, 113.9, 114.5, 116.5, 129.2, 129.3, 130.9, 131.0, 163.0, 163.7, 194.9; HRMS (EI, M⁺) calcd for C₂₅H₃₁NO₄: 409.2253. Found: 407.2096 (M⁺-2).

Acknowledgments

We are grateful for support of this research through grants from the U. S. Army Breast Cancer Research Program (DAMD17-97-1-7076) and the National Institutes of health (PHS 5R37 DK15556 [to J.A.K.], PHS 5R37 CA18119 [to B.S.K.], PHS T32 CA09067 [trainineeship for Y.R.H.]). We thank Kathryn E. Carlson for performing binding assays and Rosanna Tedesco for help with molecular graphics. NMR spectra were obtained in the Varian Oxford Instrument Center for Excellence NMR Laboratory. Funding for this instrumentation was provided in part from the W. M. Keck Foundation and the National Science Foundation (NSF CHE 96-10502). Mass spectra were obtained on instruments supported by grants from the national Institute of General Medical Sciences (GM 27019), the National Institute of Health (RR 01575), and the National Science Foundation (PCM 8121494).

References

1. Grese, T. A.; Dodge, J. A. *Curr. Pharm. Design* **1998**, *4*, 71.
2. Brzozowski, A. M.; Pike, A. C.; Dauter, Z.; Hubbard, R. E.; Bonn, T.; Engström, O.; Öhman, L.; Greene, G. L.; Gustafsson, J.-A.; Carlquist, M. *Nature* **1997**, *389*, 753.
3. Shiau, A. K.; Barstad, D.; Loria, P. M.; Cheng, L.; Kushner, P. J.; Agard, D. A.; Greene, G. L. *Cell* **1998**, *95*, 927.
4. Darimont, B. D.; Wagner, R. L.; Apriletti, J. W.; Stallcup, M. R.; Kushner, P. J.; Baxter, J. D.; Fletterick, R. J.; Yamamoto, K. R. *Genes Develop.* **1998**, *12*, 3343.
5. Katzenellenbogen, J. A.; O'Malley, B. W.; Katzenellenbogen, B. S. *Mol. Endocrinol.* **1996**, *10*, 119.
6. McDonnell, D. P.; Clemm, D. L.; Hermann, T.; Goldman, M. E.; Pike, J. W. *Mol. Endocrinol.* **1995**, *9*, 659.
7. Paige, L. A.; Christensen, D. J.; Gron, H.; Norris, J. D.; Gottlin, E. B.; Padilla, K. M.; Chang, C.; Ballas, L. M.; Hamilton, P. T.; McDonnell, D. P.; Fowlkes, D. M. *Proc. Natl. Acad. Sci. U. S. A.* **1999**, *96*, 3999.
8. Norris, J. D.; Paige, L. A.; Christensen, D. J.; Chang, C. Y.; Huacani, M. R.; Fan, D.; Hamilton, P. T.; Fowlkes, D. M.; McDonnell, D. P. *Science* **1999**, *285*, 744.
9. Chang, C. Y.; Norris, J. D.; Gron, H.; Paige, L. A.; Hamilton, P. T.; Kenan, D. J.; Fowlkes, D.; McDonnell, D. P. *Mol. Cell Biol.* **1999**, *19*, 8226.
10. Kuiper, G.; Shughrue, P. J.; Merchenthaler, I.; Gustafsson, J. A. *Frontier Neuroendocrinol* **1998**, *19*, 253.
11. Kuiper, G. G. J. M.; Gustafsson, J.-A. *FEBS Letters* **1997**, *410*, 87.
12. Kuiper, G. G. J. M.; Carlsson, B.; Grandien, K.; Enmark, E.; Häggblad, J.; Nilsson, S.; Gustafsson, J.-Å. *Endocrinol.* **1997**, *138*, 863.
13. Fink, B. E.; Mortensen, D. S.; Stauffer, S. R.; Aron, Z. D.; Katzenellenbogen, J. A. *Chem. Biol.* **1999**, *6*, 205.

14. Stauffer, S. R.; Katzenellenbogen, J. A. *J. Combinat. Chem.* **2000**, *In Press*.
15. Stauffer, S. R.; Coletta, C. J.; Tedesco, R.; Sun, J.; Katzenellenbogen, B. S.; Katzenellenbogen, J. A. *J. Med. Chem.* **2000**, *Submitted*.
16. Stauffer, S. R.; Huang, Y.; Coletta, C. J.; Katzenellenbogen, J. A. *Biorg. Med. Chem.* **2000**, *Submitted*.
17. Magarian, R. A.; Overacre, L. B.; Singh, S.; Meyer, K. L. *Curr. Med. Chem.* **1994**, *1*, 61.
18. Huang, Y.; Katzenellenbogen, J. A. *Org. Lett.* **2000**, *Submitted*.
19. Demers, J. P.; Klaubert, D. H. *Tetrahedron Lett.* **1987**, *42*, 4933.
20. Carlson, K. E.; Choi, I.; Gee, A.; Katzenellenbogen, B. S.; Katzenellenbogen, J. A. *Biochemistry* **1997**, *36*, 14897.
21. Katzenellenbogen, J. A.; Johnson, H. J., Jr.; Myers, H. N. *Biochemistry* **1973**, *12*, 4085.
22. Williams, D.; Gorski, J. *Biochemistry* **1974**, *13*, 5537.
23. McInerney, E. M.; Weis, K. E.; Sun, J.; Mosselman, S.; Katzenellenbogen, B. S. *Endocrinol.* **1998**, *139*, 4513.
24. Sun, J.; Meyers, M. J.; Fink, B. E.; Rajendran, R.; Katzenellenbogen, J. A.; Katzenellenbogen, B. S. *Endocrinology* **1999**, *140*, 800.
25. Grese, T. A.; Pennington, L. D.; Sluka, J. P.; Adrian, M. D.; Cole, H. W.; Fuson, T. R.; Magee, D. E.; Phillips, D. L.; Rowley, E. R.; Shetler, P. K.; Short, L. L.; Venugopalan, M.; Yang, N. N.; Sato, M.; Glasebrook, A. L.; Bryant, H. U. *J. Med. Chem.* **1998**, *41*, 1272.

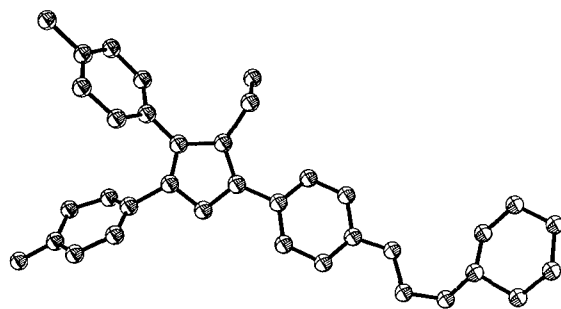


Figure 2. X-Ray crystal structure for **4** (ORTEP; ellipsoids drawn at the 35% probability level).

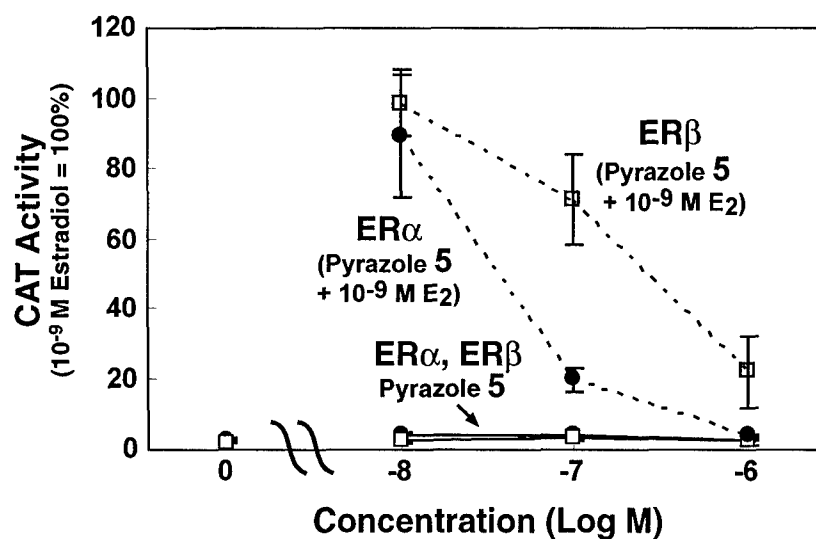


Figure 3. Transcription activation profile for pyrazole **5** with ER α and ER β . Human endometrial cancer (HEC-1) cells were transfected with expression vectors for ER α or ER β and an (ERE)₃-pS2-CAT reporter gene and were treated with indicated concentrations of pyrazole **5** alone (solid lines) or pyrazole **5** in the presence of 10⁻⁹ M estradiol (E₂) (dashed lines) for 24h. CAT activity was normalized for β -galactosidase activity from an internal control plasmid. Values are the mean \pm SD for three separate experiments, and are expressed as a percent of the ER α or ER β response with 10⁻⁹ M E₂, which is set at 100%. For some values, error bars are too small to be visible.

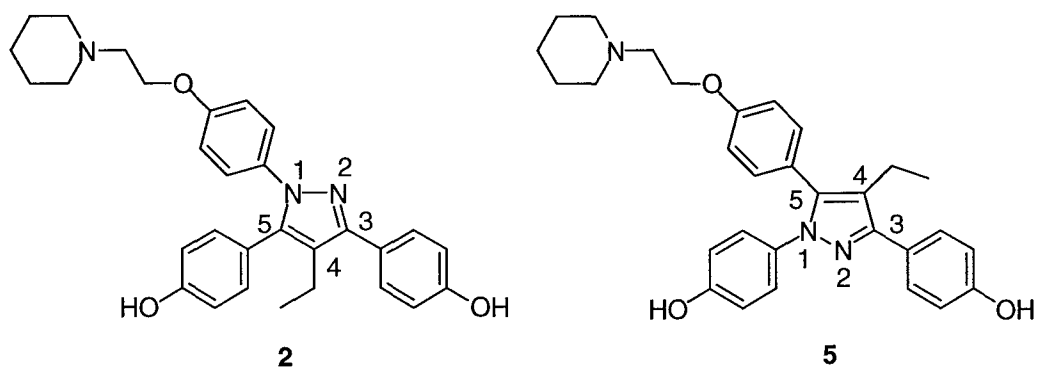


Figure 4. Pyrazoles **2** and **5** oriented with corresponding aryl rings oriented in a congruent fashion.

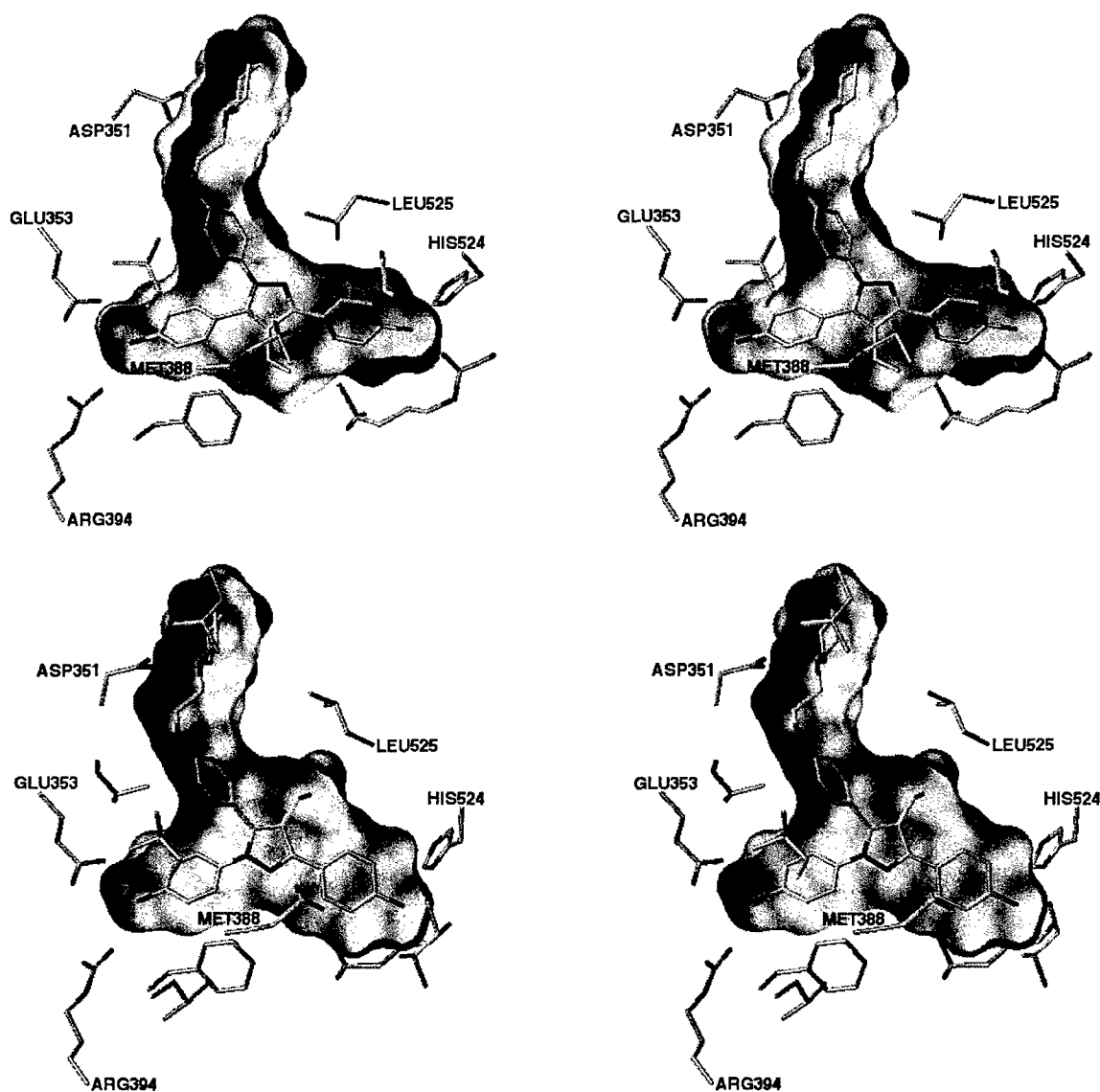
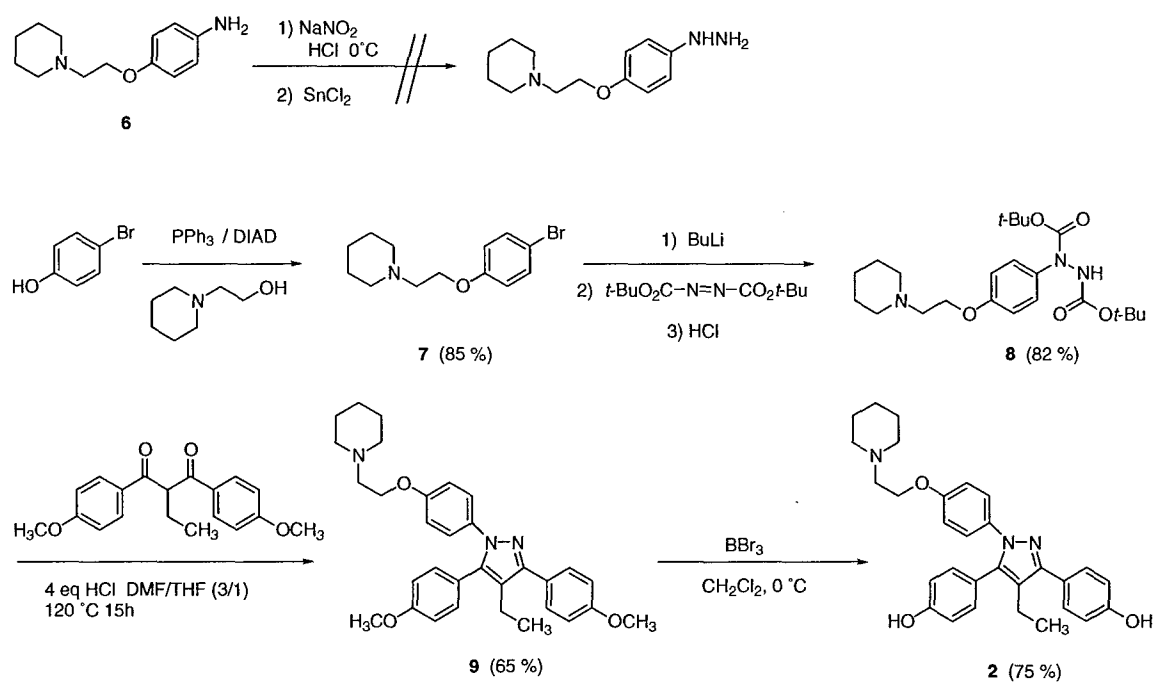
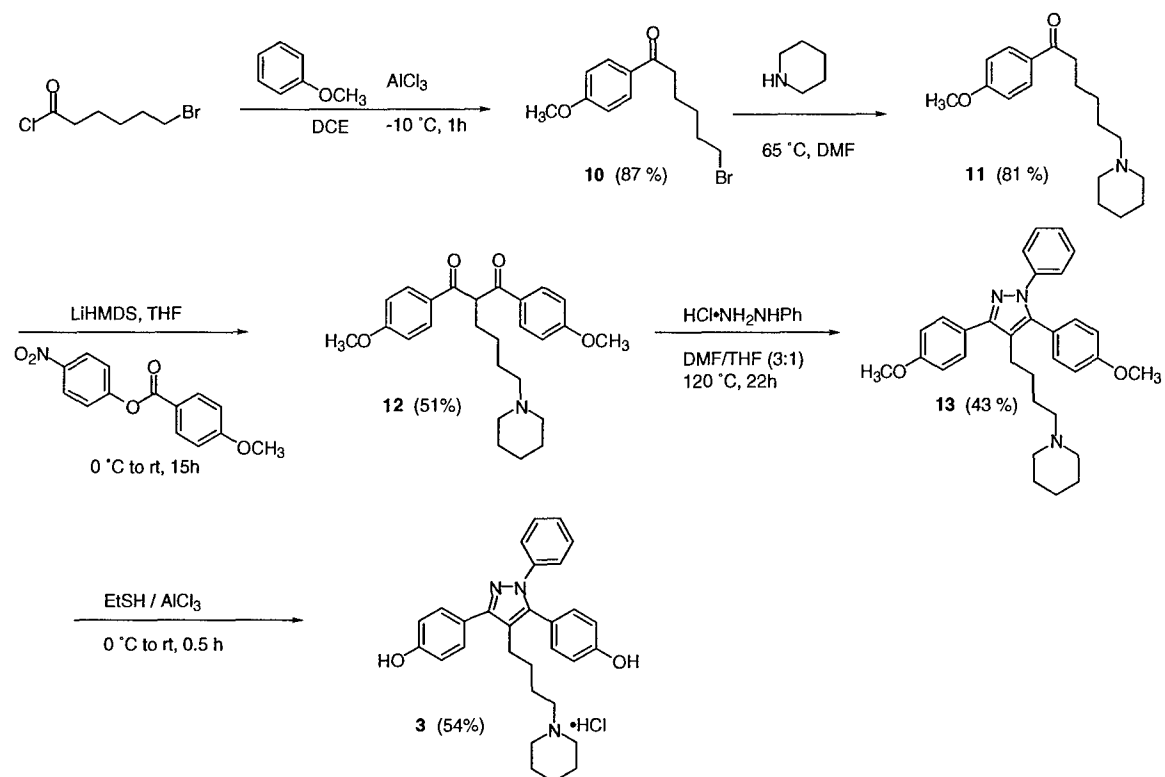


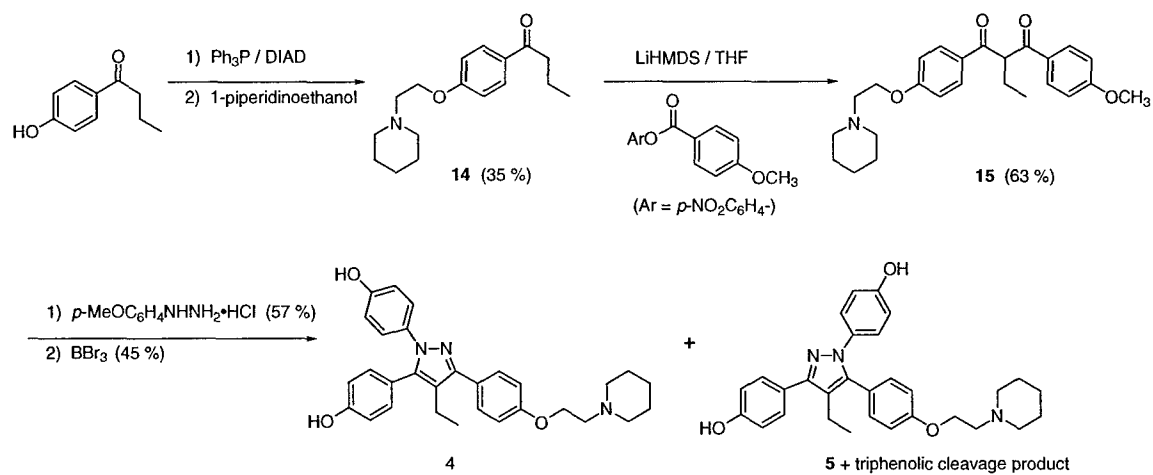
Figure 5. Crossed-stereo views of pyrazole **2** (top) and **5** (bottom) docked and minimized in ER α -raloxifene structure ligand binding pocket showing residues within 2.5 Å of ligand. The pyrazoles were initially positioned with respect to certain reference atoms of the ligand raloxifene, and then minimized together with the same contact residues in the protein using the Flexidock routine within SYBYL. For details, see the Experimental section. The yellow surface is a cutaway of the Connolly surface of the protein ligand-binding pocket.



Scheme 1. Synthesis of N(1) basic side chain containing pyrazole **2**.



Scheme 2. Synthesis of C(4) basic side chain containing pyrazole **3**.



Scheme 3. Synthesis of C(3) and C(5) basic side chain containing pyrazoles **4** and **5**.

Table 1. Estrogen Receptor Binding Affinity of Pyrazoles 1-5.

| Compound | Site of basic side chain | RBA lamb uterine cytosol ^a | RBA hER α ^a | RBA hER β ^a |
|----------|--------------------------|---------------------------------------|-------------------------------|------------------------------|
| 1 | [none] | 20.3 \pm 3 | 35.7 \pm 6 | 0.15 \pm 0.01 |
| 2 | N(1) | 1.5 \pm 0.4 | 0.65 \pm 0.13 | 0.13 \pm 0.03 |
| 3 | C(4) | 0.017 \pm 0.006 | 0.05 ^b | 0.019 ^b |
| 4 | C(3) | 0.29 \pm 0.26 | 0.13 ^b | 0.01 ^b |
| 5 | C(5) | 24.5 \pm 1 | 11.5 \pm 1 | 0.65 \pm 0.02 |

^aRelative binding affinity (RBA) where estradiol = 100%. Values are the average of repeat determinations \pm SD (n \geq 3) or \pm range (n = 2). For details of the assay procedure, see Experimental Methods. ^bSingle determinations.

Regioselective Synthesis of 1,3,5-Triaryl-4-Alkyl Pyrazoles, Novel Ligands for the Estrogen Receptor

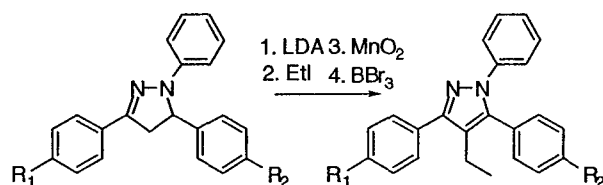
Ying R. Huang and John A. Katzenellenbogen

Department of Chemistry, University of Illinois, Urbana IL 61801

jkatzene@uiuc.edu

Received Date (will be automatically inserted after manuscript is accepted)

ABSTRACT



A regioselective synthesis of 4-alkyl-1,3,5-triarylpyrazoles has been developed for the preparation of unsymmetrically substituted systems of interest as ligands for the estrogen receptor.

In our efforts to discover novel ligands for the estrogen receptor (ER) that might act as selective estrogen receptor modifiers (SERMs),¹ we found that 1,3,5-triaryl-4-alkyl pyrazoles such as **1** and **2** (Scheme 1) were good ligands for ER, demonstrating high binding affinities and transcriptional efficacy that in some cases were very selective for the ER alpha subtype (ER α).^{2,3} Initially, we synthesized these pyrazoles by condensation of 2-alkyl-1,3-diketones with arylhydrazines.^{4,5,6} Of course, when the 1,3-diketones were unsymmetrical, this approach did

not afford any significant regioselectivity. This lack of regioselectivity became of concern when we needed the corresponding monophenols **3** and **4** for structure-activity studies to determine which phenol in pyrazole **2** mimics the A-ring of estradiol. According to a classical approach, the monophenol with the higher affinity can be presumed to be the one that corresponds to the A-ring of estradiol.^{7,8} However, when the original 1,3-dione-hydrazine condensation pyrazole synthesis was used to prepare these monophenols, only an inseparable mixture of the two regioisomers **3** and **4** was afforded (Scheme 1). Thus, a regioselective approach to these and related compounds was needed.

In a related effort, we wanted to develop these novel 1,3,5-triaryl-4-alkyl pyrazole ligands into the sort of mixed agonist/antagonists that typically have SERM

¹ Grese, T.A.; Dodge, J.A. *Current Pharmaceutical Design* **1998**, *4*, 71-92.

² Fink, B.E.; Mortensen, D.S.; Stauffer, S.R.; Aron, Z.D.; Katzenellenbogen, J.A. *Chem. Biol.* **1999**, *6*, 205-219.

³ Stauffer, S.R.; Katzenellenbogen, J.A. *J. Combinat. Chem.* **2000**, *2*, 318-329.

⁴ Fink, B.E.; Mortensen, D.S.; Stauffer, S.R.; Aron, Z.D.; Katzenellenbogen, J.A. *Chem. Biol.* **1999**, *6*, 205-219.

⁵ Stauffer, S.R.; Coletta, C.J.; Tedesco, R.; Sun, J.; Katzenellenbogen, B.S.; Katzenellenbogen, J.A. *J. Med. Chem.* submitted.

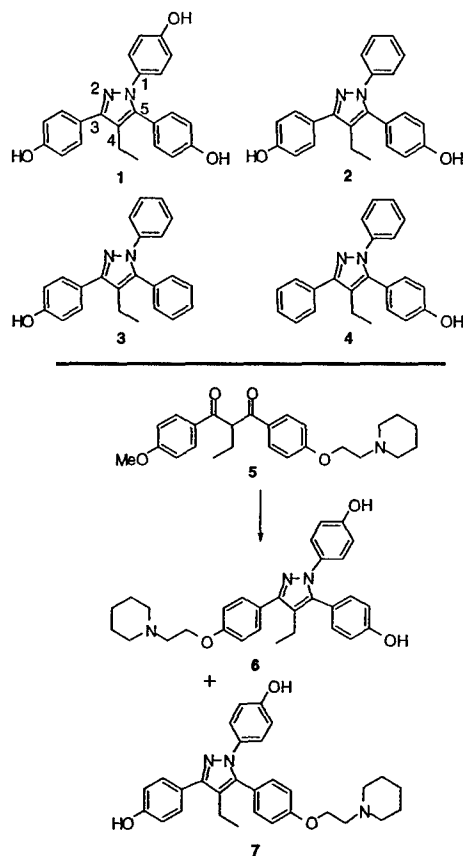
⁶ Stauffer, S.R.; Huang, Y.; Coletta, C.J.; Tedesco, R.; Katzenellenbogen, J.A. *Bioorg. Med. Chem.* Submitted.

⁷ Anstead, G.M.; Carlson, K.E.; Katzenellenbogen, J.A. *Steroids* **1997**, *62*, 268-303.

⁸ Anstead, G.M.; Peterson, C.S.; Katzenellenbogen, J.A. *J. Steroid Biochem.* **1989**, *33*, 877-887.

activity.^{9,10} This generally involves incorporating a basic or polar side chain (such as a piperidylethoxy group) onto either the C(3) or C(5) phenyl groups. However, when pyrazoles **6** and **7** were prepared by the condensation of 4-methoxyphenylhydrazine with the unsymmetrical 1,3-diketone **5**, we obtained the regioisomeric pyrazoles **6** and **7** in pure form only after exhaustive chromatography, and we had to obtain an X-ray structure of the more crystalline isomer **6** to establish the identity of these regioisomers (Scheme 1).

Scheme 1. Pyrazole ligands for the estrogen receptor alpha



The results from cell-based transcriptional assays showed that pyrazole **7** has the desired antagonistic character typical for a SERM. However, to examine this series further we required a regioselective method for the synthesis of the basic side chain derivatives of these 1,3,5-triaryl-4-alkyl pyrazole systems.

Regioselective Synthesis of the Monophenolic Tetrasubstituted Pyrazoles (3 and 4). To develop a regioselective synthesis of these tetrasubstituted pyrazoles, we investigated the reaction of α,β -unsaturated ketones with arylhydrazines, having as our initial goal the synthesis of the two monophenolic

pyrazoles **3** and **4** (Scheme 2). Although α,β -unsaturated ketone **10** condensed smoothly with phenylhydrazine to afford a single pyrazole product **12**, its α -substituted counterpart **8** failed to react under these conditions. The regioisomeric structure of **12** was assigned based on a similar type of reaction reported in the literature,^{11,12} although the mechanism that accounts for the regioselectivity was not clear at this point (*vide infra*). Pyrazole **12** was presumed to be formed through oxidation of the initially formed dihydropyrazole (pyrazoline **11**), although it was not certain whether air (the reaction was run in air) or dimethylsulfoxide served as the oxidant for this transformation. Based on these observations, we investigated methods to introduce the 4-alkyl substituent after the formation of the pyrazole system **12**.

When deprotonation at the 4-position of **12** with *s*-BuLi followed by trapping with ethyl iodide failed to give the desired product, we turned our attention to routes through the corresponding bromide **13** and iodide **14**, which were readily prepared from pyrazole **12** by treatment with the corresponding halo succinimide in CH_2Cl_2 at room temperature. When bromide **13** was treated with *n*-BuLi followed by ethyl iodide, pyrazole **12** was the only isolated product. In our attempts to effect ethyl or vinyl group substitution at C(4) of iodide **14** using various transition metal-mediated reactions (Pd, Ni), we isolated only the reduction product **12** and starting iodide **14**, suggesting that β -hydride transfer competes with reductive elimination in this hindered system. Consistent with this is the fact that we were only able to introduce an acetylene group (producing **15**) or aryl group (not shown) by this approach.¹³

Because of the difficulties we encountered in introducing the C(4)-alkyl substituent in these heterocycles *after* the pyrazoles had been formed, we wondered whether we might be able to intercept the pyrazoline intermediate and introduce the alkyl substituent *before* its oxidation to the pyrazole. Indeed, by carrying out the enone-arylhydrazine condensation reaction under inert atmosphere and eventually using DMF as solvent in place of DMSO, we were able to isolate the air-sensitive pyrazoline intermediate **11** in 61% yield (Scheme 3). Deprotonation of the acidic C(4) methylene group of **11** with LDA at -78°C in THF, followed by trapping of the resulting anion with ethyl iodide, afforded the ethyl-substituted pyrazoline **16** (as a racemate) in 63% yield, with only small amounts of pyrazole **12** as the side product. Pyrazoline **16** was formed as a single diastereomer, and the 4,5-substituents are presumed to be *trans* to each other, based on the 3.7 Hz vicinal coupling constant between the two methine

⁹ Grese, T.A.; Dodge, J.A. *Current Pharmaceutical Design* **1998**, *4*, 71-92.

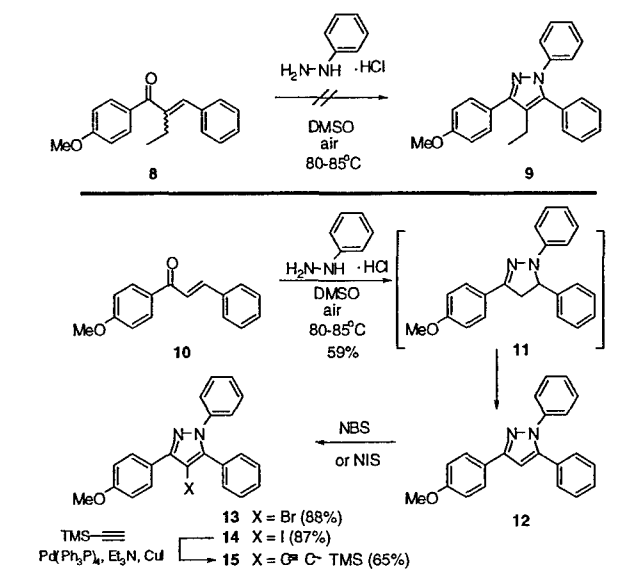
¹⁰ Magarian, R.A.; Overacre, L.B.; Singh, S.; Meyer, K.L. *Curr. Med. Chem.* **1994**, *1*, 61-104.

¹¹ Elguero, J. In *Comprehensive Heterocyclic Chemistry*, Vol. 5; Katritzky and Rees, Eds.; Pergamon: Oxford, 1985; Vol. 5, p 167.

¹² Elguero, J. In *Comprehensive Heterocyclic Chemistry II*; Katritzky, Rees and Scriven, Eds.; Pergamon: Oxford, 1996; p 1.

¹³ Routes involving palladium-mediated coupling of aryl groups to other pyrazole systems have been described: Reference 5 and Wang, X.; Tan, J.; Grozinger, K. *Tetrahedron Lett*, **2000**, *41*, 4713-4716.

Scheme 2. Regiospecific preparation of 1,3,5-triaryl-4-halopyrazoles and their reactions.



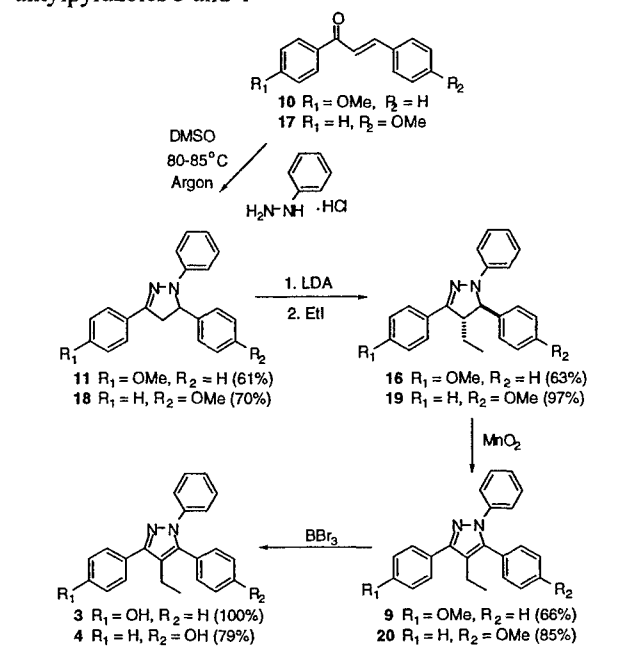
protons.¹⁴ In contrast to the air-sensitivity of its unsubstituted counterpart **11**, the C(4)-alkylated pyrazoline **16** is reasonably stable. It can be stored for a prolonged period of time without apparent oxidation or decomposition, and subsequent oxidation to the corresponding pyrazole actually requires rather harsh conditions. Initially, we used MnO_2 , either at high temperature (reflux benzene) or with ultrasonic agitation, and we obtained the desired 1,3,5-triaryl-4-alkylpyrazoles **9** in 66% yield, but the reaction took 48 h. Later, DDQ was found to be a more efficient oxidant. After demethylation of the protected pyrazole **9** with BBR_3 , we obtained the first desired monophenolic pyrazole **3**. The other desired monophenolic pyrazole (**4**) was obtained by the same reaction sequence, starting from enone **17**. Although it is apparent that the two regioisomers **3** and **4** are different and we were quite confident in our structural assignments based on literature precedent,^{15 16 17 18} the regioselectivity of this route was firmly established only later, by X-ray crystallography (*vide infra*).

With both pyrazole isomers **3** and **4** in hand, we determined their relative binding affinities for ER, and, as described elsewhere,⁵ we were able to conclude that the

C(3) phenol of these pyrazoles is the ring that mimics the A-ring of estradiol.

Regioselective Synthesis of Tetrasubstituted Pyrazoles with Basic Side Chains (7, 33-41). For the synthesis of pyrazole **7** and its analogs, we prepared α,β -unsaturated ketone **21** by an aldol condensation of 4-methoxyacetophenone and *p*-hydroxybenzaldehyde, according to a literature procedure¹⁹ with modifications (Scheme 4). Despite numerous attempts, we were unable to obtain good yields in this simple reaction. However, we were able to isolate the highly crystalline enone **21** easily.

Scheme 3. Regioselective synthesis of 1,3,5-triaryl-4-alkylpyrazoles **3** and **4**



Enone **21**, protected as its silyl ether (**22**), reacted with 4-methoxyphenylhydrazine to give pyrazoline **23**. This material was alkylated, as before, with various iodides to give pyrazolines **24-26**, which were oxidized with either MnO_2 or DDQ to afford the desired pyrazoles **27-29**. Fluoride ion cleavage of the silyl group then gave the C(5) phenolic pyrazoles **30-32**. An X-ray structure of one of these pyrazoles (**31**, Scheme 4) secured the structure of this compound, in the process confirming the regioselectivity of this route to pyrazoles. Installation of the piperidinylethoxy side chain was accomplished by a Mitsunobu reaction. Although BBR_3 cleaved all three ether groups, $\text{AlCl}_3\text{-EtSH}$ selectively cleaved only the methyl ethers, leaving the basic side chain unaffected and giving pyrazoles **33-35** in very high yield. A number of other side chain derivatives (**36-41**) were prepared in the C(4) ethyl series. Pyrazole **41** was prepared by a closely related route (not shown). We are currently investigating

¹⁴ Vicinal coupling constants were calculated using the Karplus relationship within Macromodel v7.0. Monte Carlo conformational searches were conducted using the Amber force field with CHCl_3 as a solvent model. All generated conformers from Monte Carlo searches underwent full matrix assisted minimization using the FMR function with a convergence criteria of 0.001 Kcal/mol, and the Boltzman-averaged constants for the cis and trans compounds are estimated to be 9.3 Hz and 4.8 Hz, respectively. Thus, pyrazolines **16** and **19** are presumed to be the trans isomers. NOE experiments on these pyrazolines gave ambiguous results regarding stereochemistry.

¹⁵ Sangwan, N.; Rastogi, S.N. *Indian J. Chem.* **1979**, *18B*, 65.

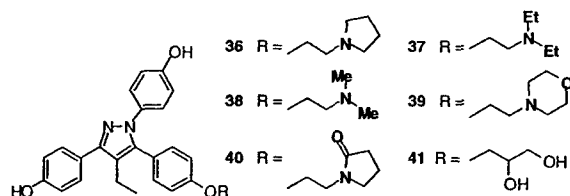
¹⁶ Gupta, S.; Rastogi, S.N. *Indian J. Chem.* **1995**, *34B*, 245.

¹⁷ Kaufman, F.B.; Engler, E.M. *J. Am. Chem. Soc.* **1979**, *101*, 547.

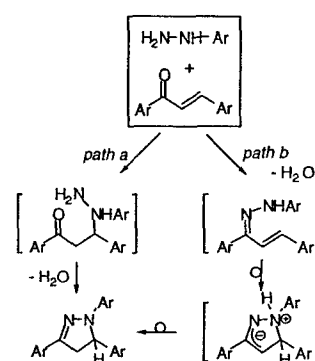
¹⁸ Marzinzik, A.L.; Felder, E.R. *J. Org. Chem.* **1998**, *63*, 723.

¹⁹ Kaufman, F.B.; Engler, E.M. *J. Am. Chem. Soc.* **1979**, *101*, 547.

Basic of Regioselectivity. The regioselectivity of this pyrazole synthesis derives from the initial enone-arylhydrazine condensation, which results in the attachment of the aryl-substituted hydrazine nitrogen to the enone β -carbon and the unsubstituted hydrazine nitrogen to the enone carbonyl carbon. Two mechanisms seem plausible for this transformation (Scheme 5), and they differ in the timing of bond formation. In path a, the aryl-substituted nitrogen reacts first, undergoing a Michael-type addition to the β -carbon of the enone which is followed by an intramolecular imine formation between the carbonyl group and the free amine. In path b, imine formation between the unsubstituted nitrogen and the

[illegible]

Scheme 5. Possible mechanistic pathways for the regiospecific formation of pyrazolines



Supporting Information. Procedures for the preparation of all of the compounds mentioned in this paper and their spectroscopic characterization are found in the Supporting Information section.



DEPARTMENT OF THE ARMY

US ARMY MEDICAL RESEARCH AND MATERIEL COMMAND
504 SCOTT STREET
FORT DETRICK, MARYLAND 21702-5012

REPLY TO
ATTENTION OF:

MCMR-RMI-S (70-1y)

26 Aug 02

MEMORANDUM FOR Administrator, Defense Technical Information
Center (DTIC-OCA), 8725 John J. Kingman Road, Fort Belvoir,
VA 22060-6218


SUBJECT: Request Change in Distribution Statement

1. The U.S. Army Medical Research and Materiel Command has reexamined the need for the limitation assigned to technical reports written for this Command. Request the limited distribution statement for the enclosed accession numbers be changed to "Approved for public release; distribution unlimited." These reports should be released to the National Technical Information Service.

2. Point of contact for this request is Ms. Kristin Morrow at DSN 343-7327 or by e-mail at Kristin.Morrow@det.amedd.army.mil.

FOR THE COMMANDER:

Encl


PHYLLIS M. RINEHART
Deputy Chief of Staff for
Information Management

ADB274369
ADB256383
ADB264003
ADB274462
ADB266221
ADB274470
ADB266221
ADB274464
ADB259044
ADB258808
ADB266026
ADB274658
ADB258831
ADB266077
ADB274348
ADB274273
ADB258193
ADB274516
ADB259018
ADB231912
ADB244626
ADB256677
ADB229447
ADB240218
ADB258619
ADB259398
ADB275140
ADB240473
ADB254579
ADB277040
ADB249647
ADB275184
ADB259035
ADB244774
ADB258195
ADB244675
ADB257208
ADB267108
ADB244889
ADB257384
ADB270660
ADB274493
ADB261527
ADB274286
ADB274269
ADB274592
ADB274604

ADB274596
ADB258952
ADB265976
ADB274350
ADB274346
ADB257408
ADB274474
ADB260285
ADB274568
ADB266076
ADB274441
ADB253499
ADB274406
ADB262090
ADB261103
ADB274372